



Eidgenössische Technische Hochschule Zürich
Swiss Federal Institute of Technology Zurich



Institut für
Technische Informatik und
Kommunikationsnetze

Andreas Germann

Evaluation of AQM Schemes to Support Low Latency in the Internet

18. September 2017

Master Thesis MA-2017-07
July 2017 to September 2017

Tutor: Prof. Dr. Laurent Vanbever
Supervisors: Mirja Kuehlewind, Brian Trammell

Acknowledgements

I want to thank my tutor Prof. Dr. Laurent Vanbever and my supervisors Mirja Kuehlewind and Brian Trammel for their support while working on this project.

Abstract

In this work, we evaluated different AQM schemes that can be used in the internet. Since low latency becomes a requirement for increasing amounts of applications and traffic and since queuing remains a significant source of latency, we wanted to find out how well these AQM schemes would perform with respect to low latency requirements.

For these evaluations, we implemented different AQM schemes for a network simulator and ran simulations. Based on these results we evaluated the performance of these schemes with respect to queuing delays and link utilization.

Our results showed that simple AQM with a single queue only rarely could achieve low queuing delays and that they had to sacrifice link utilization when trying. Some more complex schemes with two queues also had a hard time achieving low queuing delays but did not loose link utilization when trying. Other schemes with two queues were able to achieve very low queuing delays but also had to sacrifice link utilization.

Contents

1	Introduction	7
2	Background	9
2.1	Explicit Congestion Notification	9
2.2	TCP Congestion Control	9
2.2.1	Classic Congestion Control	10
2.2.2	Scalable Congestion Control	12
2.2.3	Scalable vs Classic	13
2.3	Active Queue Management	14
2.3.1	Random Early Detection	15
2.3.2	Curvy Random Early Detection	15
2.3.3	Proportional Integral Controller Enhanced	16
2.3.4	Proportional Integral Controller Squared	17
2.4	Low Latency Low Loss Scalable Throughput	18
2.4.1	Basic Concept	18
2.4.2	DualQ Coupled AQM	18
2.5	Network Simulator 3	21
2.5.1	Direct Code Execution	21
2.5.2	Link Models	21
2.6	Jain's Fairness Index	22
3	Simulation	23
3.1	AQM Implementations	23
3.1.1	Single Queue AQM	23
3.1.2	Dual Queue Uncoupled AQM	24
3.1.3	DualQ Coupled AQM	25
3.2	Kernel Modifications	27
3.3	Simulation Network	27
3.3.1	Static Link Model	27
3.3.2	LTE Network	28
3.4	Simulation Scenarios	28
4	Results	31
4.1	Metrics	31
4.2	Static Link Simulations	31
4.2.1	Single Queue AQM	32
4.2.2	Dual Queue Uncoupled AQM	34
4.2.3	DualQ Coupled AQM	38
4.2.4	Comparison	43
4.3	LTE Link Simulations	44
4.3.1	Single Queue AQM	44
4.3.2	Dual Queue Uncoupled AQM	46
4.3.3	DualQ Coupled AQM	49
4.3.4	Comparison	50
4.4	Conclusion	52
4.4.1	AQM Schemes	52
4.4.2	TCP Settings	52

5 Summary and Outlook	55
5.1 Summary	55
5.2 Outlook	56
A Plots	57
A.1 Plots from Static Link Simulations	57
A.2 Plots from LTE Link Simulations	87
B Data	119
B.1 Data from Static Link Simulations	120
B.2 Data from LTE Link Simulations	130
C Original Problem	139

Chapter 1

Introduction

In today's internet, delays are increasingly becoming a problem. More and more applications and traffic require low latencies to provide a satisfying service. Examples for such applications are voice over IP, video telephony or interactive web applications. Recent efforts to reduce latency by placing servers closer to the users were of limited success since queuing persists as an intermittent source of delay. Queuing causes spikes in latency when buffers fill up due to congestion. Even when using modern active queue management (AQM), queueing can still cause significant delays. [26]

AQM are algorithms that control the size and thereby also the delay of a queue through pre-emptive drops. This leads to a trade-off of latency against throughput. Low queuing delays are achieved by reducing the amount of packets in the queues. This can leave the queue temporarily empty which leads to underutilization of the link and loss of throughput. Allowing high queuing delays results in higher amounts of packets in the queues and higher link utilization.

Low Latency Low Loss Scalable Throughput (L4S) is a proposed algorithm that provides an ultra low latency service in parallel to the classic best-effort service. This is done by separating incoming traffic into the two classes based on an identifier and then applying different control schemes to achieve the respective goal. To achieve ultra low latency the low-latency class is given priority over the best-effort class. [11]

In this project we implement different AQM schemes in a network simulator. With these implementations, we run simulations in different scenarios to gather data on the performance of these schemes. Based on the results of these simulations we will evaluate the performance of the different algorithms. This should give insight into their advantages, drawbacks and problems.

Chapter 2

Background

2.1 Explicit Congestion Notification

Explicit Congestion Notification (ECN) is an extension of TCP/IP [15]. ECN allows a router to send congestion signals without dropping packets. To do that, a router marks packets instead of dropping them.

If a router wants to send a congestion signal, it marks a packet. Upon receiving a marked packet, the endpoint of a connection informs the sender by marking the acknowledgement packet.

Using ECN implicates a problem with fairness called ECN unfairness. ECN unfairness describes different scenarios where bandwidth is distributed unfairly between flows because of ECN. Corrupted ECN signals and the ignoring of ECN feedback are mentioned as reasons for ECN unfairness. But there is a case without signal corruption or disobedience to feedback that can cause ECN unfairness. In this case, non-ECN flows receive less bandwidth than ECN flows because their packets are dropped instead of marked. This happens especially often in situations where an AQM reaches high drop probabilities.

The RED algorithm described in Section 2.3.1 is mentioned as an example. When the queue length exceeds the maximum threshold, only ECN flow receive throughput since all non-ECN packets are dropped.

2.2 TCP Congestion Control

TCP congestion controls are algorithms designed to control the sending rate of network devices [8]. Their goal is to adjust the sending rate according to the currently available bandwidth. On one hand, they should keep the sending rate high in order to achieve a high link utilization. On the other hand, they should keep the rate low enough to avoid congestions and congestive breakdowns.

The sending rate in TCP is controlled by the congestion window. The congestion window defines how many packets a connection is allowed to have in flight simultaneously. If the congestion window is full, the sender has to wait for acknowledgements before he can send further packets. Congestion controls define how the congestion window is changed. The difference between congestion controls is how and when they change the congestion window. Generally, the absence of packet losses indicates that the network is not congested and the congestion window can be increased. When a packet loss is detected, this indicates a congestion and the congestion window has to be reduced. Like losses, ECN feedback is also a congestion signal and should lead to a congestion window reduction.

A lot of congestion controls use slow-start, an algorithm for increasing the congestion window. It is comprised of two phases, the slow-start phase and the congestion-avoidance phase. In the slow-start phase, the congestion window is increased quickly in order to bring the connection

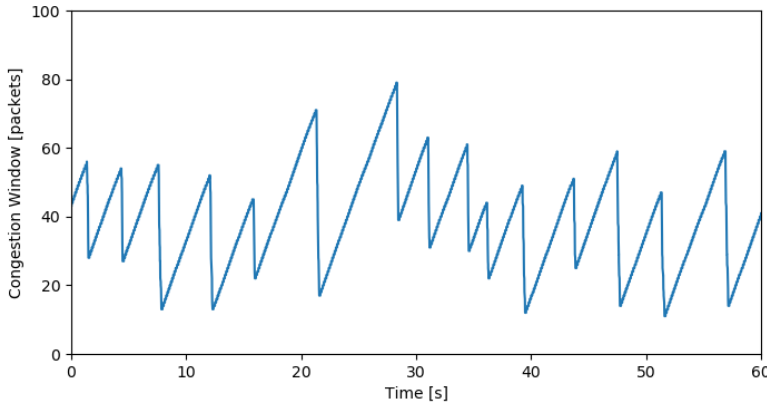


Figure 2.1: Congestion window over time in Reno

up to speed. In the congestion avoidance phase, the window is increased slowly. Also, a lot of algorithms use fast-recovery/fast-retransmission, an algorithm that can sometimes skip the slow-start phase after a loss. If the sender registers a packet loss of a specific packet, it can perform a fast retransmission of this packet. If it succeeds, the slow-start phase is skipped, the congestion window is increased and the control continues in the congestion-avoidance phase. Since this work is about congestion and since the congestions controls in our simulations will mostly be in the congestion-avoidance phase, we will focus on the congestion-avoidance behaviour of the algorithms.

2.2.1 Classic Congestion Control

One class of congestion controls that we used in our simulations are classic congestion controls [16] [24]. Classic congestion controls are in the sense classic that they the ones currently being used in today's internet. They work by the AIMD (additive increase/multiplicative decrease) principle. The main difference to scalable congestion controls explained in Section 2.2.2 is that the congestion window reduction is quite aggressive when congestion signals are registered.

Reno

Reno is a simple classic congestion control algorithm [8]. Reno uses slow-start and fast-recovery/fast-retransmission.

In the congestion-avoidance phase and the absence of losses, it increases the congestion window by one over the current congestion window for every acknowledgement received. This leads to an effective increase of one packet every round-trip-time.

In case of losses or the receiving of ECN feedback, the congestion window is reduced. Simplified, it is halved. Actually, it is set to one packet but due fast-recovery/fast-retransmission, the slow-start phase can be skipped and the congestion window restored to half its previous value, continuing in the congestion-avoidance phase.

Figure 2.1 shows an example plot of the Reno congestion window over time in steady state.

Cubic

Cubic is another classic congestion control [17] [24]. It also uses slow-start and fast-recovery/fast-retransmission.

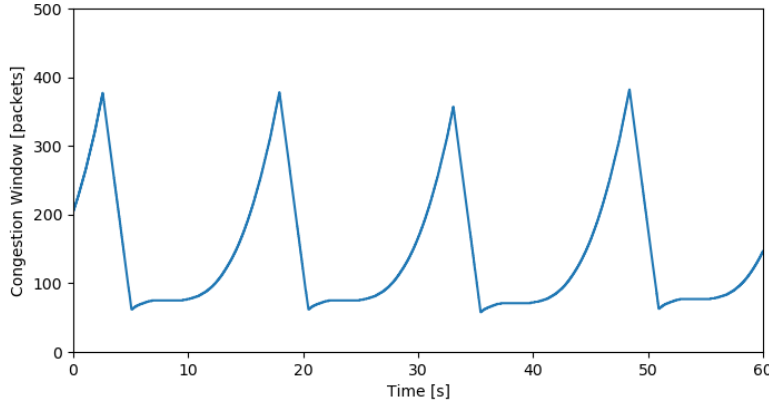


Figure 2.2: Congestion window over time in Cubic

Like Reno, Cubic increases its congestion windows for every received acknowledgement. In the congestion-avoidance phase, Cubic uses a cubic congestion window growth function depending on the time since the last loss or ECN feedback. This function is shown in Equation 2.1. The factor β is the decrease factor and is recommended to be 0.7. The factor C defines the aggressiveness of the algorithm and is recommended to be 0.4. W_{max} is the stored congestion window from before the last reduction.

$$W(t) = C * (t - K)^3 + W_{max} \quad (2.1)$$

$$K = \sqrt[3]{\frac{W_{max} * (1 - \beta)}{C}}$$

The cubic growth function has three regions. One region is the TCP-friendly region. Here, the growth function is compared to a standard TCP growth function (Equation 2.2) with β_{aimd} equals 0.5. If $W(t)$ is smaller than $W_{aimd}(t)$, then the congestion window should be set to $W_{aimd}(t)$ whenever an acknowledgement is received. This should ensure that the congestion window in Cubic grows at least as fast as in the linearly growing standard TCP.

The other two regions are the convex and the concave region. In these two regions, the congestion window is set to $W(t + RTT)$ from Equation 2.1 for every acknowledgement received. As long as the congestion window has not reached w_{max} , the cubic function is in its concave region. Here it grows quickly at first and slows down when approaching W_{max} . Once the congestion window goes past W_{max} , it enters the convex region and grows increasingly fast.

$$W_{aimd}(t) = W_{max} * \beta_{aimd} + 3 * \frac{1 - \beta_{aimd}}{1 + \beta_{aimd}} * \frac{t}{RTT} \quad (2.2)$$

The window reduction in Cubic works like the one in Reno with fast-recovery/fast-retransmission and slow-start. But simplified, the congestion window is reduced by 70%. Also, the congestion window before the reduction is saved as the new W_{max} . This is shown in Equation 2.3.

$$W_{max} = cwnd \quad (2.3)$$

$$cwnd = cwnd * (1 - beta)$$

Figure 2.2 shows an example plot of the Cubic congestion window over time in steady state.

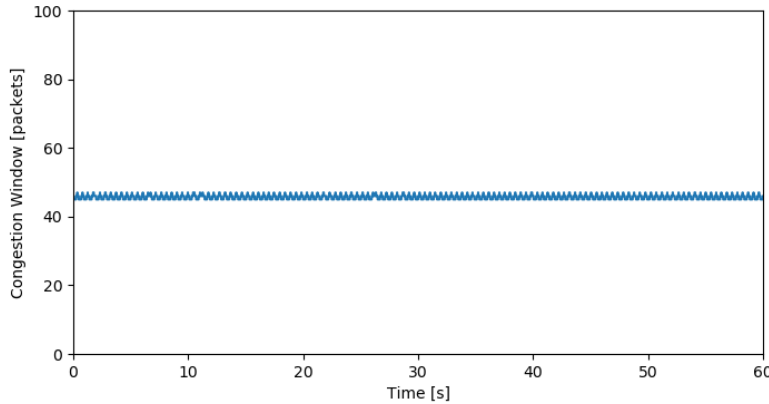


Figure 2.3: Congestion window over time in DCTCP

2.2.2 Scalable Congestion Control

Another class of congestion controls are scalable congestion controls [5] [20]. Compared to classic congestion controls, scalable congestion controls reduce the congestion window more conservatively.

Data Center TCP

Data Center TCP (DCTCP) is a scalable congestion control [5] [7]. Like Reno, it also uses slow-start and fast-recovery/fast-retransmission.

In the congestion-avoidance phase, the congestion window is also increased by one packet every round-trip-time.

The difference lies in the congestion window decrease mechanism. DCTCP distinguishes between losses and ECN feedback. For ECN feedback, it reduces the congestion window based on an exponentially weighted moving average of the ratio between bytes where the acknowledgement was marked and bytes where the acknowledgement was not marked. For losses, DCTCP behaves like Reno, halving the congestion window.

The exponentially weighted moving average α is updated according to Equation 2.4 approximately once very round-trip-time. The factor g sets the weight between old and the values. g is recommended to be $\frac{1}{16}$.

Upon receiving an ECN feedback, DCTCP reduces the congestion window according to Equation 2.5. The reduction by the factor of $\frac{\alpha}{2}$ ensures that for high congestion when α is close to 1, DCTCP halves its congestion window like in the Reno algorithm.

$$\alpha = (1 - g) * \text{alpha} + g * (\text{marked_bytes_acknowledged}/\text{bytes_acknowledged}) \quad (2.4)$$

$$\text{cwnd} = \text{cwnd} * (1 - \frac{\alpha}{2}) \quad (2.5)$$

Figure 2.3 shows an example plot of the DCTCP congestion window over time in steady state.

Relentless

Relentless is a simple implementation of a scalable congestion control [20] [21]. It also uses slow-start and fast-recovery/fast-retransmission.

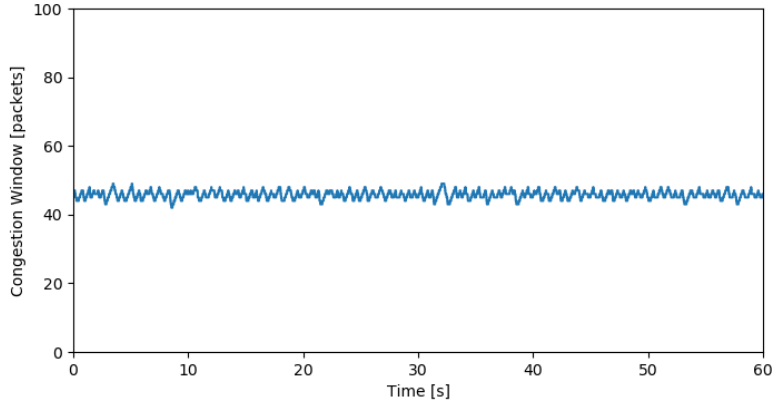


Figure 2.4: Congestion window over time in Relentless

The increase mechanism is again the same as in Reno, increasing the congestion window by one packet every round-trip-time.

The reduction mechanism of Relentless is very simple. The congestion window is reduced by one packet for every loss or ECN feedback. This is similar to DCTCP but leaves out the smoothing of the moving average function.

Figure 2.4 shows an example plot of the Relentless congestion window over time in steady state.

2.2.3 Scalable vs Classic

Buffer Size

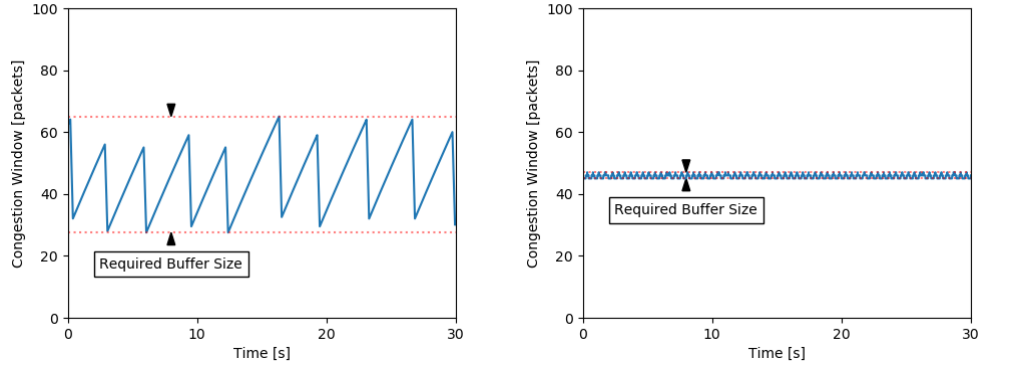
Compared to classic congestion control, scalable congestion control offers three improvements. [7]. The first improvement is that scalable congestion control can achieve full link utilization with less buffer size than classic congestion control. The second, following from the first, is that scalable congestion control can achieve lower queuing delays since the buffer size can be smaller. And third, if a buffer is managed by an AQM, the lower buffer utilization of scalable congestion control leaves more capacity for bursts.

Figures 2.5a and 2.5b show example plots of the congestion windows of Reno and DCTCP in steady state with similar throughputs and round-trip-times. The required buffer sizes to achieve full link utilization are also plotted. Reno and DCTCP are used as examples for classic and scalable congestion controls. The same principle goes for other congestion controls in the respective classes.

Throughput Equation

One big problem with scalable congestion control is that it is not AIMD-friendly meaning that it starves out competing flows that use AIMD or classic congestion controls. This is due to the difference in throughput equations. [13] [14]

The throughput equations states the throughput of a flow that uses a certain congestion control. Different congestion controls have different throughput equations. The throughput equations for Reno, Cubic, DCTCP [13] and Relentless [14] are stated in Equations 2.6. They depend on the maximum segment size (MSS), the round-trip-time RTT and the drop rate p .



(a) Congestion window and required buffer size for full link utilization in Reno (b) Congestion window and required buffer size for full link utilization in DCTCP

Figure 2.5: Comparison of the congestion windows of Reno and Cubic

$$\begin{aligned}
 \text{throughput_reno} &= \frac{MSS * 1.22}{RTT * \text{drop_rate}^{0.5}} \\
 \text{throughput_cubic} &= \frac{MSS * 1.17}{RTT^{0.25} * \text{drop_rate}^{0.75}} \sim \frac{MSS * 1.68}{RTT * \text{drop_rate}^{0.5}} \quad (\text{in TCP-friendly region}) \\
 \text{throughput_dctcp} &= \frac{MSS * 2}{RTT * \text{drop_rate}} \\
 \text{throughput_relentless} &= \frac{MSS * 0.49}{RTT * \text{drop_rate}}
 \end{aligned} \tag{2.6}$$

There is a major difference between the throughput equations of classic and scalable congestions controls. While the classic ones contain the drop rate as a square root, the scalable ones do contain it directly.

Assuming similar RTT and MSS and drop probability, the classic congestion controls have a much lower throughput than the scalable ones. That is the reason why flow with scalable congestion control starve out competing flows with classic congestion control if no special measures are adopted.

2.3 Active Queue Management

Active Queue Management (AQM) describes schemes that aim to control filling levels and delays of queues. [6] Queues in network devices serve as buffers to prevent losses when more packets come in than can go out. An ongoing congestion causes such queues to fill up. This can lead to massive drops in case of an overflow as well as large queuing delays.

AQM was originally developed to conserve throughput by preventing an excessive build-up of packets in case of a congestion. Such an excessive build-up can ultimately lead to the buffer overflowing resulting in massive packet loss. AQM controls the queue length by randomly dropping packets if it detects a congestion. This signals the senders to reduce their sending rate and mitigates the congestion. The cost of these pre-emptive drops should outweigh the cost of a buffer overflow with massive packet losses.

Later, AQM was also used to control queuing delays since latency became increasingly important and since queuing remained a significant source of delay. In this case, the goal is to keep the queue short in order to reduce delay. At the same time, the queue should not run empty because that would lead underutilization of the link. Controlling the queue length is a trade-off between latency and throughput.

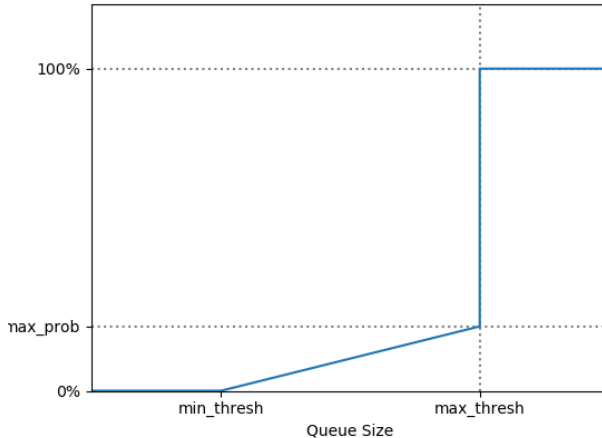


Figure 2.6: Drop probability function of RED

The difference between AQM schemes is how the drop probability is implemented which determines how the queue length or delay is controlled.

If available, AQM can also use ECN marks instead of drops or a mixture of drops and marks.

2.3.1 Random Early Detection

Random Early Detection (RED) is a simple AQM [19] [12]. It randomly marks or drops packets with a drop probability depending on the current queue length .

RED uses three parameters. The minimum threshold defines the queue length up to which no packets are dropped or marked. The maximum threshold defines the queue length above which all packets are dropped or marked. The maximum drop probability defines the drop probability when the queue length is equal to the maximum threshold.

Between minimum and maximum threshold, the drop probability is a linear function that equals 0 at the minimum threshold and equals the maximum drop probability at the maximum threshold.

The maximum drop probability is recommended to be one or two percent. For the thresholds, there are no special recommendations.

Figure 2.6 shows the basic graph of the drop probability function of RED.

2.3.2 Curvy Random Early Detection

Curvy Random Early Detection (CRED) is another simple AQM [10]. It randomly drops or marks packets with a drop probability depending on the current queue delay. The AQM is called curvy because it uses an exponential function for the drop probability.

CRED uses two parameters to calculate the drop probability. The slope factor Dq defines the queue delay above which all packets are dropped or marked. The curviness factor U defines the exponent for the drop probability function.

The drop probability function is described in Equation 2.7. The drop probability is bounded to 1 for queue delays above the slope factor.

$$\text{drop_probability} = \left(\frac{\text{queue_delay}}{Dq} \right)^U \quad (2.7)$$

The current queue delay can either be measured by using timestamps or estimated using the current queue length and a measurement of the dequeuing rate. There are no recommenda-

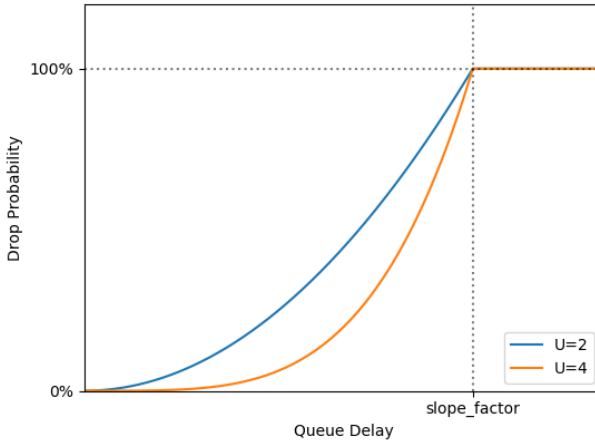


Figure 2.7: Drop probability function of CRED

tions for the parameters.

Figure 2.7 shows two plots of the CRED drop probability function with different curviness factors U .

2.3.3 Proportional Integral Controller Enhanced

Proportional Integral Controller Enhanced (PIE) is a more complex AQM [23] [22]. It uses current and past queuing delays for the calculation of the drop probability. The PIE algorithm consists of two parts.

The first part is the drop probability calculation. This function periodically updates the drop probability depending on the current, previous and target queue delay as well as the current drop probability. After the calculation, the current queuing delay is stored for the next calculation. Algorithm 1 shows the drop probability calculation as it is defined in [22].

The second part is the early drop function that decides whether a packet is dropped or marked. A packet is dropped or marked randomly using the calculated drop probability.

Random dropping is prevented if the previous queuing delay and the drop probability are low enough or if the queue is almost empty.

Random dropping is also prevented if PIE is in burst protection. Burst protection keeps PIE from dropping packets during short bursts. If the link is not congested for a while, burst protection is activated. In the case of a congestion, the burst protection deactivates after a certain time.

The current queue delay can either be measured by using timestamps or estimated using the current queue length and a measurement of the dequeuing rate.

These are recommended values for the PIE parameters from [22].

Target delay	: 15 milliseconds
Burst protection period	: 150 milliseconds
Update period	: 15 milliseconds
Alpha	: 0.125
Beta	: 1.25

The full proposed pseudo code of PIE can be seen in [22].

```

p = alpha * (current_delay - target_delay) + beta * (current_delay - previous_delay);
if drop_prob < 0.000001 then
| p /= 2048;
else if drop_prob < 0.00001 then
| p /= 512;
else if drop_prob < 0.0001 then
| p /= 128;
else if drop_prob < 0.001 then
| p /= 32;
else if drop_prob < 0.01 then
| p /= 8;
else if drop_prob < 0.1 then
| p /= 2;
else
| p = p;
end
drop_prob += p;
if cur_queue_delay == 0 AND old_queue_delay == 0 then
| drop_prob *= 0.98;
end
if drop_prob < 0 then
| drop_prob = 0;
end
previous_delay=current_delay;

```

Algorithm 1: Drop probability calculation of PIE from [22]

2.3.4 Proportional Integral Controller Squared

Proportional Integral Controller Squared (PI2) is another AQM [13]. It is loosely based on PIE. A special thing about this AQM is that it can control scalable and classic congestion controls at the same time. This is done by adjusting the drop probability according to the congestion control. However, this required a reliable distinction between the congestion controls. The ECT(1) code-point is proposed for such a distinction.

The drop probability calculation is shown in Equation 2.8. The drop probability is updated periodically. The current queue delay can either be measured by using timestamps or estimated using the current queue length and a measurement of the dequeuing rate.

$$\begin{aligned} drop_prob = & drop_prob \\ & + \alpha * update_period * (cur_queue_delay - ref_queue_delay) + \quad (2.8) \\ & + \beta * update_period * (cur_queue_delay - old_queue_delay) \end{aligned}$$

After the distinction, the drop probability is adjusted for the congestion control. For a flow with classic congestion control, the drop probability is first scaled and then squared as shown in Equation 2.9. For scalable congestion controls, the drop probability would be left as it is.

$$drop_prob_classic = \left(\frac{drop_prob}{K} \right)^2 \quad (2.9)$$

This different treatment accounts for the difference in the throughput equation of classic and scalable congestion controls described in Section 2.2.3 and allows them to coexist. The squaring adjusts the different powers of the drop rate in the throughput equations. The scaling shifts the throughput distribution to adjust for the constants.

Two is recommended as scaling factor since it is the power of two that should achieve the fairest throughput distribution. Powers of two are favourable since divisions by two can be

implemented cheaply using bit shifts.

These are recommended values for the PI2 parameters from [22].

Target delay	: 15 or 20 milliseconds
Update period	: 16 or 32 milliseconds
Alpha	: 10
Beta	: 100
K	: 2

2.4 Low Latency Low Loss Scalable Throughput

Low Latency Low Loss Scalable Throughput (L4S) is a proposed algorithm that aims to provide a low-latency service parallel to the current best-effort service [11].

In connection with L4S, we will call the low-latency service L4S service and the best-effort service classic service. The same goes for the respective AQM elements like for example queues or drop probabilities.

2.4.1 Basic Concept

The basic concept of L4S contains three elements [11]. These are separation, identification and scalable congestion control.

Separation means the separation of L4S traffic and classic traffic so that both of them do not affect each other. Mainly, the L4S traffic needs to be protected from the potentially high latency of the classic traffic. Also, the classic traffic needs to be protected from the less sensitive scalable congestion control of the L4S traffic. But even if the two classes are separated, they should still share the link capacity freely without having fixedly assigned shares.

Identification means the necessity to clearly identify the respective classes in order to correctly separate incoming traffic. A recommendation for this identifier is the ECT(1) code-point [25].

And scalable congestion control is necessary for the L4S traffic in order to avoid the problem of link utilization. Since the L4S traffic seeks low latency, only a small buffer can be used. And as mentioned in Section 2.2.3, when only a small buffer is available, scalable congestion control achieves higher utilization than classic congestion control.

Also, scalable congestion control requires ECN which can prevent the large spikes in latency that occur when packets are lost. L4S also requires ECN since the ECT(1) code-point is recommended to be used as identifier. DCTCP is mentioned as a possible scalable congestion control.

2.4.2 DualQ Coupled AQM

DualQ Coupled AQM is a proposed implementation of L4S [26]. DualQ Coupled AQM uses the ECT(1) code-point to classify incoming packets. The traffic is separated into two queues, one for L4S and one for classic traffic. These queues run an AQM that is coupled through the drop probability. This coupling means that the drop probability for the classic Queue is equal to the scaled and squared drop probability of the L4S queue. Equation 2.10 shows this coupling.

$$\text{drop_probability_C} = \left(\frac{\text{drop_probability_L}}{K} \right)^2 \quad (2.10)$$

The squaring of the drop probability is necessary due to the different powers of the drop rate in the throughput equations of classic and scalable congestion control described in Section 2.2.3. With the scaling factor K , this steady state distribution can be shifted. Two is recommended for K since it is a power of two and since it approximates throughput equivalence between

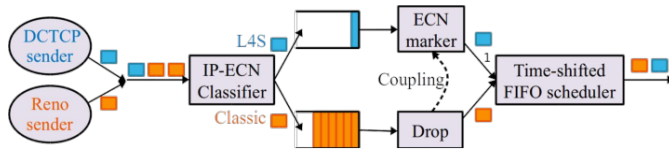


Figure 2.8: Function principle of DualQ Coupled AQM (Graphic from [9])

L4S and classic flows. Using powers of two for K has the advantage that divisions are cheaply implementable through bit shifts.

To achieve a low latency in the L4S queue, the L4S queue is to be scheduled with priority. This priority can be strict but does not have to be.

Two possible implementations of DualQ Coupled AQM are proposed. One uses PI2 as AQM and the other CRED.

Figure 2.8 shows the function principle of DualQ Coupled AQM.

DualQ Coupled AQM with PI2

This proposed implementation of DualQ Coupled AQM uses the AQM PI2 described in Section 2.3.4. It consists of an enqueueing function, a dequeuing function and a drop probability calculation function that periodically updates the drop probabilities.

The drop probabilities are calculated based on the current queuing delay. As long as the classic queue is not empty, its queue delay is used for the calculation. If it is empty, the queue delay of the L4S queue is used. The new drop probabilities are calculated according to Equation 2.11.

$$\begin{aligned}
 \text{classic_drop_probability} &= \text{classic_drop_probability} \\
 &+ \alpha * \text{update_period} * (\text{current_queue_delay} - \text{target_queue_delay}) \\
 &+ \beta * \text{update_period} * (\text{current_queue_delay} - \text{old_queue_delay})
 \end{aligned}$$

$$\text{l4s_drop_probability} = K * \text{classic_drop_probability} \quad (2.11)$$

At enqueueing, the queues are checked whether there is space. If there is, the packet is classified using the ECT(1) code-point and enqueued in the respective queue.

For dequeuing, the queues are scheduled with a shifted FIFO scheduler with the shift in favour of the L4S queue. This means, the classic queue is only scheduled if the L4S queue is empty or if the oldest packet in the classic queue is more than a certain time older than the oldest in the L4S queue.

If an L4S packet is dequeued it is decided whether it will be marked. The packet is marked randomly with the L4S drop probability. If the packet has been in the queue longer than a time threshold and if the queue is currently longer than a length threshold, the packet is marked deterministically.

If a classic packet is dequeued it is randomly dropped or marked with the square of the classic drop probability.

This algorithm has an overload protection that would switch to dropping if it detected an unresponsive ECN flow. We will not explain this part since we did not examine the security properties of these algorithms in this work. The overload protection can be seen in the pseudo code in [26].

The current queue delay can either be measured by using timestamps or estimated using the current queue length and a measurement of the dequeuing rate. The proposed pseudo code uses timestamps.

These are recommended parameter values for the DualQ Coupled AQM with PI2 from [26].

Target delay	: 15 milliseconds
Update period	: 16 milliseconds
FIFO time shift	: 2 * target delay (30 milliseconds)
Time threshold	: 1 millisecond
Length threshold	: 2 packets (or 2 * MTU)
Maximum classic drop probability	: 0.25
Maximum L4S drop probability	: min (K * $\sqrt{\text{classic_drop_prob_max}}$, 1)
Alpha	: 10
Beta	: 100
K	: 2

The complete, proposed pseudo code of DualQ Coupled AQM with PI2 can be seen in [26].

DualQ Coupled AQM with CRED

This proposed implementation of DualQ Coupled AQM uses the AQM CRED described in Section 2.3.2. It only has an enqueueing and a dequeuing function.

The enqueueing here works like the enqueueing in DualQ Coupled AQM with PI2. The queues are checked whether they have free space and then the packet is sorted into the respective queue depending on the ECT(1) code-point.

For dequeuing, strict priority scheduling in favour of the L4S queue is used. If an L4S packet is dequeued, it is randomly marked with the L4S drop probability. And if the L4S queue exceeds a certain length threshold, the packet is marked deterministically.

If a classic packet is dequeued, it is randomly dropped or marked with the classic drop probability. If a packet from the classic queue is dropped, another one is dequeued until the classic queue is empty or one packet was not dropped.

The L4S drop probability and the classic drop probability are calculated according to Equation 2.13. For the calculation of the L4S drop probability, the current queue delay of the classic queue is used. For the calculation of the classic drop probability, an exponentially weighted moving average (EWMA) of the classic queue delay is used. This calculation can be seen in Equation 2.12.

The current queue delay can either be measured by using timestamps or estimated using the current queue length and a measurement of the dequeuing rate. The proposition does not specify which.

$$Q_C = 2^{-smoothing_factor} * \text{classic_queue_delay} + (1 - 2^{-smoothing_factor}) * Q_C \quad (2.12)$$

$$\text{classic_drop_probability} = \frac{Q_C}{2^{classic_scaling_factor}} \quad (2.13)$$

$$l4s_drop_probability = \frac{\text{classic_queue_delay}}{2^{l4s_scaling_factor}}$$

We assume there is a typo or a sign error in the draft. The formula for the L4S drop probability in Equation 2.13 seems incorrect since it does not conform to the throughput equivalence equation in Section 2.4.2. This is discussed further in Section 3.1.3.

These are recommended parameter values for the DualQ Coupled AQM with CRED from [26].

Classic scaling factor	: -1
L4S scaling factor	: Classic scaling factor + K' ($K' = \log_2 K$) (We assume this to be an error)
Smoothing factor	: 5
L4S length threshold	: 5 packets (or 5 * MTU)
K (k)	: 2

The complete, proposed pseudo code of DualQ Coupled AQM with CRED can be seen in [26].

2.5 Network Simulator 3

The Network Simulator 3 (NS-3) is an open source software for network simulations [1]. We used this software to simulate a router handling congestions with different AQM schemes.

2.5.1 Direct Code Execution

Direct Code Execution (DCE) is a feature of NS-3 [2]. DCE allows a user to run real-world kernel code libraries on the simulated devices. Using original kernel code allows the use of the real world protocol implementations. This should give a more realistic behaviour of the different algorithms in the simulation.

For our simulations we used the linux kernel version 4.7.0 -rc5 [4].

2.5.2 Link Models

In NS-3, different link models can be used for simulations. With these models, different kinds of networks can be simulated. For our simulations we used the static link model and the LTE link model.

Static Link Model

The static link model simulates a point-to-point link that is statically defined by a bandwidth and a delay. [1]

LTE Model

The LTE model allows simulations of an LTE network [3]. For our simulations, the important aspects of the model are the bearers and the bearer scheduling.

In LTE, there are so-called bearers. Simplified, bearers are virtual channels. For every user device in an LTE network a default bearer is opened but additional dedicated bearers can be added. Dedicated bearers can be used to separate specific traffic like for example voice over IP. The LTE model of NS-3 simulates this bearer system and allows a user to add his own bearers depending on what he wants to simulate. Each bearer maintains its own queue.

Bearers have to be scheduled for transmission by the LTE network.

NS-3 has different schedulers implemented. For our simulations, we used the proportional fair scheduler. The proportional fair scheduler calculates a priority for each bearers according to Equation 2.14 where R_i is the achievable throughput of bearer i in the coming time slot and T_i is the achieved throughput in the past of bearer i . T_i is calculated using an exponentially weighted moving average.

The bearers are scheduled with these calculated priorities.

$$\text{priority_bearer_}i = \frac{R_{_i}}{T_{_i}} \quad (2.14)$$

2.6 Jain's Fairness Index

Jain's fairness index is a measure for how fair bandwidth was distributed between multiple flows [18]. It is calculated with from the throughputs achieved by the individual flows. The calculation can be seen in Equation 2.15 where n is the total number of flows and $t_{_i}$ is the throughput of flow i .

$$\text{jain_fairness_index} = \frac{(\sum_{i=0}^n t_{_i})^2}{n * (\sum_{i=0}^n t_{_i}^2)} \quad (2.15)$$

Jain's fairness index is bounded between 0 and 1. The distribution was absolutely fair if the index equals one.

Chapter 3

Simulation

3.1 AQM Implementations

For our simulations, we implemented different algorithms and AQM schemes in order to evaluate their performance in different scenarios. We implemented three groups of algorithms. The simplest implementations use a single queue with an AQM. Their results should show how established algorithms perform in our simulations and serve as a reference for the other implementations.

Some more complex algorithms use two queues where low-latency and classic traffic can be separated. Both queues run independent AQM schemes without coupling. The two queues are scheduled with a weighted round robin scheduler. These implementations are simplifications of the proposed DualQ Coupled AQM described in Section 2.4.2. For one, their results should show the change in performance between separated treatment and Single Queue AQM implementations. And furthermore, these results should show how the additional step of coupling and priority scheduling does further change the performance.

The most complex implementations are the DualQ Coupled AQM implementations described in Section 2.4.2. Based on these results we want to evaluate the performance of this proposed algorithm.

3.1.1 Single Queue AQM

The Single Queue AQM implementations work like a classic buffer. Incoming packets are stored in a FIFO queue until they can be passed on. Packets are treated equally independent of their traffic class. We implemented the Single Queue AQM with RED and PIE described in Section 2.3.1 and 2.3.3.

In early simulations we saw that DualQ Coupled AQM could keep queuing delays in the order of a few milliseconds. Since the Single Queue AQM implementations would have to compete with that, we decided to use a target delay of five milliseconds.

Since these implementations do not separate low-latency and classic flows, the Single Queue AQM implementations can only work fairly if all flows use either classic or scalable congestion controls (See Section 2.2.3). And since current traffic in the internet uses classic congestion controls, the low-latency flows must do that as well. Therefore, classic congestion controls were used on all flows in the simulations with Single Queue AQM.

Single Queue AQM with RED

NS-3 already contains an implementation of RED but we implemented our own. The reasons were that the out-of-the-box implementation did not support ECN and that we wanted to have an exact implementation of RED as it is in [12]. We implemented RED according to that description.

The parameters for RED were set according to the recommendations in [12] and our own experimental simulations. The maximum drop probability was set to 0.02 or 2% as recommended. Since RED does not take a target delay as parameter, we experimentally determined the thresholds that would correspond to the target of five milliseconds. To reduce the number of parameters, we decided to use a minimum threshold of one third the maximum threshold. The experimental simulations were made for a single Reno-controlled flow and the link speed used in the simulations.

This resulted in a maximum threshold of 34 packets. Dividing by three resulted in a minimum threshold of 11 packets.

Single Queue AQM with PIE

NS-3 also already contains an implementation of PIE but again we implemented our own. Again, the reasons were that the included NS-3 implementation did not support ECN and that we wanted an exact implementation according to [22]. Our implementation of PIE followed that description. For our PIE implementation, we used timestamps to determine the queue delay and not an estimation through dequeuing rate and queue length.

The parameters for PIE were set according to the recommendations in [22] except for the target queue delay and the update period of the drop probability. Like for Single Queue RED, the target queue delay was set to five milliseconds and the update period as well.

The update period was reduced since the recommended one would have been higher than the target delay. Early simulations showed that PIE could keep the target better with a reduced update period. The update period was set equal to the target delay since it is equal to the target delay in [22] as well.

3.1.2 Dual Queue Uncoupled AQM

The Dual Queue Uncoupled AQM implementations work with two FIFO queues with one for the classic traffic and one for the low-latency traffic. Like in [26], we use the ECT(1) code-point as a class identifier. Incoming packets were separated into the two queues based on the ECT(1) code-point. The two queues were scheduled with a weighted round robin scheduler. The weight was assigned according to the number of flows in each class. The flow numbers are not determined by the queues themselves but given to them as an argument. An actual implementation would have to determine the numbers by itself. For the Dual Queue Uncoupled AQM implementations we also used the AQM schemes RED and PIE described in Sections 2.3.1 and 2.3.3.

Both queues ran independent instances of the same AQM.

For the low-latency queue, a low target queue delay was set in order to serve the low latency requirement. Again, since the AQM would have to compete with DualQ Coupled AQM, this delay was set to five milliseconds.

The classic queue AQM was set up with a high target queue delay in order to achieve high throughput. Also, we saw in early simulations that a high classic target delay improved the performance of the low-latency AQM. When the target delay of the classic queue AQM was set too low, the classic queue often got empty in which case the low-latency queue received more throughput. Once the low-latency queue received more throughput, the low-latency senders increased their sending rate. When the classic queue then filled again and reclaimed the throughput, the increased sending rate leading to longer queue and increased delay.

Therefore, the classic target delay was set so high that the classic queue delay should never run empty.

Since these implementations did separate low-latency and classic traffic, scalable congestion control could be used on the low-latency flows. Since the throughput was distributed by the scheduler, the scalable congestion control flows in the low-latency queue could not starve the classic congestion control flows in the classic queue. So classic and scalable congestion

control could coexist.

Dual Queue Uncoupled AQM with RED

For Dual Queue Uncoupled AQM with RED, we again used the basic RED implementation from [12]. The difference was that here we ran two instances of the algorithm in parallel. Since RED does not hold a state, the only difference between the instances were the parameters.

Like in the Single Queue AQM implementations, the parameters were set according to the recommendations in [19] and our own experimental simulations. For both instances, the maximum drop probability was set to 0.02 or 2% as recommended.

The minimum and the maximum threshold for the low-latency instance were again determined experimentally. And like in Single Queue RED, we used a ratio of 1:3 between minimum and maximum threshold to simplify the determination. Since the average queue length in RED is different for scalable and classic congestion control, we ran additional simulations for a single DCTCP controlled flow. Based on these simulations we set the thresholds corresponding to a target delay of five milliseconds.

The base minimum and maximum thresholds for classic congestion controls were like in the Single Queue AQM implementation 11 and 34 packets. The simulations showed that the base maximum threshold for scalable congestion control should be five packets and the minimum threshold therefore two packets.

The weighted round robin scheduler assigned throughput according to the flow counts and the delays do also depend on the throughput beside the queue length. Therefore, the resulting values were scaled in each simulation for the expected throughput of the low-latency traffic. Equation 3.1 shows the scaling.

$$\begin{aligned} \text{max_thresh_low_latency} &= \max\left(\frac{\text{low_latency_flows}}{\text{low_latency_flows} + \text{classic_flows}} * \text{base_max_thresh}, 1\right) \\ \text{min_thresh_low_latency} &= \min\left(\frac{\text{max_thresh_low_latency}}{3}, \text{max_thresh_low_latency} - 1\right) \end{aligned} \quad (3.1)$$

The minimum and the maximum threshold for the classic AQM instance needed to be set to high values in order to keep the throughput high and the classic queue full. Therefore, the minimum and maximum threshold were set to 100 and 300 packets.

Dual Queue Uncoupled AQM with PIE

For Dual Queue Uncoupled AQM with PIE, we again used the same basic PIE implementation described in Section 2.3.3. Again, two instances of the algorithm were run in parallel. Here, the difference included state variables aside from the parameters.

Like in the Single Queue AQM implementation, the parameters were set according to the recommendations from [22] with the exception of the target queue delay and the update period. For the low-latency instance, the target delay and the update period was again set to five milliseconds.

The target delay of the classic AQM instance was set to 500 milliseconds to achieve high throughput and keep the classic queue full. For the classic instance, the update period was taken from the recommendations in [22] since it was still lower than the target delay.

3.1.3 DualQ Coupled AQM

DualQ Coupled AQM was implemented as described in Section 2.4.2. We implemented three versions of this algorithm.

Proposed Implementations

[26] contains two proposed implementations for DualQ Coupled AQM. One is using PI2 and the other is using CRED.

The proposed implementation using PI2 is a fully elaborated algorithm that we implemented according to the pseudo code from [26].

The proposition using CRED is not as elaborate. Our implementation follows the pseudo code from [26] aside from three points.

First, the proposed pseudo code does not allow to use ECN marking in the classic queue. For our implementation we decided to add this option.

Second, the proposition mentions two mechanism to determine the queue delays. One is the use of timestamps, the other is a delay estimation based on the queue length and the dequeuing rate. But it is not specified, which one should be used. We decided to use timestamps.

And third, we think that there is an error in the pseudo code concerning the drop probability calculation. The drop probability calculation from [26] does not satisfy the throughput equivalence equation described Section 2.4.2. This drop probability calculation is shown in Equation 3.2.

$$\begin{aligned} \text{classic_drop_probability} &= \left(\frac{Q_C}{2^{\text{classic_scaling_factor}}} \right)^2 \\ l4s_drop_probability &= \frac{\text{classic_queue_delay}}{2^{l4s_scaling_factor}} \end{aligned} \quad (3.2)$$

In steady state, the exponentially weighted moving average Q_C should approximate the current queuing delay. And according to [26], $l4s_scaling_factor = \text{classic_scaling_factor} + \log_2 K$. This results in the drop probabilities and coupling shown in Equation 3.3.

$$\begin{aligned} \text{classic_drop_probability} &= \left(\frac{\text{classic_queue_delay}}{2^{\text{classic_scaling_factor}}} \right)^2 \\ l4s_drop_probability &= \frac{\text{classic_queue_delay}}{2^{\text{classic_scaling_factor} + \log_2 K}} \\ &= \frac{\text{classic_queue_delay}}{2^{\text{classic_scaling_factor}} * K} \\ \Rightarrow \text{classic_drop_probability} &= (l4s_drop_probability * K)^2 \end{aligned} \quad (3.3)$$

In order for the drop probabilities to satisfy the equivalence equation, the L4S scaling factor needs to be $\text{classic_scaling_factor} - \log_2 K$ instead of $\text{classic_scaling_factor} + \log_2 K$. We assume this is a sign error in [26].

For our implementation, we changed the calculation to satisfy the equivalence equation.

DualQ Coupled AQM with PIE

Additionally to the two proposed implementations, we implemented a third version based on the PIE algorithm described in 2.3.3. The basic design was still the one of DualQ Coupled AQM from with two queues, priority scheduling, identifier and coupling.

For this implementations we used the unchanged drop probability calculation function of PIE described in Section 2.3.3.

The enqueueing function was changed to be able to serve two queues. After checking whether the queues still have free space, the incoming packets were classified based on the ECT(1) code-point.

After the classification, the drop decision was made. Classic packets were dropped or marked according to the classic PIE scheme. L4S packets were marked randomly with the L4S drop probability which was equal to the square root of the classic drop probability times the scaling factor. Equation 3.4 shows the calculation of the L4S drop probability. Also, L4S packets were marked deterministically if the queue delay and the queue length exceeded certain thresholds. This deterministic marking and its thresholds were borrowed from the proposed implementation with PI2 in [26].

$$l4s_drop_probability = \sqrt{classic_drop_probability} * K \quad (3.4)$$

If the incoming packet was not dropped, it was enqueued in the respective queue.

The dequeuing function implemented a strict priority scheduling in favour of the L4S queue.

The queue delays were determined using timestamps.

3.2 Kernel Modifications

For our simulations we used the linux kernel version 4.7.0-rc5 [4]. For the purpose of this simulation, we made some modifications to the kernel code.

The first modification concerns the ECN behaviour. We changed the kernel code to use ECT(1) instead of ECT(0) in order to mark traffic as low-latency traffic. This modification was used for the low-latency and L4S senders.

The second modification concerns the congestion control. DCTCP is already implemented in [4]. But since we wanted to compare the AQM schemes with another scalable congestion control, we additionally implemented Relentless [21].

Our implementation was based on the existing DCTCP implementation [4]. Most of the DCTCP code was left as it is. The reduction function was changed to reduce the congestion window by half a packet for every received ECN feedback. If an ECN feedback acknowledged multiple packets, the reduction was increased accordingly.

[21] recommends a reduction by one packet for every received ECN feedback but we wanted to tune Relentless to approximately the same sensitivity as DCTCP. DCTCP halves its congestion window when all packets in a round-trip-time are marked [7]. With a reduction of half a packet per ECN feedback, Relentless is similarly sensitive.

3.3 Simulation Network

3.3.1 Static Link Model

The first simulations used the static link model described in Section 2.5.2 for the simulation network. These simulations should provide insight into of the performance that these AQM schemes would have in a wired network.

We set up our simulation network with bandwidths of 1 gigabit per second on the access links and 10 megabits per second on the congested link. The base round-trip-time, was set to 100 milliseconds.

For the simulations with the static link model, we implemented all the AQM schemes mentioned in Section 3.1.

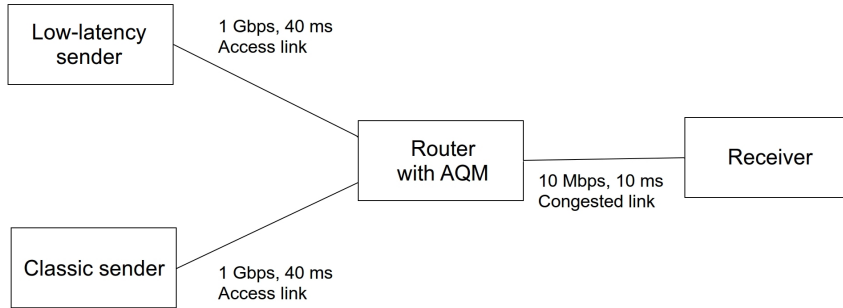


Figure 3.1: Static link simulation network

Figure 3.1 shows the static link network used for the simulations.

3.3.2 LTE Network

The second simulations used the LTE link model described in Section 2.5.2 for the congested link. These simulations should demonstrate the performance of the AQM schemes in a mobile network.

For these simulations, the parameters of the congested link were defined by the LTE model of NS-3. We saw that the maximum bandwidth was around 17.5 megabits per second. We also saw that the base round-trip-time of the LTE link was in the order of a few milliseconds.

The access links to the LTE base station were set up with a bandwidth of 1 gigabit per second and a base round-trip-time of 100 milliseconds.

For these simulations, we implemented the Single Queue and Dual Queue Uncoupled AQM schemes described in Sections 3.1.1 and 3.1.2. From the DualQ Coupled AQM schemes described in Section 3.1.3, we could only implement the version with PIE. These implementations were more complicated since they had to be written inside the code of the NS-3 LTE module [3] itself.

This imposed some restrictions. For example, we could only implement AQM schemes that work at enqueueing. The dequeuing functions were more complex since they did not simply dequeue packet by packet but also grouped them into transmission units. If we wanted to include AQM schemes in these functions, we would also have had to make sure that these AQM schemes do not interfere with this grouping. This would have significantly added complexity. Ultimately, we did not have enough time to do this.

We also used the bearer scheduling mechanisms that were already implemented in the LTE module [3]. Due to time limits, we did not look closely into these schedulers. They were quite complex since they had to cooperate with other elements of the LTE model. This made it more complicated to implement our own schedulers and we did not have enough time to do this. Therefore, we used the included proportional fair scheduler described in Section 2.5.2 instead of the weighted round robin or priority schedulers.

Figure 3.2 shows the LTE network used for the simulations.

3.4 Simulation Scenarios

For our simulation scenarios we used several parameters. The most important ones were the flow counts in each class. Additionally we used different congestion controls and turned ECN on and off for the classic flows.

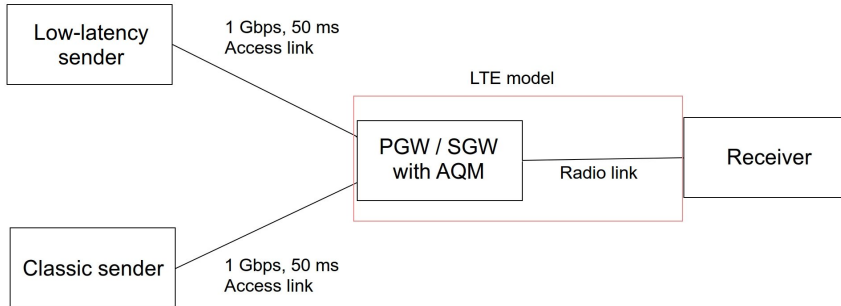


Figure 3.2: LTE simulation network

The flow configurations we used were all combination of one, five and ten flows in both traffic classes. These simulations should show how the AQM schemes perform with different flow counts per class and different ratios of flow counts between the classes.

We also ran the simulations with different combinations of congestion controls in both the low-latency senders and the classic senders. For the low-latency senders Reno, Cubic, DCTCP and Relentless were used depending on what was sensible to be used for the current AQM. For the classic senders, Reno and Cubic were used. These different simulations should show whether the choice of congestion control has a significant impact on the performance of the AQM schemes.

Also, we ran the simulations with ECN activated and deactivated for the classic flows. ECN was always activated for the low-latency flows because the ECT(1) code-point was necessary for the traffic class separation and because ECN was necessary for the scalable congestion controls. These simulations should show, whether the using ECN on the classic flows has an impact on the performance of the AQM schemes.

In all our simulations we used a segment size of 1502 bytes.

Chapter 4

Results

4.1 Metrics

For evaluating the results of our simulations we used metrics concerning the delays and the throughput.

We evaluated the delays by looking at the maximum and the average queue delay. For the implementations with two queues, this was extended to maximum and average queue delays of the classic and the low-latency or L4S queue.

Since only the low-latency or L4S traffic seek low latency, the main metric in the implementations with two queues were the maximum and average low-latency or L4S queue delays.

The throughput was evaluated by looking at the link utilization and the fairness. The utilization should show how much resources were wasted by a certain algorithm. The fairness should show, how fairly the available bandwidth was distributed between the two traffic classes.

In order to measure the fairness, we used Jain's fairness index described in Section 2.6. For the calculation of the index we assumed that within the traffic classes, the throughput was assigned fairly.

For our purposes we modified the fairness index. In Jain's classic fairness index, it is not shown, which class got more throughput in the case of unfairness. Therefore, we changed the index depending on which class received more throughput.

When the classic traffic class received more throughput, the fairness index was left as it is. When the low-latency or L4S traffic class received more throughput, the sign of the index was flipped and two was added to it. This modified index is still the fairest when it is close to one. But it shows now which class received more throughput depending if it is below or above one. Equation 4.1 shows the calculation performed when the low-latency or L4S class received more throughput.

$$\text{modified_jain_index} = (2 - \text{jain_index}) \quad (4.1)$$

4.2 Static Link Simulations

This section discusses the results from our simulations in the static link network.

In the following passages, we only use examples to visualize our findings. The full data and all plots can be found in Appendices A.1 and B.1.

4.2.1 Single Queue AQM

In our simulations, we saw that Single Queue PIE achieved the target delay of 5 milliseconds only for two total flows. For more flows, the average queue delay increased, up to a maximum of 8.8 milliseconds.

Single Queue RED missed the target delay for all flow combinations. The lowest average queue delays were achieved with only two flows, having been between 7.8 and 11 milliseconds. For more flows, the average queue delays went up to between 18 and 28 milliseconds.

Like the average queue delays, the maximum queue delays in both single queue AQM were the lowest for two flows and went up for more flows. And like for the average queue delay, PIE achieved lower maximum queue delays than RED.

We think the reason for this is that the target delay of five milliseconds translates to a too small queue size. With a segment size of 1502 bytes and a bandwidth of 10 megabits per second, one packet takes about 1.2 milliseconds to transmit. This means that a queue of more than four packets already exceeds the target delay. This gives the AQM too little space to work, especially for higher flow counts.

By trying to reach such a low delay, the single queue AQM often underutilized the link. RED was loosing up to 14.5% utilization and PIE up to 17.5%.

In most cases, the available bandwidth was shared fairly between the flows with the exception of ECN unfairness (See Section 2.1) that occurred when using RED.

Influence of Flow Counts

In general, the queue delays in Single Queue AQM schemes increased with the number of flows. The main increase in delay was from two to six flows. Above six flows, the increase slowed down.

Also, ECN unfairness in RED became more severe with increasing classic flow counts. We think, this comes from the increasing size and frequency of spikes due to more flows. These spikes would cause the queue to exceed the maximum threshold (See Section 2.3.1). In that case, the drop probability would be 100% leading to more severe ECN unfairness.

Activating ECN also lead to an increase in maximum queue delay. We think this is because unlike dropped packets, marked packets were enqueued anyway, adding to the queue length and delay.

The Figures 4.1 and 4.2 show the resulting metrics from simulations with Single Queue AQM across all flow count combinations. These plots should visualize the influence of the flow counts. We chose the results from the simulations with Cubic as examples. The results from the simulations with Reno showed similar effects.

Influence of TCP Settings

When ECN was deactivated on the classic links, single queue RED encountered ECN unfairness.

Activating ECN also generally lead to an increase in maximum delay since the packets that would be dropped without ECN are marked and enqueued anyway, increasing the delay.

Using Cubic instead of Reno as congestion control decreased the maximum delays and increased the utilization.

We think the reason for this was the different growth function of cubic. Since the bandwidth was quite stable, the Cubic algorithm (See Section 2.2.1) only rarely reached the phase of fast, exponential growth. Therefore, the congestion window of Cubic was growing slower around the saturation point than that of Reno. This lead to lower peaks in queue length and queue delay.

Also, Cubics initial fast growth in the concave phase brought up the congestion window faster than the linear growth of Reno leading to higher utilization.

The Figures 4.3a and 4.3b show examples of congestion window traces from our single queue

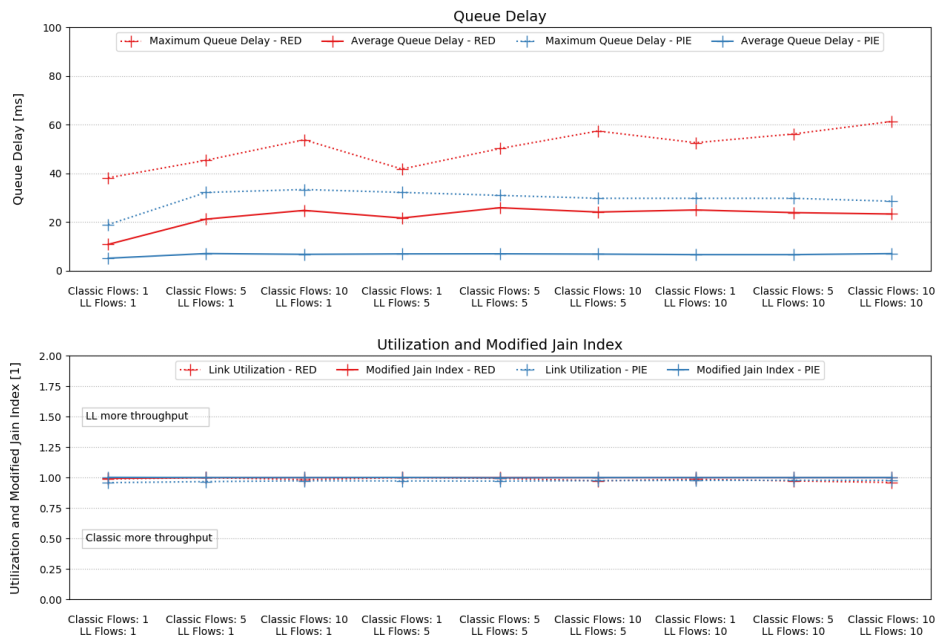


Figure 4.1: Average and maximum queue delays, link utilization and modified Jain index over all flow count combinations for the Single Queue AQM simulations using Cubic on all flows and activating ECN on the classic flows

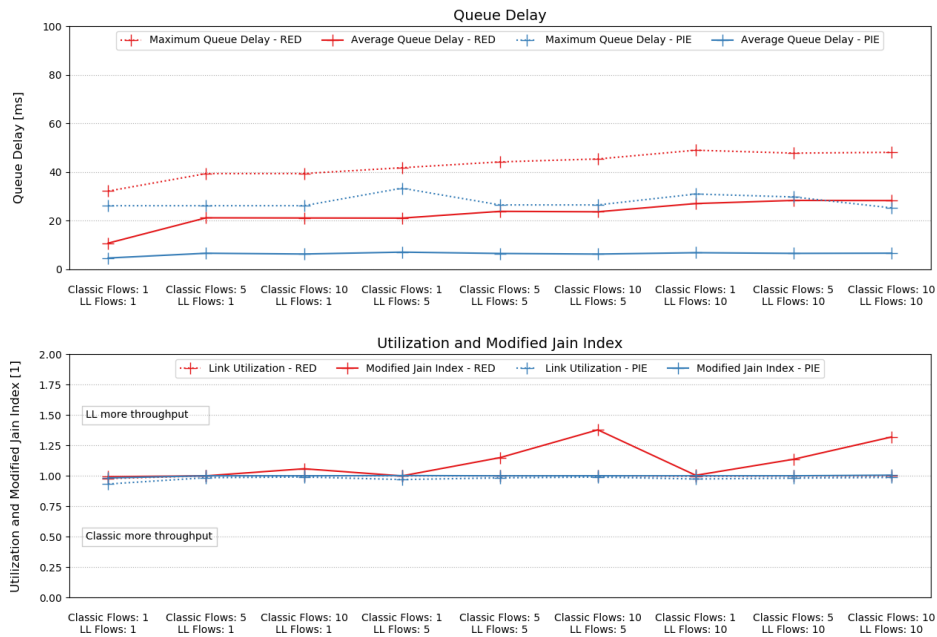


Figure 4.2: Average and maximum queue delays, link utilization and modified Jain index over all flow count combinations for the Single Queue AQM simulations using Cubic on all flows and deactivating ECN on the classic flows

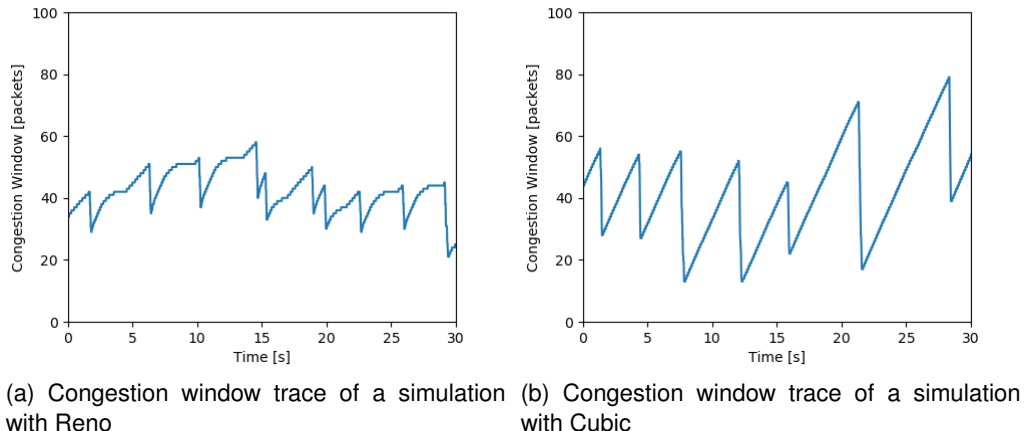


Figure 4.3: Comparison of the congestion windows of Reno and Cubic from our Single Queue PIE simulations

PIE simulations using Reno and Cubic. They show the aforementioned differences between Cubic and Reno.

Figure 4.4 shows the resulting metrics from simulations with Single Queue AQM across all available TCP settings. These plots should visualize the influence of the TCP settings. We chose the results from the simulations with 5 low-latency and 5 classic flows as an example. The results from the simulations with other flow configurations showed similar effects.

4.2.2 Dual Queue Uncoupled AQM

Unlike in Single Queue AQM, scalable congestion control could be used for the low-latency flows in Dual Queue Uncoupled AQM. In our simulations with Dual Queue Uncoupled AQM we also looked at the difference that scalable congestion control can make.

With classic congestion control, the PIE implementations also only achieved the low-latency target delay of 5 milliseconds when there were only 2 flows. For more flows, the average low-latency queue delay increased, up to a maximum of 23 milliseconds.

The RED implementation could never keep the low-latency target delay. With only two flows, the average low-latency queue delay was the lowest between 8.3 and 12 milliseconds. For more flows, the average low-latency queue delay increased to between 18 and 25 milliseconds. For PIE and RED, the maximum low-latency queue delays were also the lowest for only two flows and increased for more.

With scalable congestion control, the average low-latency queue delays of PIE were very similar to the ones with classic congestion control. But the maximum low-latency queue delay tended to be smaller with scalable than with classic congestion control.

The low-latency queue delays in the RED implementation were significantly smaller when using scalable congestion control. Now, RED was sometimes able to keep the low-latency target delay, especially for low flow counts. But the RED implementation still had cases where the average low-latency queue delay went up to 17 milliseconds. And like in the PIE implementations, scalable congestion control resulted in lower maximum low-latency queue delays than classic congestion control in Single Queue RED.

The average and maximum queue delays of the classic queue were in the order of hundreds or sometimes thousands of milliseconds for both PIE and RED as well as classic and scalable congestion control. These high delays came by design. The AQM of the classic queue has a very high target delay in order to keep it at a high filling level. This high filling level should keep the classic queue from running empty, allowing it to use all available bandwidth, serving its goal

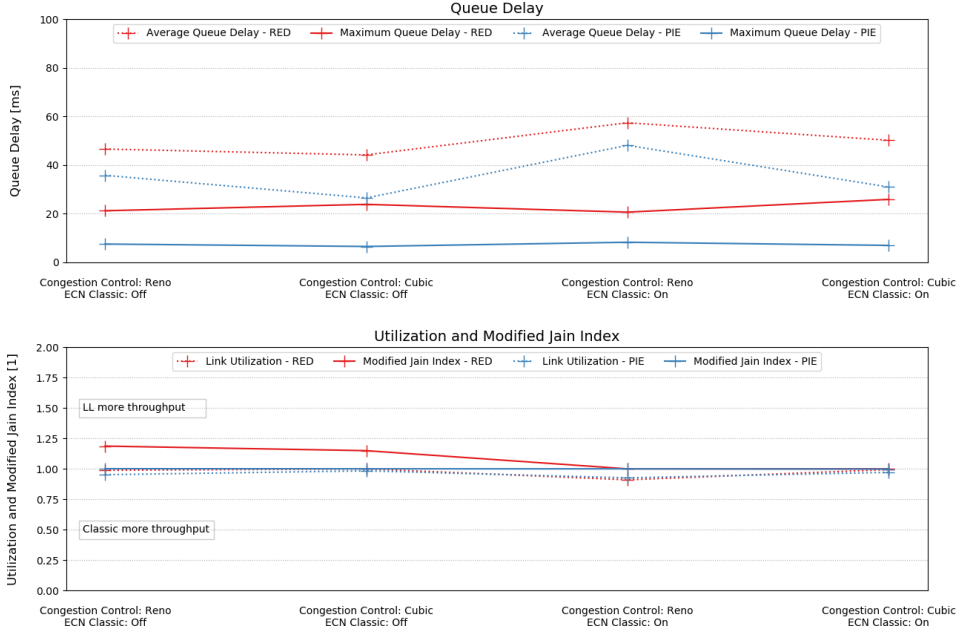


Figure 4.4: Average and maximum queue delays, link utilization and modified Jain index over all available TCP settings for the Single Queue AQM simulations with 5 low-latency and 5 classic flows

of high throughput.

By design, both implementations achieved almost full link utilization for classic and scalable congestion control. The lowest link utilization was 99.88%. Dual Queue Uncoupled AQM was designed to achieve full link utilization by keeping the classic queue from running empty. So when the low-latency queue had to give up bandwidth in order to achieve its target delay, the classic queue could absorb it.

Because of that, the important metric concerning throughput was the allocation. With both scalable and classic congestion control, this allocation was fair in most cases.

Influence of Flow Counts

The low-latency queue delays generally increased with the number of flows. Additionally, the low-latency delays increased when there were more classic than low-latency flows.

We think, this is an effect of the weighted round robin scheduler. When the low-latency class had less flows than the classic class, then it also got scheduled less often. This lead to longer intervals between dequeues and therefore higher delays.

In cases where there were more low-latency than classic flows, the low-latency queue delay was generally the lowest. But in these cases, the low-latency queue was often also not able to fully use the assigned throughput. Since this bandwidth was not lost but absorbed by the classic queue, this did not lead to a lower utilization but to unfairness.

We think the reason for this is that with higher numbers of flows, the low-latency class received more throughput which made it easier to achieve its target delay. But often, when the target delay went down the fairness did as well. Also, the choice of congestion control had a significant influence on this.

Figure 4.5 shows the resulting metrics from simulations with Dual Queue Uncoupled AQM across all flow count combinations when using classic congestion controls on the low-latency

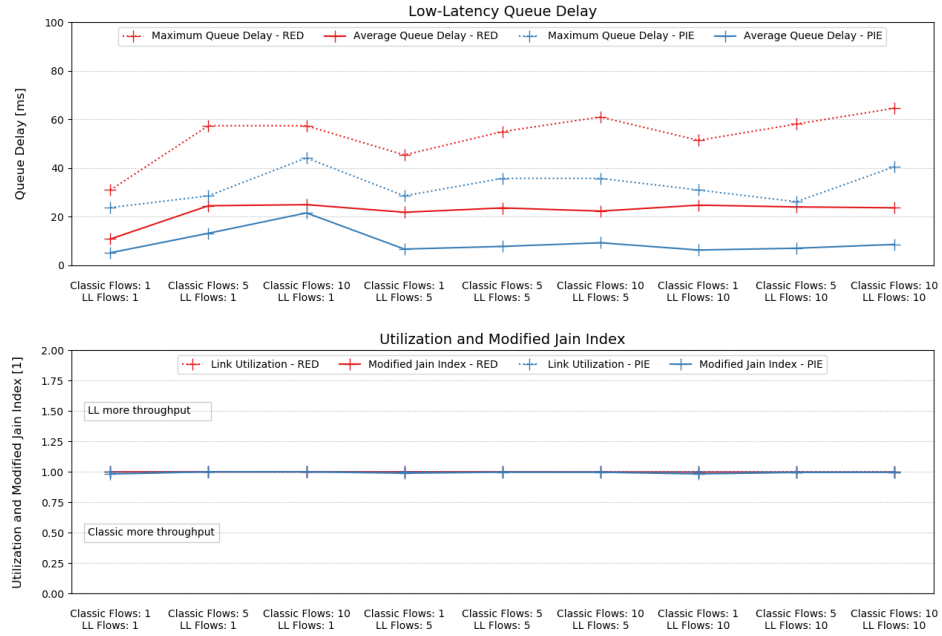


Figure 4.5: Average and maximum queue delays, link utilization and modified Jain index over all flow count combinations for the Dual Queue Uncoupled AQM simulations using Cubic on all flows and activating ECN on the classic flows

flows. Figure 4.6 shows the same for when using scalable congestion controls on the low-latency flows. These plots should visualize the influence of the flow counts. We chose the results from the simulations with Cubic, DCTCP and ECN activated as examples. The results from the simulations with other congestion controls or ECN deactivated showed similar effects.

Influence of TCP Settings

When using classic congestion control, both RED and PIE showed the aforementioned problem of unfairness. With Reno, this unfairness was in most cases more severe than with Cubic. And Cubic also tended to achieve lower maximum low-latency queue delays.

We think, the reason for this is the same as in the Single Queue AQM.

Figures 4.7a and 4.7b show examples of low-latency sender congestion window traces from our Dual Queue Uncoupled RED simulations using Reno and Cubic. Like in the Single Queue AQM case, the differences leading to lower maximum delay and higher utilization can be seen in these plots.

When using scalable congestion control, the aforementioned problem with unfairness persists for RED when Relentless is used. For PIE and for RED with DCTCP, the bandwidth distribution is always very fair.

The unfairness in RED with Relentless was in some cases even more severe than with classic congestion controls. Apart from the difference in fairness, Relentless also reached lower average low-latency queue delays.

We think the reason for this is that neither RED nor Relentless contain any smoothing function. This lead to more fluctuations in the congestion window. With the limited buffer size due to delay constraints this caused the low-latency queue to give up more throughput. This also reduced the average queue length and therefore the average low-latency queue delay.

Figures 4.8a and 4.8b show examples of low-latency sender congestion window traces from our Dual Queue Uncoupled RED simulations using DCTCP and Relentless. It can be seen that

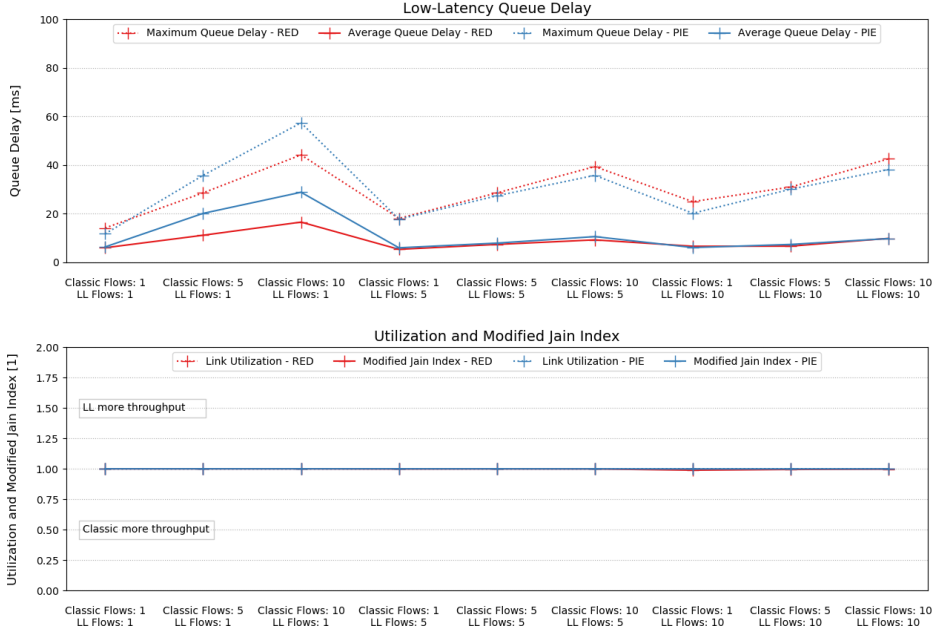


Figure 4.6: Average and maximum queue delays, link utilization and modified Jain index over all flow count combinations for the Dual Queue Uncoupled AQM simulations using DCTCP on low-latency flows, Cubic on classic flows and activating ECN on the classic flows

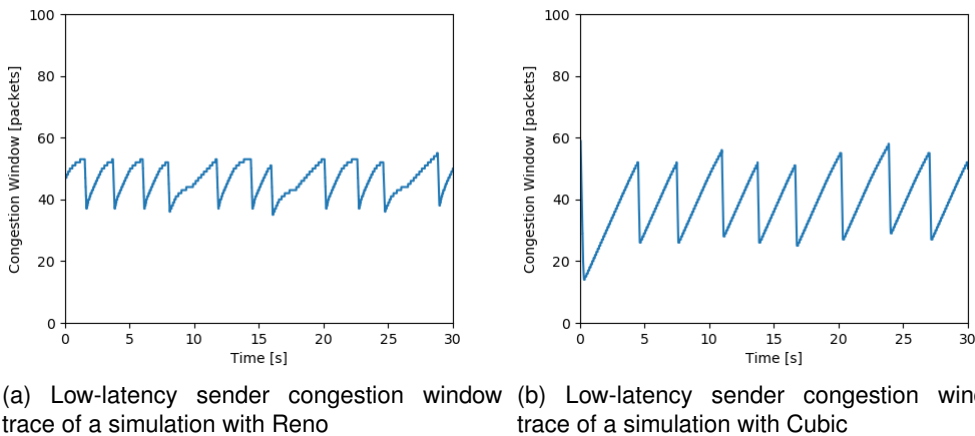


Figure 4.7: Comparison of the congestion windows of Reno and Cubic from our Dual Queue Uncoupled RED simulations

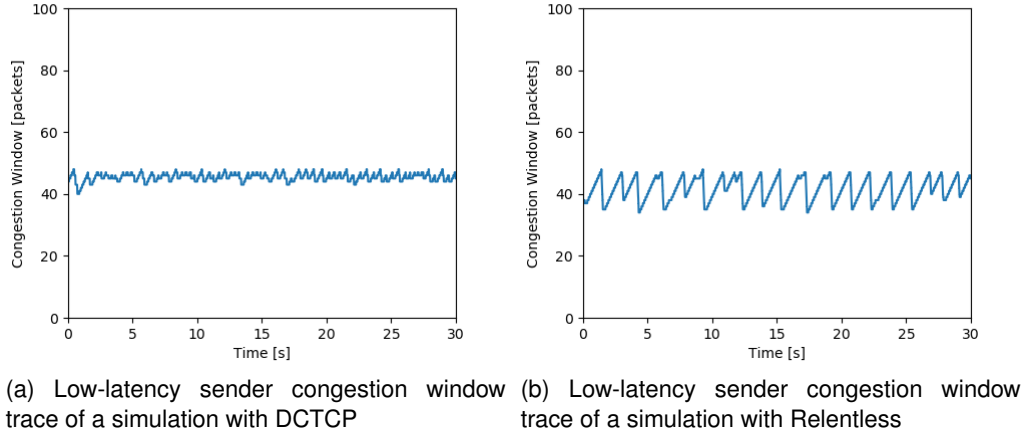


Figure 4.8: Comparison of the congestion windows of DCTCP and Relentless from our Dual Queue Uncoupled RED simulations

the congestion window trace of Relentless is much less smooth than the one of DCTCP.

When scalable congestion control was used on the low-latency flows, the choice of classic congestion control on the classic flows did not have a significant effect on the low-latency delays or the fairness.

This makes sense since these congestion controls were only used to control the classic queue which is kept at a high filling level anyway.

Figure 4.9 shows the resulting metrics for simulations with Dual Queue Uncoupled AQM across all available TCP settings when using classic congestion controls on the low-latency flows. Figure 4.10 shows the same for when using scalable congestion controls on the low-latency flows. These plots should visualize influence of the TCP settings. We chose the results from the simulations with 5 low-latency and 5 classic flows as examples. The results from the simulations with other flow configurations showed similar effects.

4.2.3 DualQ Coupled AQM

In our simulations, DualQ Coupled AQM achieved very low delays in the L4S queue. The average L4S queue delays were between 1.0 and 3.1 milliseconds for CRED, between 1.7 and 3.3 milliseconds for PI2 and between 1.1 and 2.1 milliseconds for PIE. The maximum L4S queue delays were between 4.5 and 19 milliseconds for CRED, between 10 and 35 milliseconds for PI2 and between 4.5 and 14 milliseconds for PIE.

While all implementations achieved similarly low average L4S queue delays. The PI2 implementation tended to reach higher maximum L4S queue delays. We think this is due to the scheduler. While the scheduler for CRED and PIE were strict priority schedulers, PI2 used a shifted FIFO scheduler (See Sections 2.4.2 and 3.1.3). With this non-strict priority scheduler, the L4S queue could sometimes loose its priority leading to higher maximum delays.

The classic queue delays in the DualQ Coupled AQM simulations were lower than the ones in the Dual Queue Uncoupled AQM simulations.

The average classic queue delays were between 7.6 and 86 milliseconds for CRED, between 15 and 19 milliseconds for PIE and between 16 and 36 milliseconds for PIE. The maximum classic queue delays were between 37 and 350 milliseconds for CRED, between 39 and 62 milliseconds for PIE and between 50 and 325 milliseconds for PIE.

Note again that, the CRED and PIE implementations reached similar delays in the classic queue but the PI2 implementation did not. Like for the L4S queue delays, we think the reason for this was the non-strict priority scheduling of PI2 that sometimes suspended the priority of the L4S queue.

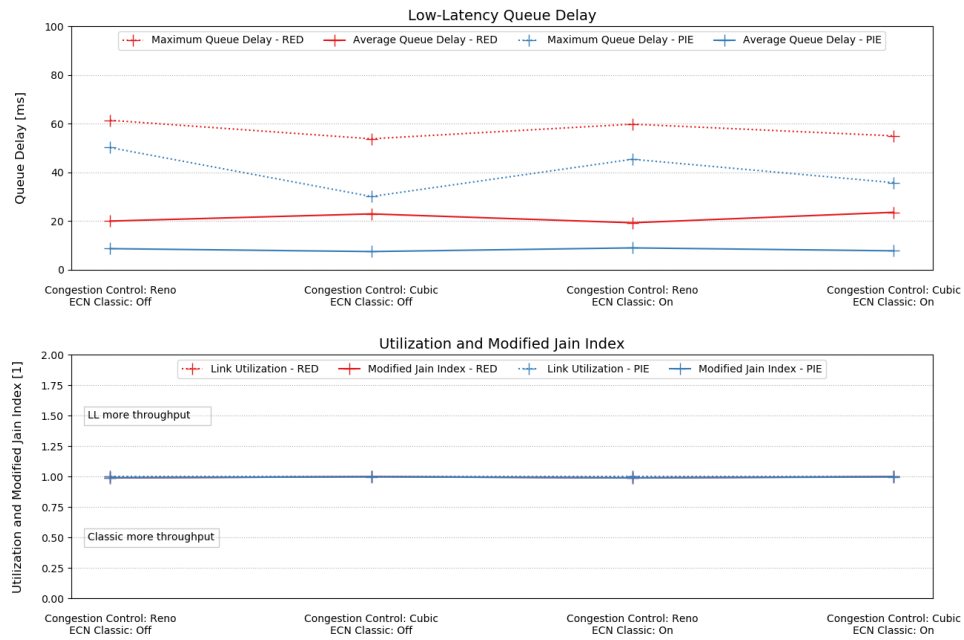


Figure 4.9: Average and maximum queue delays, link utilization and modified Jain index over all available TCP settings for the Dual Queue Uncoupled AQM simulations with 5 low-latency and 5 classic flows when using classic congestion control on all flows

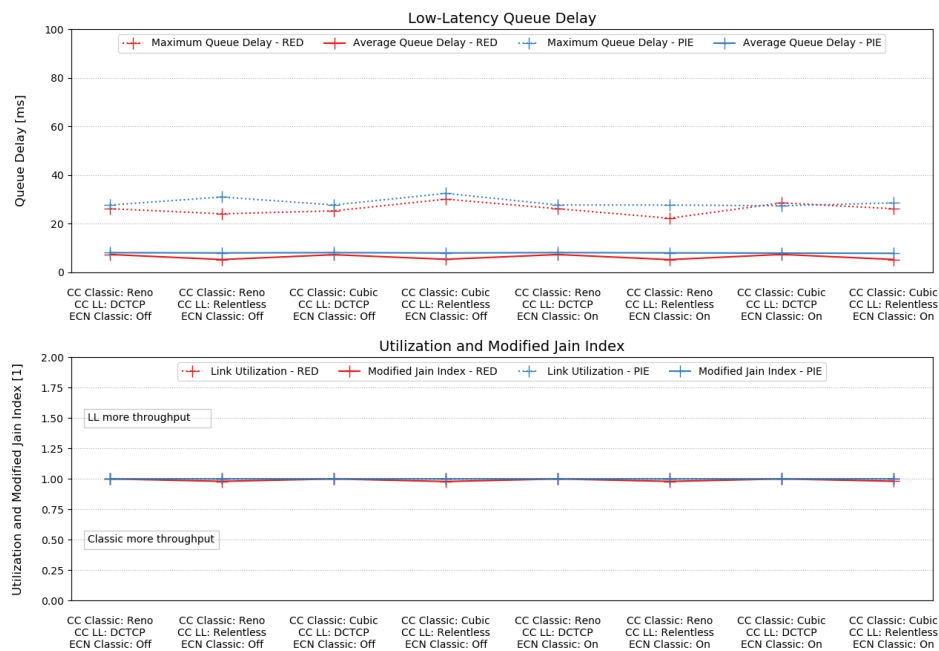


Figure 4.10: Average and maximum queue delays, link utilization and modified Jain index over all available TCP settings for the Dual Queue Uncoupled AQM simulations with 5 low-latency and 5 classic flows when using scalable congestion control on low-latency flows on low-latency flows

Classic Congestion Control	Flow Combination [L4S Flows : Classic Flows]								
	1:1	1:5	1:10	5:1	5:5	5:10	10:1	10:5	10:10
Cubic	39	49	54	43	48	50	48	45	47
Reno	41	56	61	44	54	60	50	54	61

Table 4.1: Maximum classic queue delay in milliseconds from the DualQ Coupled PI2 simulations using DCTCP and activating ECN on the classic flows

In the simulations, DualQ Coupled AQM experienced losses of link utilization up to 12%. The highest link utilization was generally achieved by CRED, followed by PI2 and PIE.

The highest losses were seen when there was only one classic flow. This makes sense since with only one flow, the AQM is most likely to cause the classic queue to run empty.

All implementations experienced some problems in terms of fairness.

In a lot of cases, the L4S queue achieved less throughput than the classic queue. We think, one general reason for this is the choice of the factor K that scales the drop probabilities in the coupling. [26] recommends 2 since multiplication and division by powers of 2 is cheaply implementable using bit shifts. But according to the throughput equations described in Section 2.2.3, the scaling factor with DCTCP should be 1.22 for Reno and 1.68 for Cubic. This puts the L4S queue at a disadvantage.

And like with Single Queue RED, ECN unfairness occurred with the CRED implementation.

Influence of Flow Counts

With increasing L4S flow counts, all implementations encountered increasing L4S queue delays.

In the PIE and CRED implementations, the L4S queue delays tended to decrease with increasing classic flow counts. We think, the reason for this is that the AQM which depended on the classic queue had to work more aggressively for more flows leading to tighter control on the L4S queue.

In the PI2 implementation, the L4S queue delays tended to increase with the classic flow count. We also saw that more classic flows also increased the maximum classic queue delay. We think, this caused the L4S queue to loose the priority more often since DualQ Coupled PI2 used a shifted FIFO scheduler.

Table 4.1 shows the maximum classic queue delays from the the simulations with DualQ Coupled PI2 when DCTCP was used on the L4S flows and ECN was activated on the classic flows. DCTCP and activated ECN was chosen as an example. The maximum classic queue delays were similar when using Relentless or when deactivating ECN on the classic flows. In can be seen that the maximum classic queue delay increases with the classic flow count.

For unbalanced flow counts, the fairness tended to decrease at the expense of the class with more flows. For CRED, this effect was seen the least. It was seen a bit stronger for PI2 and strongest for PIE.

Also, ECN unfairness became more severe with increasing classic flow counts. Like in Single Queue RED, we think this comes from increasing size and frequency of spikes in the classic queue length. These spikes would cause the queue delay to exceed the slope factor (See Section 2.3.2). In that case, the drop probability would be 100% leading to more severe ECN unfairness.

Figures 4.11 and 4.12 show the resulting metrics from simulations with DualQ Coupled across all flow count combinations. These plots should visualize the influence of the flow counts. We chose the results from the simulations with DCTCP and Cubic as examples. The results from

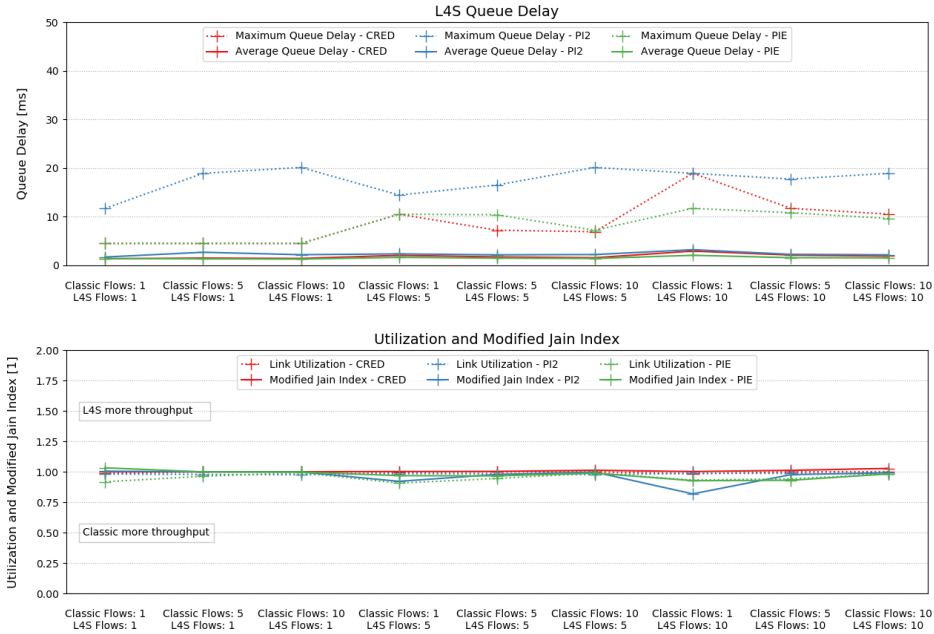


Figure 4.11: Average and maximum queue delays, link utilization and modified Jain index over all flow count combinations for the DualQ Coupled AQM simulations using DCTCP on L4S flows, Cubic on classic flows and activating ECN on the classic flows

the simulations with other congestion controls showed similar effects.

Influence of TCP Settings

When ECN was deactivated on the classic links, the implementations with CRED encountered ECN unfairness (See Section 2.1).

In PI2 and for larger classic flow counts, using Cubic instead of Reno on the classic flows tended to result in lower maximum L4S queue delays. We saw that in these cases, the maximum classic queue delay was also lower. And since the PI2 implementations uses a shifted FIFO scheduler, we assume that the L4S queue less often lost the priority when classic queue delays were lower.

We think the reason for the lower classic queue delays was the same as in Single Queue and Dual Queue Uncoupled AQM cases.

Table 4.1 shows the maximum classic queue delays from the the simulations with DualQ Coupled PI2 when DCTCP was used on the L4S flows and ECN was activated on the classic flows. DCTCP and activated ECN was chosen as an example. The maximum classic queue delays were similar when using Relentless or when deactivating ECN on the classic flows.

Just as for Dual Queue Uncoupled AQM, Relentless also achieved lower delays than DCTCP. But Relentless also gave up more throughput. Like in the Dual Queue Uncoupled AQM cases, we think that the reason is the lack of a smoothing function leading to large fluctuations in the congestion window.

Figures 4.13a and 4.13b show examples of low-latency sender congestion window traces from our DualQ Coupled PI2 simulations using DCTCP and Relentless. It can be seen that the congestion window trace of DCTCP is smoother than the one of Relentless.

Figure 4.14 shows the resulting metrics from simulations with DualQ Coupled AQM across all available TCP settings. These plots should visualize the influence of the TCP settings. We

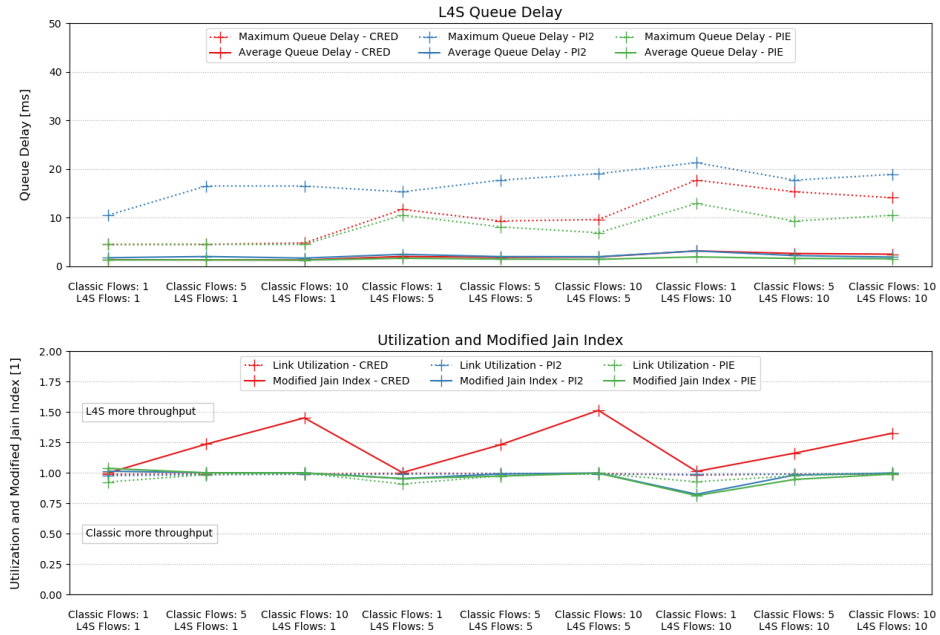


Figure 4.12: Average and maximum queue delays, link utilization and modified Jain index over all flow count combinations for the DualQ Coupled AQM simulations using DCTCP on L4S flows, Cubic on classic flows and deactivating ECN on the classic flows

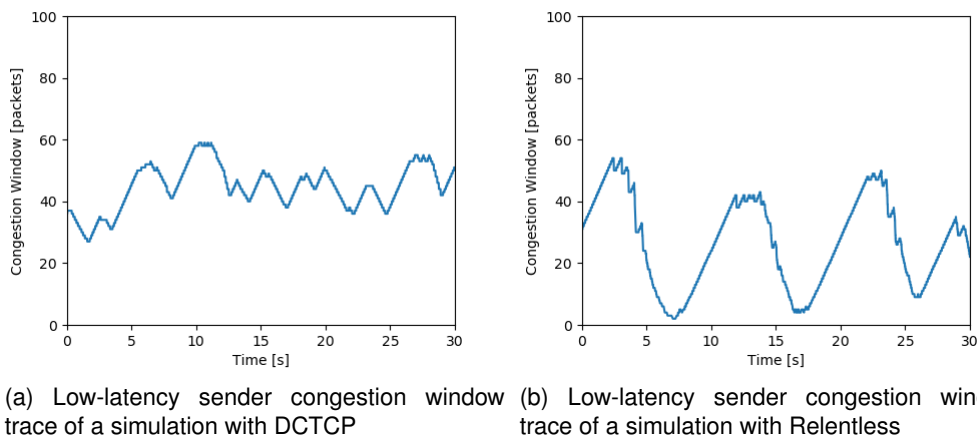


Figure 4.13: Comparison of the congestion windows of DCTCP and Relentless from our DualQ Coupled PI2 simulations

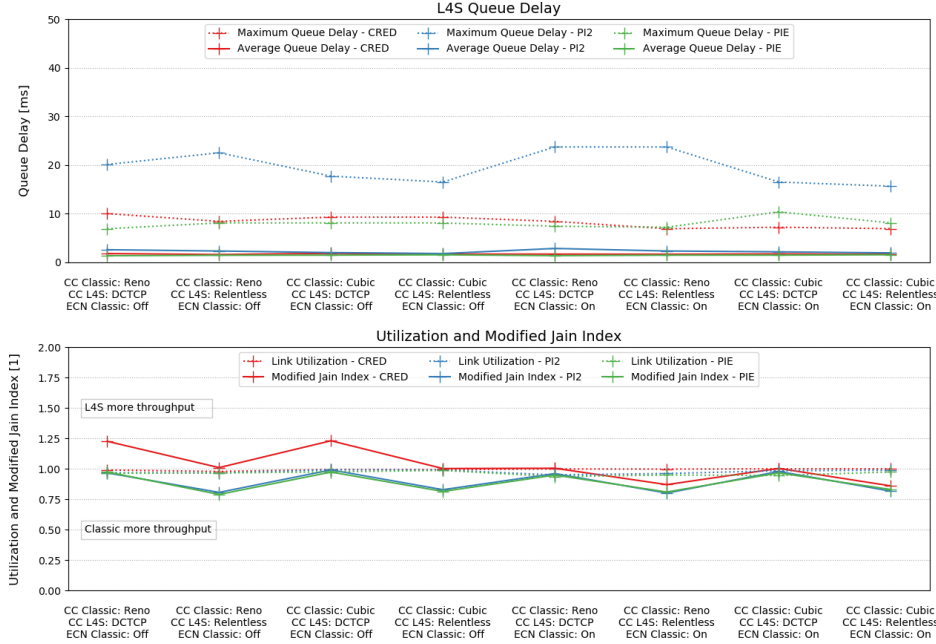


Figure 4.14: Average and maximum queue delays, link utilization and modified Jain index over all available TCP settings for the DualQ Coupled AQM simulations with 5 low-latency and 5 classic flows

chose the results from the simulations with 5 low-latency and 5 classic flows as an example. The results from the simulations with other flow configurations showed similar effects.

4.2.4 Comparison

In our simulations we saw that Single Queue AQM could reach a low target delay only for low flow counts. And by trying to achieve a low delay, they sacrificed link utilization. Also, the ECN unfairness that was discovered, poses a problem for the use of ECN in Single Queue RED.

Dual Queue Uncoupled AQM also often exceeded the target delay when using classic congestion control on the low-latency flows. Compared to the Single Queue AQM, Dual Queue Uncoupled AQM in some cases even had higher delays, especially in cases with more classic than low-latency flows. As stated above, we think this is an inherent problem of the scheduler. Switching to scalable congestion control reduced the delays in Dual Queue Uncoupled AQM, especially for the RED implementation. But in cases with more classic than low-latency flows, the problem with the scheduler persisted.

The delays of the classic queue were quite high, in the order of hundreds and sometimes thousands of milliseconds. This was to be expected due to the design of Dual Queue Uncoupled AQM.

But, unlike the Single Queue AQM, Dual Queue Uncoupled AQM achieved almost full link utilization. Here, the problem concerning throughput was the fairness. Like in the Single Queue AQM, once the low-latency queue achieved a lower delay, it had to give up throughput. This throughput was absorbed by the classic queue and lead to unfairness.

Some scalable congestions control partially solved this problem as they should (See Section 2.2.3). With DCTCP, the bandwidth allocation was quite fair in all cases. Relentless also achieved a quite fair allocation with PIE. But with RED, Relentless in some cases even deteriorated the fairness.

The DualQ Coupled implementations were able to achieve very low L4S queue delays. Its L4S queue delays were lower than the delays in Single Queue AQM or the low-latency queue delays in Dual Queue Uncoupled AQM. Also, the delays of the classic queue were lower in DualQ Coupled AQM than the ones in Dual Queue Uncoupled AQM.

But DualQ Coupled AQM had to sacrifice link utilization, unlike Dual Queue Uncoupled AQM. And like in the Single Queue RED, the ECN unfairness spotted in DualQ Coupled CRED poses a problem for the use of ECN. But unlike in Single Queue AQM, the use of ECN is necessary for DualQ Coupled AQM.

4.3 LTE Link Simulations

In this section we discuss the results from the simulations in the LTE network. Due to implementation restrictions, a proportional fair scheduler was used on all implementations with two queues. Since DualQ Coupled AQM requires a priority scheduler, the significance of its results in these simulations are limited.

Due to time constraints, our knowledge of this scheduler is limited to the general idea. We did not have time to look into the implementation in the LTE model of NS-3 [3].

Also, the bandwidth of the congested link was defined by the LTE model. We saw that this bandwidth was 17.53 megabits per second.

In the following passages, we only use examples to visualize our findings. The full data and all plots can be found in Appendices A.2 and B.2.

4.3.1 Single Queue AQM

The the Single Queue AQM implementation in some cases achieved the target delay. The average delays were between 5.1 and 8.5 milliseconds for PIE and between 5.4 and 9.8 milliseconds for RED. The maximum delays were 18 and 46 for PIE and between 11 and 34 for RED.

Compared to the static link simulations, PIE achieved similar delays in both networks. RED achieved lower delays in the LTE network than in the static link network. We think the reason for this is that due to the higher bandwidth, the target delay is easier to keep since the serialization time of a packet decreases.

But due to these low delays, the link was often underutilized due to the queue running empty. Here, the losses were larger than in the static link network. PIE suffered losses up to 34% and RED up to 64%.

Like in the static link network, the bandwidth was shared fairly in most cases with the exception of ECN unfairness in RED (See Section 2.1).

Influence of Flow Counts

In the simulations with PIE, the flow counts did not show any clear influence on the queue delays. In the ones with RED, the delays tended to increase with the number of flows.

The utilization tended to increase with the flow counts, especially when increasing from two to six flows.

The Figures 4.15 and 4.16 show the resulting metrics from simulations with Single Queue AQM across all flow count combinations. These plots should visualize the influence of the flow counts. We chose the results from the simulations with Cubic as examples. The results from the simulations with Reno showed similar effects.

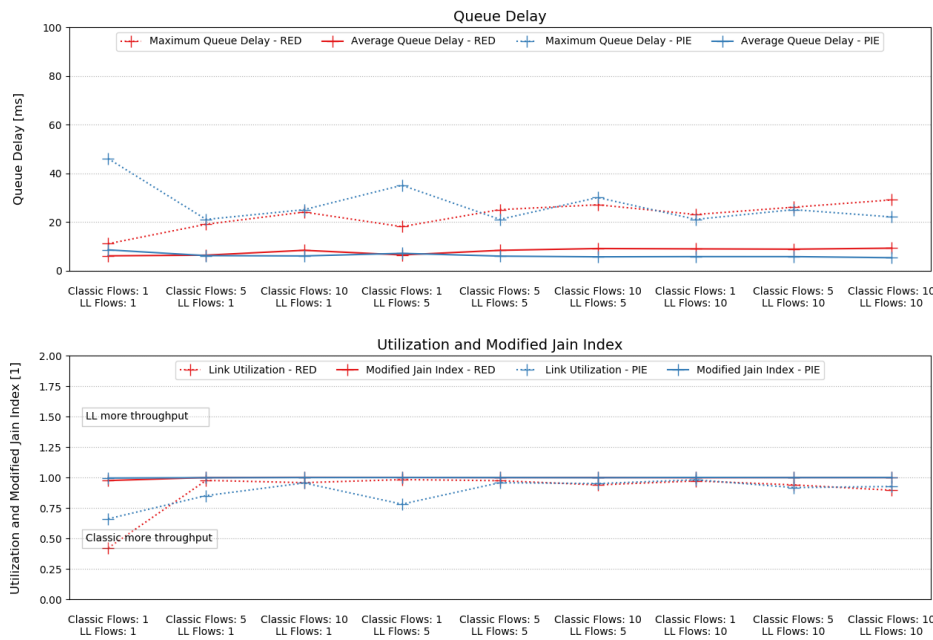


Figure 4.15: Average and maximum queue delays, link utilization and modified Jain index over all flow count combinations for the Single Queue AQM simulations using Cubic on all flows and activating ECN on the classic flows

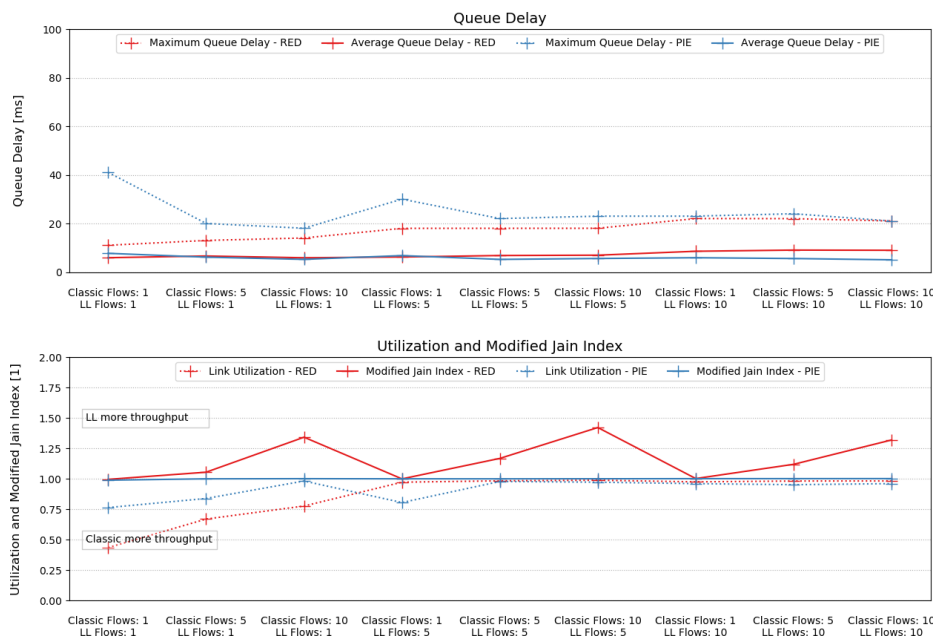


Figure 4.16: Average and maximum queue delays, link utilization and modified Jain index over all flow count combinations for the Single Queue AQM simulations using Cubic on all flows and deactivating ECN on the classic flows

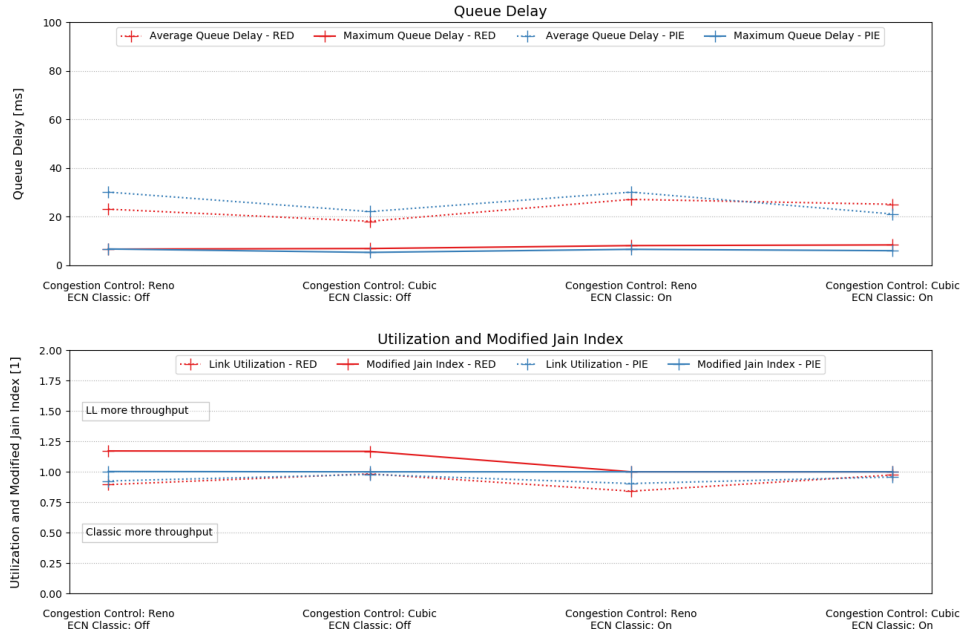


Figure 4.17: Average and maximum queue delays, link utilization and modified Jain index over all available TCP settings for the Single Queue AQM simulations with 5 low-latency and 5 classic flows

Influence of TCP Settings

Like in the static link network, deactivating ECN on the classic link lead to ECN unfairness. Activating ECN also lead to an increase in maximum queue delay. Like in the static link network, we think this is because unlike dropped packets, marked packets were enqueued anyway, adding to the queue size and delay.

Figure 4.17 shows the resulting metrics from simulations with Single Queue AQM across all available TCP settings. These plots should visualize the influence of the TCP settings. We chose the results from the simulations with 5 low-latency and 5 classic flows as an example. The results from the simulations with other flow configurations showed similar effects.

4.3.2 Dual Queue Uncoupled AQM

The results from these simulations differed from the simulations in the static link network. We assume, the reason for this is that here a the proportional fair scheduler was used instead of a weighted round robin.

Here, Dual Queue Uncoupled PIE very often achieved the target delay in the low-latency queue, independent from the use of classic or scalable congestion control on the low-latency flows. With classic congestion control, PIE achieved an average low-latency queue delays between 5.0 and 6.6 milliseconds and with scalable congestion control between 4.8 and 5.9 milliseconds. The main difference between scalable and classic congestion control for the PIE implementation was in the maximum low-latency queue delay. It decreased from between 23 and 50 milliseconds to between 8 and 34 milliseconds when scalable congestion control was used.

With the RED implementations, the target delay was only achieved in a few specific flow combinations. Furthermore, the average low-latency queue delay tended to be larger for scalable congestion control having been between 1.2 and 19 milliseconds for classic and

between 1.3 and 30 milliseconds for scalable congestion control. The use of scalable or classic congestion control had no significant impact on the maximum low-latency queue delay.

Like in the static link network simulations, the classic queue delays were in the order of hundreds of milliseconds. But again, this comes by design.

Compared to the static link network simulations, Dual Queue Uncoupled AQM tended to achieve lower delays. We think, there are two reasons for this. First, as in the Single Queue AQM case, the total bandwidth was higher so the transmission time per packet went down. Second, it seems like the scheduler assigned disproportionately much throughput to one traffic class if it had less flows than the other. We think, this leads to shorter dequeuing intervals.

As in the static link model, Dual Queue Uncoupled AQM achieved almost always full link utilization. The fairness depended on the flow counts.

Influence of Flow Counts

The main observation concerning flow counts was, that the proportional fair scheduler (See 2.5.2) assigned disproportionately much throughput to one traffic class if it has less flows than the other.

This leads to a number of other effects.

First, the low-latency queue delays in RED depended on the ratio between the low-latency and the classic flow count. If there were more classic than low-latency flows, the delays were lower. And if there were more low-latency than classic flows, the delays were higher.

We think, the reason for this are the RED parameters and the scheduler. The thresholds of RED were set using base values that were scaled according to the expected throughput (See Section 3.1.2). And the expected throughput was calculated assuming a fair distribution.

In case of more classic than low-latency flows, the scheduler assigned more throughput to the low-latency class than expected. Therefore, the thresholds were set too low, leading to a low delay. In case of more low-latency than classic flows, the scheduler assigned less throughput to the low-latency class than expected. In this case, the thresholds were set too high, leading to high delays.

This is an implementation error, raising the question how significant the results of the simulations with Dual Queue Uncoupled RED are.

Of course, this disproportionate assignment of throughput also lead to unfairness in favour of the class with less flows.

And as in the static link network simulations, Dual Queue Uncoupled AQM achieved almost full link utilization.

The low-latency queue delays of the PIE implementation were not affected by the disproportionate bandwidth distribution, since the PIE takes the target delay itself as a parameter.

Figure 4.18 shows the resulting metrics from simulations with Dual Queue Uncoupled AQM across all flow count combinations when using classic congestion controls on the low-latency flows. Figure 4.19 shows the same for when using scalable congestion controls on the low-latency flows. These plots should visualize the influence of the flow counts. We chose the results from the simulations with Cubic, DCTCP and ECN activated on classic flows as examples. The results from the simulations with other congestion controls or ECN deactivated on classic flows showed similar effects.

Influence of TCP Settings

In the case where scalable congestion control was used on the low-latency link, we saw some differences between Relentless and DCTCP.

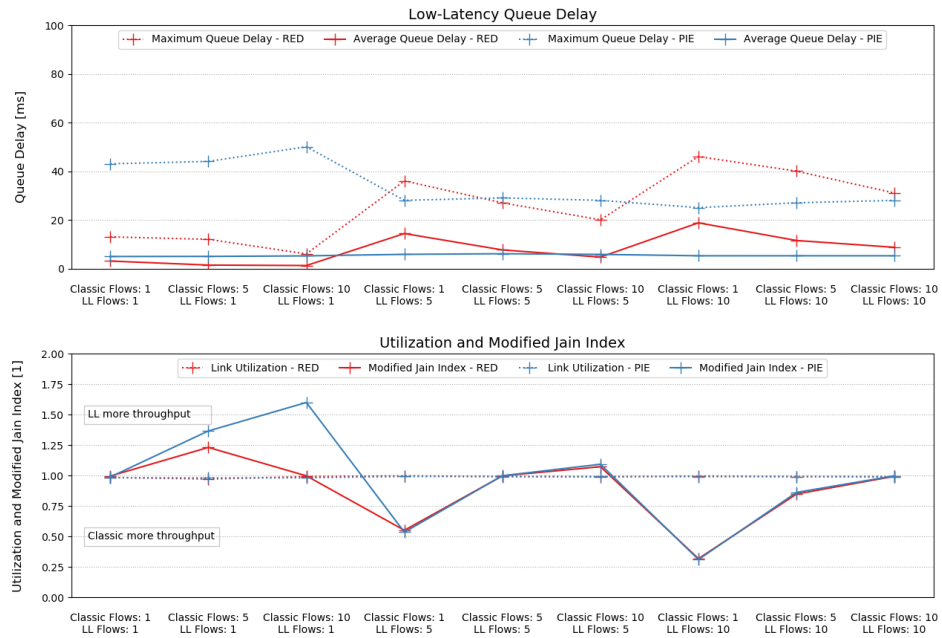


Figure 4.18: Average and maximum queue delays, link utilization and modified Jain index over all flow count combinations for the Dual Queue Uncoupled AQM simulations using Cubic on all flows and activating ECN on the classic flows

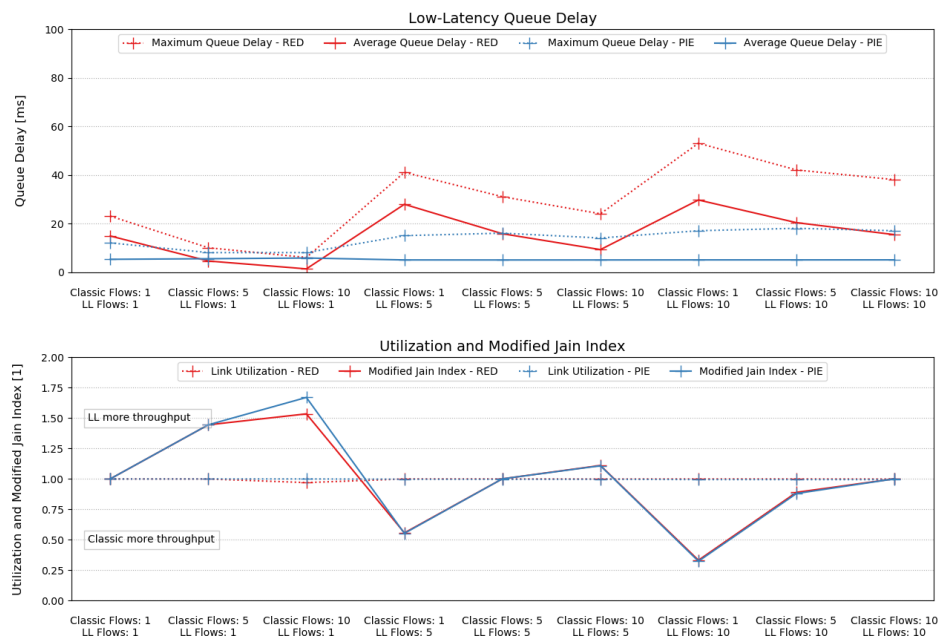


Figure 4.19: Average and maximum queue delays, link utilization and modified Jain index over all flow count combinations for the Dual Queue Uncoupled AQM simulations using DCTCP on low-latency flows, Cubic on classic flows and activating ECN on the classic flows

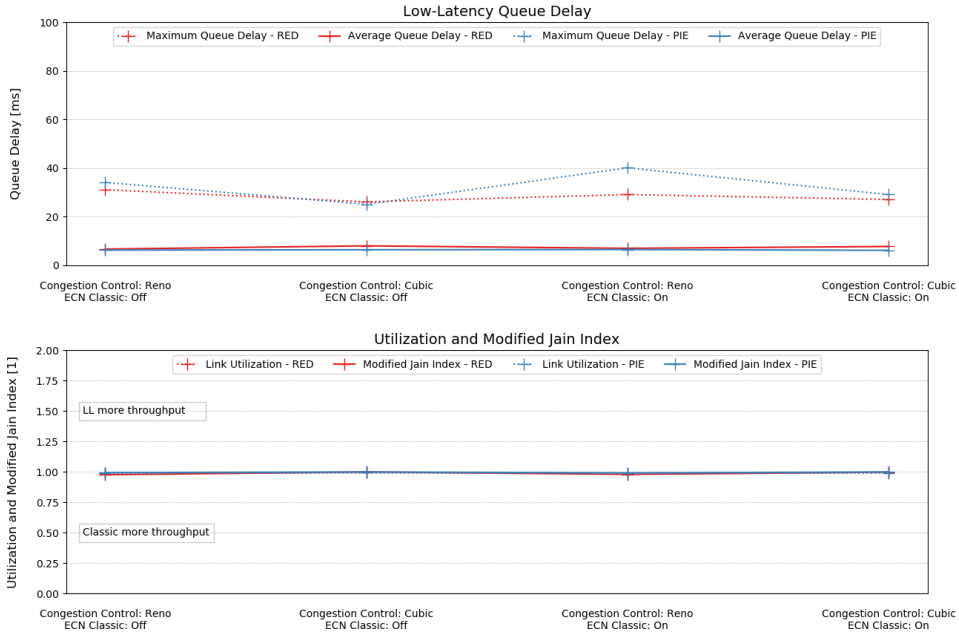


Figure 4.20: Average and maximum queue delays, link utilization and modified Jain index over all available TCP settings for the Dual Queue Uncoupled AQM simulations with 5 low-latency and 5 classic flows when using classic congestion control on all flows

For PIE, Relentless tended to lead to higher maximum low-latency queue delays than DCTCP. But we saw no difference in the average low-latency queue delay or the throughput between DCTCP and Relentless.

For RED, the low-latency class tended to achieve a lower average delay with Relentless than with DCTCP. At the same time, Relentless often also caused the low-latency class to give up more throughput.

We assume, the reasons for this are the same as in the static link model.

Figure 4.20 shows the resulting metrics from simulations with Dual Queue Uncoupled AQM across all available TCP settings when using classic congestion control on the low-latency flows. Figure 4.21 shows the same for when using scalable congestion control on the low-latency flows. These plots should visualize the influence of the TCP settings. We chose the results from the simulations with 5 low-latency and 5 classic flows as examples. The results from the simulations with other flow configurations showed similar effects.

4.3.3 DualQ Coupled AQM

In the simulations with the DualQ Coupled AQM, we saw that DualQ Coupled AQM definitely requires priority scheduling.

DualQ Coupled PIE achieved very low average L4S queue delays between 1.1 and 3.5 milliseconds and maximum delays between 4 and 20 milliseconds.

But this often lead to underutilization of the link with losses going up to 25%. Since the L4S queue had to give up throughput in order to achieve the low delay, the classic queue would have had to absorb it. Since the classic queue is also controlled by PIE, this was not always possible. The utilization mainly increased for higher classic flow counts. We think, this is because then the classic queue would run empty less often.

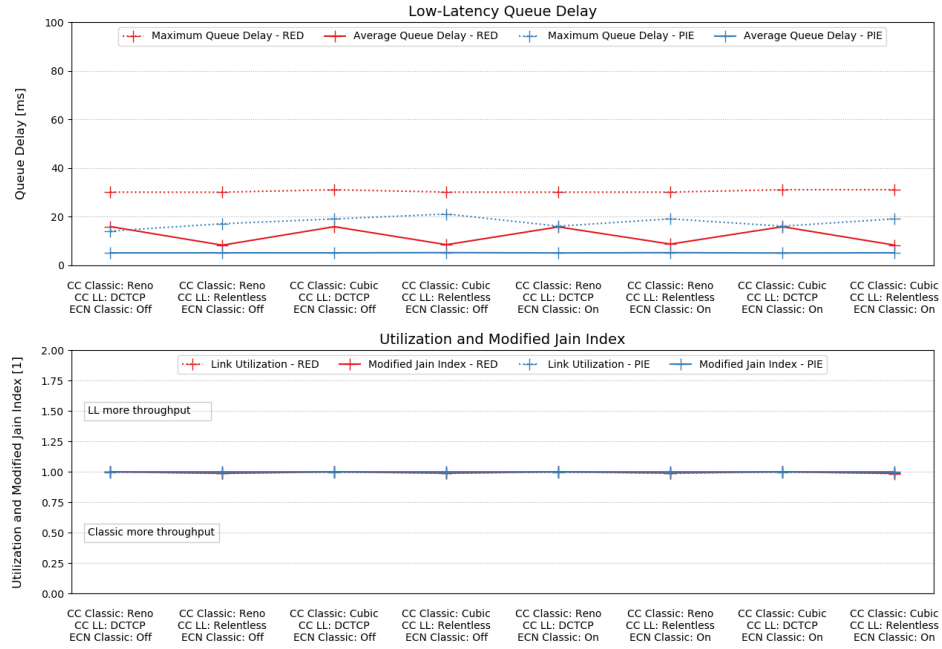


Figure 4.21: Average and maximum queue delays, link utilization and modified Jain index over all available TCP settings for the Dual Queue Uncoupled AQM simulations with 5 low-latency and 5 classic flows when using scalable congestion control on low-latency flows and classic congestion control on low-latency flows

Also here, the scheduler assigned disproportionately much throughput to the traffic class with fewer flows. Since the L4S queue was at a fundamental disadvantage, the classic queue always achieved a higher per-flow-throughput.

Figure 4.22 shows resulting metrics from simulations with DualQ Coupled AQM across all flow count combinations. These plots should visualize the influence of the flow counts. We chose the results from the simulations with DCTCP, Cubic and ECN activated on the classic flows as examples. The results from the simulations with other congestion controls or deactivated ECN on the classic flows showed similar effects.

The classic queue achieved average delays between 9.7 and 20 milliseconds and maximum delays between 38 and 88 milliseconds.

Like in the static link network simulations, DCTCP achieved higher throughputs than Relentless without any significant change in the low-latency queue delays. We think the reason for this is the same as in the static link network.

Figure 4.23 shows the resulting metrics from simulations with DualQ Coupled AQM across all available TCP settings. These plots should visualize the influence of the TCP settings. We chose the results from the simulations with 5 low-latency and 5 classic flows as an example. The results from the simulations with other flow configurations showed similar effects.

4.3.4 Comparison

We saw that the Single Queue AQM still could not achieve the target delay for higher flow counts. And it lost utilization when low delays were achieved.

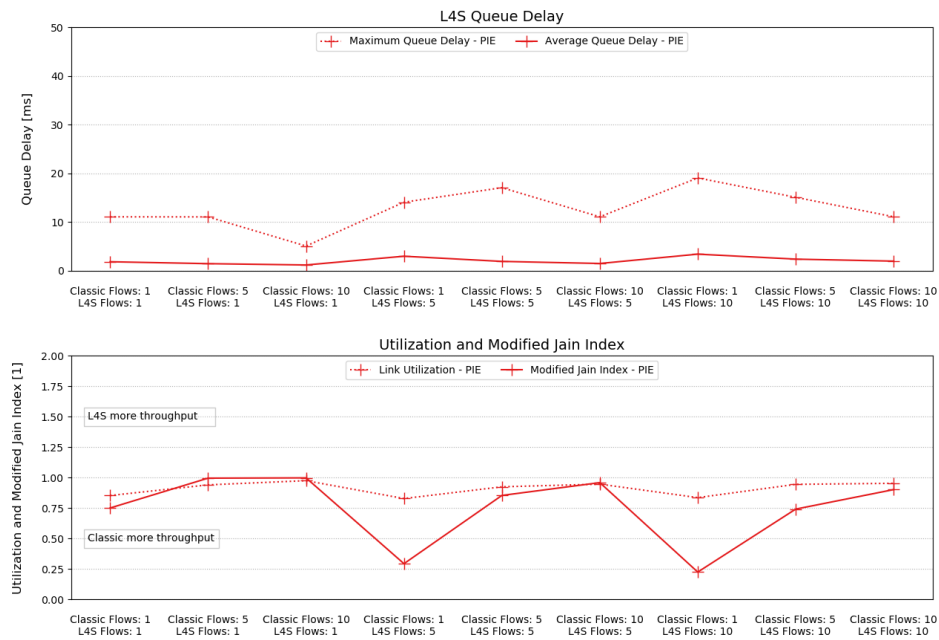


Figure 4.22: Average and maximum queue delays, link utilization and modified Jain index over all flow count combinations for the DualQ Coupled AQM simulations using DCTCP on L4S flows, Cubic on classic flows and activating ECN on the classic flows

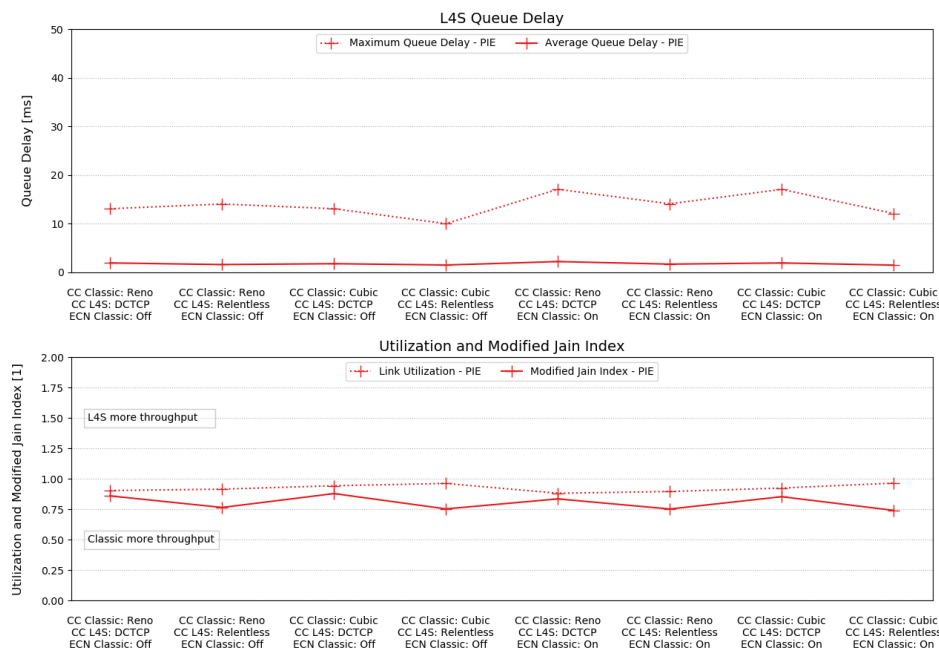


Figure 4.23: Average and maximum queue delays, link utilization and modified Jain index over all available TCP settings for the DualQ Coupled AQM simulations with 5 low-latency and 5 classic flows

In these simulations, Dual Queue Uncoupled PIE achieved the target delay without trading away a high link utilization. The use of scalable instead of classic congestion control, lead to a significant decrease in maximum low-latency queue delay. The average low-latency delay was more or less unchanged.

Dual Queue Uncoupled RED only achieved the target delay for certain flow combinations because of an implementation error.

DualQ Coupled AQM achieved low L4S queue delays but had to give up a lot of throughput to do so.

4.4 Conclusion

4.4.1 AQM Schemes

In our simulations we saw that the Single Queue AQM implementations had limits concerning achievable delays and link utilization. Low target delays could only be achieved in cases with very few flows. For higher numbers of flows, the available queue size corresponding to the delay seemed to be too small for AQM schemes to work on.

Also, low delays came at the cost of link utilization. This is a known problem described in Section 2.2.3.

Compared to the Single Queue AQM, Dual Queue Uncoupled AQM implementations were able to achieve full link utilization while trying to achieve low delays in the low-latency queue. Concerning delays, we saw that the scheduling of the two queues could cause problems. In the static link network simulations, where we used a weighted round robin scheduler, this scheduler lead to increased delays when there were much more classic than low-latency flows. In the LTE network simulations, where a proportional fair scheduler had to be used, this problem was alleviated at the cost of fairness. Other schedulers might further improve the performance of this algorithm. Depending on the requirements, this could be seen as a better performance.

The Dual Queue Uncoupled AQM approach also allowed the use of scalable congestion control. While a high link utilization was given by design, using classic congestion controls often lead to the low-latency queue having to give up assigned throughput because it ran empty (See Section 2.2.3). Using an elaborate scalable congestion control algorithm like DCTCP allowed the low-latency queue to fully use the assigned throughput in most cases. The less elaborate Relentless algorithm on the other hand, in some cases even deteriorated the fairness further.

In order to achieve full link utilization, the classic queue was kept full at all times. In some cases, this lead to massive classic queue delays in the order of hundreds or thousands of milliseconds. We think, this something that should be taken into consideration.

The DualQ Coupled AQM implementations were able to achieve very low delays. In the LTE network simulations, we saw that the priority scheduling is a very important part of this algorithm. Here, we had to use a proportional fair scheduler which caused the L4S queue to give up a lot of throughput while trying to achieve the low delay.

DualQ Coupled AQM also lost utilization when the classic queue was running empty. Possibly, this could be solved by increasing the target delays used in the AQM schemes.

Unlike with Dual Queue Uncoupled AQM, the average classic queue delays with DualQ Coupled AQM stayed below 100 milliseconds and the maximum classic queue delays all stayed below 350 milliseconds. This might be an advantage over Dual Queue Uncoupled AQM.

4.4.2 TCP Settings

For Single Queue AQM and Dual Queue Uncoupled AQM, we ran simulations using the classic congestion controls Cubic and Reno. In these simulations we saw that in most cases, Cubic achieved lower maximum delays and higher throughput than Reno.

For Dual Queue Uncoupled and DualQ Coupled AQM, we ran simulations using the scalable congestion controls DCTCP and Relentless. We saw that Relentless often achieved lower lower delays than DCTCP. At the same time, DCTCP achieved higher throughput than Relentless.

The main influence of turning on ECN on the classic flows or not were the occurrences of ECN unfairness. Aside from that, ECN caused an increase in maximum queue delays for Single Queue AQM.

Chapter 5

Summary and Outlook

5.1 Summary

In this work, we wanted to evaluate the performance of AQM schemes that can be used in the internet. We wanted to find out which algorithms can achieve very low queuing delays in order to serve the low-latency requirement that an increasing amount of applications and traffic has today. Furthermore, we wanted to see what concessions have to be made in order to achieve these low delays.

In order to answer these questions, we implemented different AQM algorithms for the network simulator NS-3 and ran simulations. Based on the results from these simulations, we evaluated the performance of the algorithms. For the first simulations we were using a static link model, simulating a wired network. In the second, we used an LTE link model. This should give insight into how these algorithms perform in wired and in mobile networks.

We implemented three algorithms.

The first algorithm used a single queue, controlled by a traditional AQM scheme.

The second algorithm was the DualQ Coupled AQM algorithm from [26]. It uses two queues to separate traffic based on whether they seek low latency or not. The queue of the low-latency traffic is scheduled with priority. A traditional AQM schemes is used for controlling the two queues with a coupling between them.

The third algorithm was a simplification of DualQ Coupled AQM. It also separates the traffic into two queues. Both queues run independent instances of a traditional AQM but with different target delays. The two queues are scheduled by a weighted round robin scheduler.

In our static link network simulations, we saw that the algorithms using a single queue often failed to achieve a low delay and that they lost link utilization by trying.

The simplification of DualQ Coupled AQM also often failed to achieve the low target delay. But this implementation always achieved full link utilization due to its design.

DualQ Coupled AQM achieved very low delays. But this algorithm sometimes also lost link utilization.

Our LTE network simulations were hindered by implementation issues. The DualQ Coupled AQM algorithm could not be implemented with priority scheduling. We therefore had to use a proportional fair scheduler. For the simplification of DualQ Coupled AQM, we also had to use a proportional fair scheduler.

These simulations also showed that the algorithms with a single queue often failed to keep a low target delay. And that trying to achieve it lead to underutilization of the link.

Here, DualQ Coupled also achieved very low delays but the low latency seeking traffic only achieved little throughput. this is probably due to the lack of priority scheduling.

And the simplification of DualQ Coupled AQM was in most cases able to achieve the low target delay which came in some cases at the cost of fairness but without loss of link utilization.

5.2 Outlook

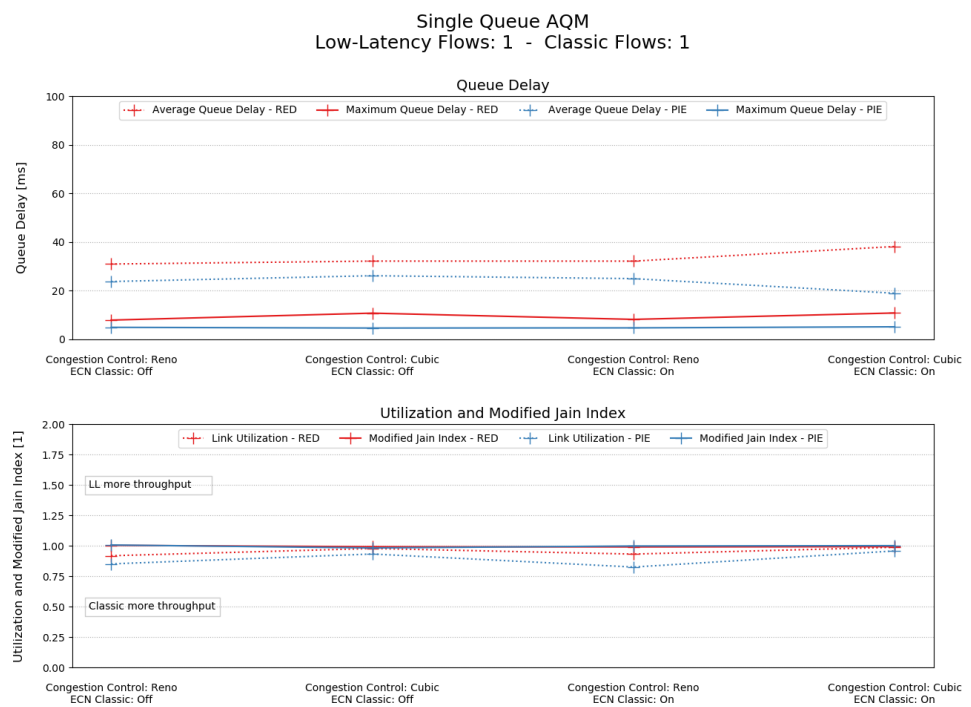
In the future, the DualQ Coupled AQM algorithm from [26] could be correctly implemented for the LTE module of NS-3. This could show whether the low delays achieved using the static link model can also be achieved in a mobile environment.

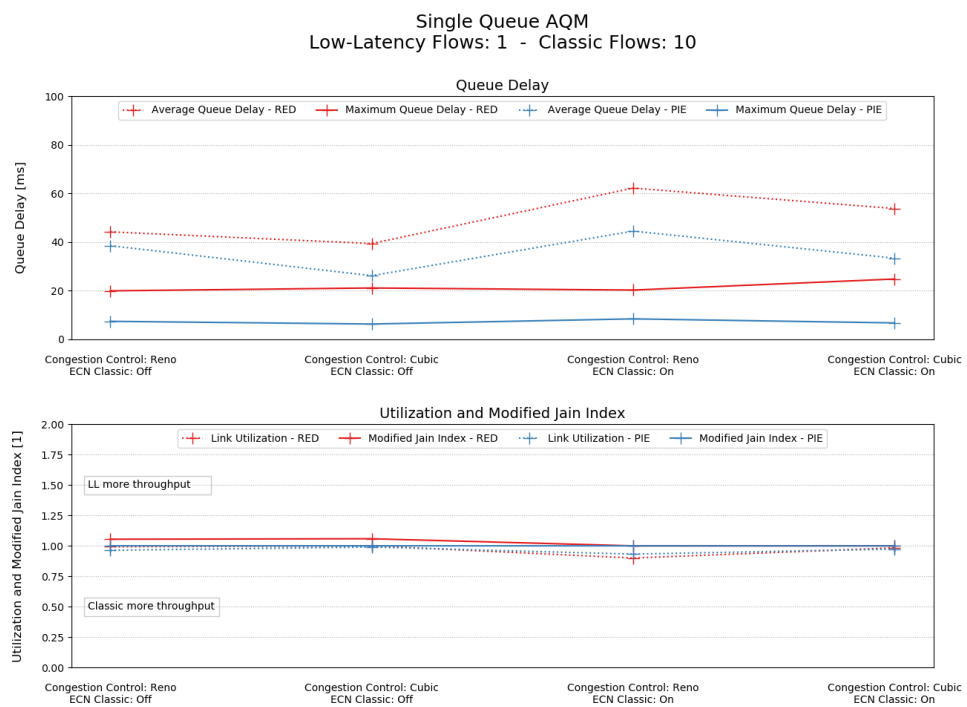
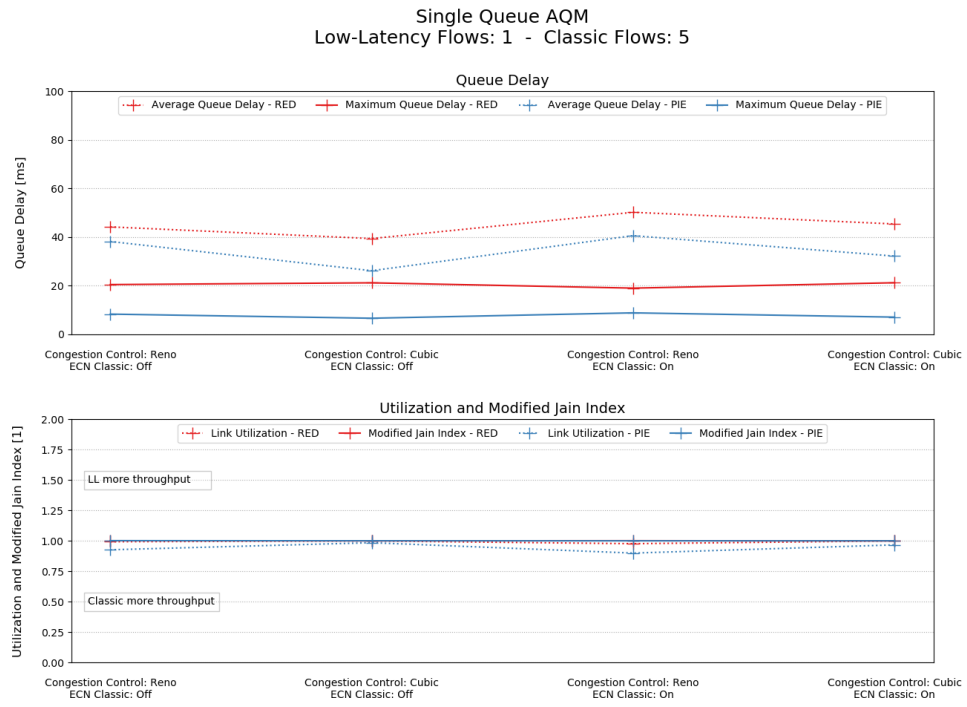
Also, Dual Queue Uncoupled AQM could be implemented with another scheduler than a weighted round robin. Since the simulations in the LTE network with a proportional fair scheduler resulted in lower delays, changing the scheduler could also lead to lower delays when using the static link model.

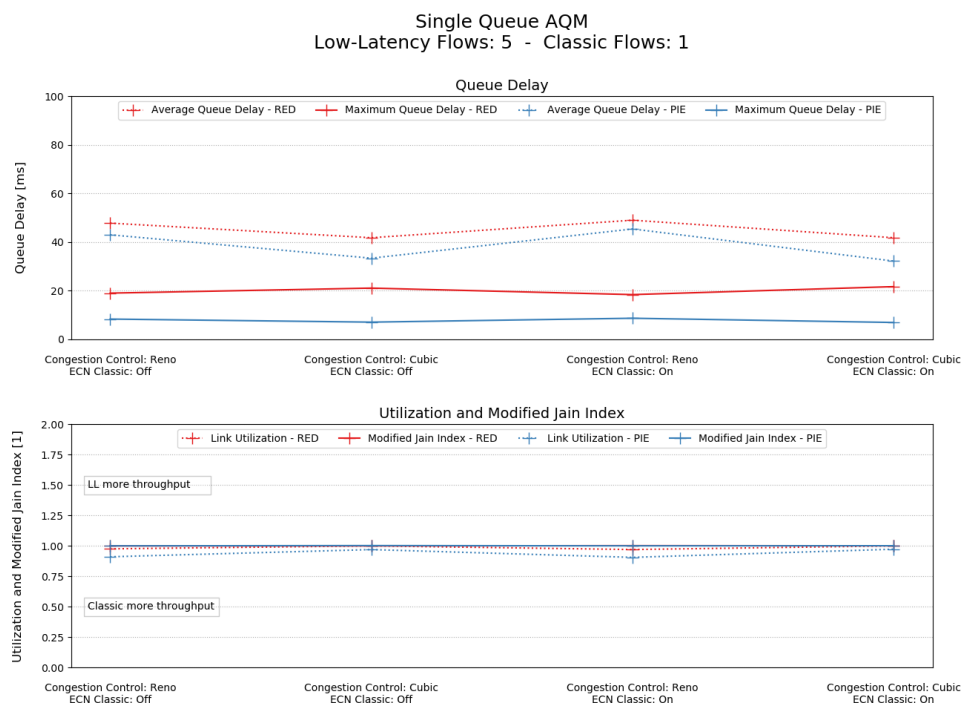
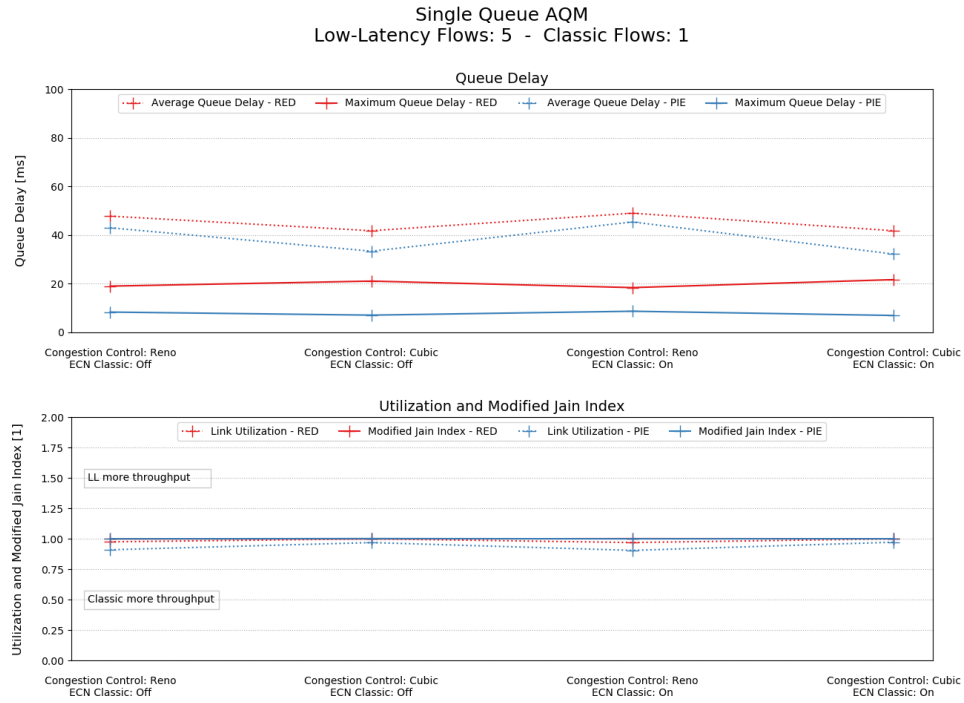
Appendix A

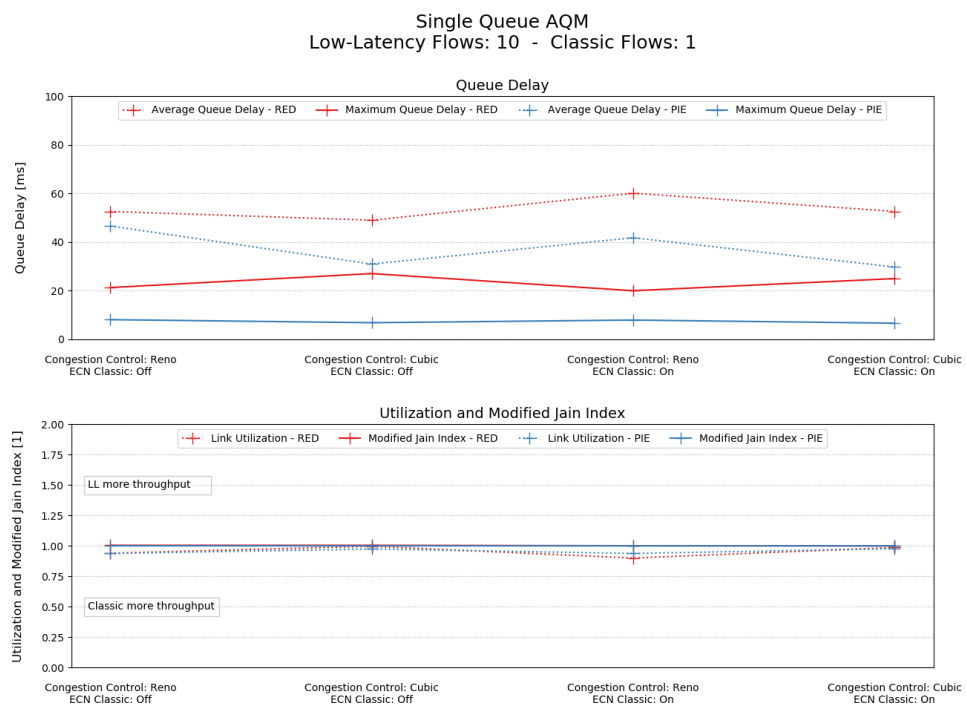
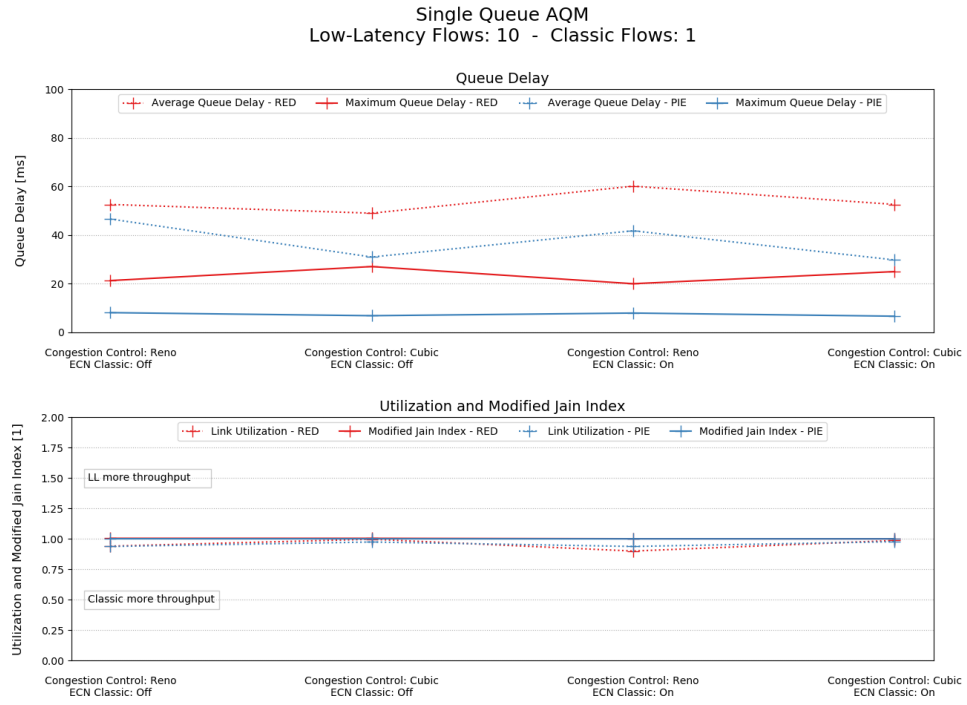
Plots

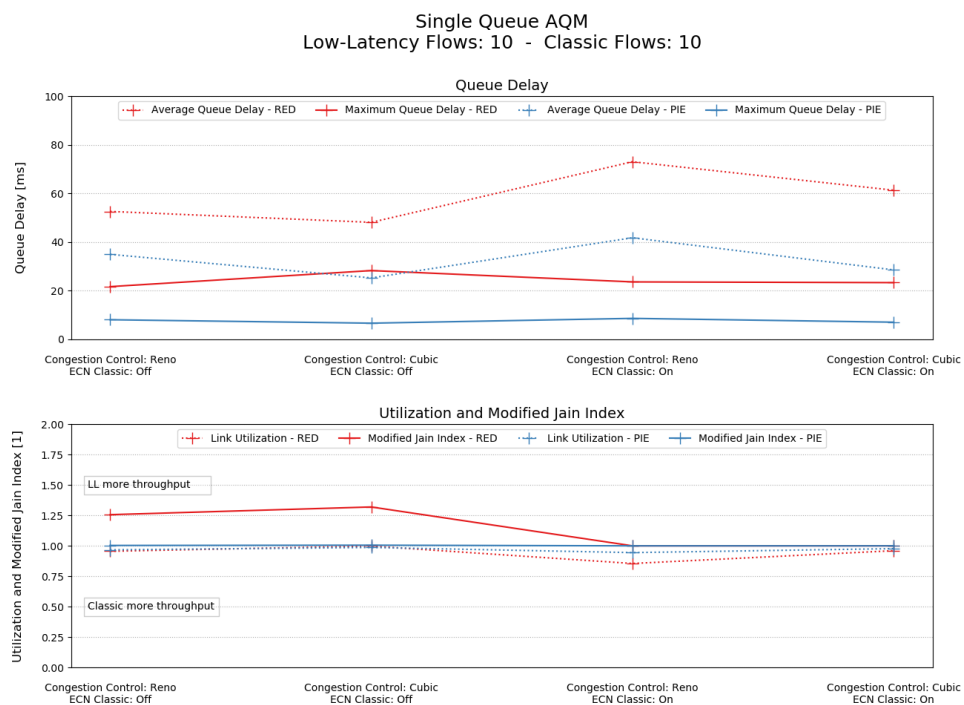
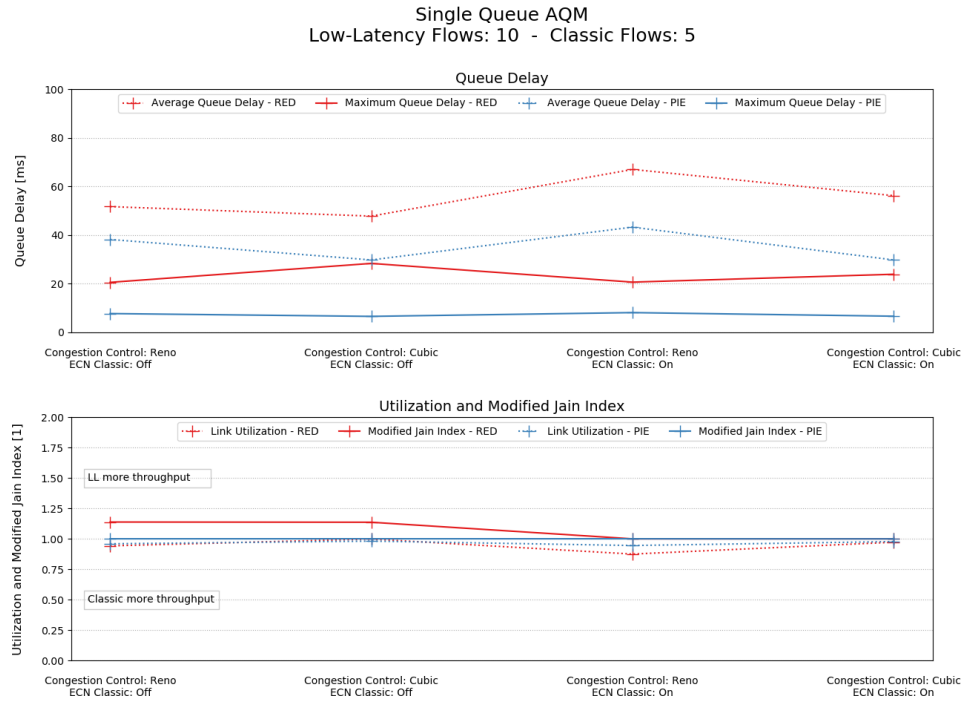
A.1 Plots from Static Link Simulations

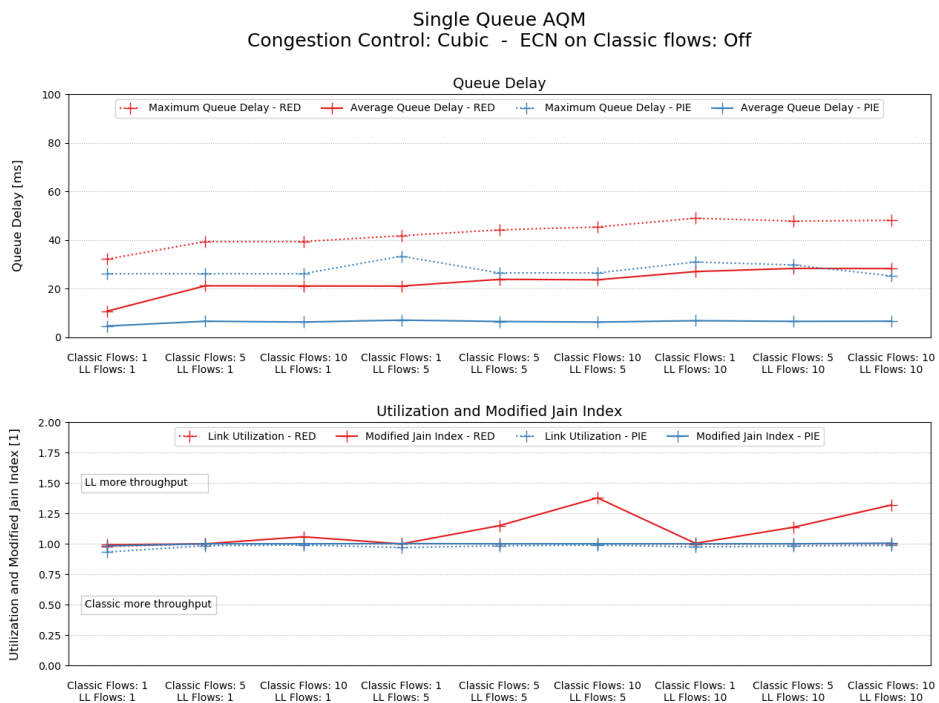
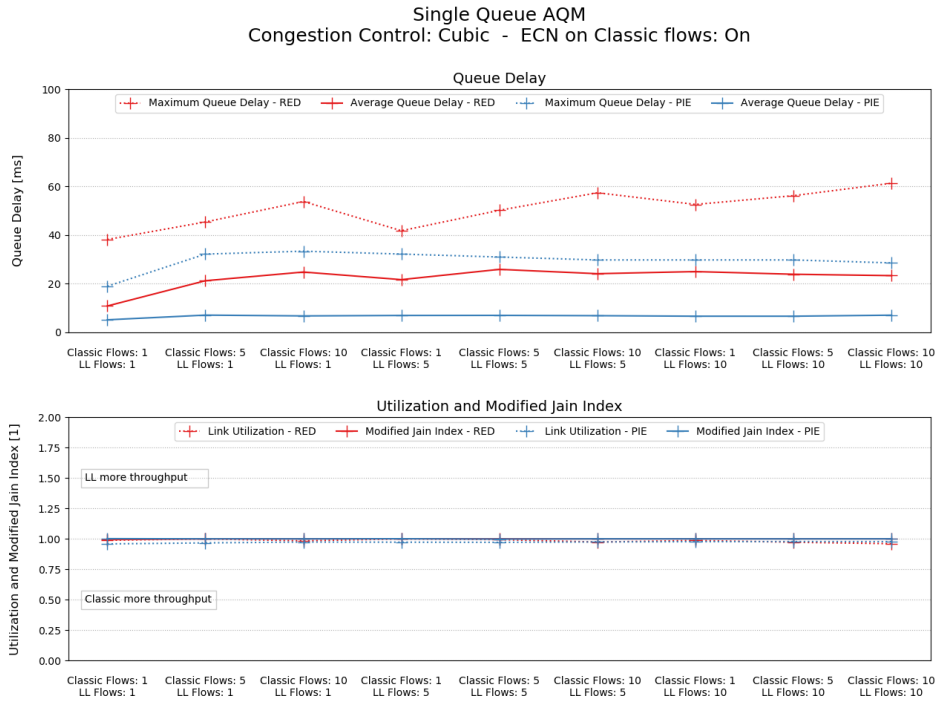


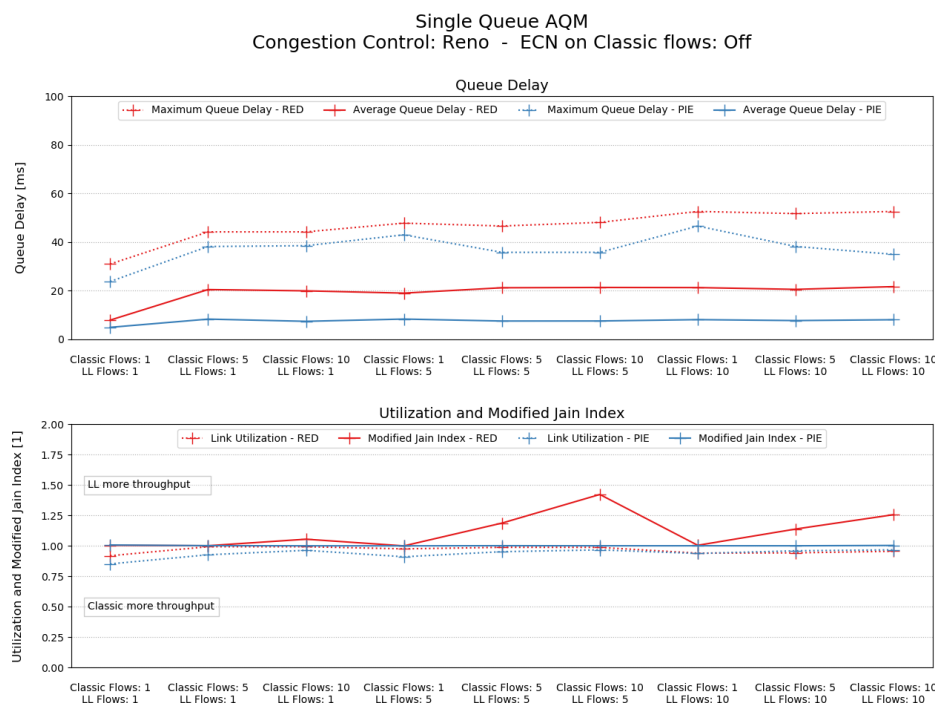
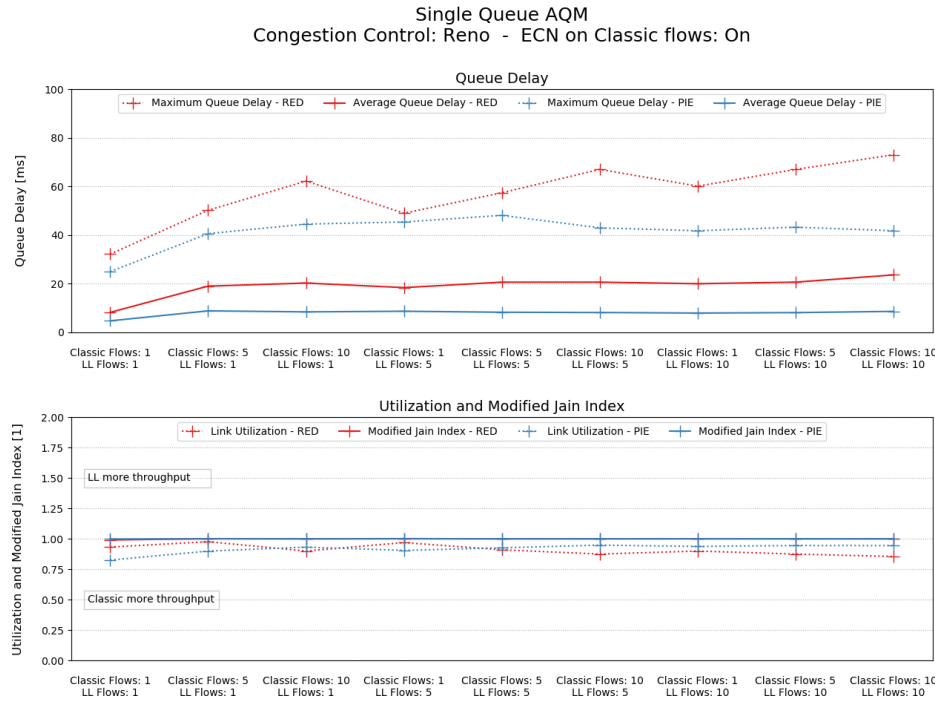


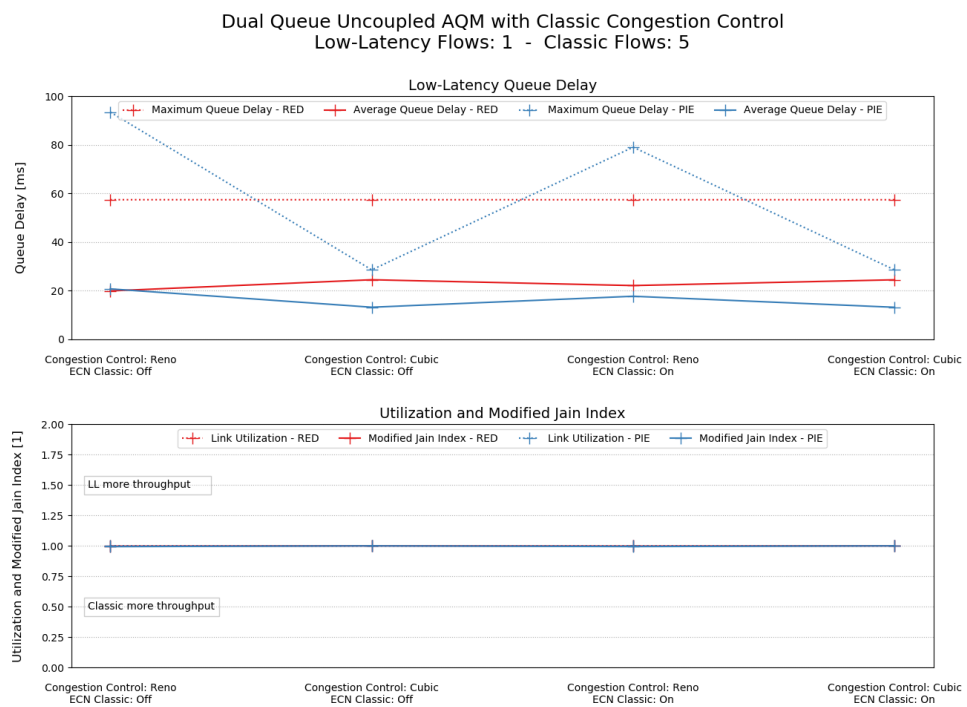
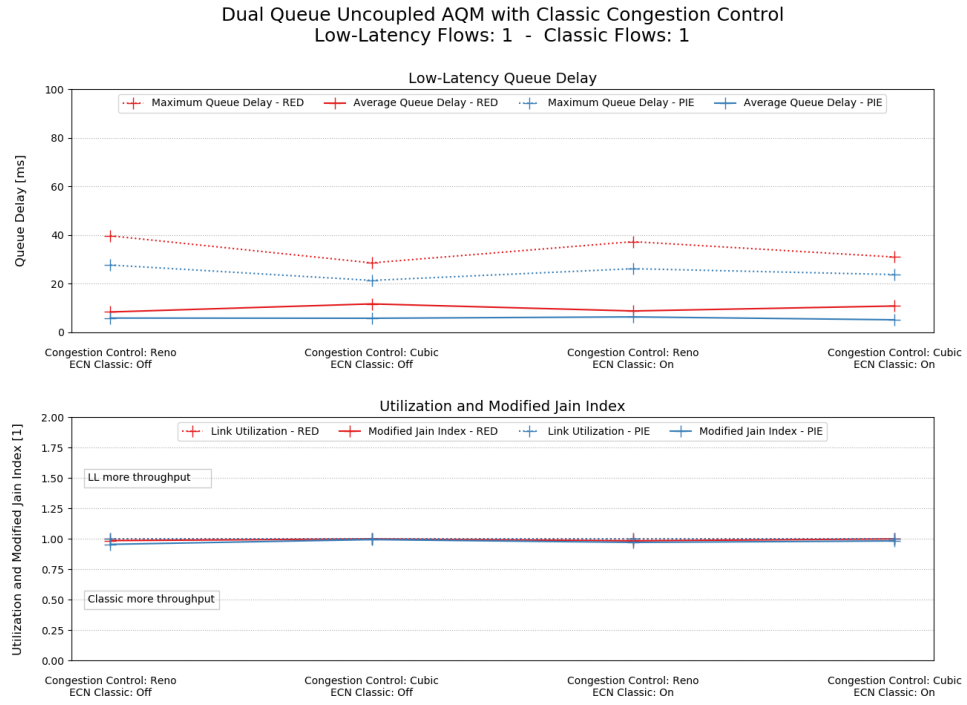


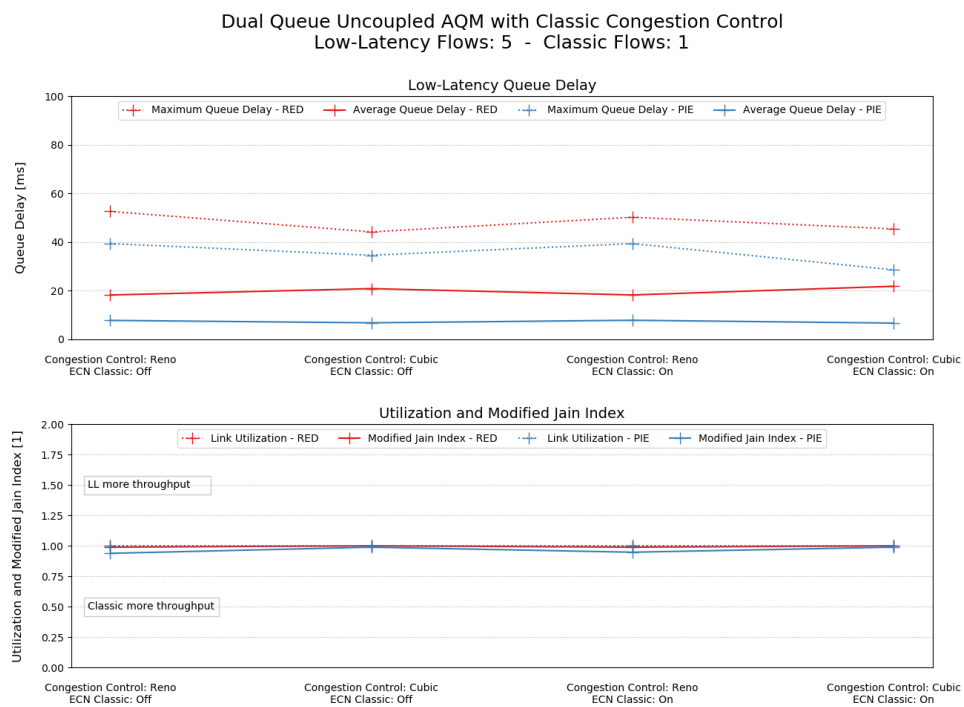
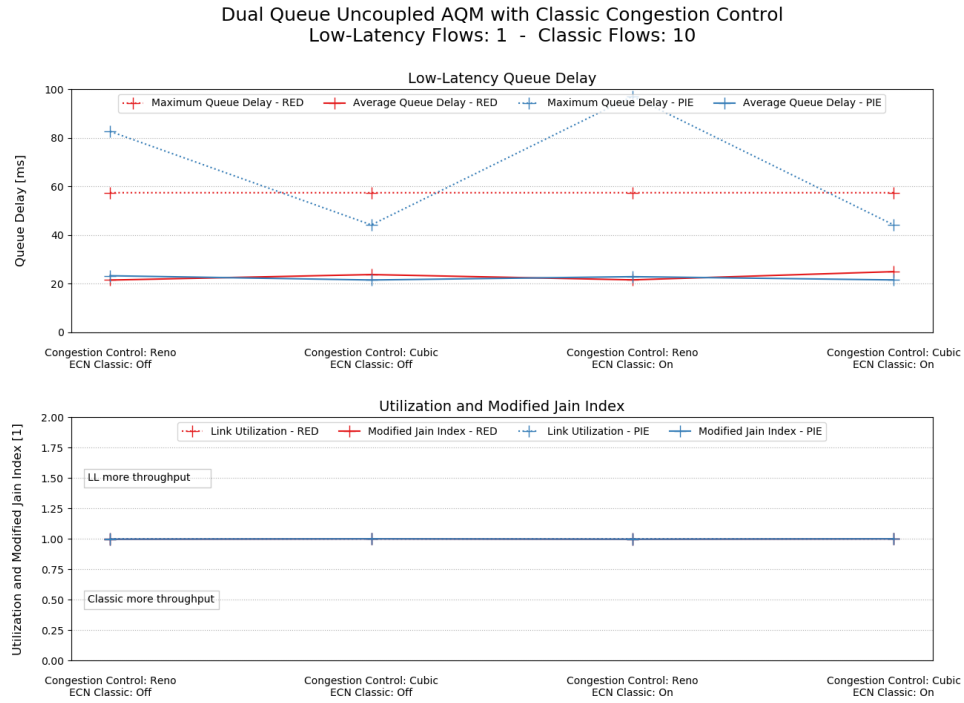




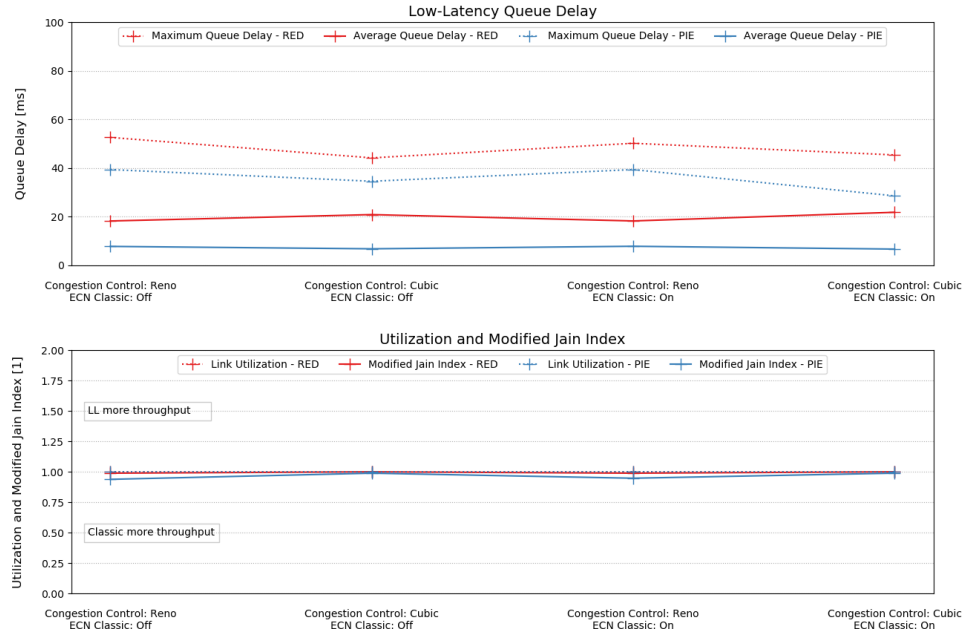




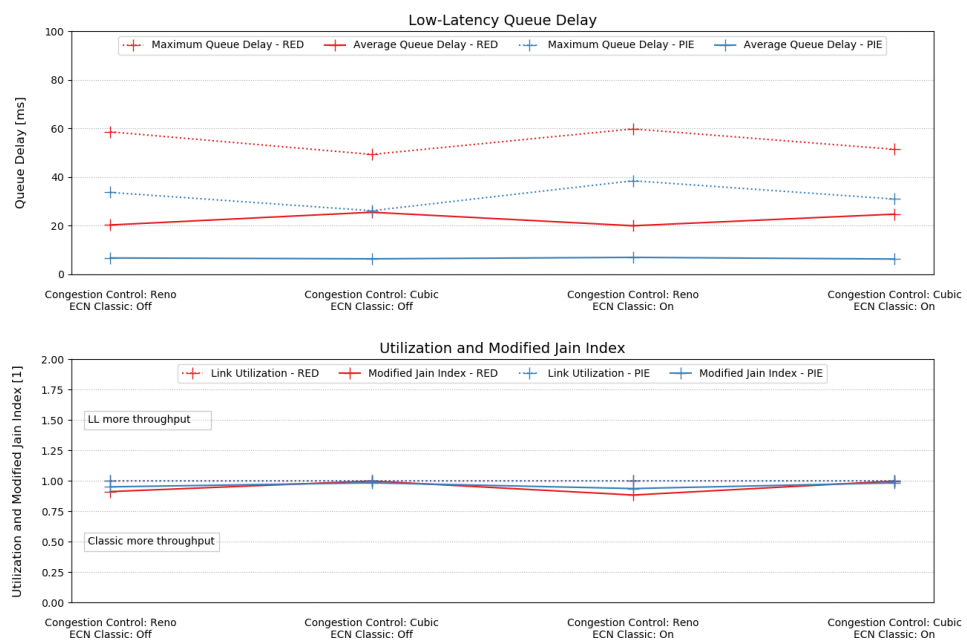


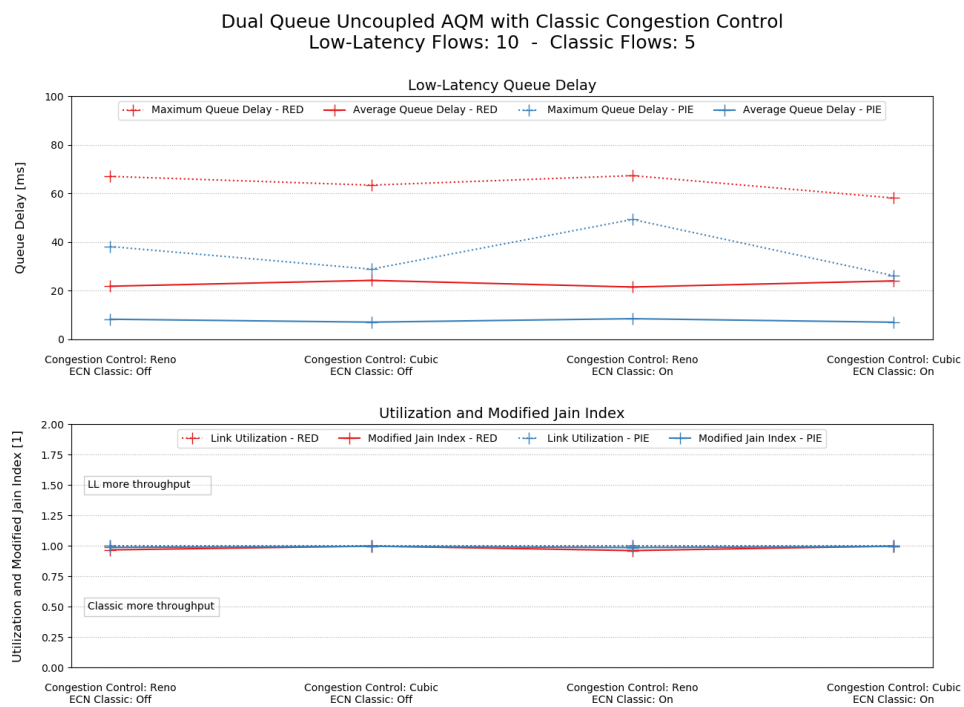
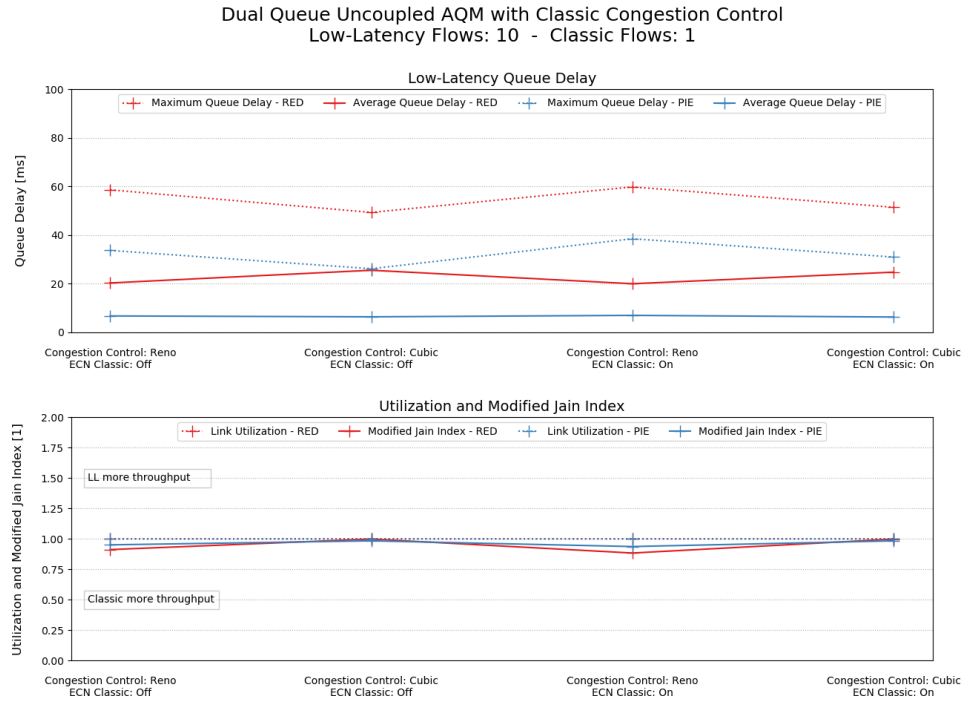


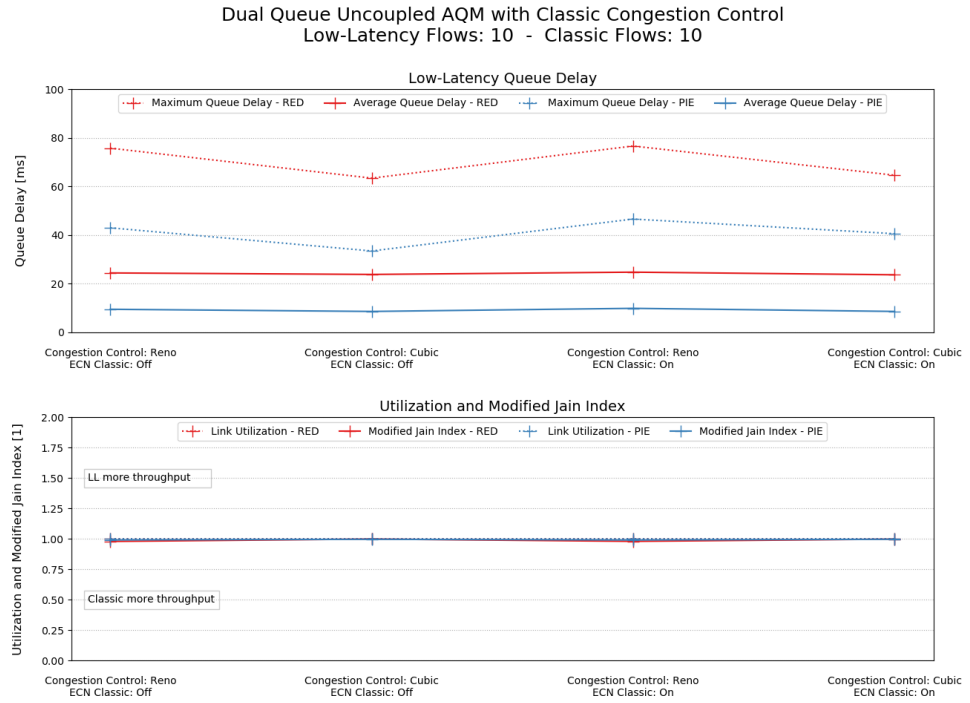
Dual Queue Uncoupled AQM with Classic Congestion Control
Low-Latency Flows: 5 - Classic Flows: 1



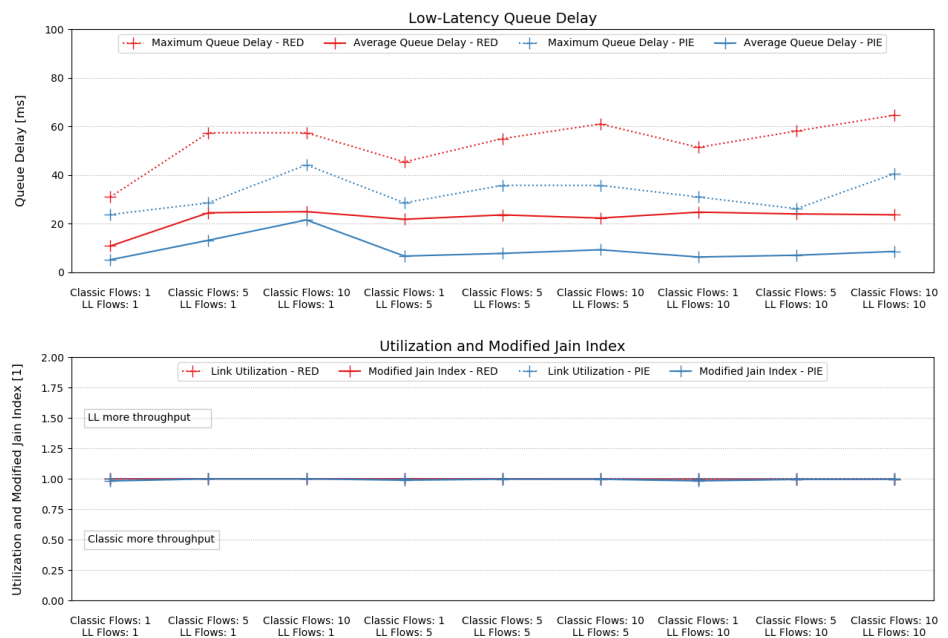
Dual Queue Uncoupled AQM with Classic Congestion Control
Low-Latency Flows: 10 - Classic Flows: 1

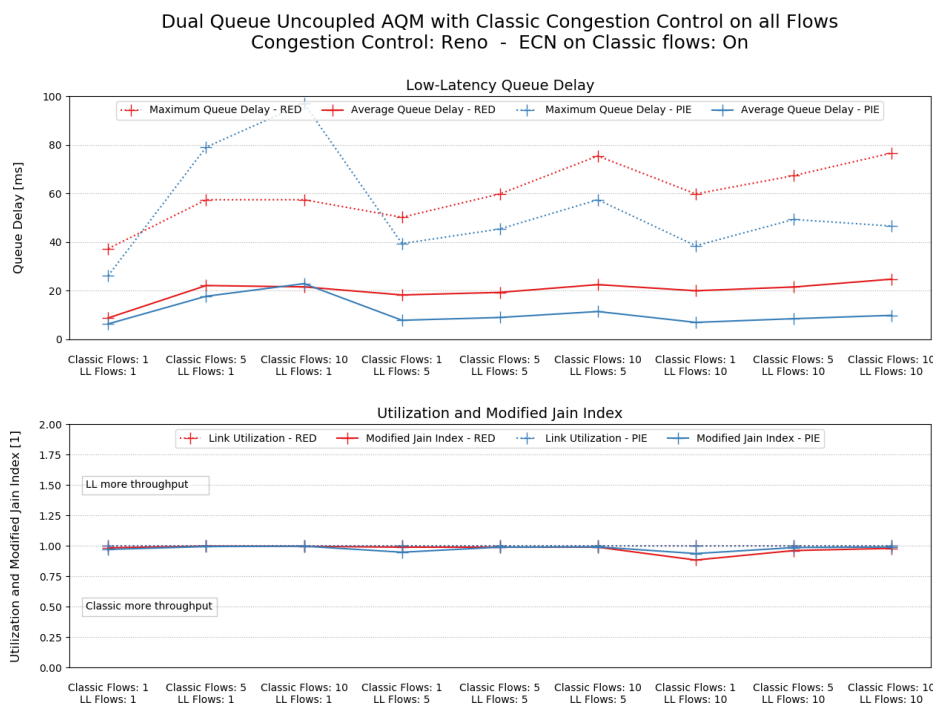
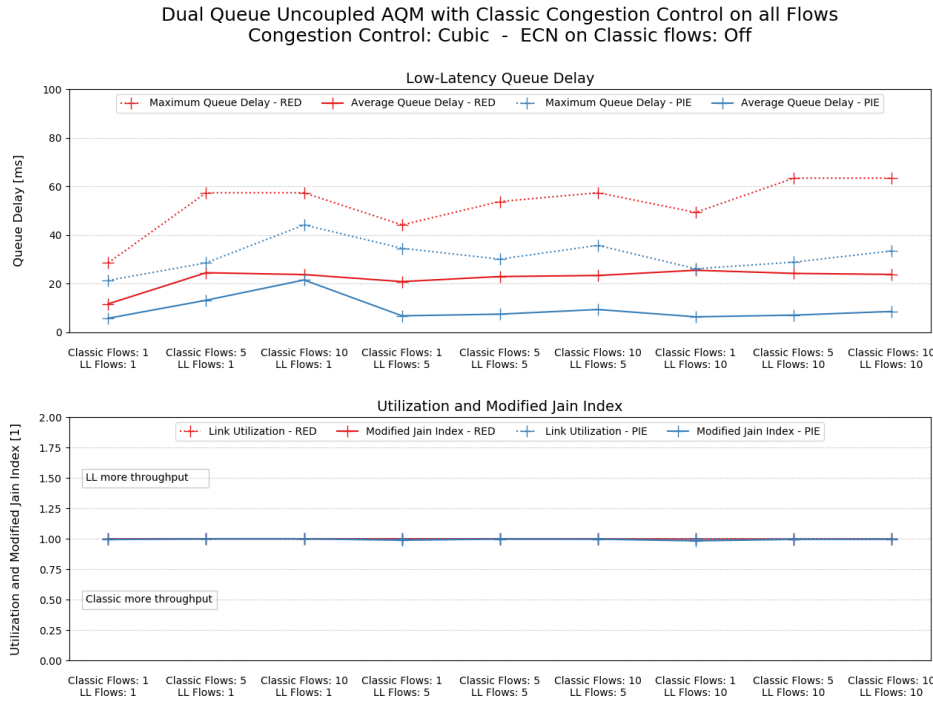


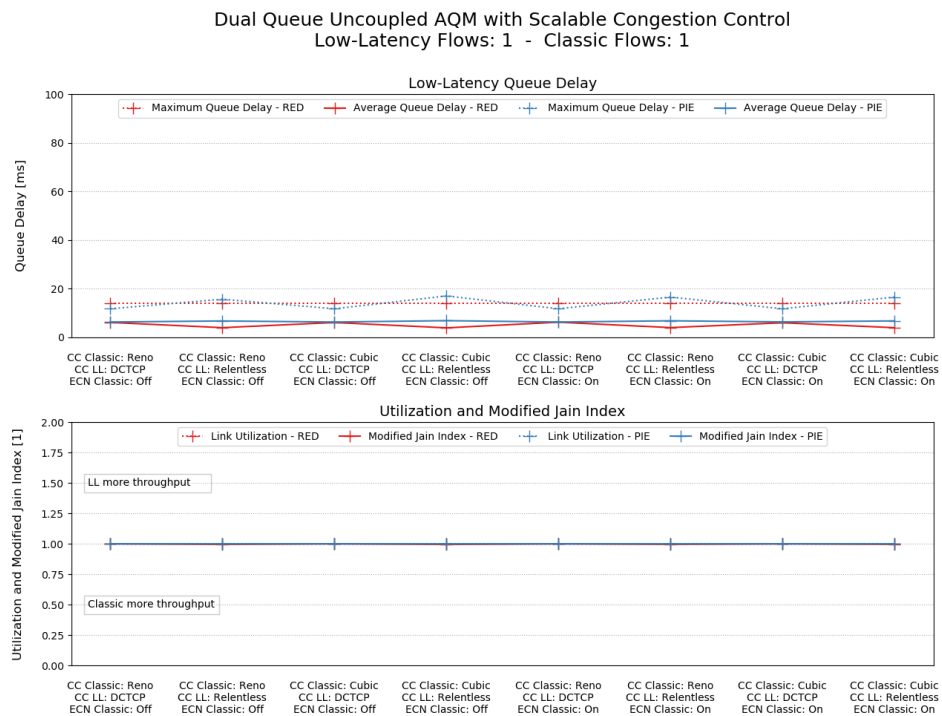
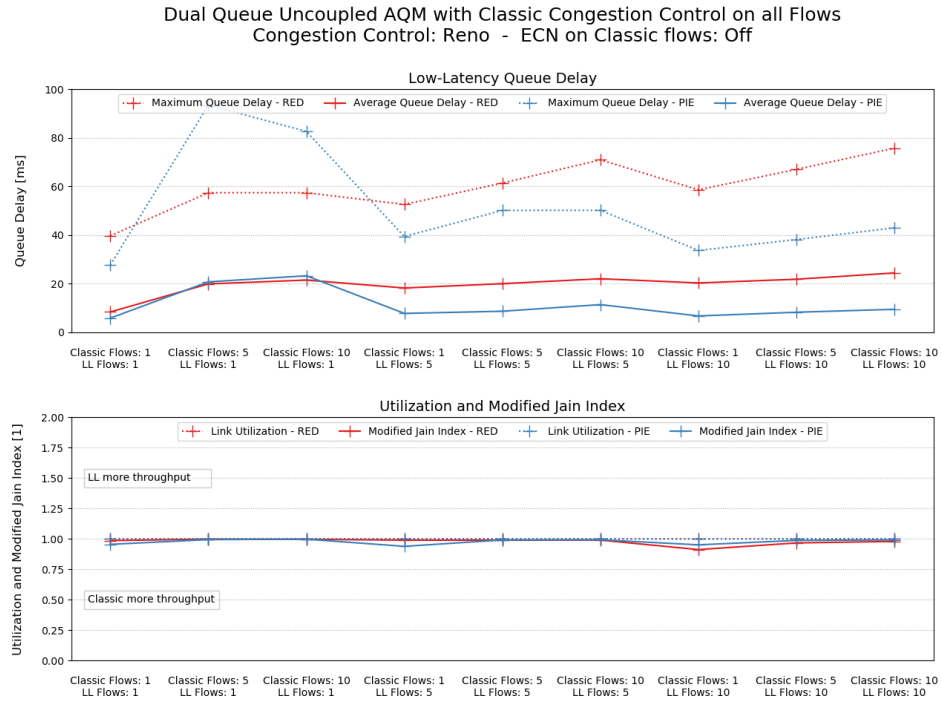


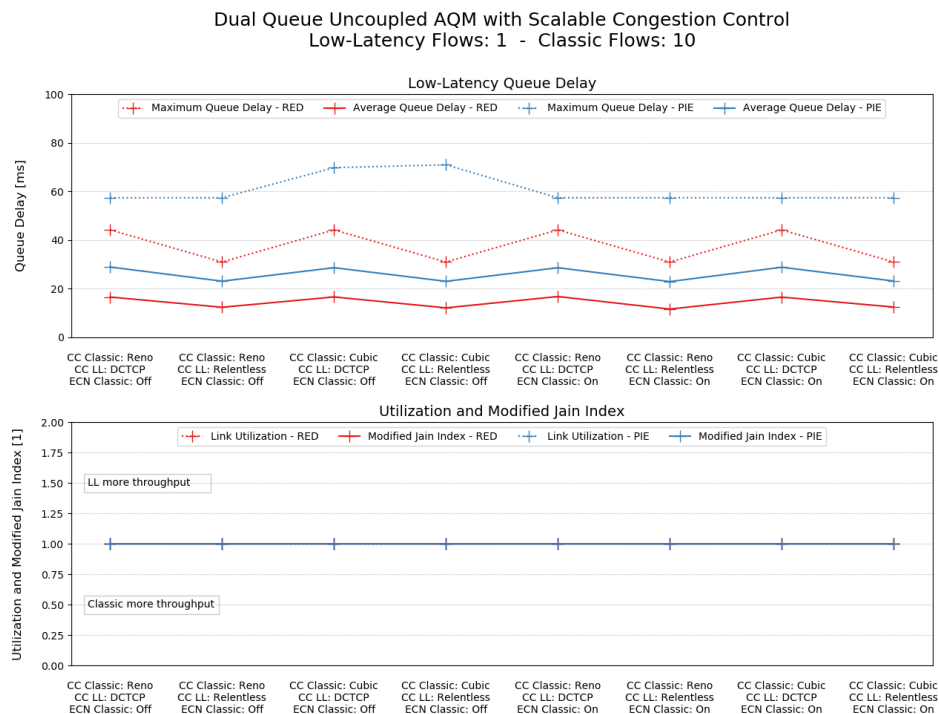
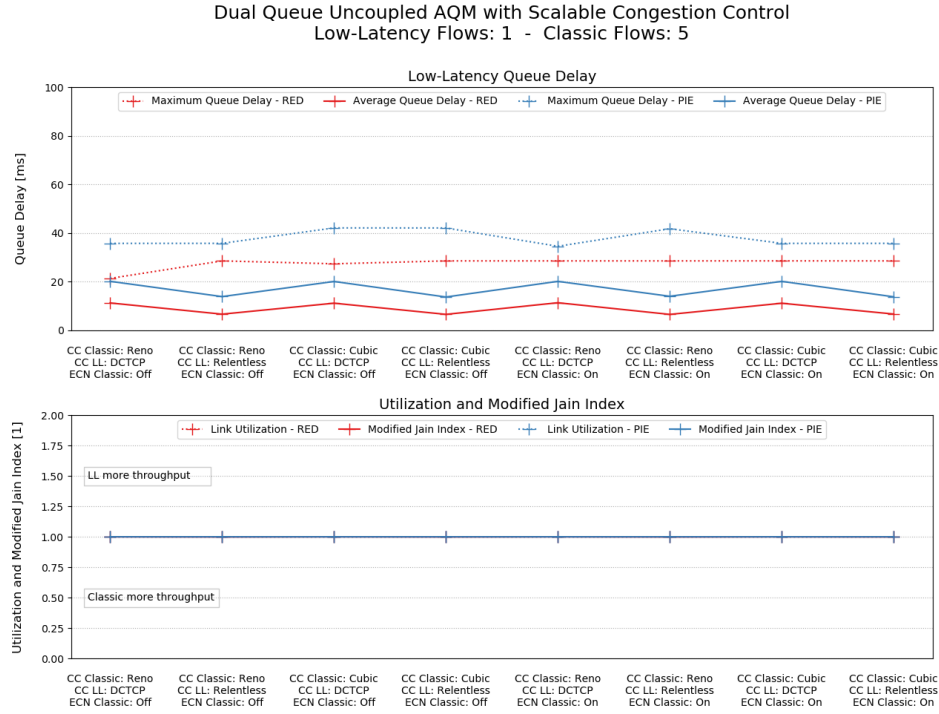


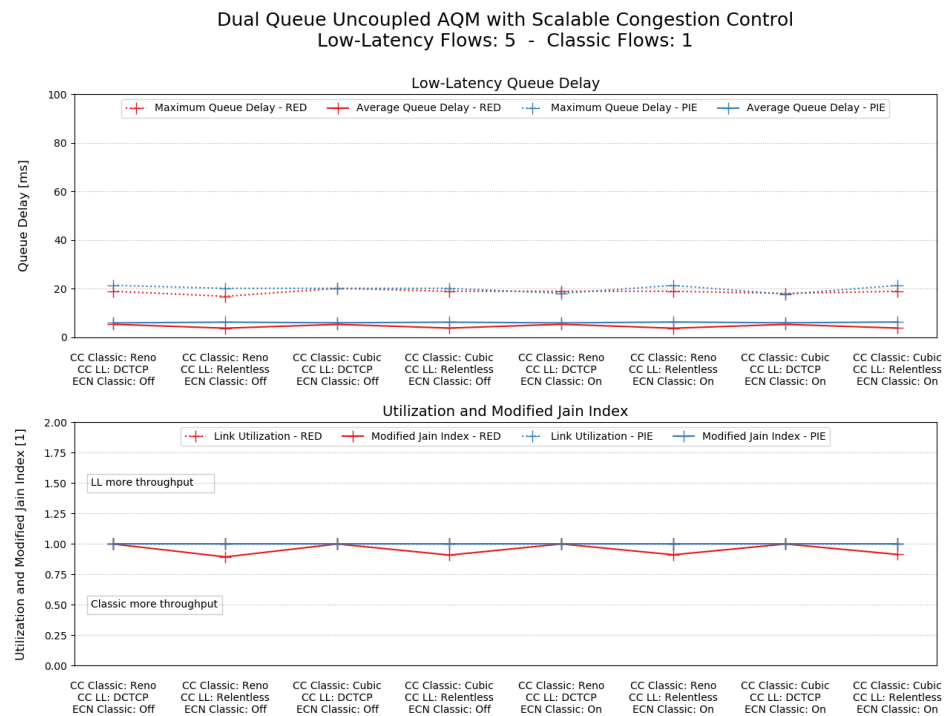
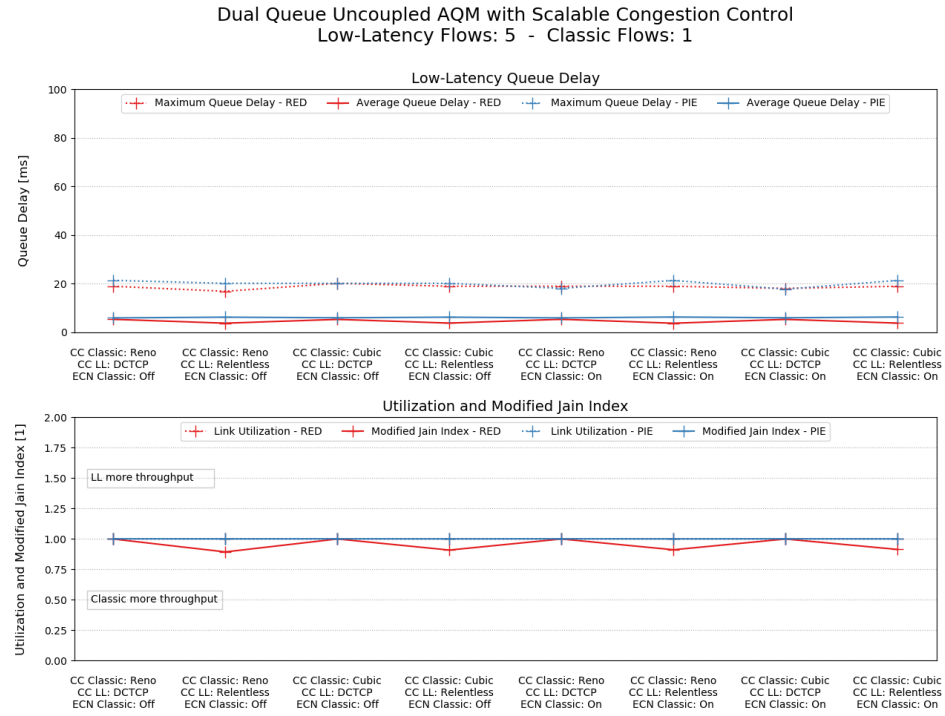
Dual Queue Uncoupled AQM with Classic Congestion Control on all Flows
Congestion Control: Cubic - ECN on Classic flows: On

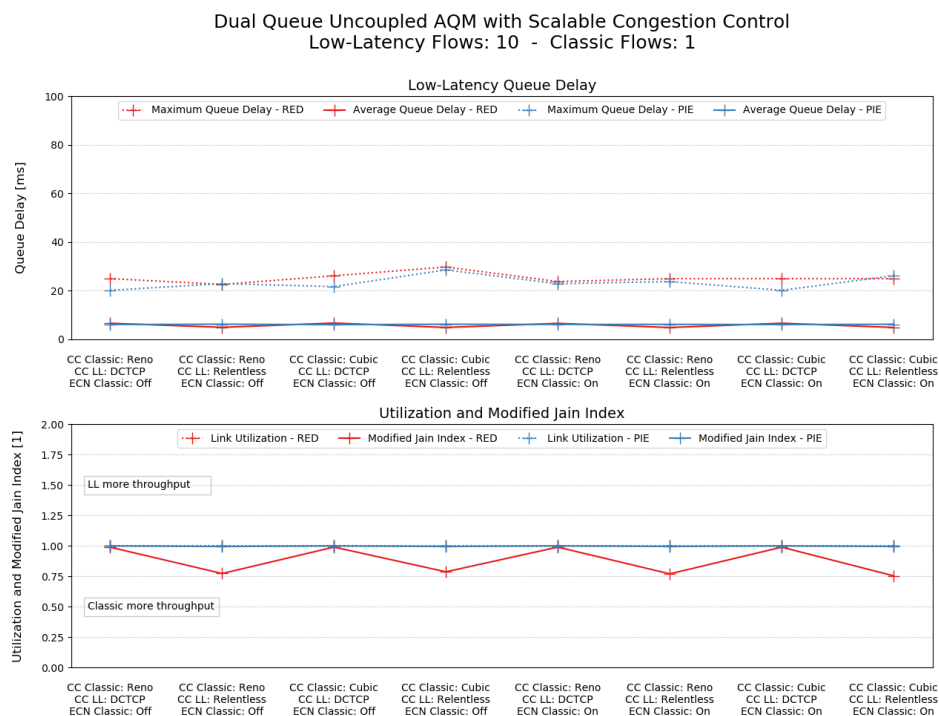
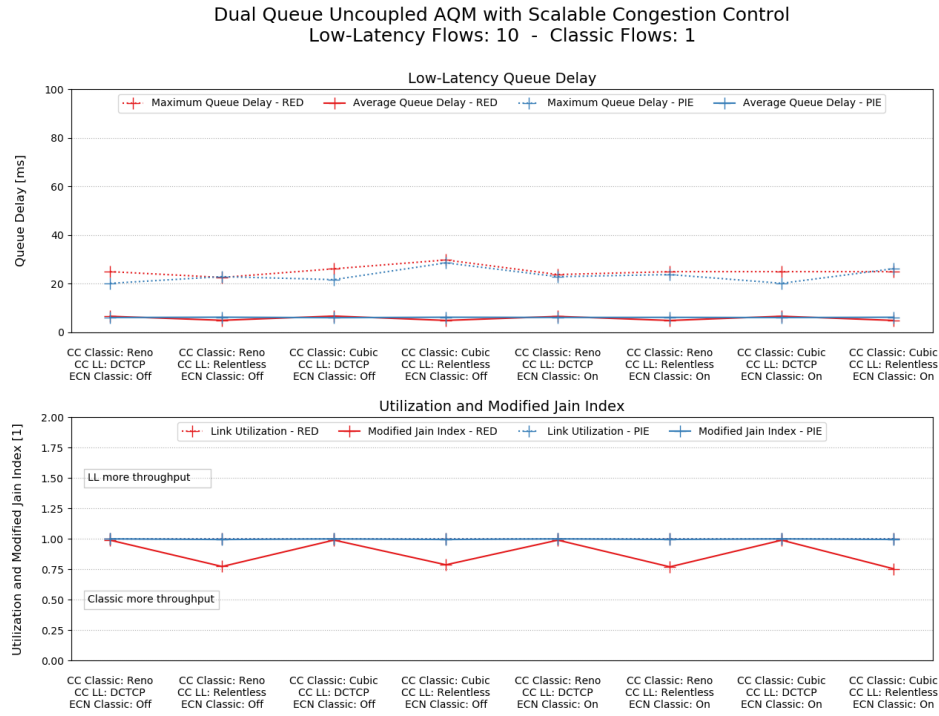




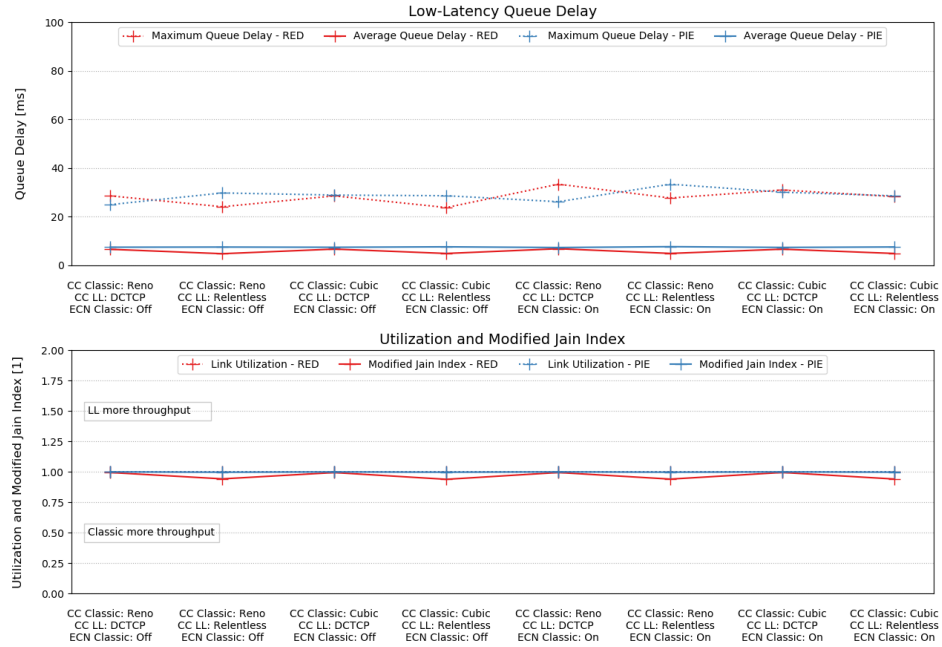




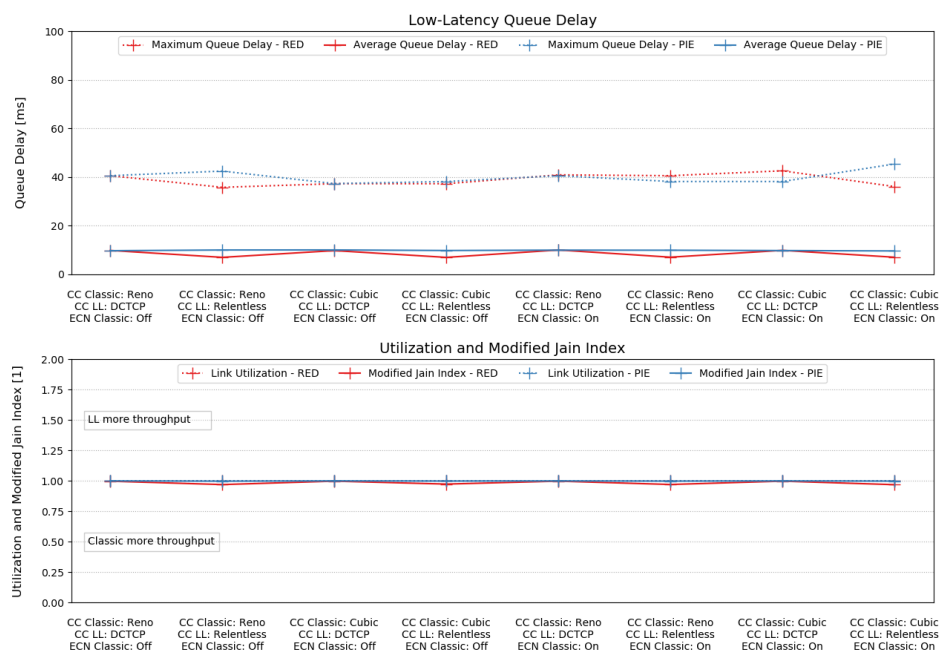


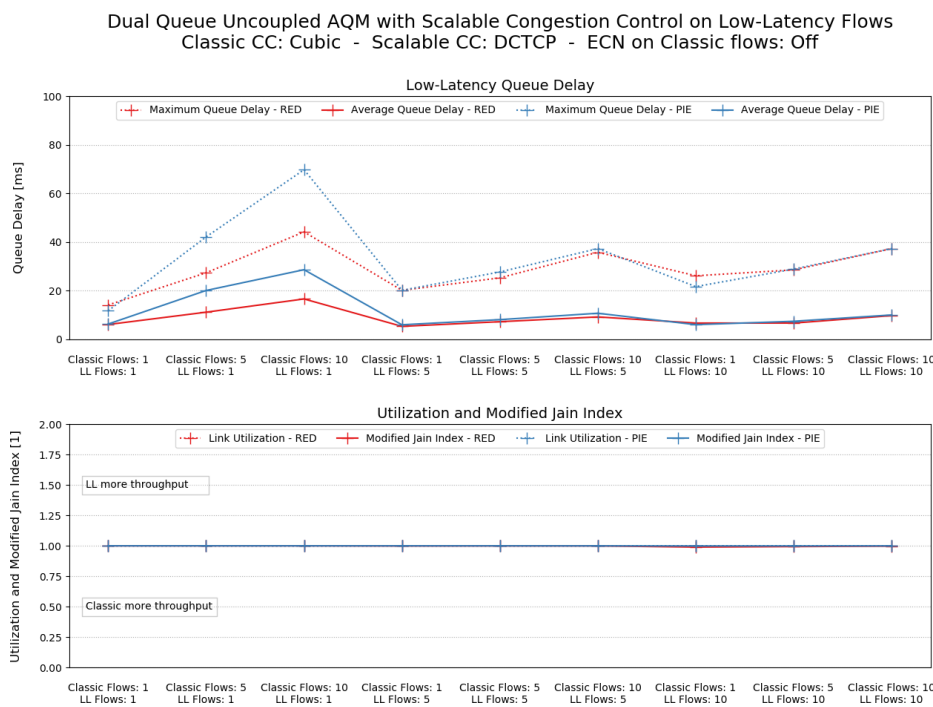
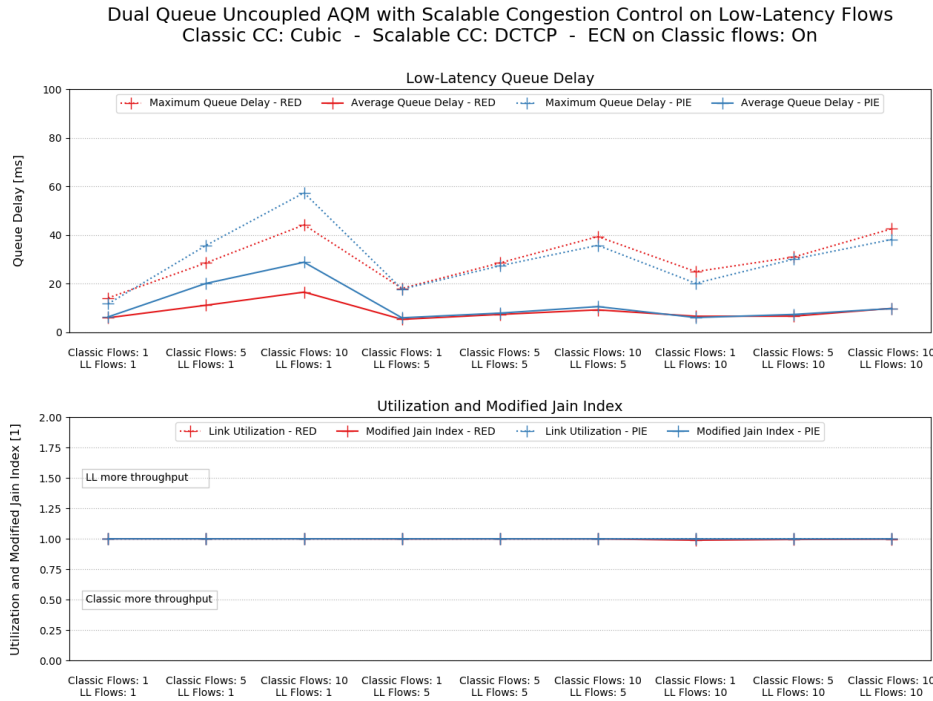


Dual Queue Uncoupled AQM with Scalable Congestion Control
Low-Latency Flows: 10 - Classic Flows: 5

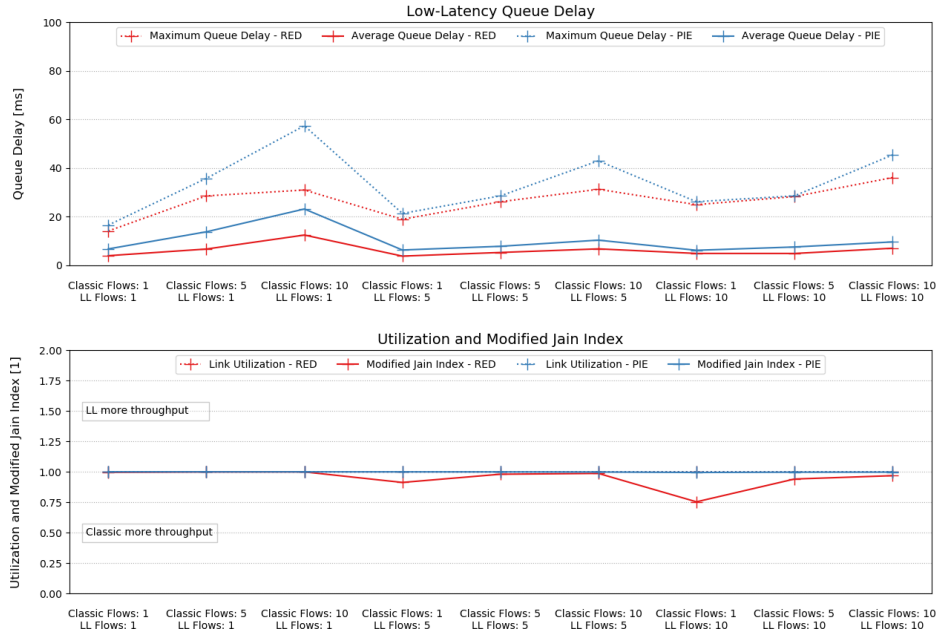


Dual Queue Uncoupled AQM with Scalable Congestion Control
Low-Latency Flows: 10 - Classic Flows: 10

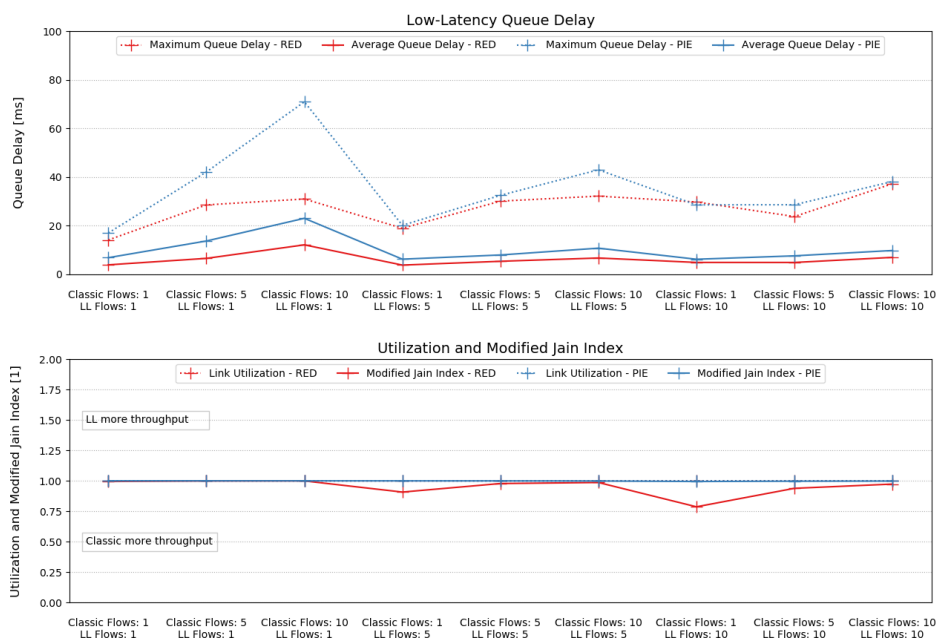


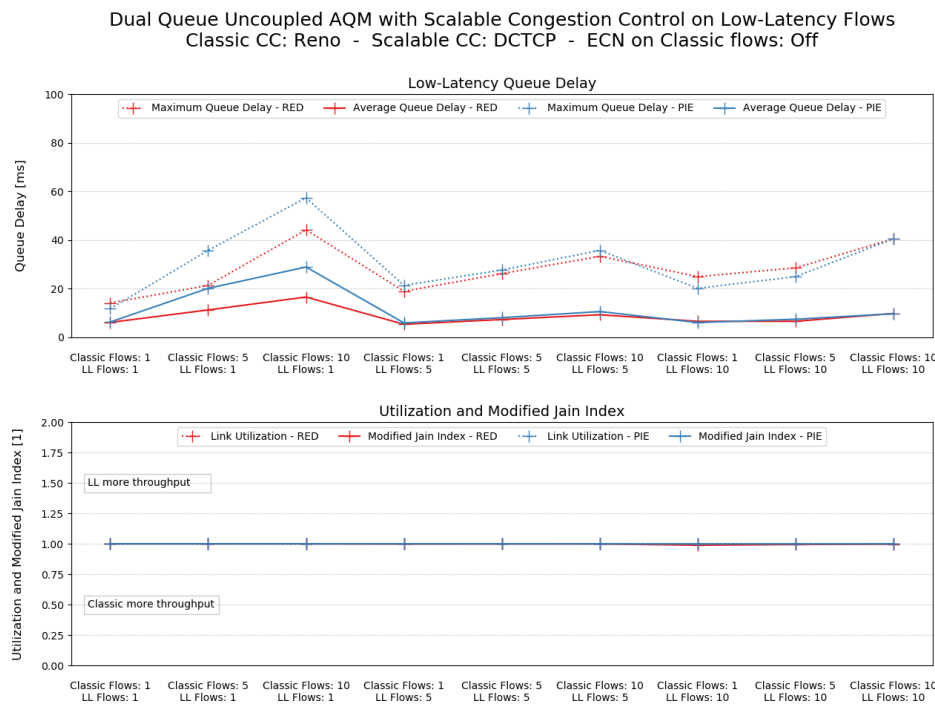
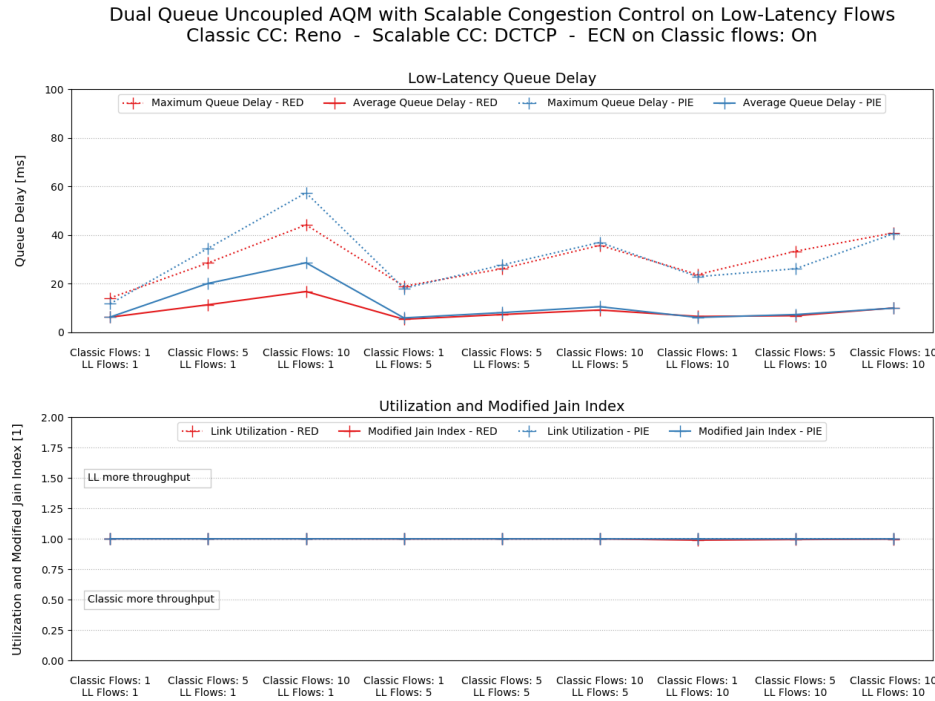


Dual Queue Uncoupled AQM with Scalable Congestion Control on Low-Latency Flows
 Classic CC: Cubic - Scalable CC: Relentless - ECN on Classic flows: On

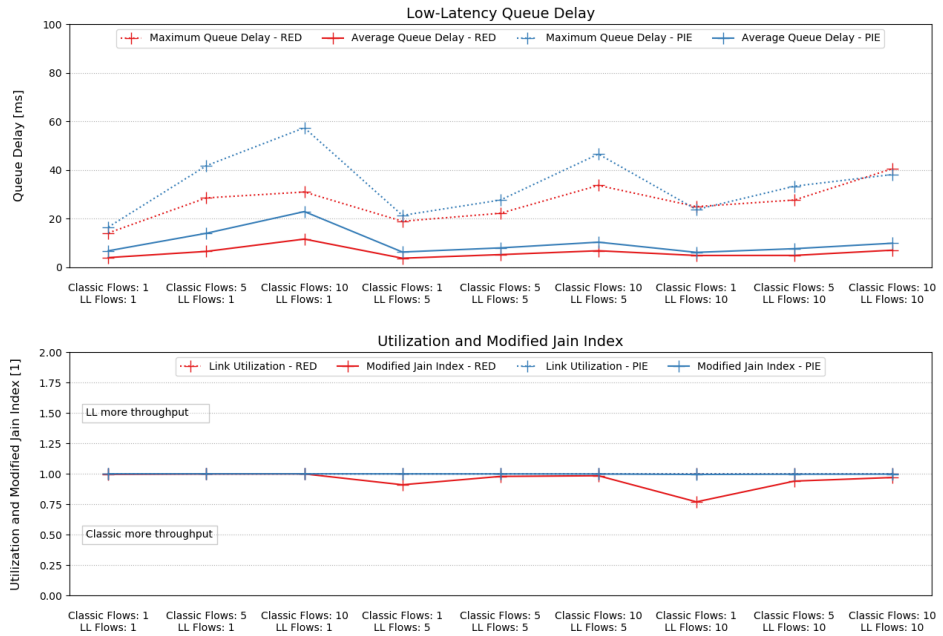


Dual Queue Uncoupled AQM with Scalable Congestion Control on Low-Latency Flows
 Classic CC: Cubic - Scalable CC: Relentless - ECN on Classic flows: Off

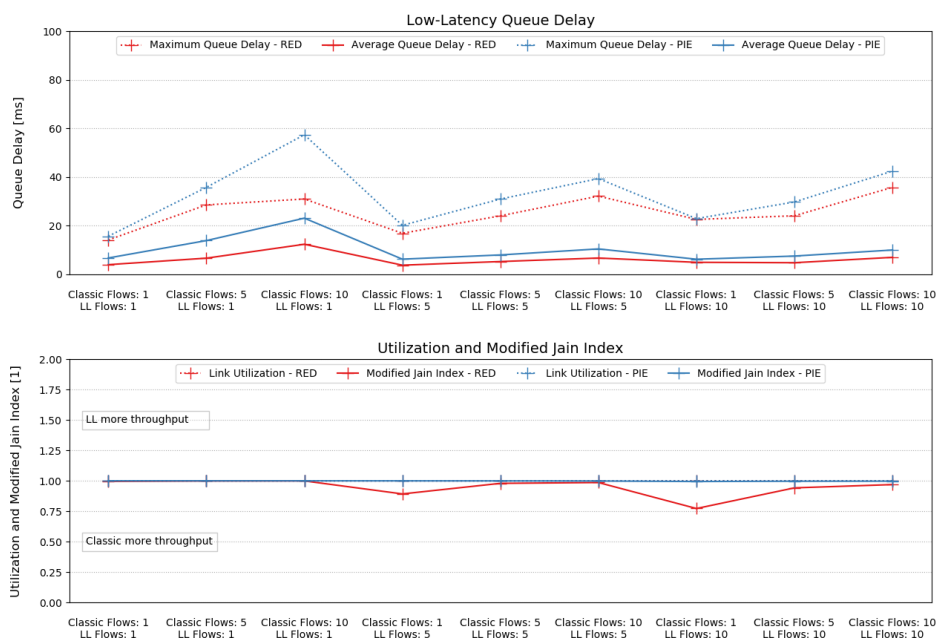


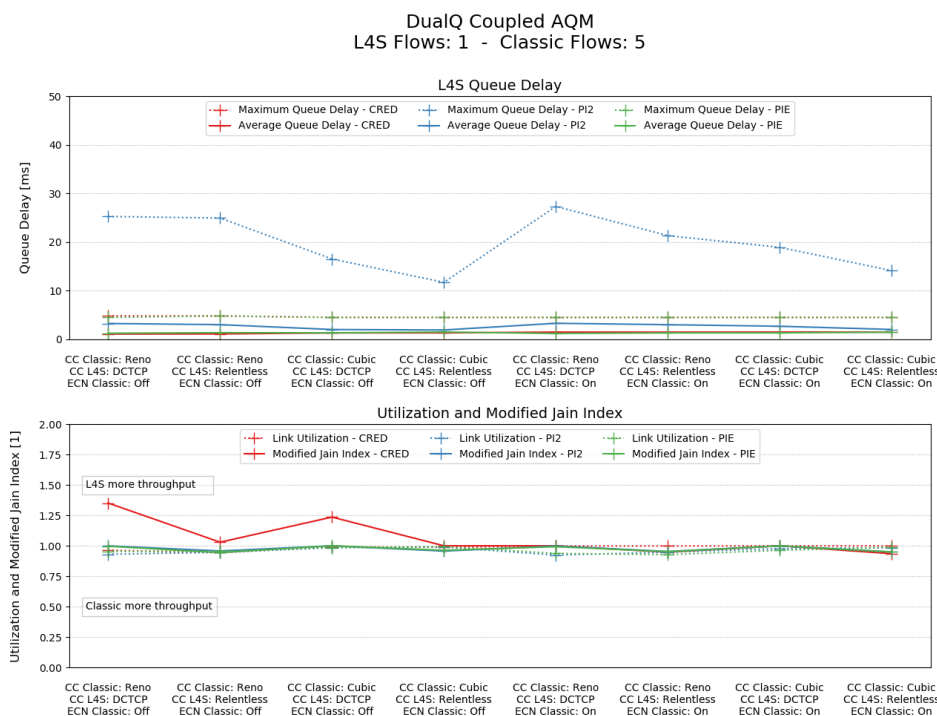
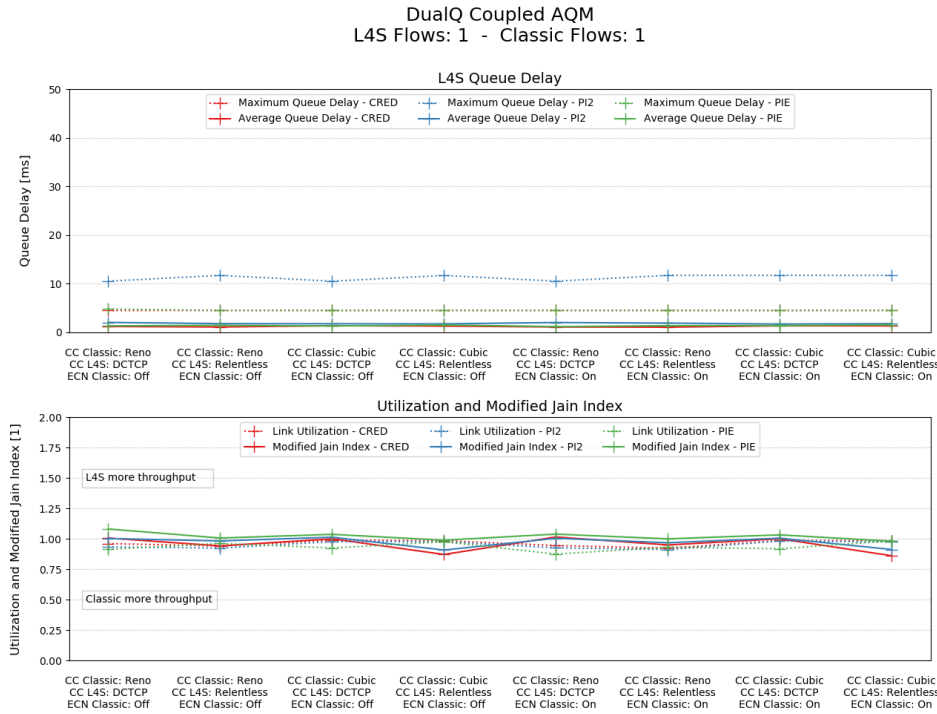


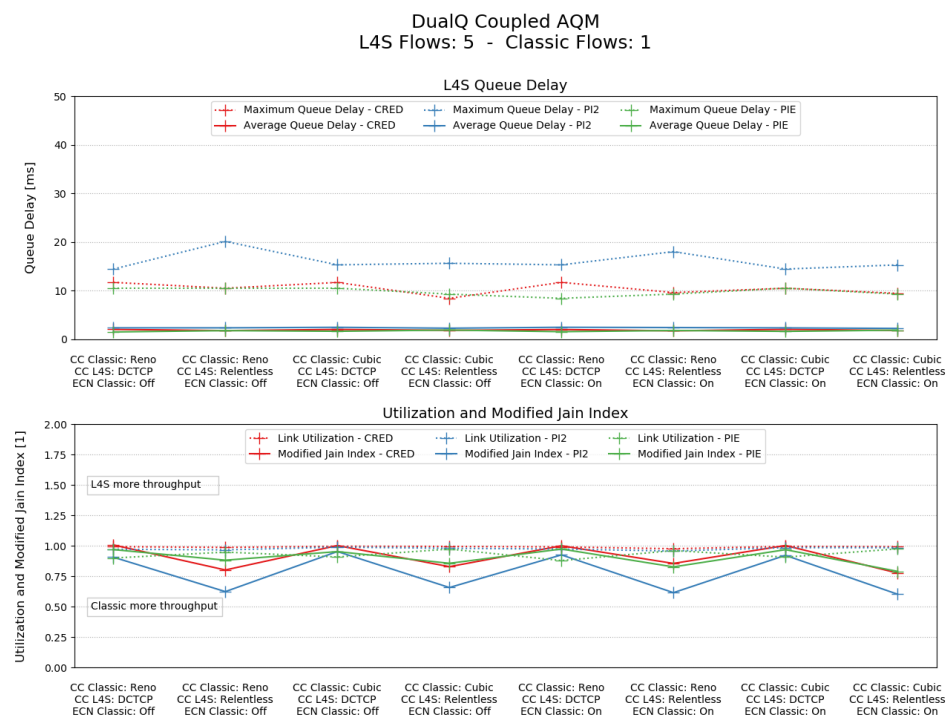
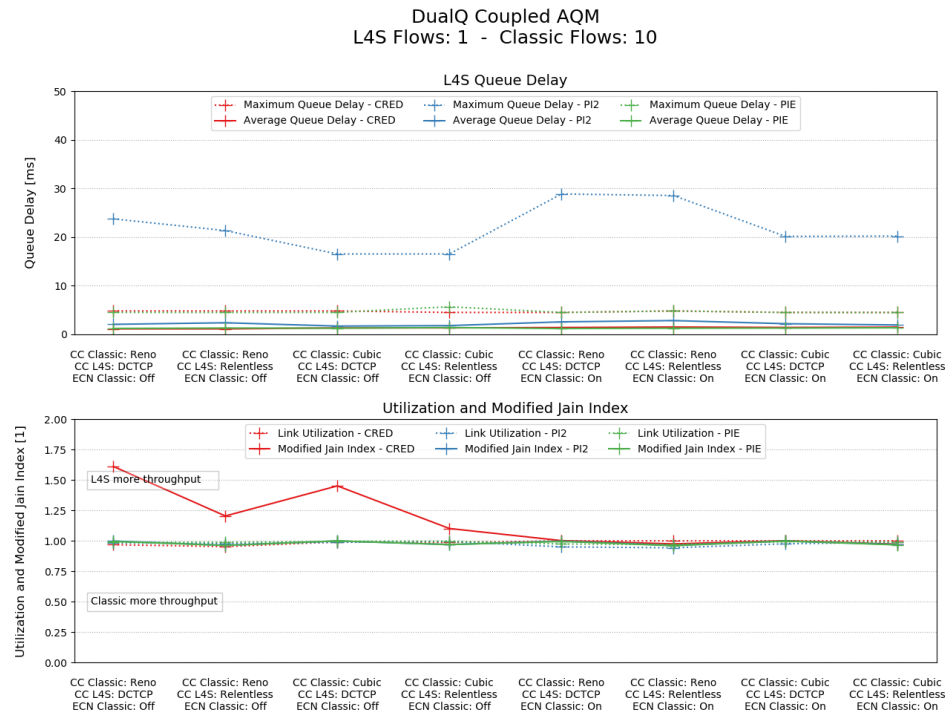
Dual Queue Uncoupled AQM with Scalable Congestion Control on Low-Latency Flows
 Classic CC: Reno - Scalable CC: Relentless - ECN on Classic flows: On

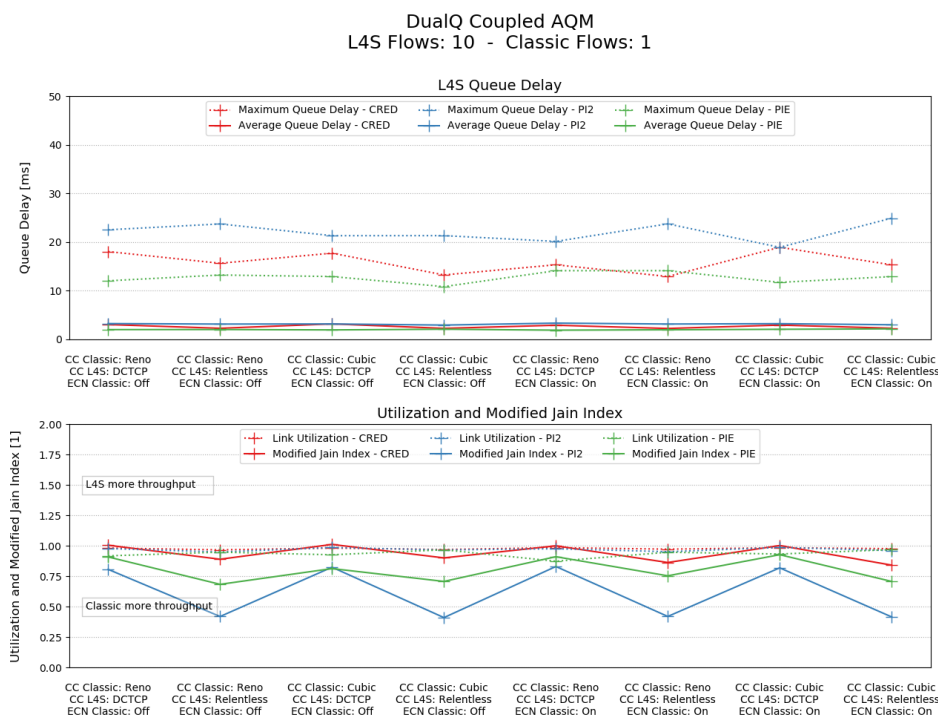
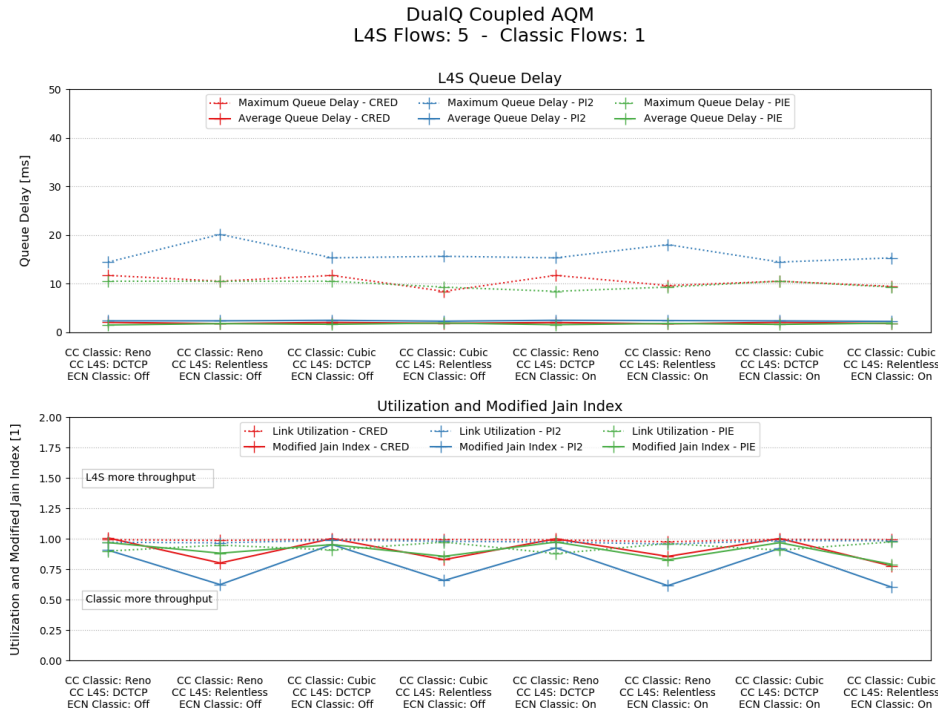


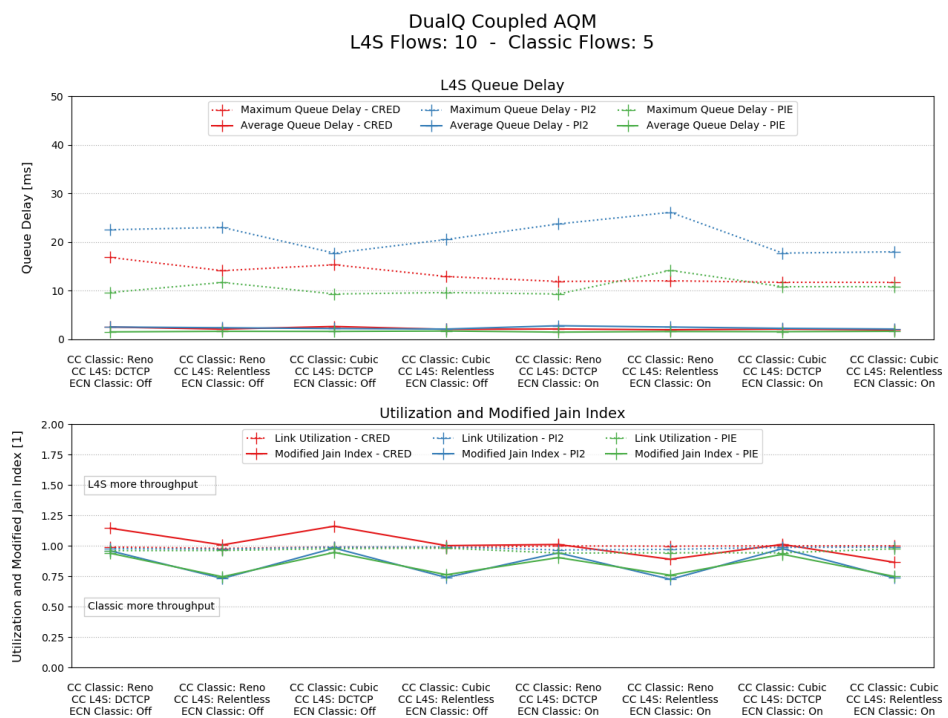
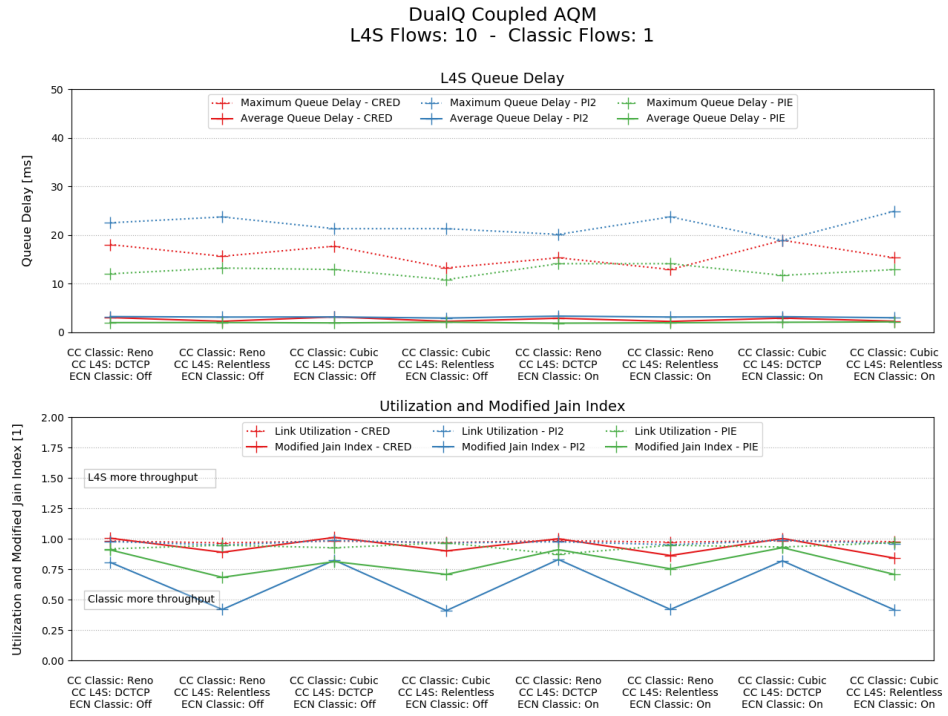
Dual Queue Uncoupled AQM with Scalable Congestion Control on Low-Latency Flows
 Classic CC: Reno - Scalable CC: Relentless - ECN on Classic flows: Off

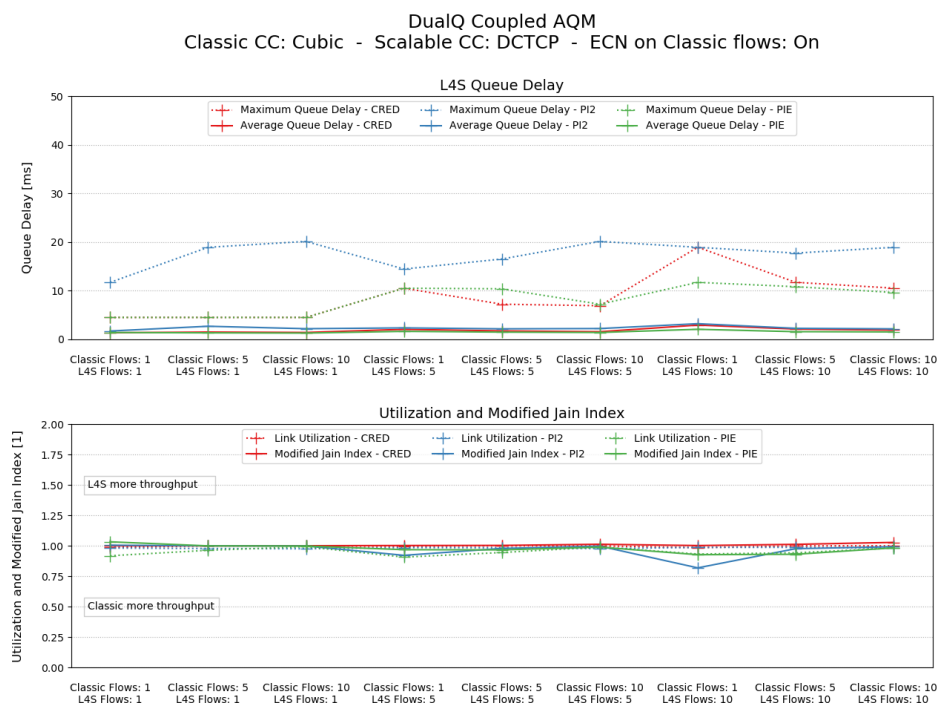
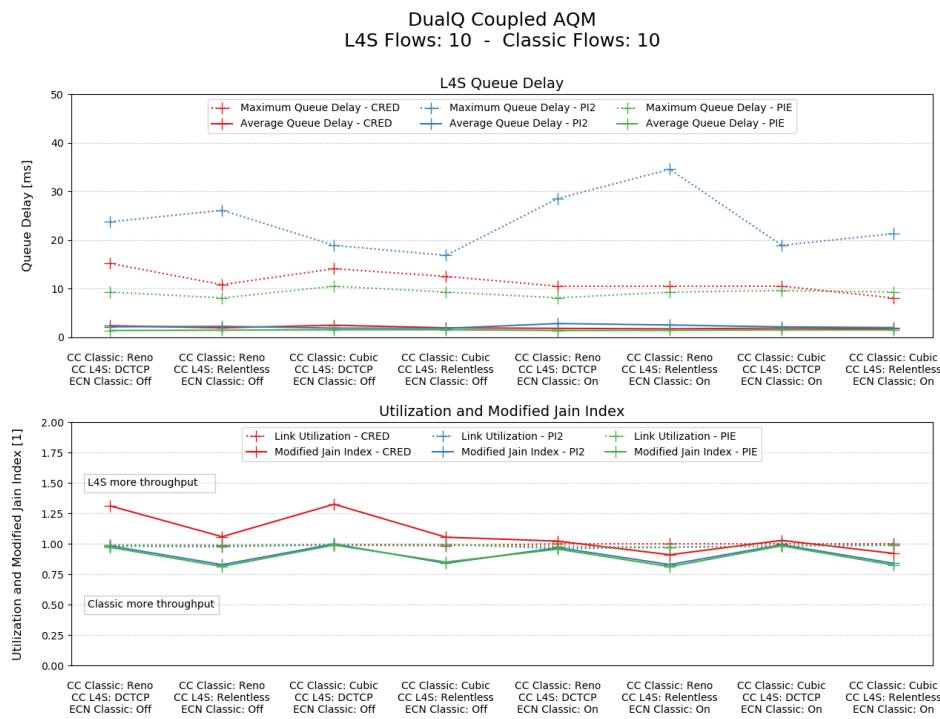


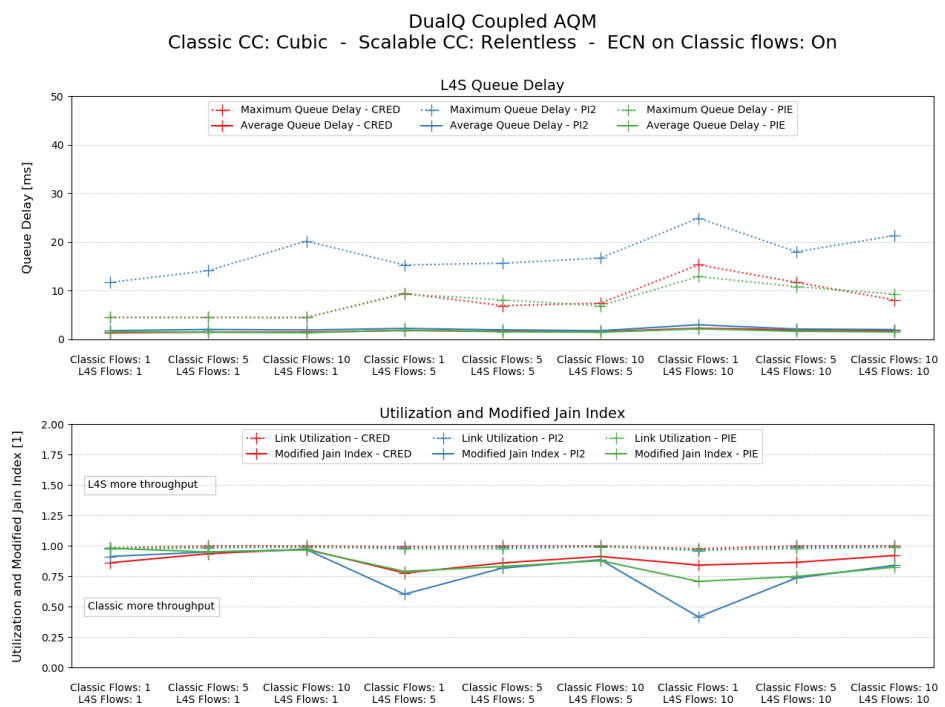
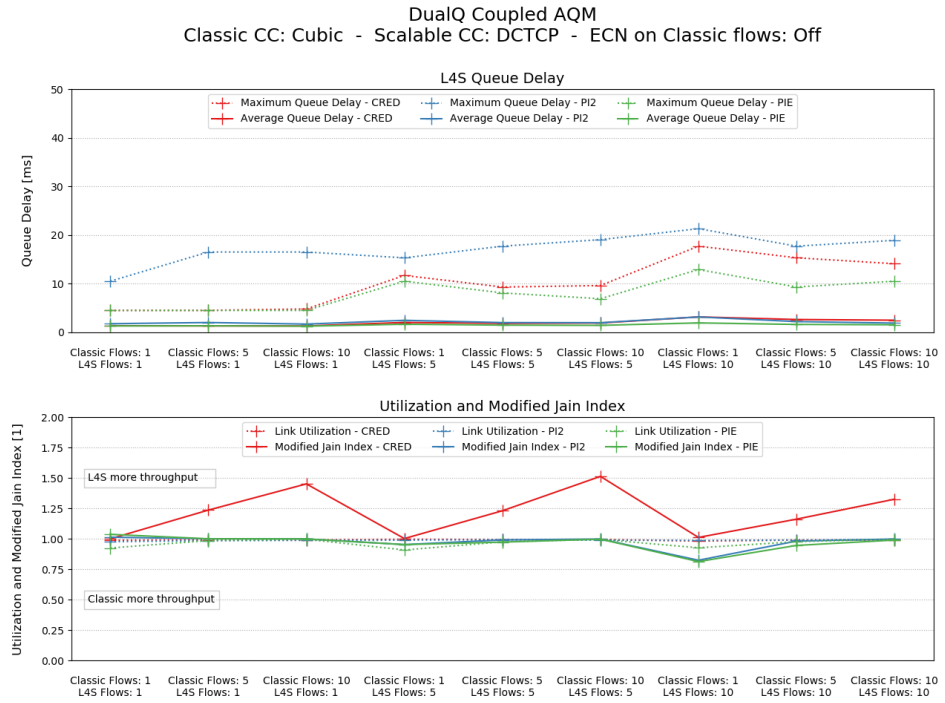


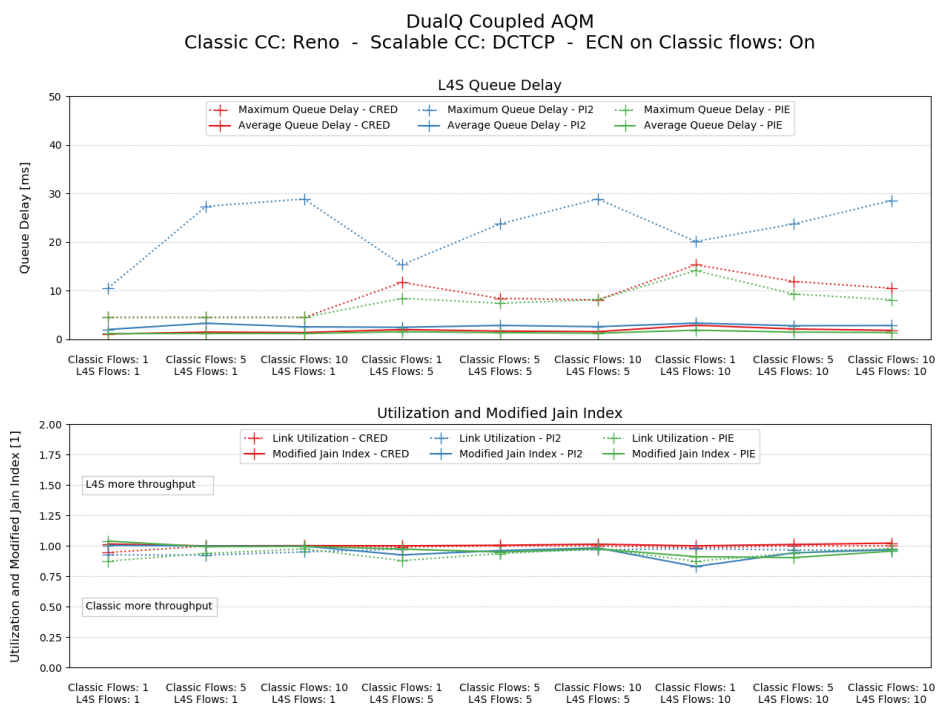
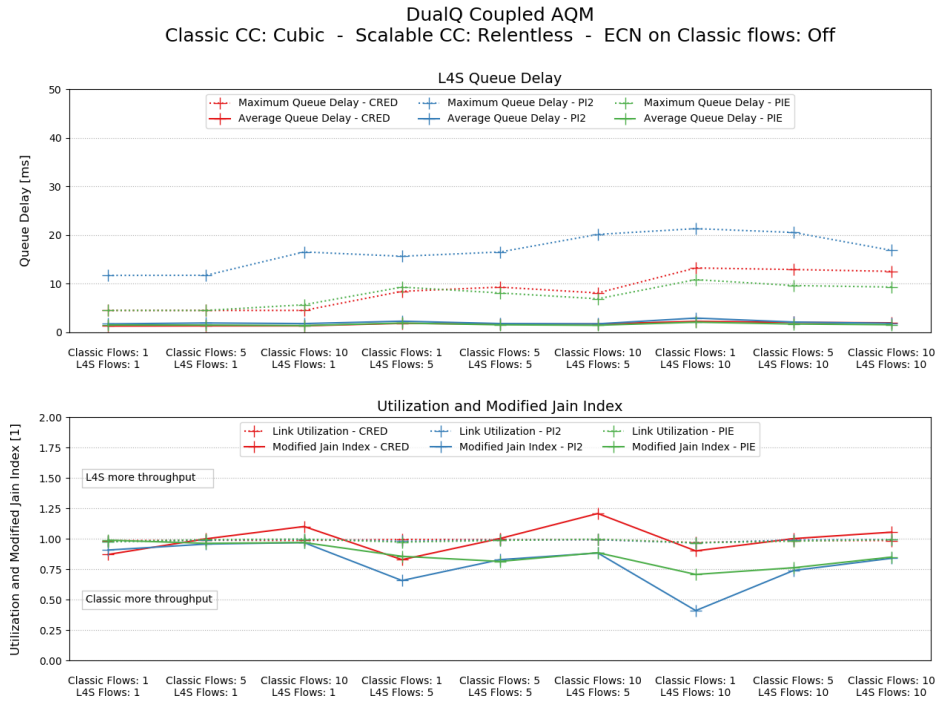


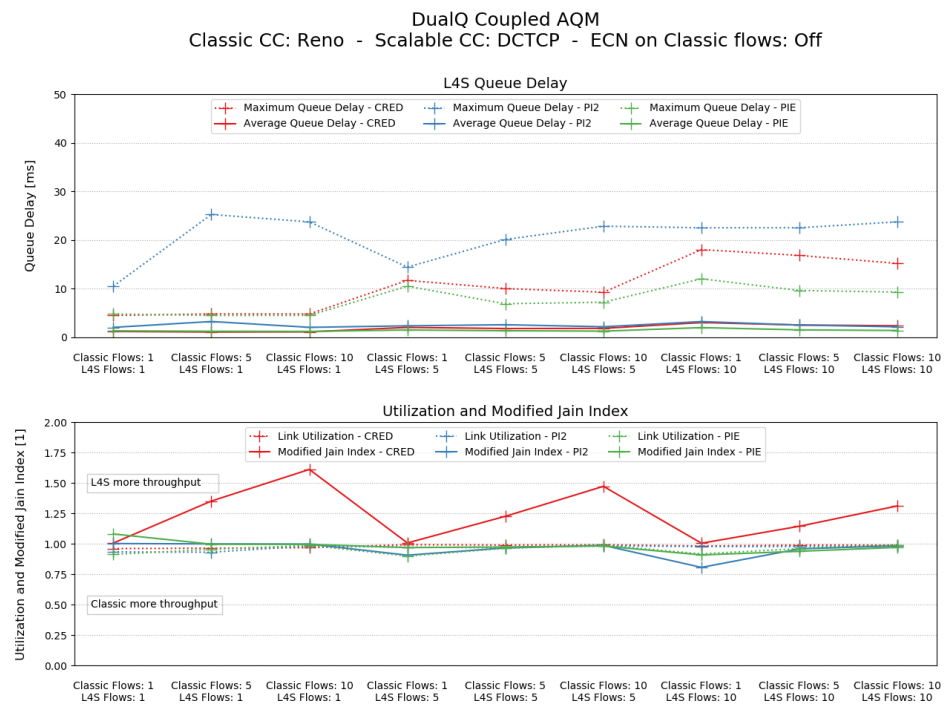
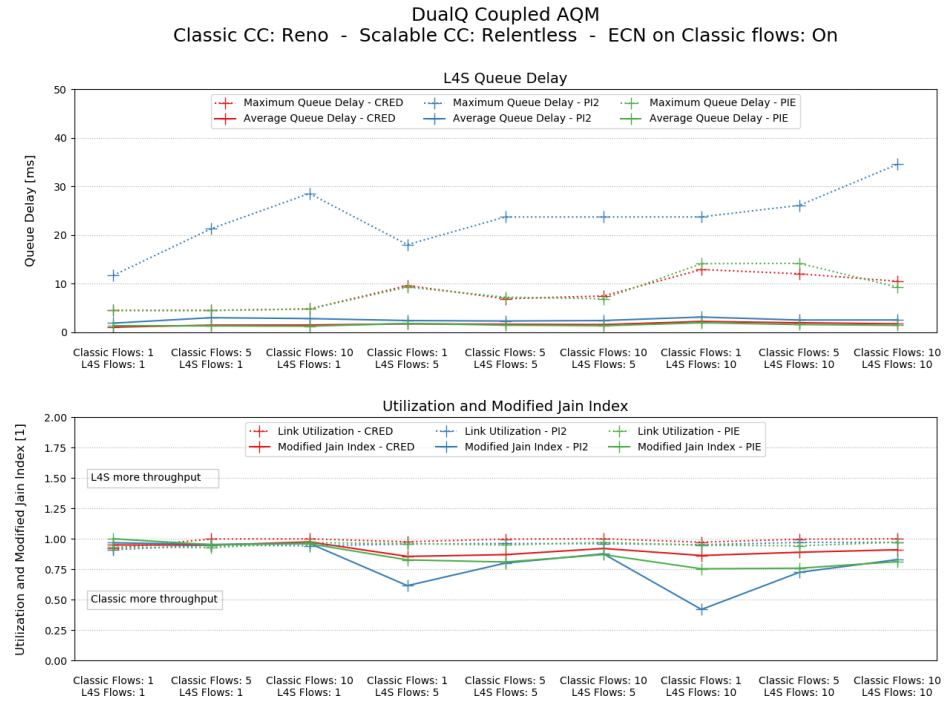


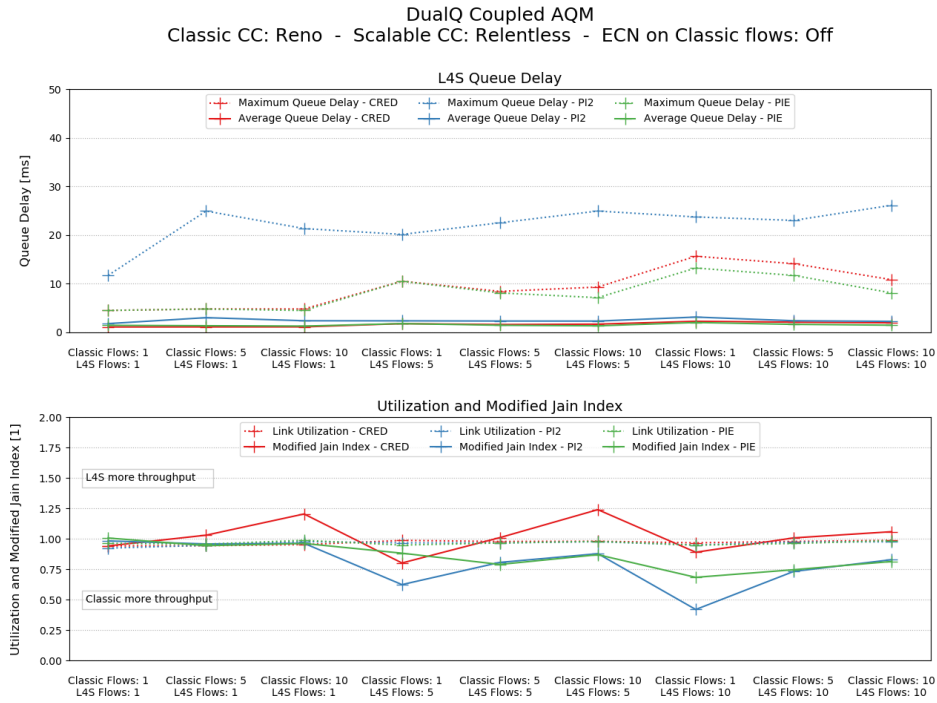




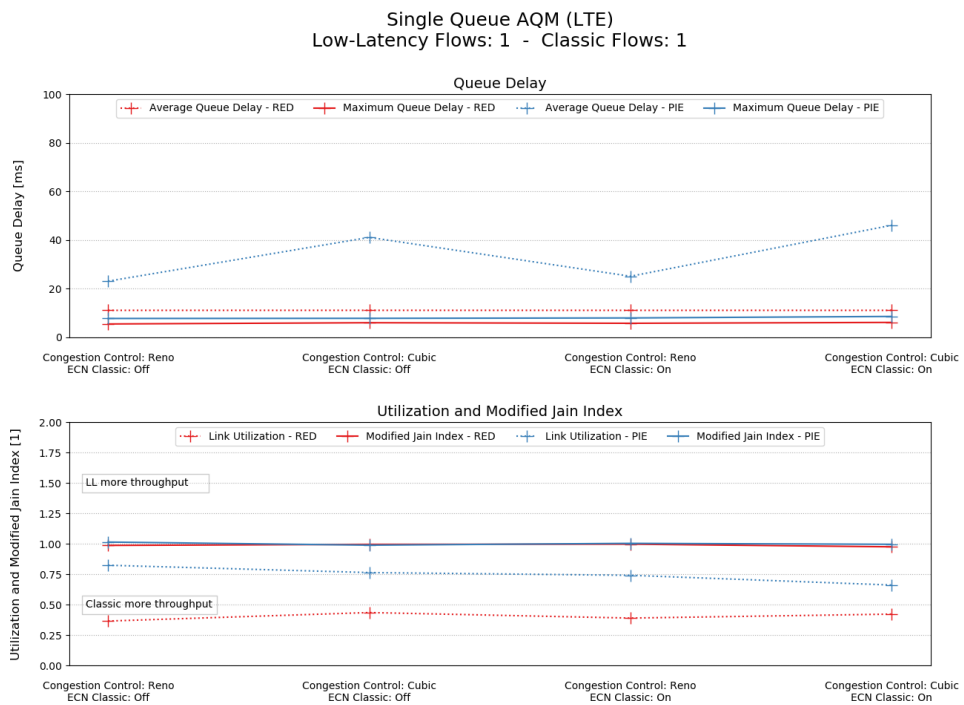


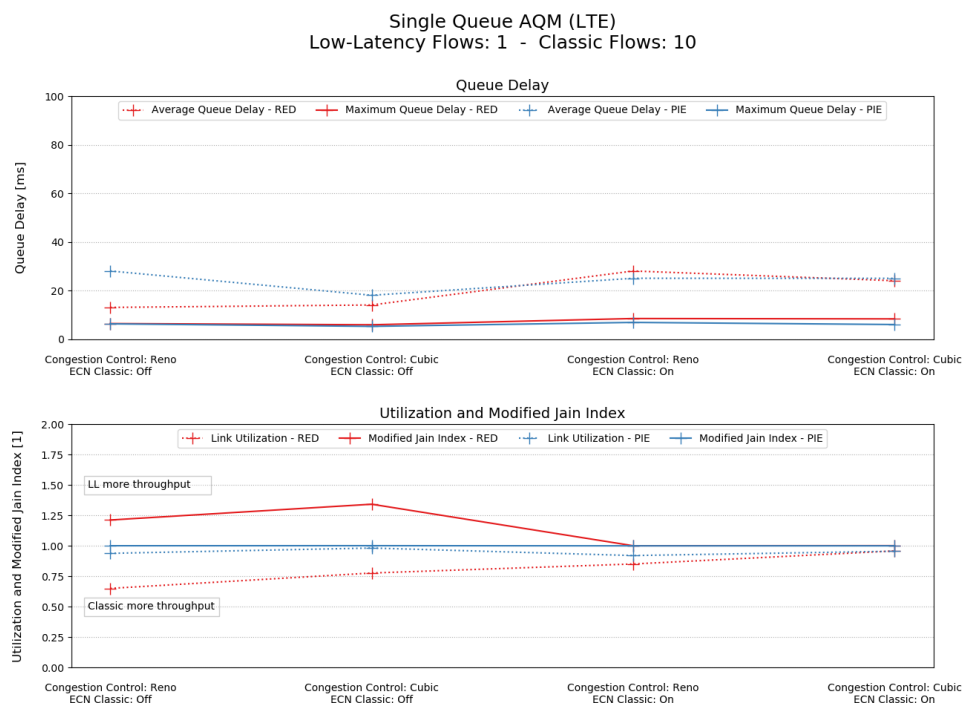
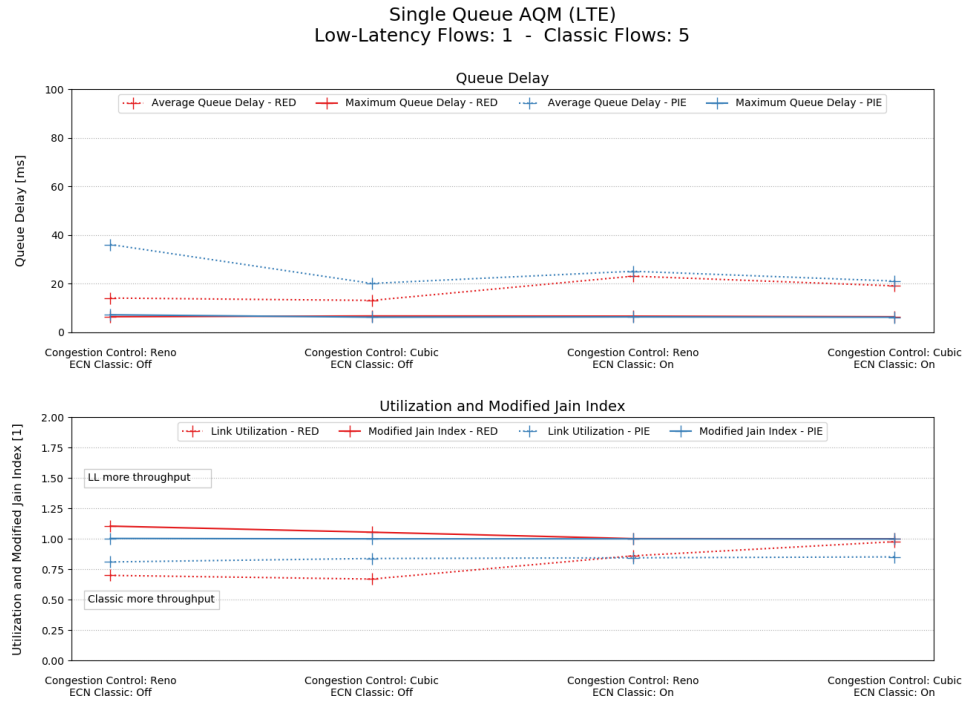


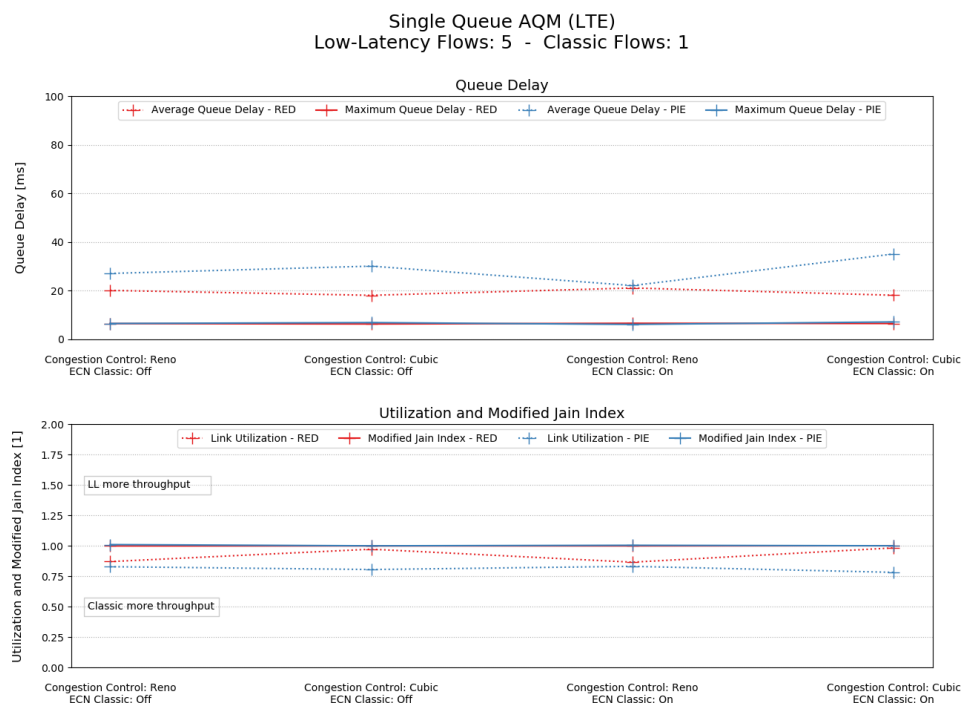
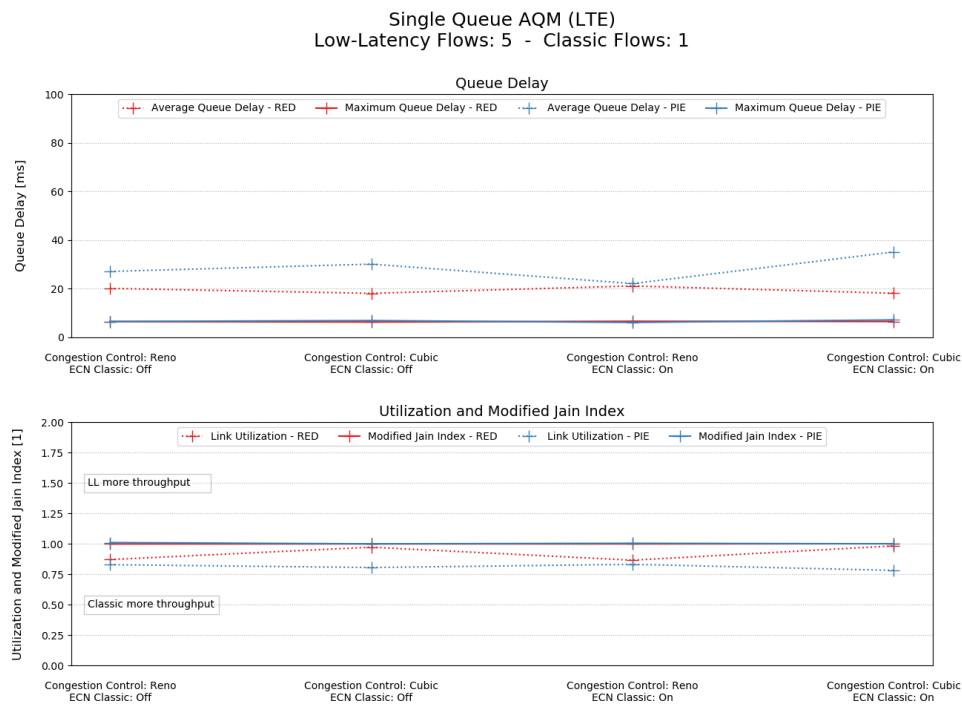


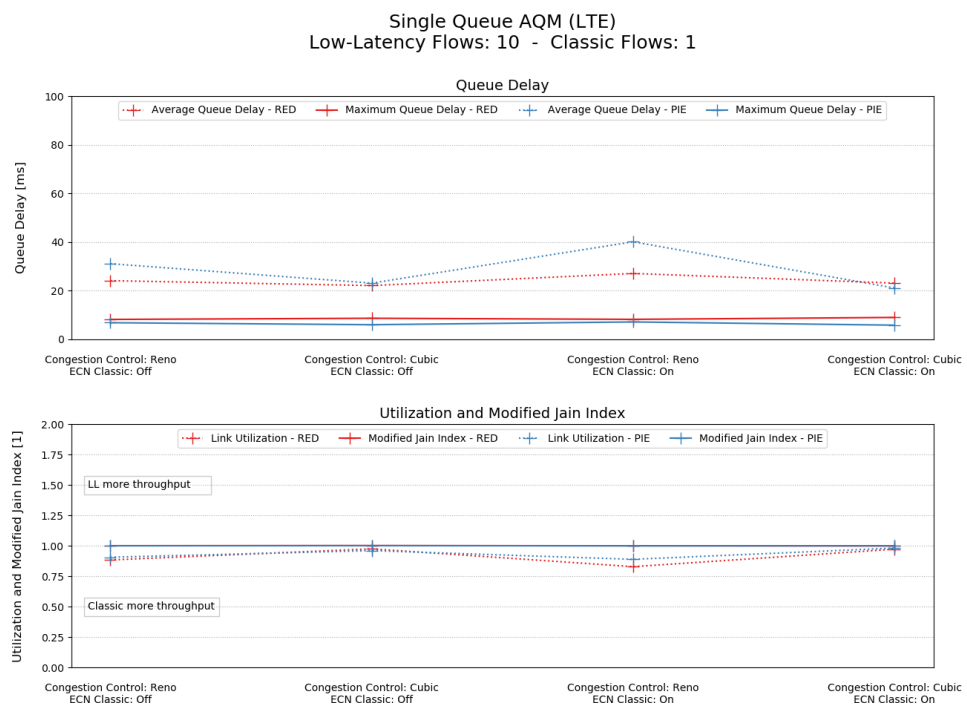
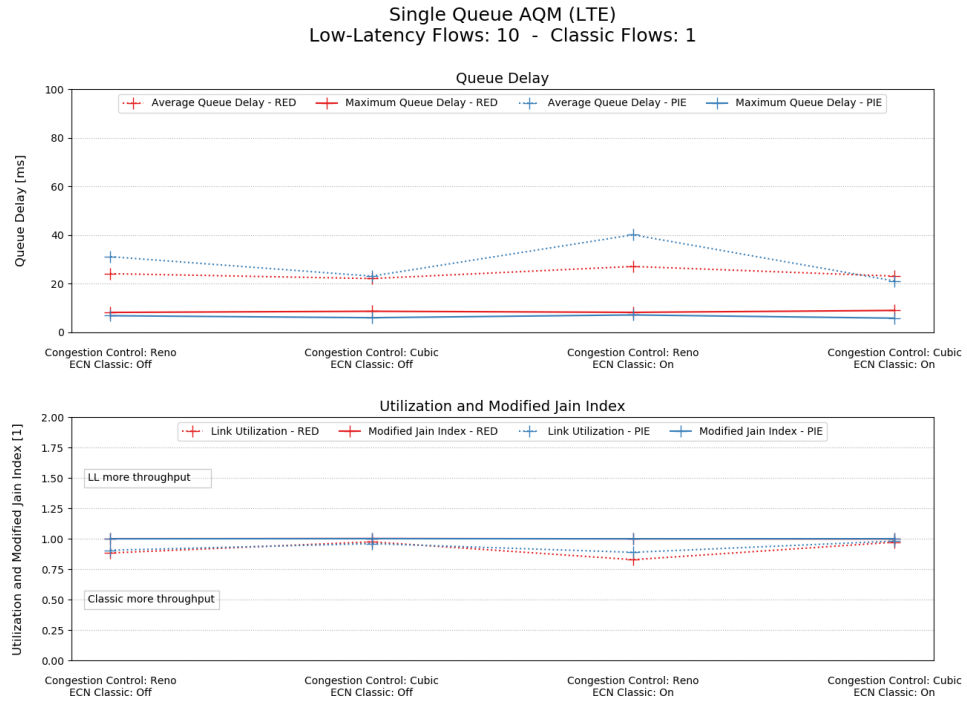


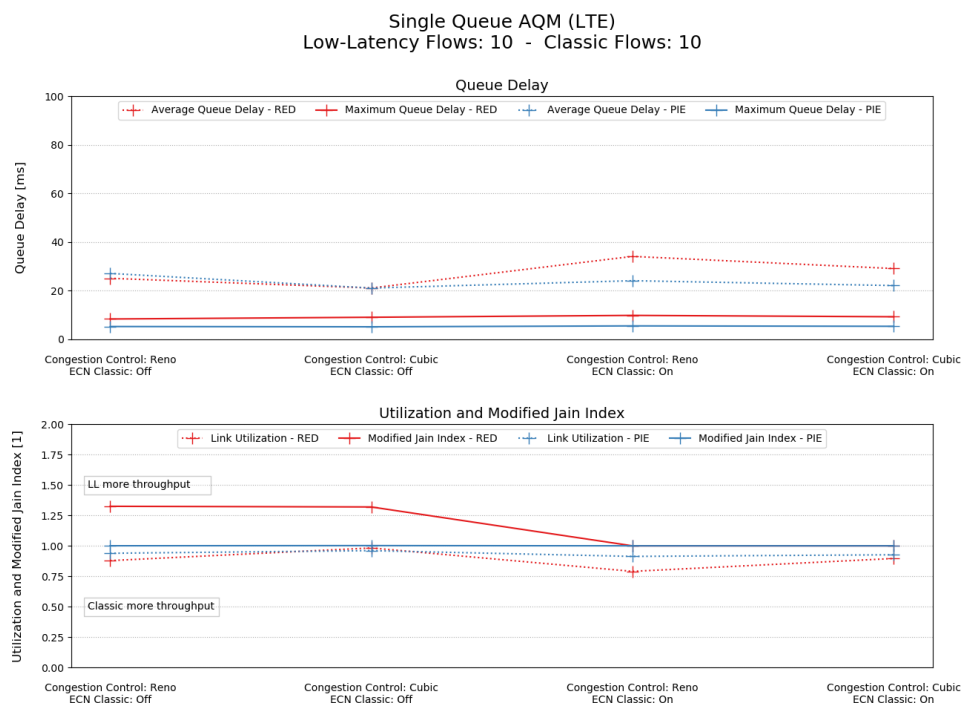
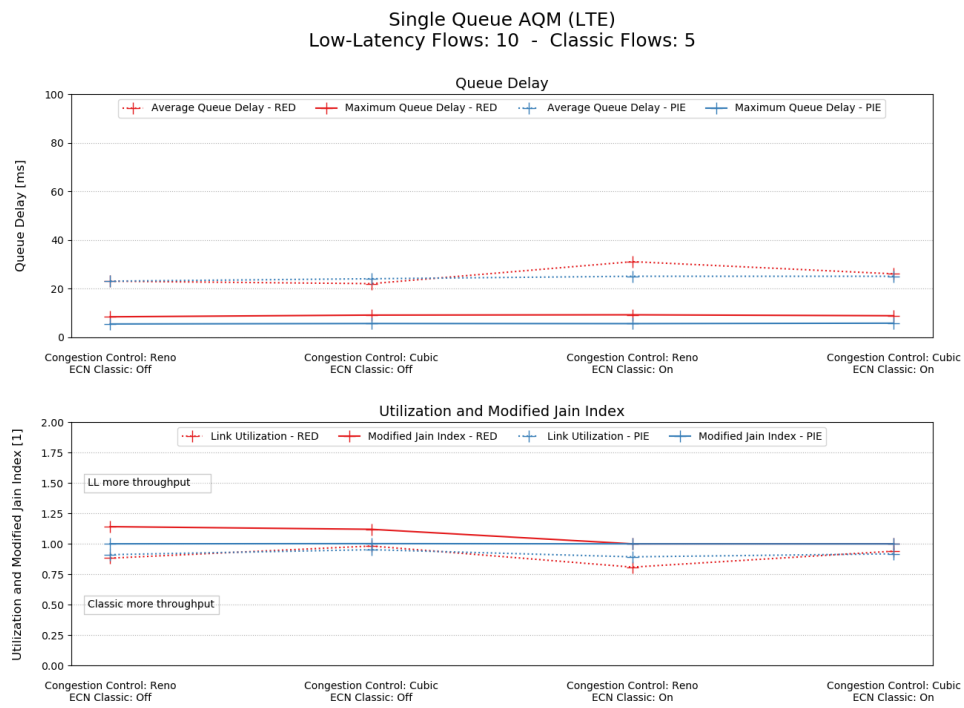
A.2 Plots from LTE Link Simulations

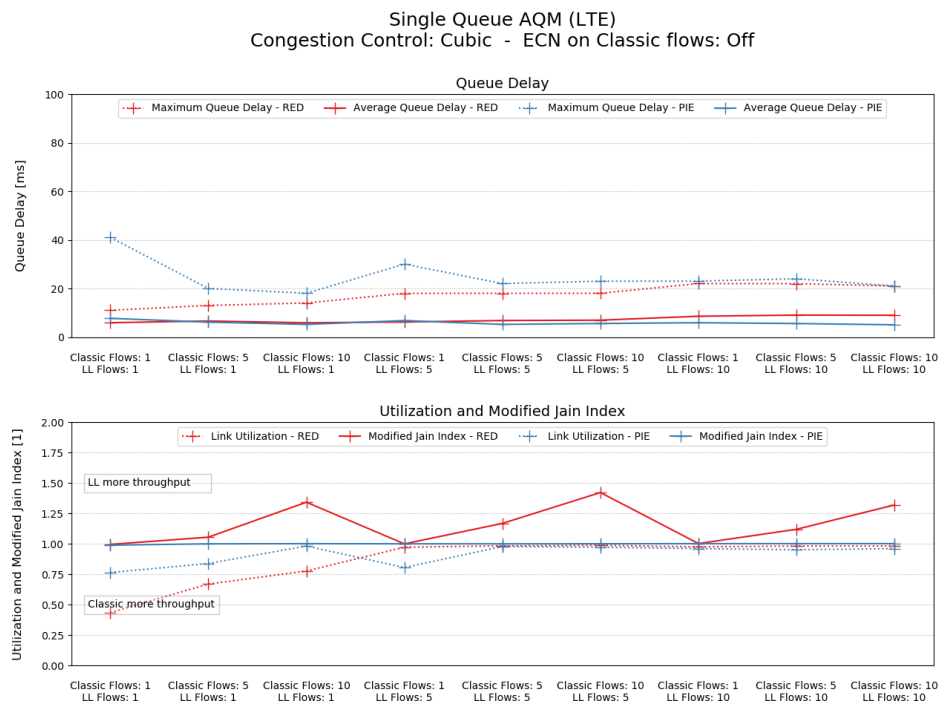
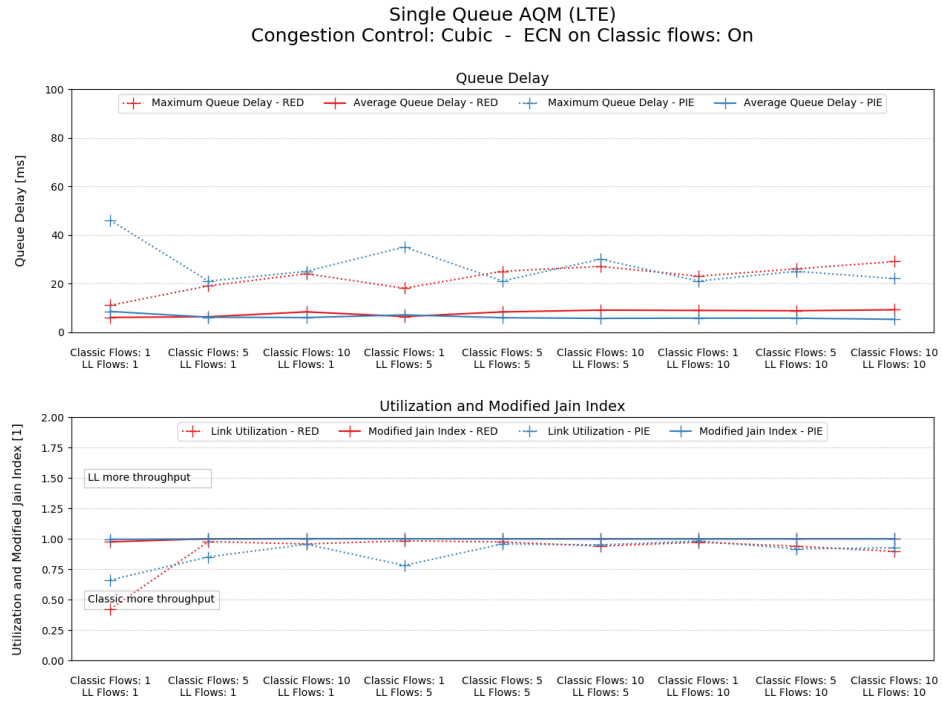


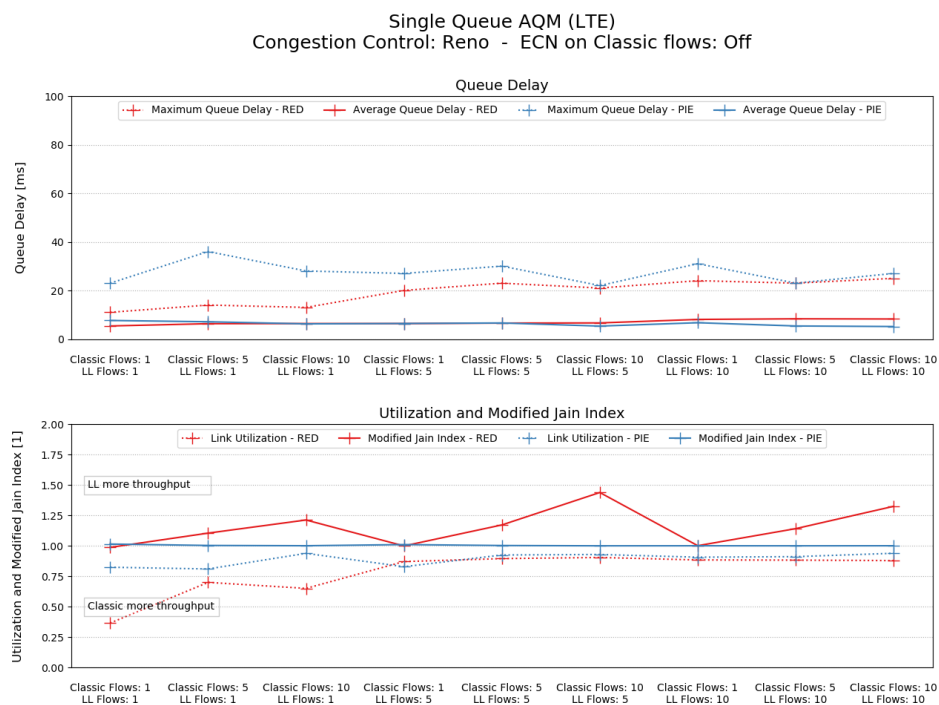
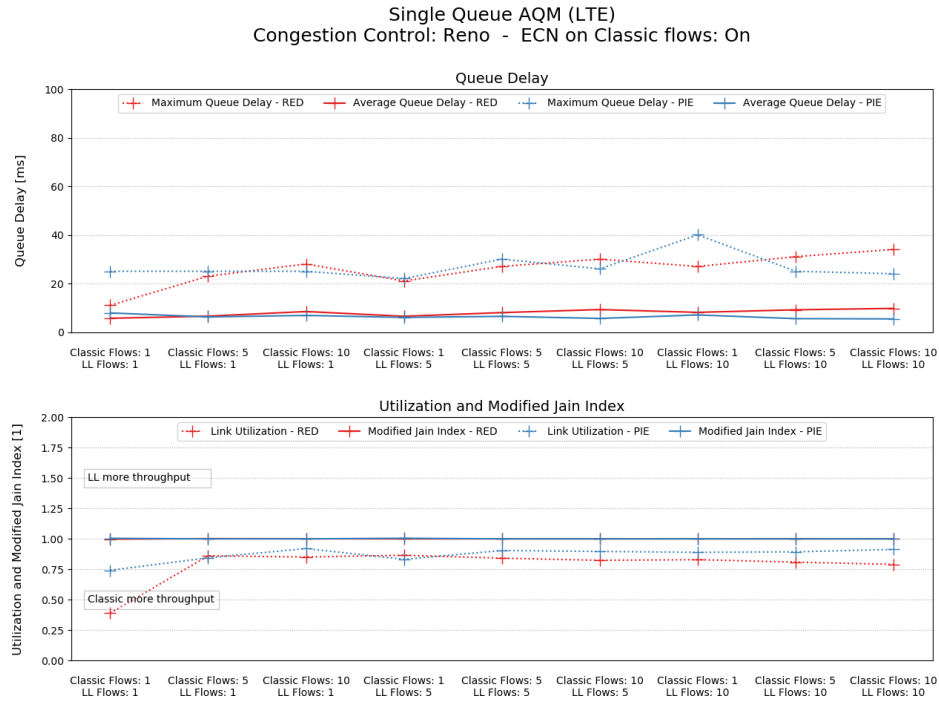




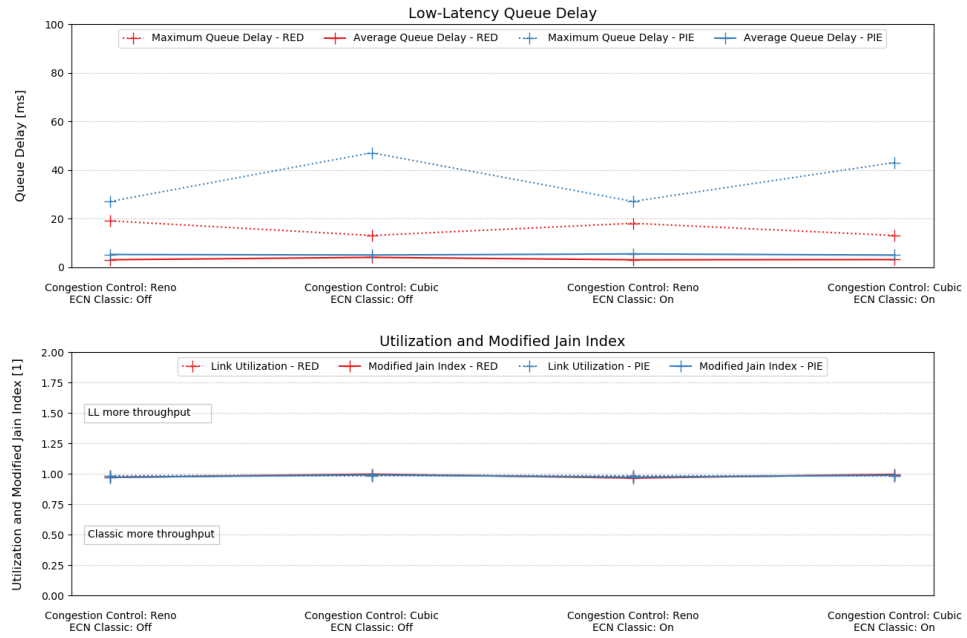




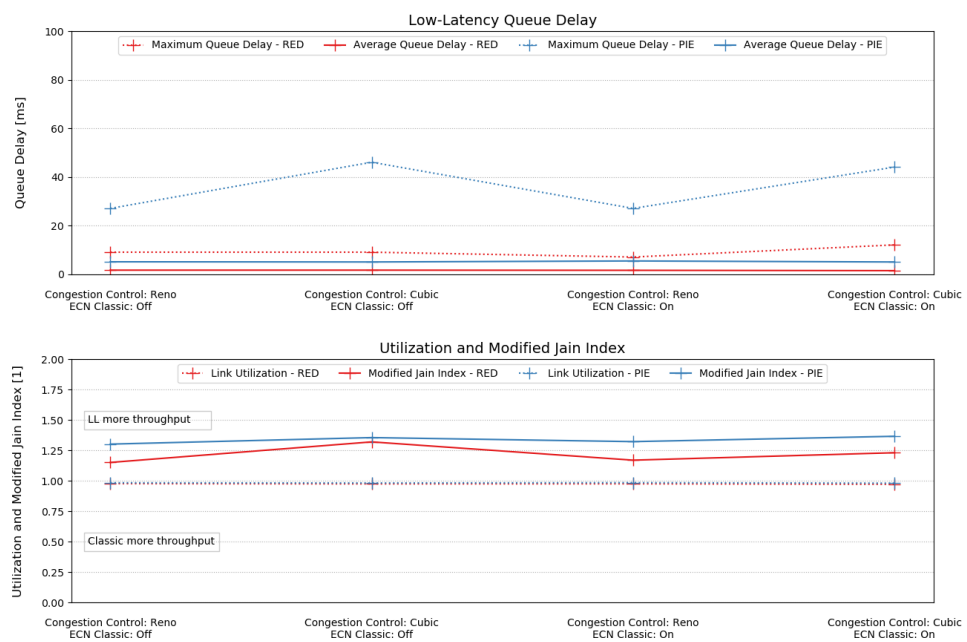


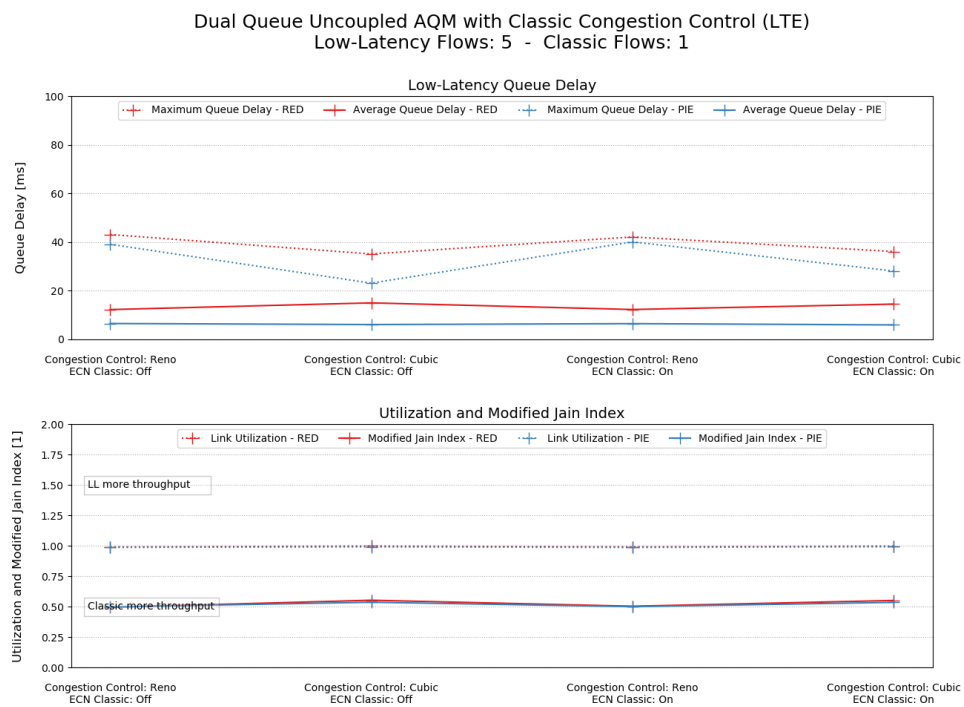
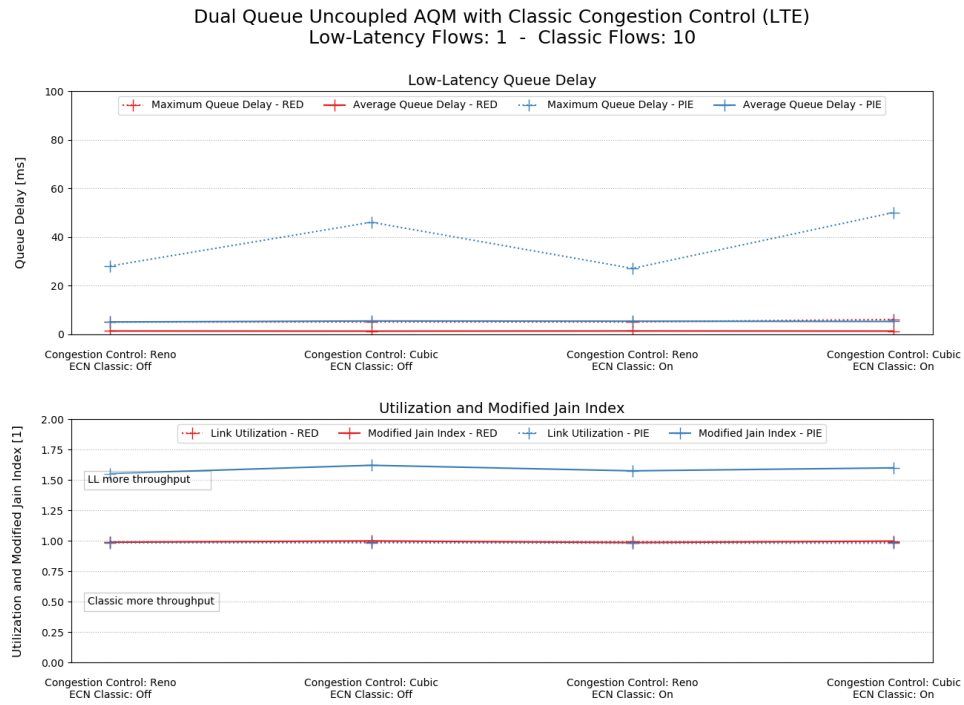


Dual Queue Uncoupled AQM with Classic Congestion Control (LTE)
Low-Latency Flows: 1 - Classic Flows: 1

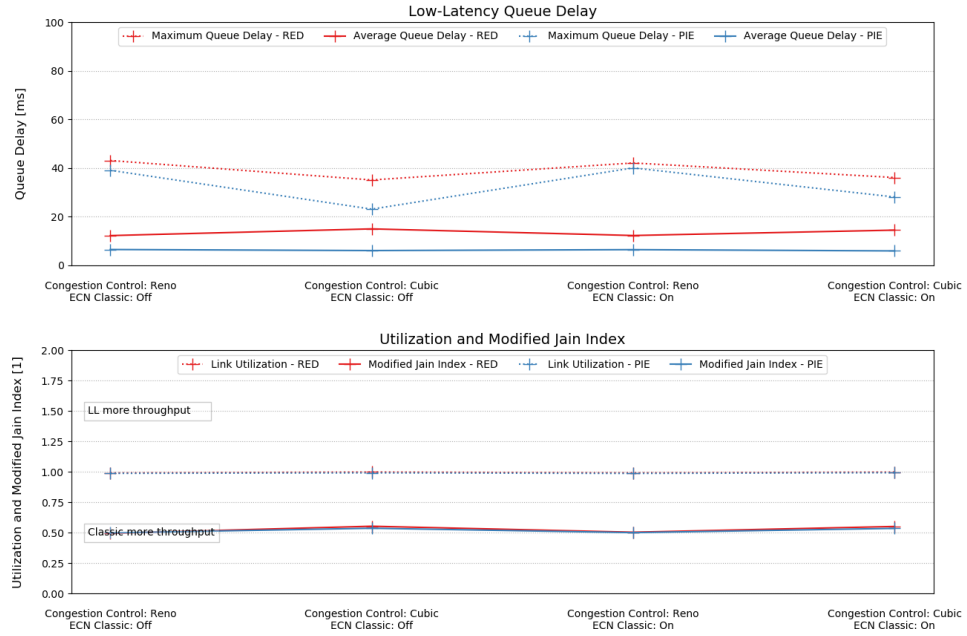


Dual Queue Uncoupled AQM with Classic Congestion Control (LTE)
Low-Latency Flows: 1 - Classic Flows: 5

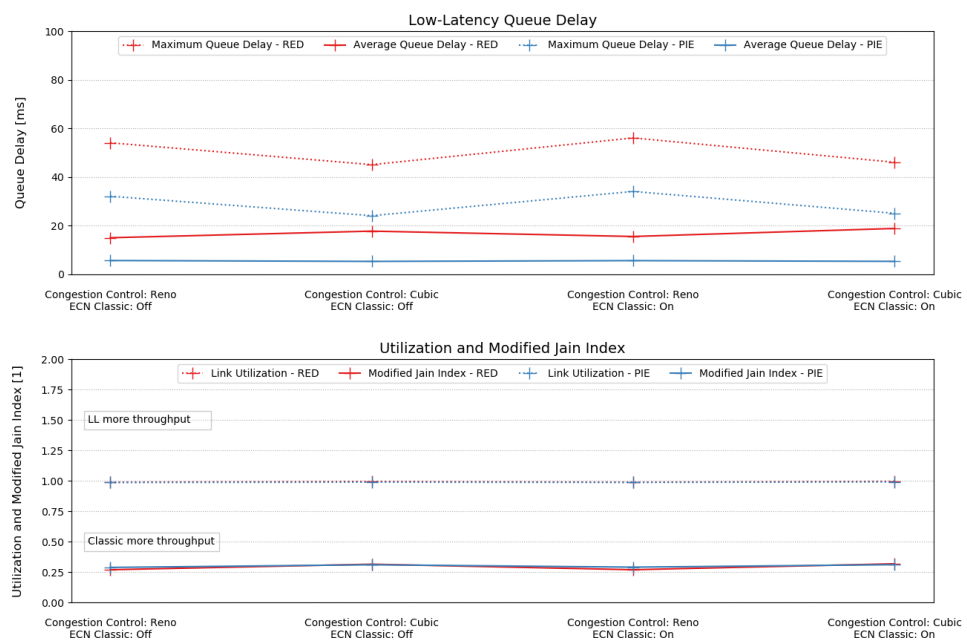


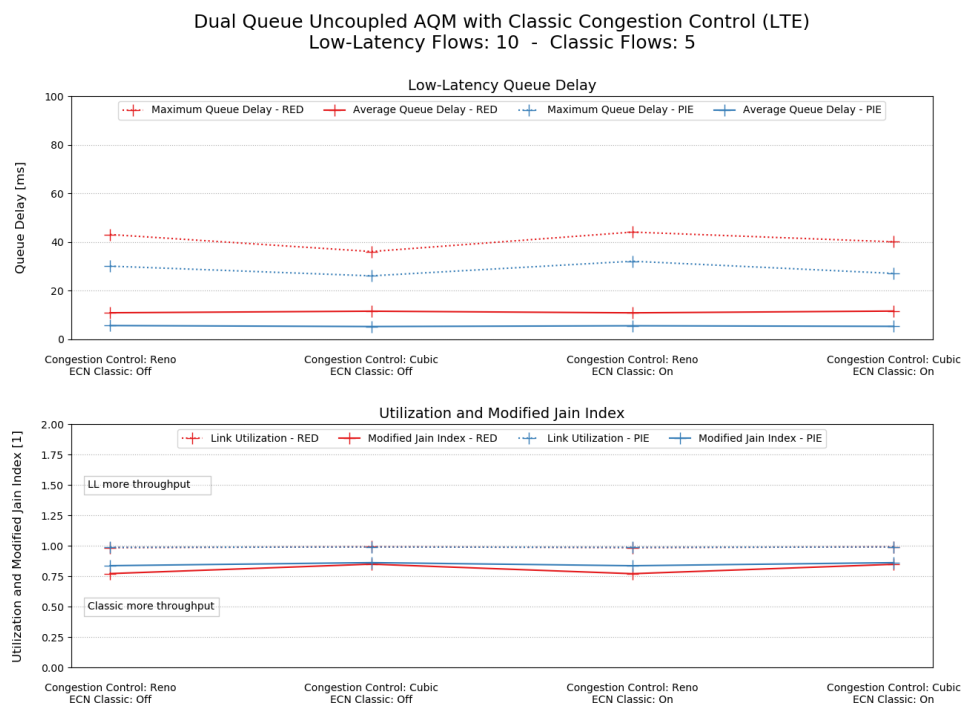
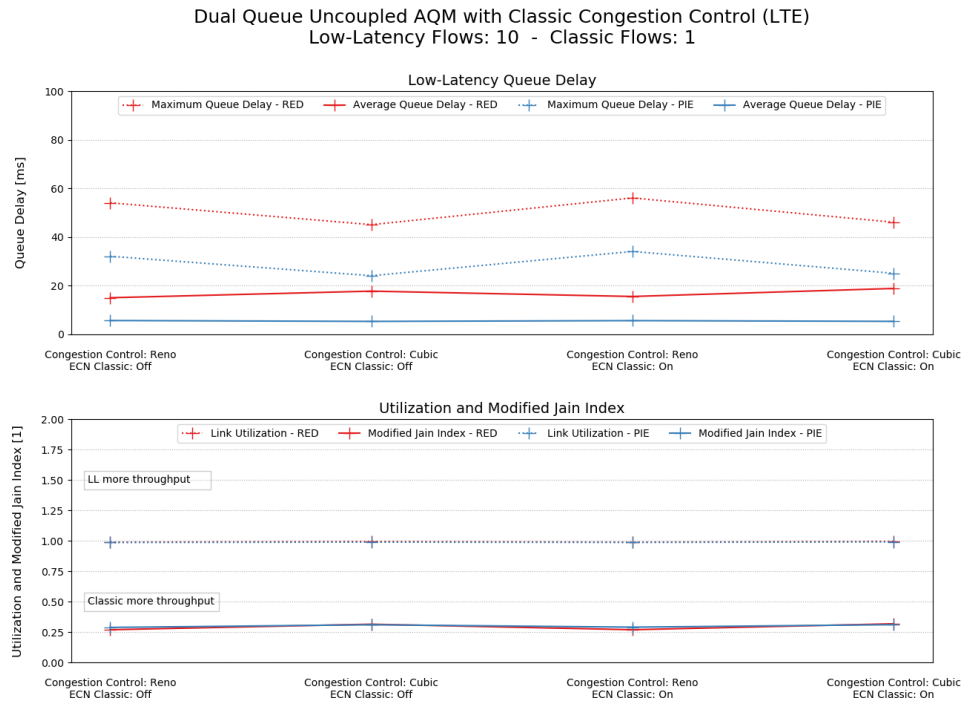


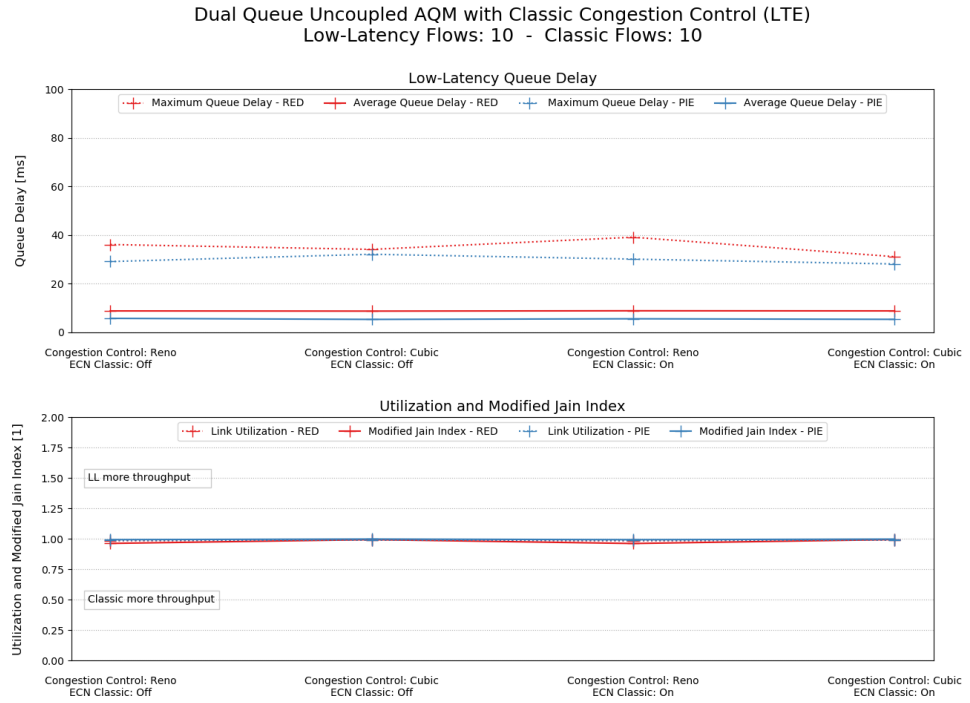
Dual Queue Uncoupled AQM with Classic Congestion Control (LTE)
Low-Latency Flows: 5 - Classic Flows: 1



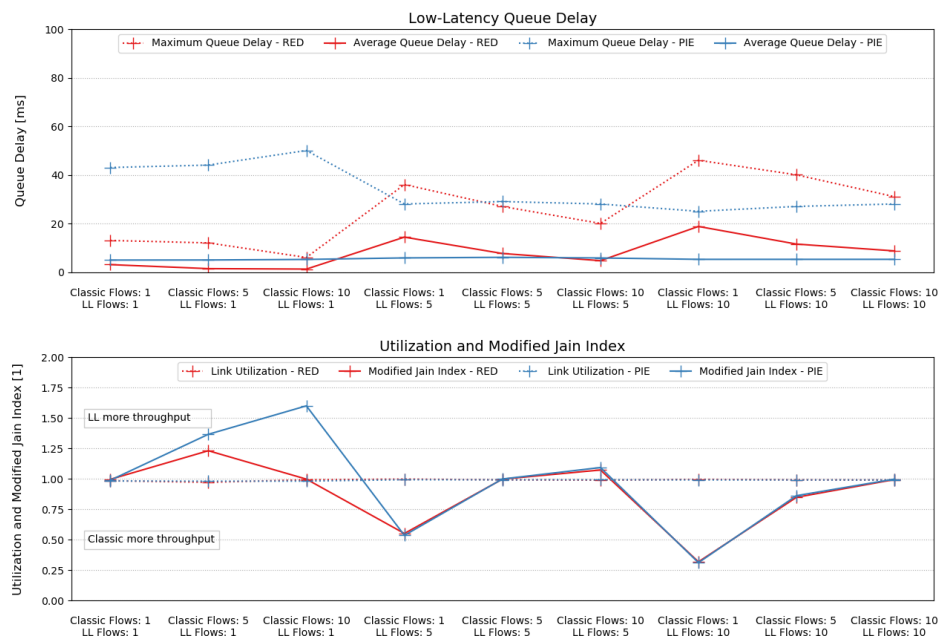
Dual Queue Uncoupled AQM with Classic Congestion Control (LTE)
Low-Latency Flows: 10 - Classic Flows: 1

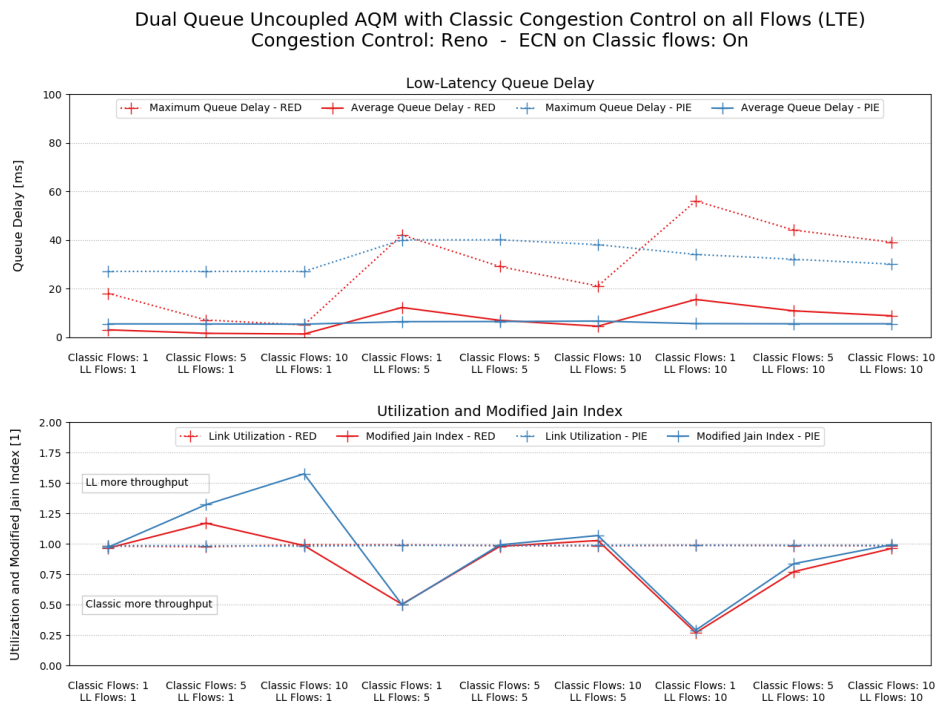
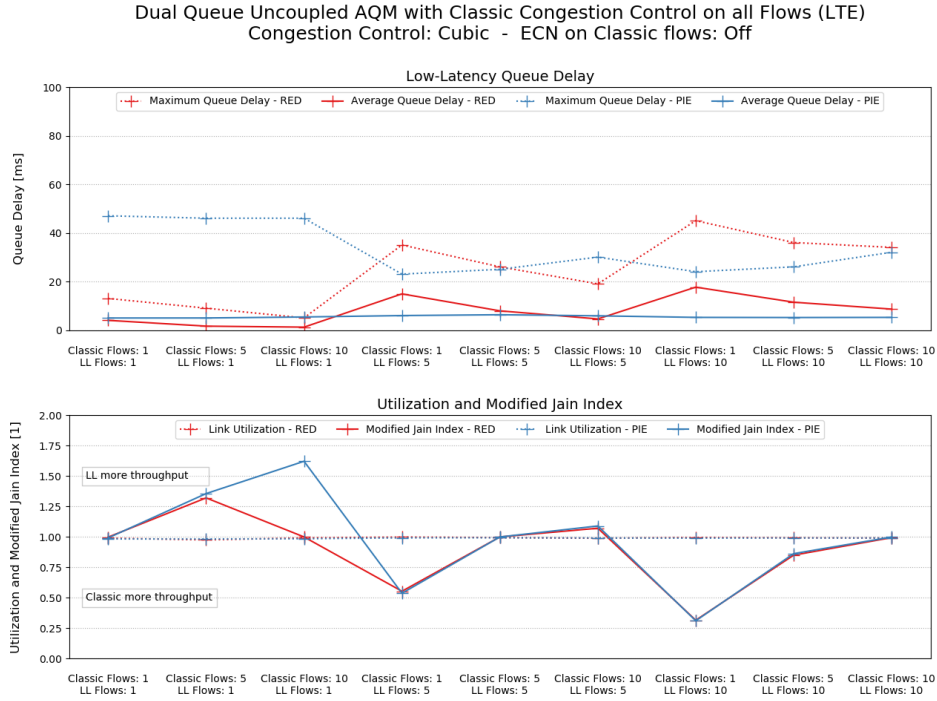




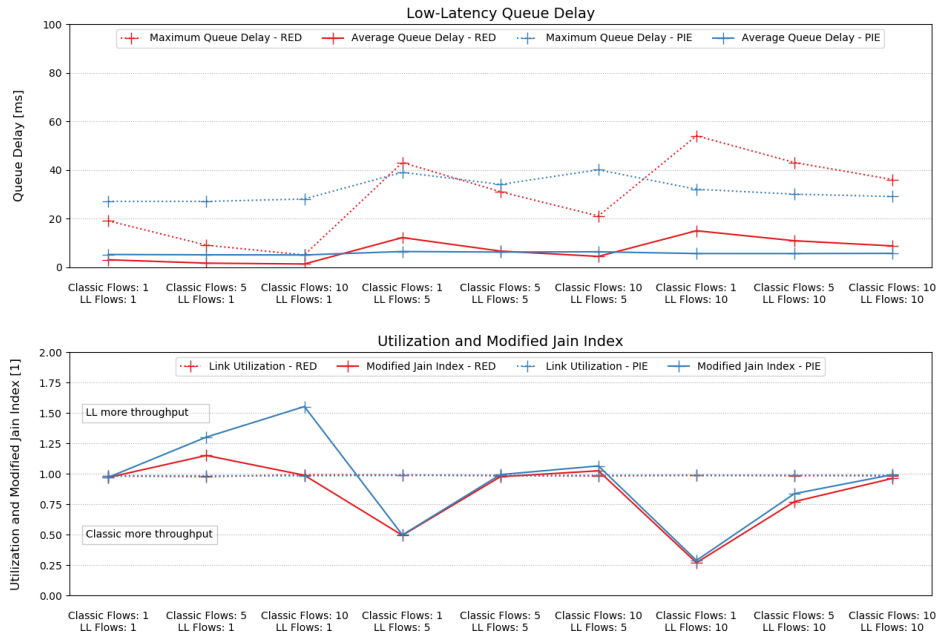


Dual Queue Uncoupled AQM with Classic Congestion Control on all Flows (LTE) Congestion Control: Cubic - ECN on Classic flows: On

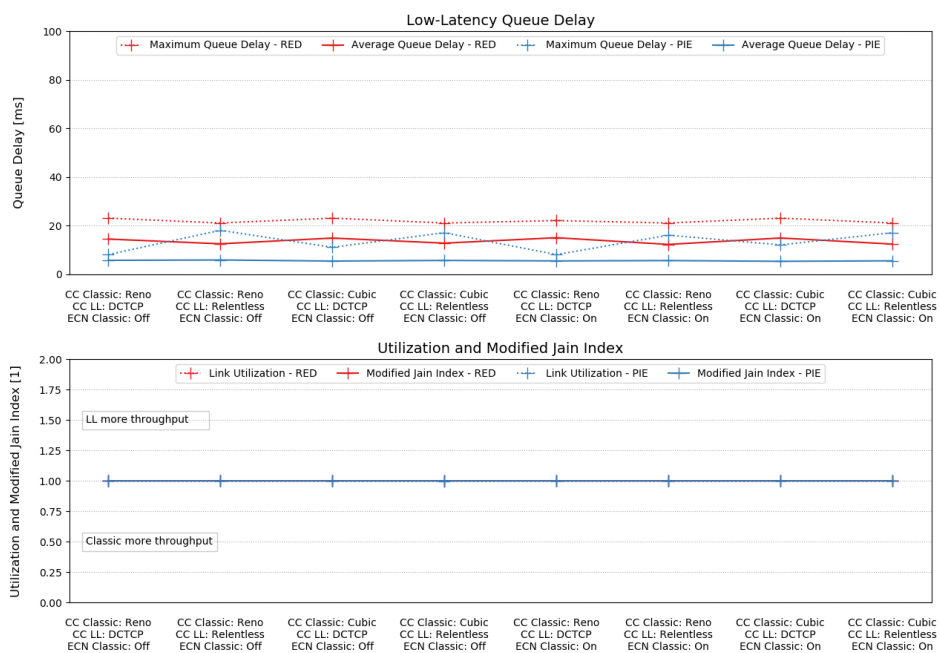


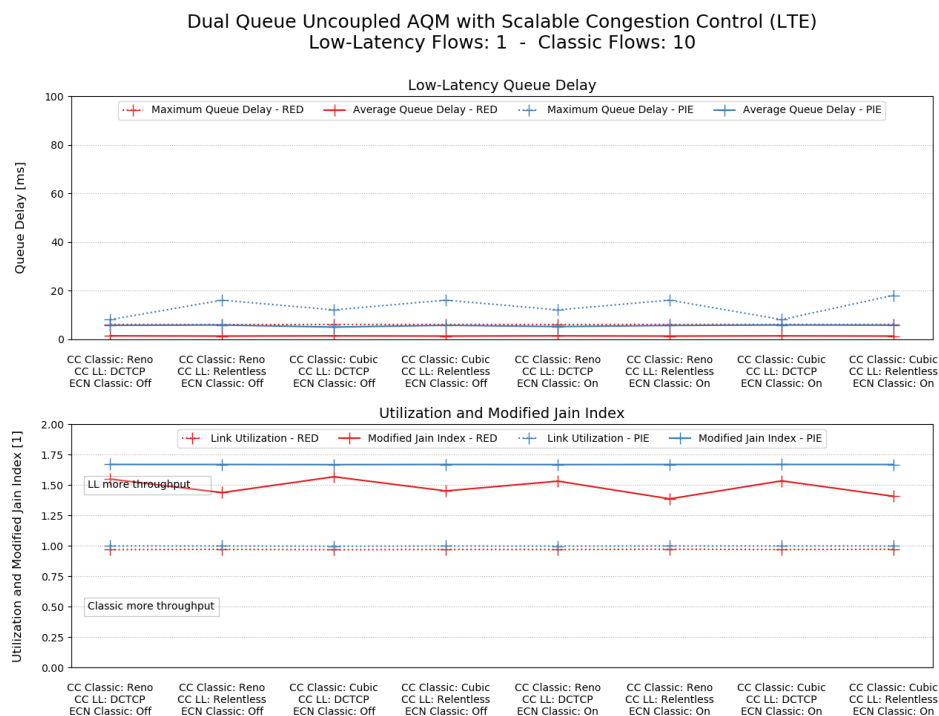
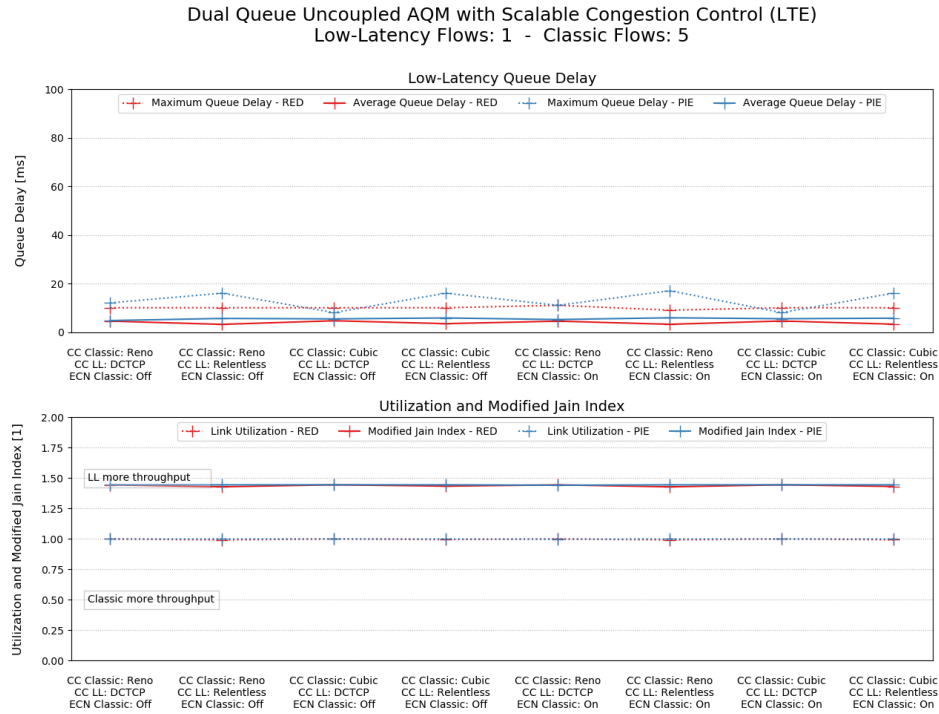


Dual Queue Uncoupled AQM with Classic Congestion Control on all Flows (LTE)
Congestion Control: Reno - ECN on Classic flows: Off

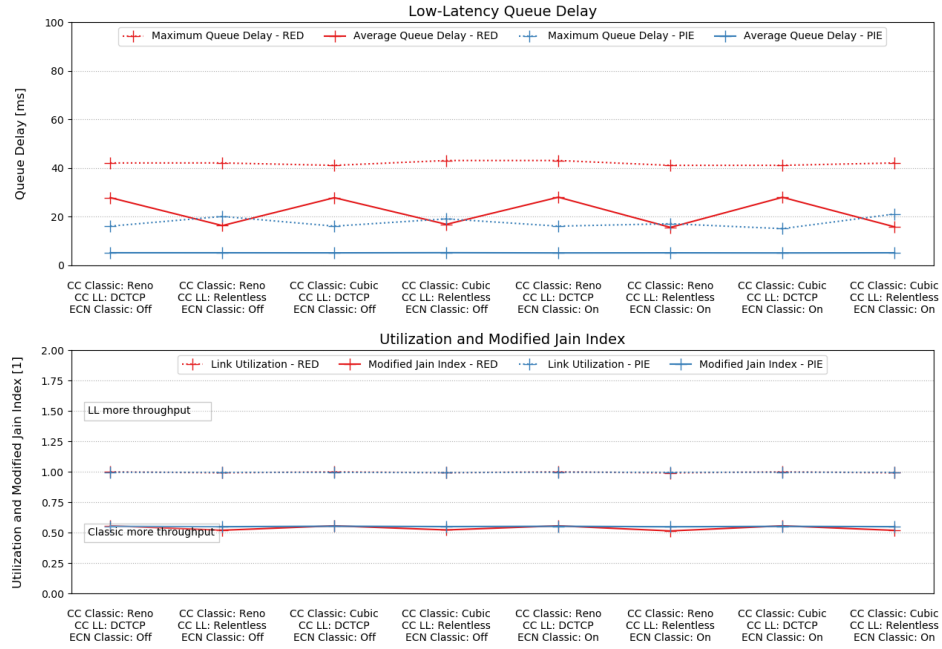


Dual Queue Uncoupled AQM with Scalable Congestion Control (LTE)
Low-Latency Flows: 1 - Classic Flows: 1

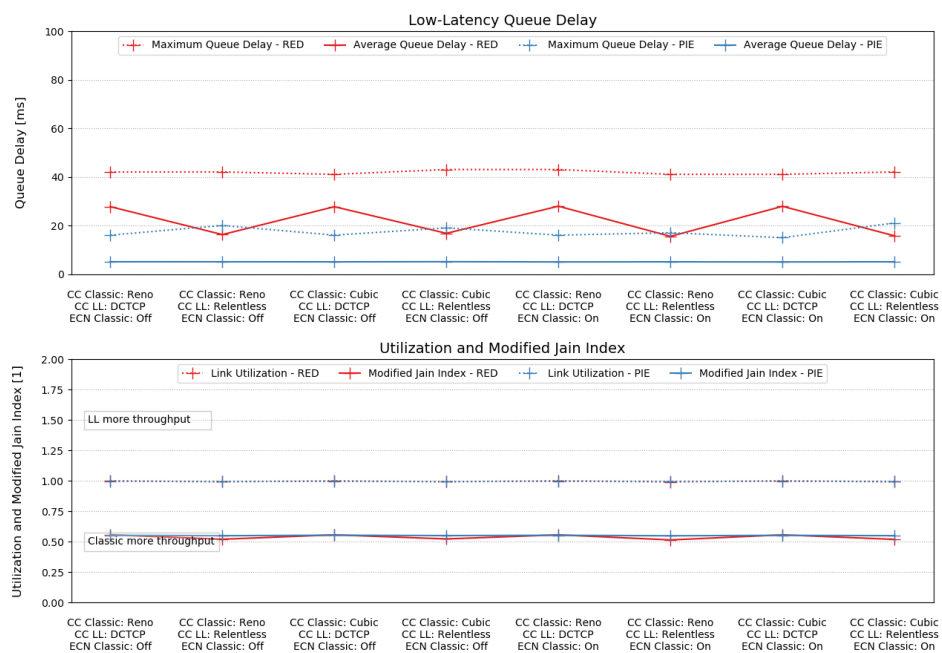


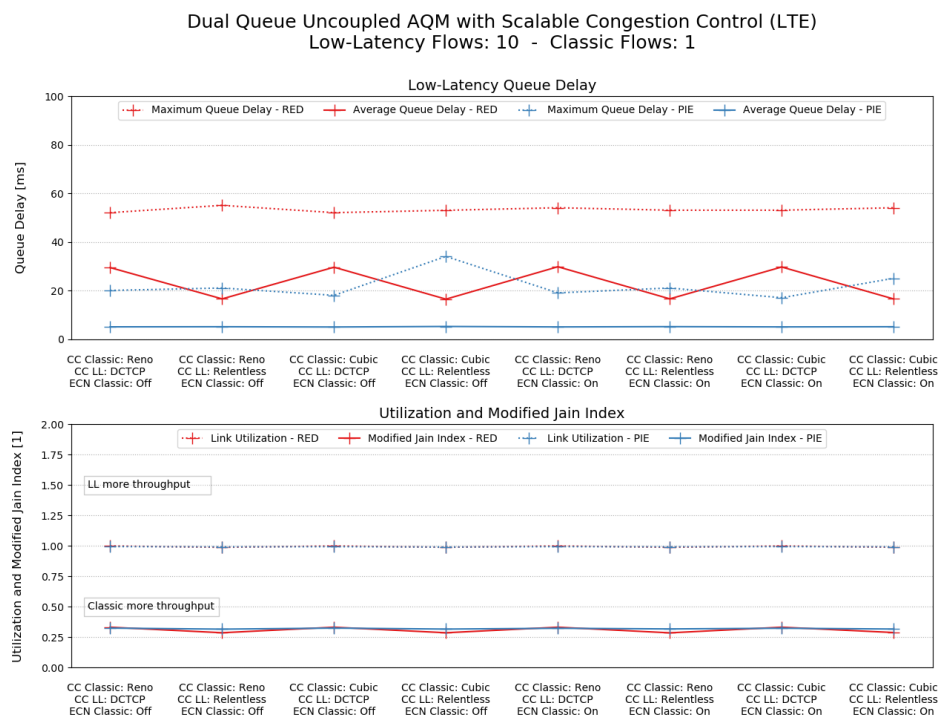
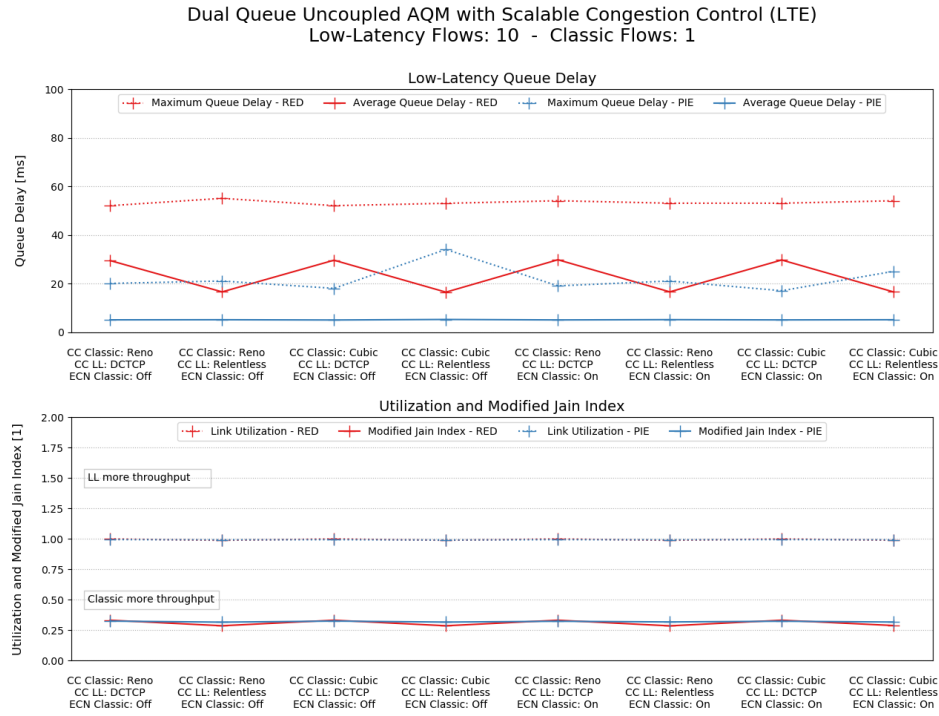


Dual Queue Uncoupled AQM with Scalable Congestion Control (LTE)
Low-Latency Flows: 5 - Classic Flows: 1

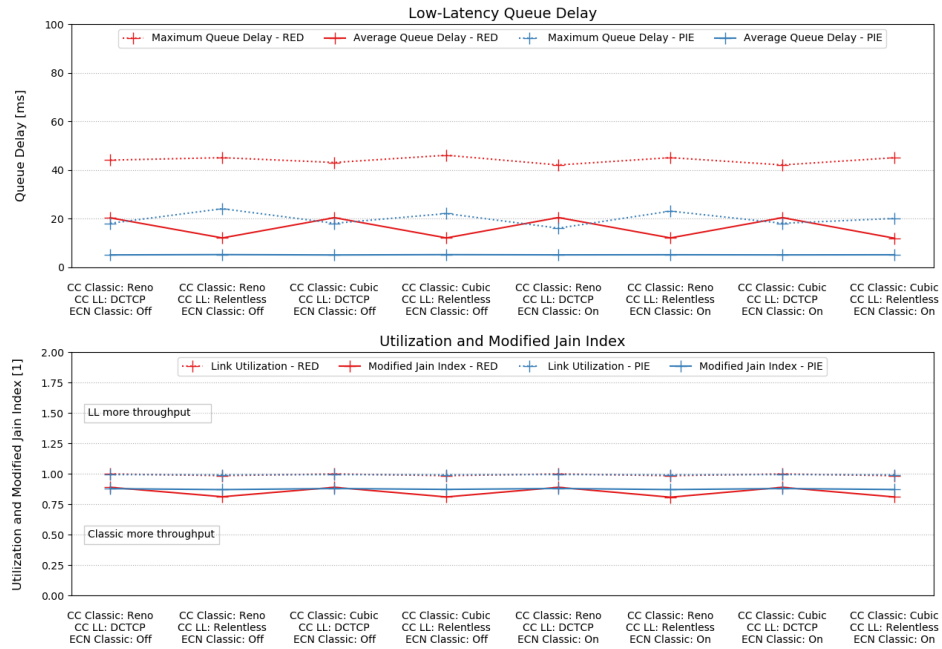


Dual Queue Uncoupled AQM with Scalable Congestion Control (LTE)
Low-Latency Flows: 5 - Classic Flows: 1

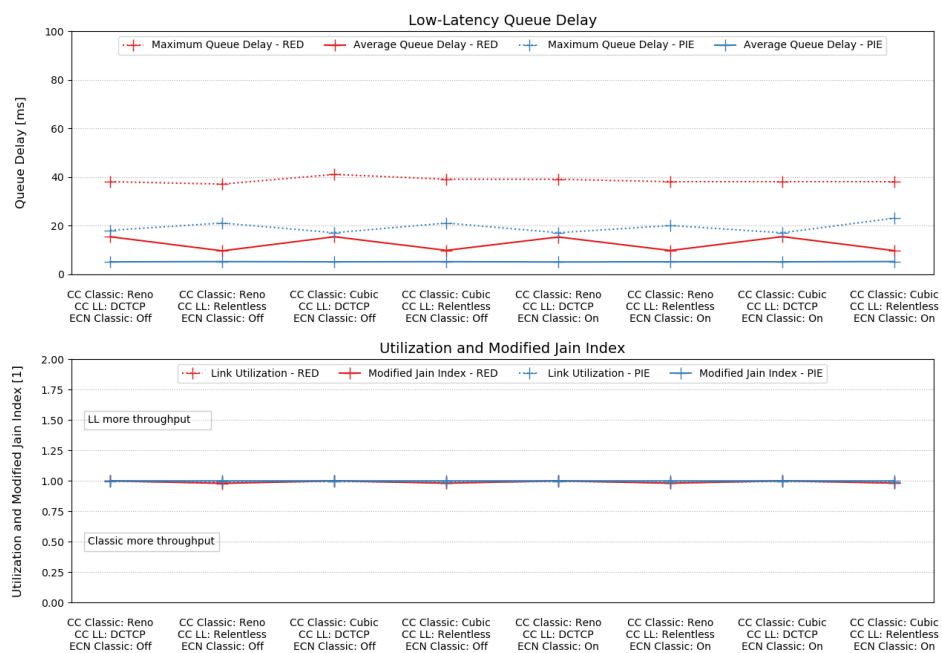


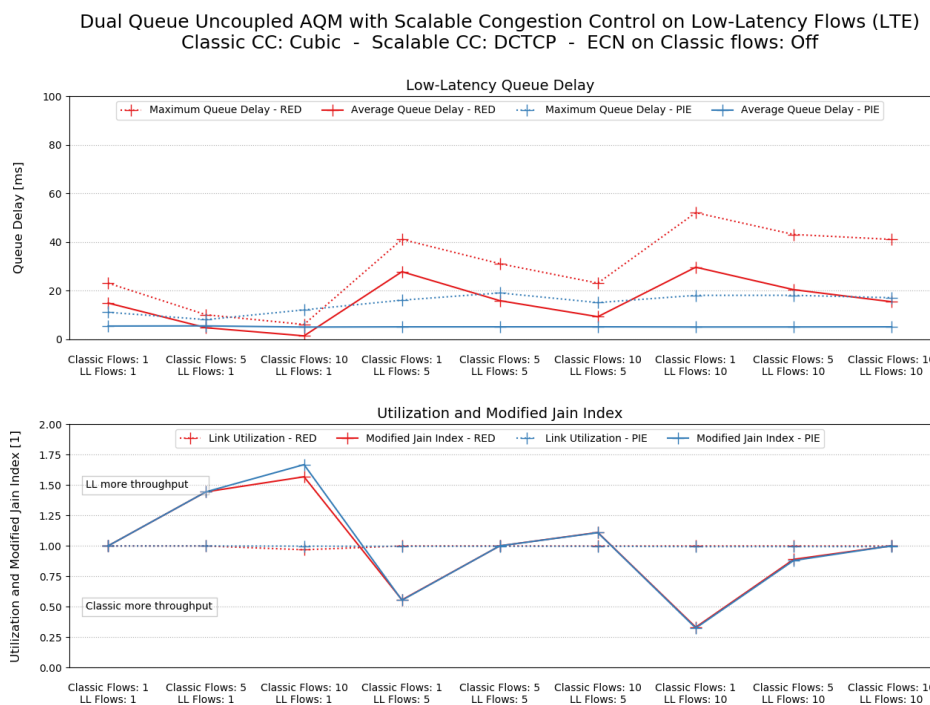
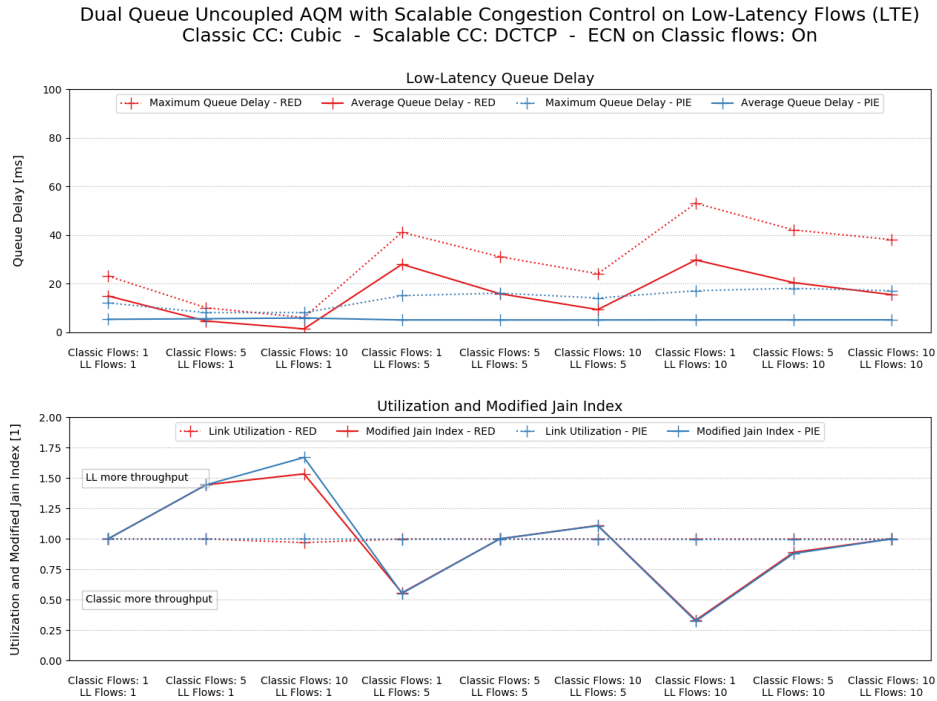


Dual Queue Uncoupled AQM with Scalable Congestion Control (LTE)
Low-Latency Flows: 10 - Classic Flows: 5

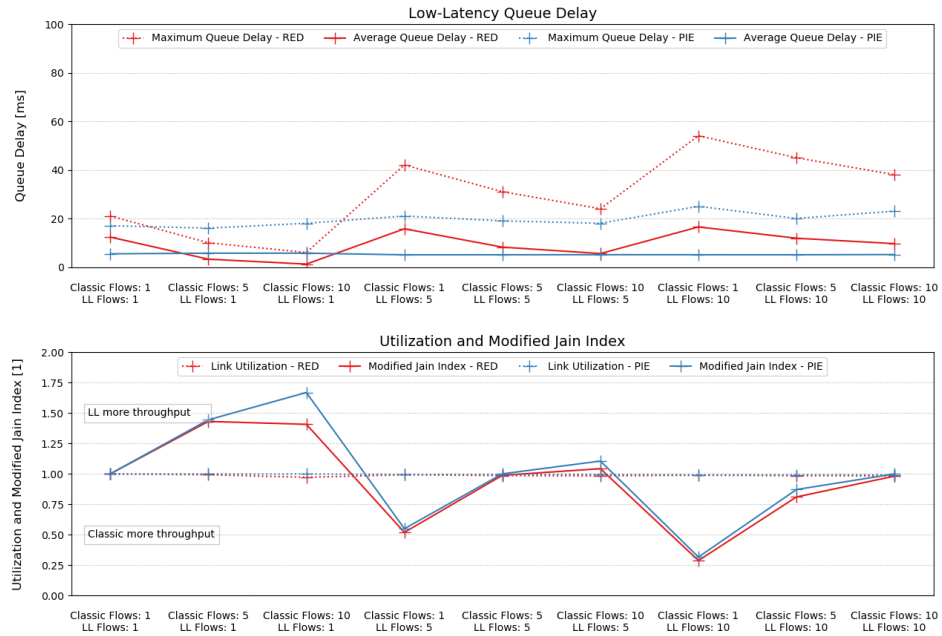


Dual Queue Uncoupled AQM with Scalable Congestion Control (LTE)
Low-Latency Flows: 10 - Classic Flows: 10

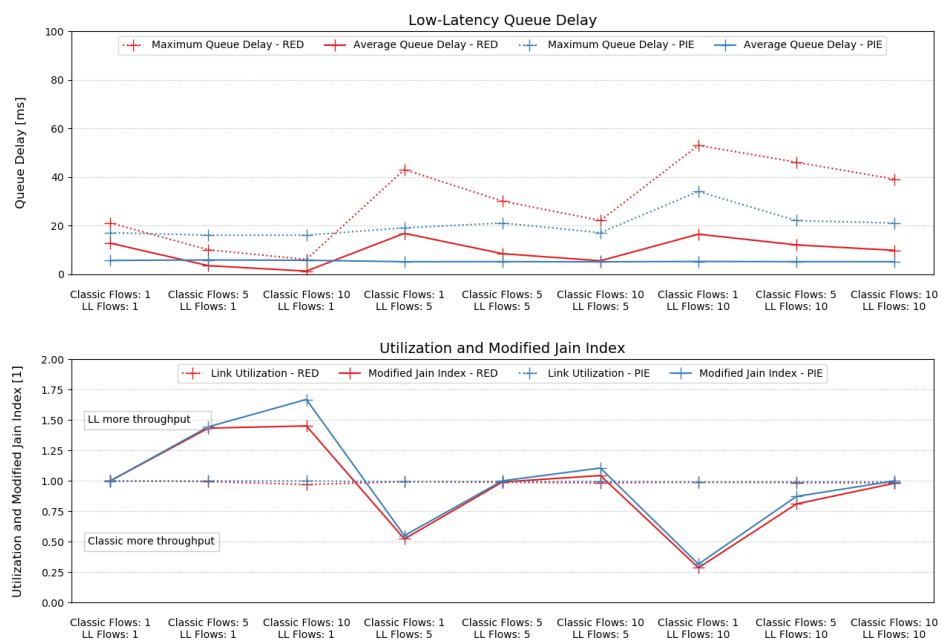


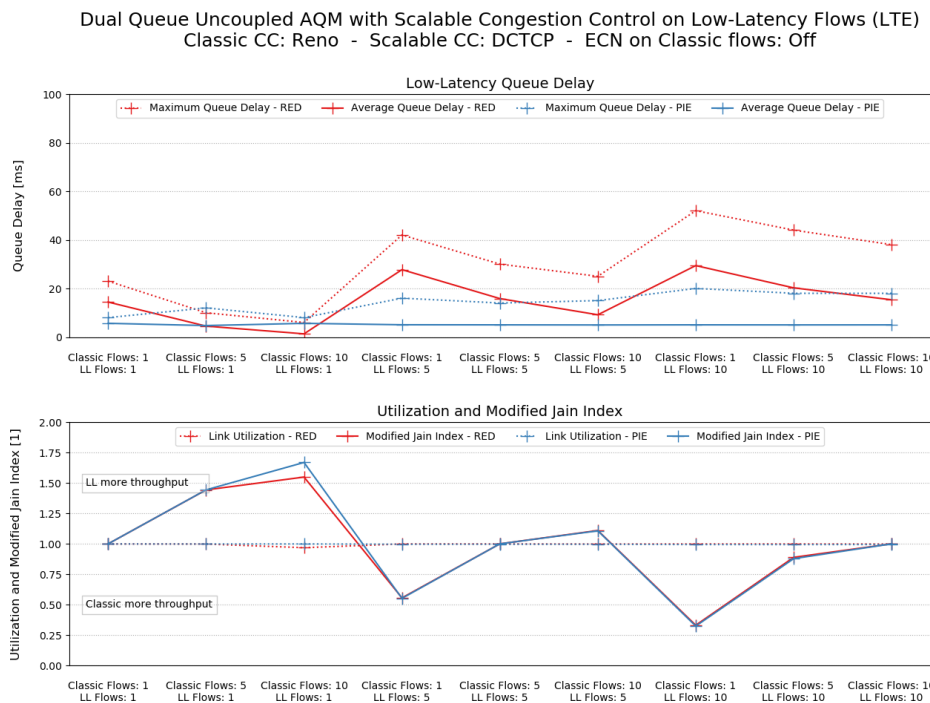
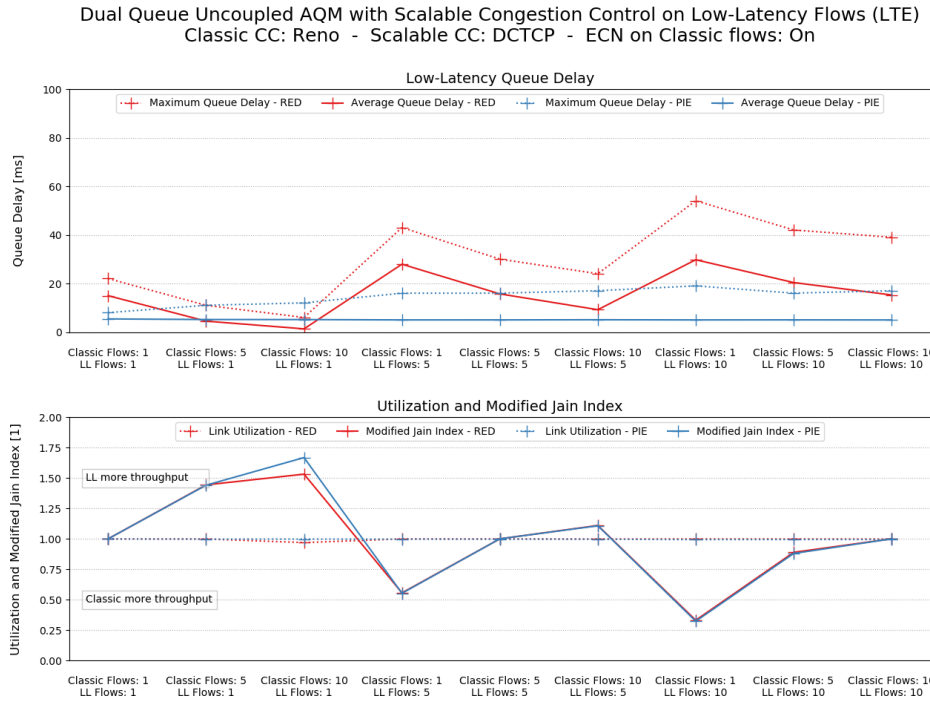


Dual Queue Uncoupled AQM with Scalable Congestion Control on Low-Latency Flows (LTE)
 Classic CC: Cubic - Scalable CC: Relentless - ECN on Classic flows: On

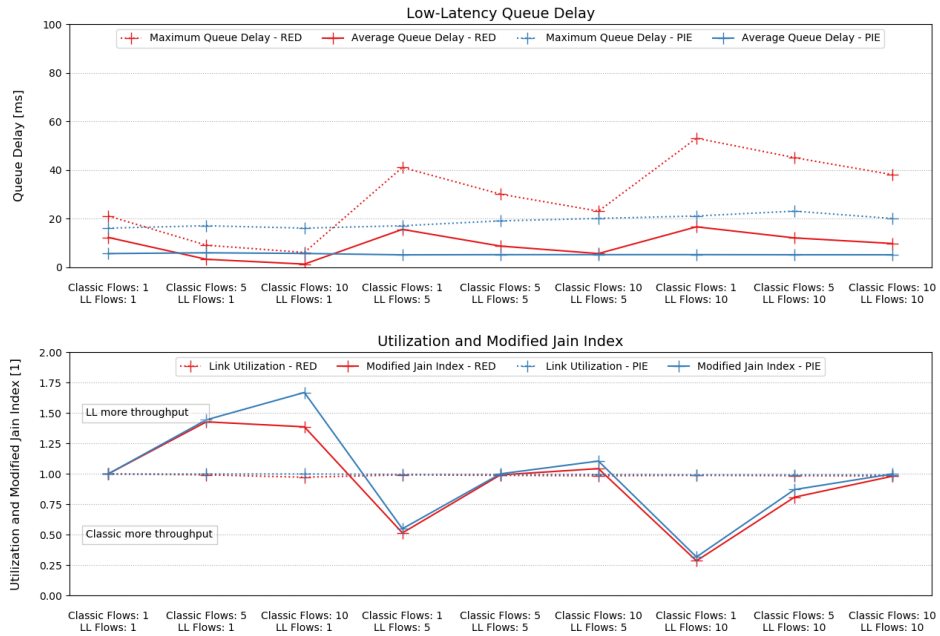


Dual Queue Uncoupled AQM with Scalable Congestion Control on Low-Latency Flows (LTE)
 Classic CC: Cubic - Scalable CC: Relentless - ECN on Classic flows: Off

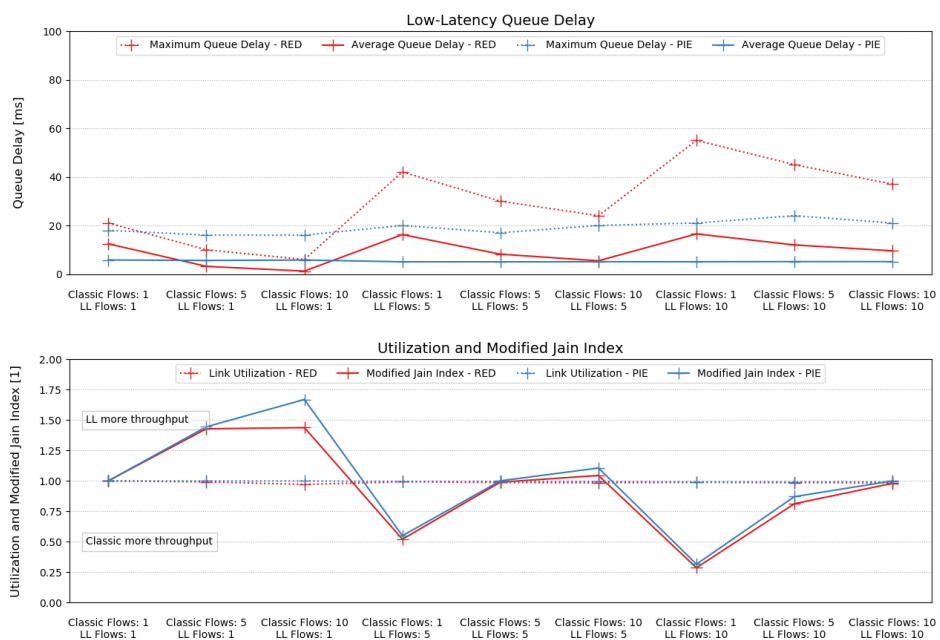


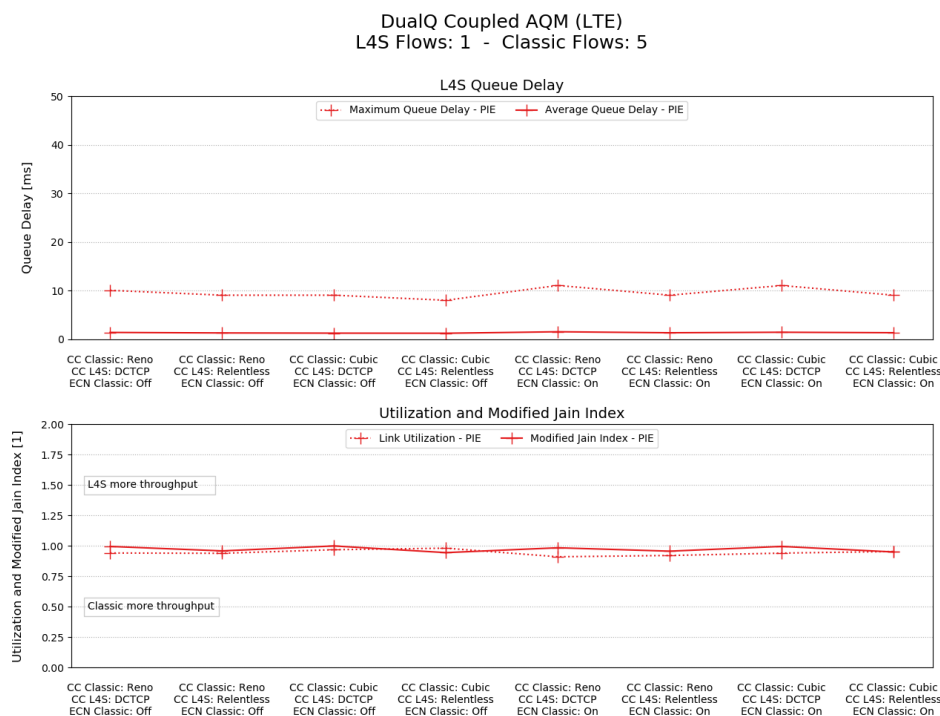
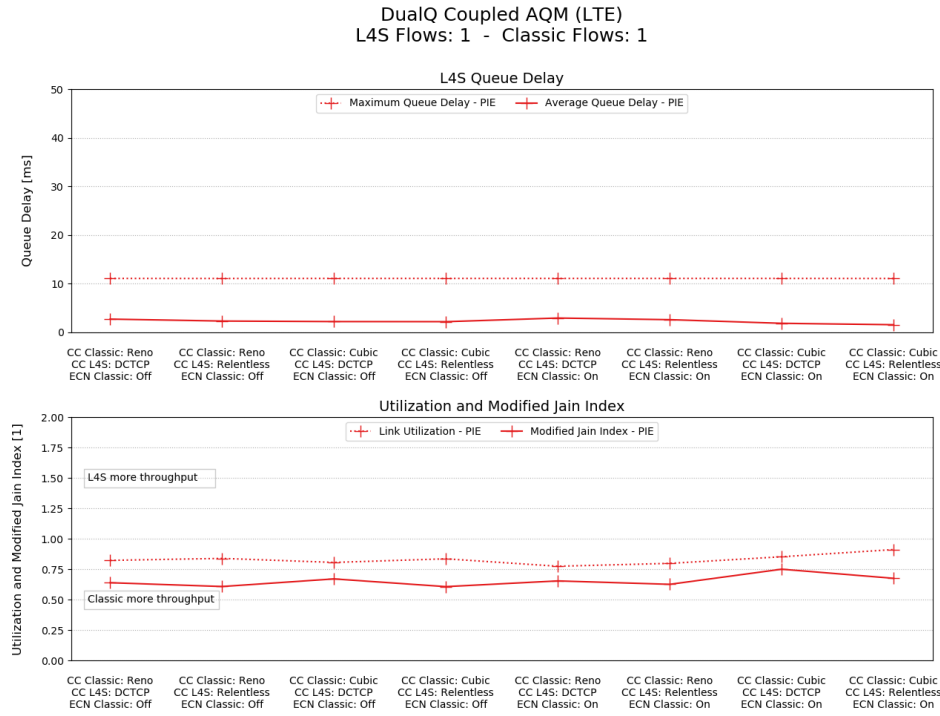


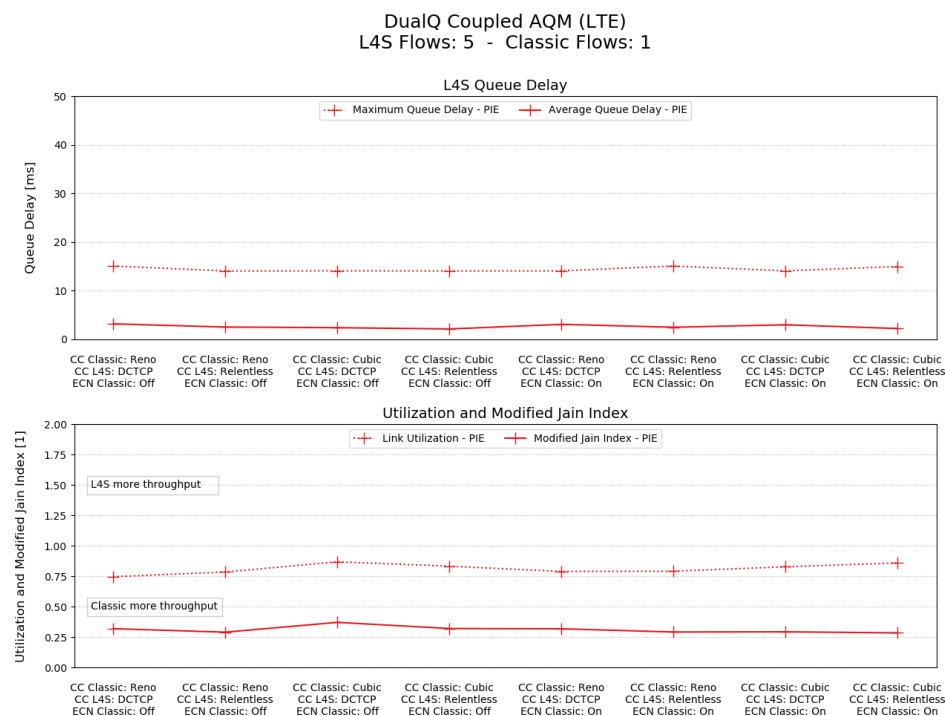
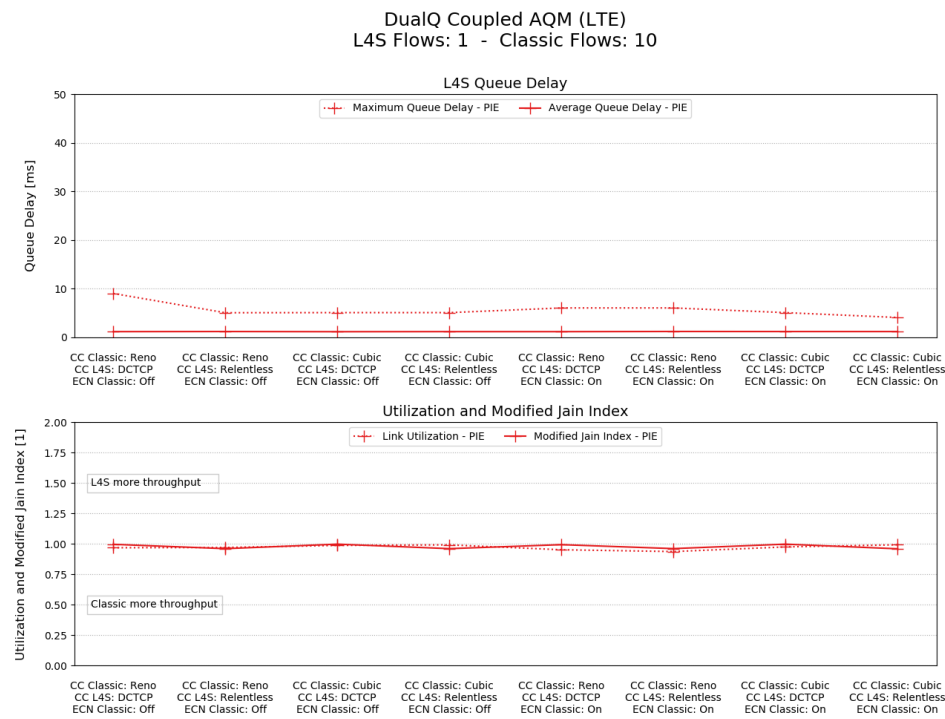
Dual Queue Uncoupled AQM with Scalable Congestion Control on Low-Latency Flows (LTE)
 Classic CC: Reno - Scalable CC: Relentless - ECN on Classic flows: On

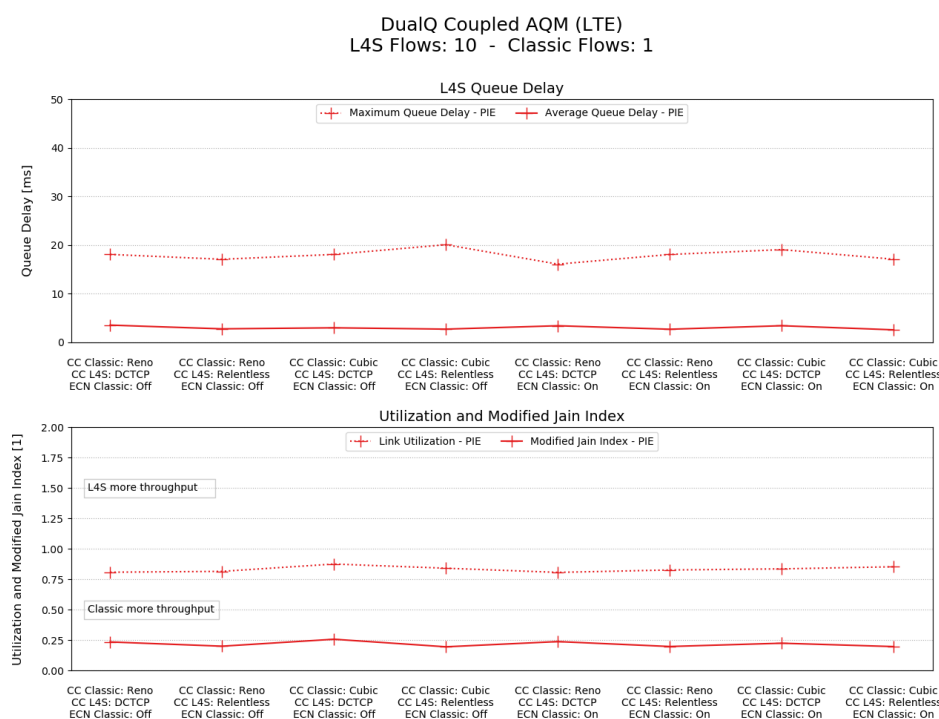
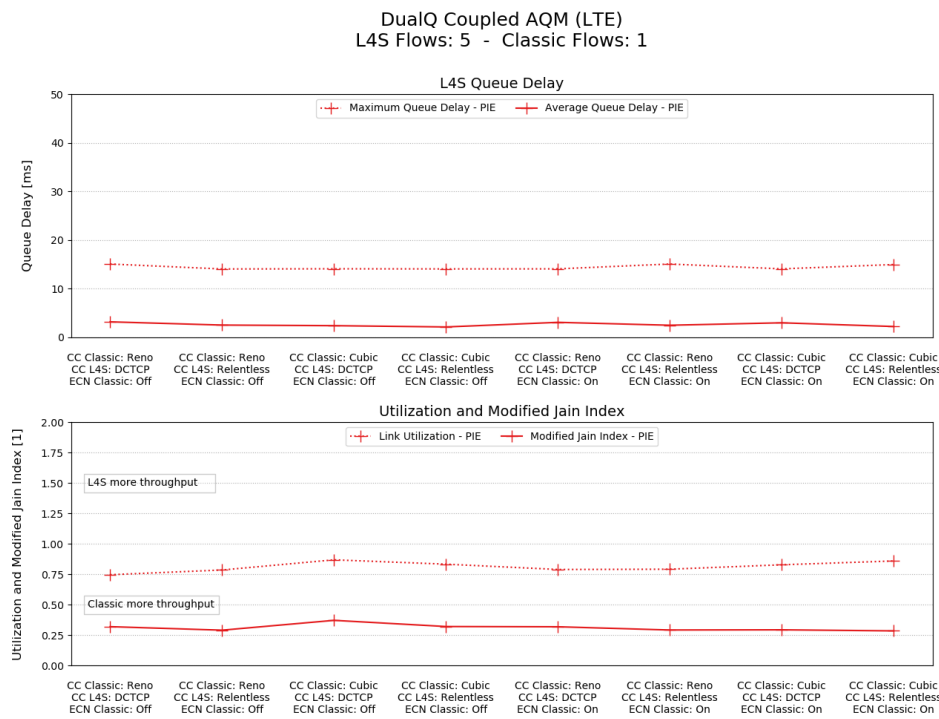


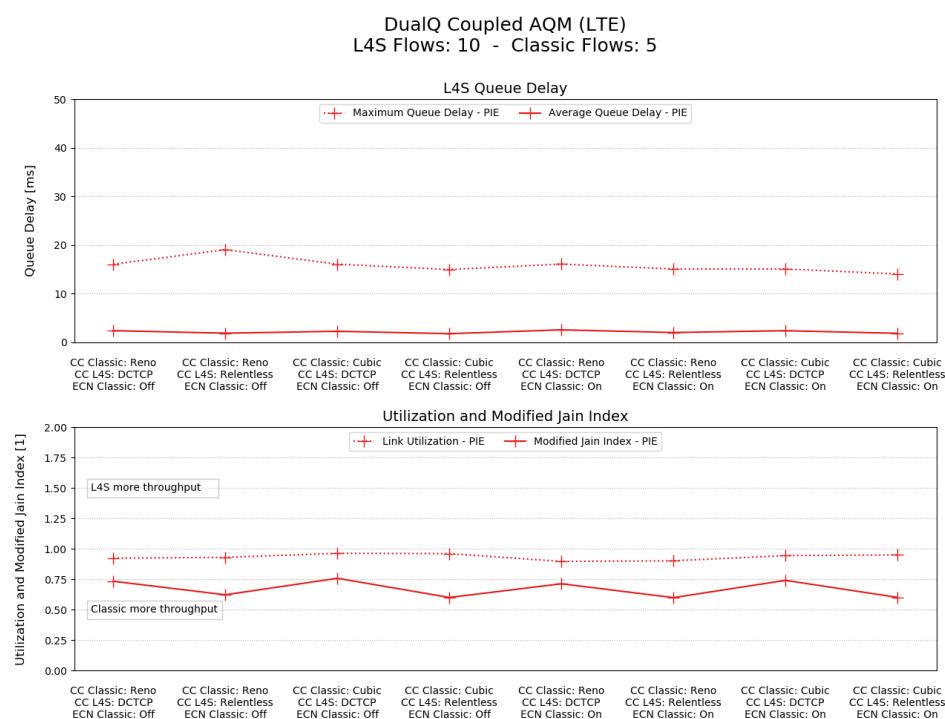
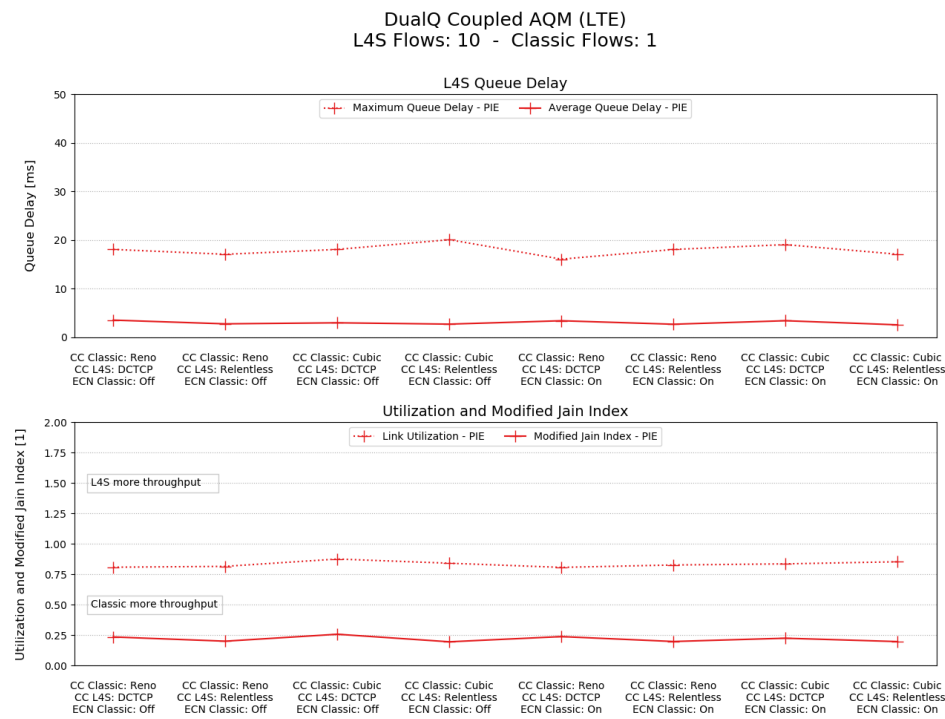
Dual Queue Uncoupled AQM with Scalable Congestion Control on Low-Latency Flows (LTE)
 Classic CC: Reno - Scalable CC: Relentless - ECN on Classic flows: Off

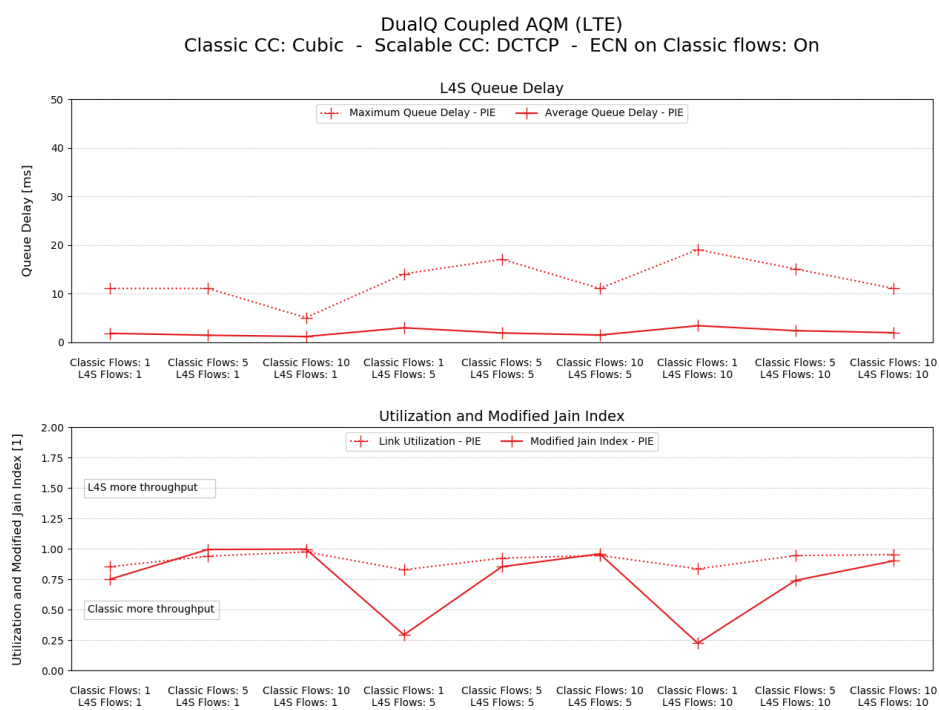
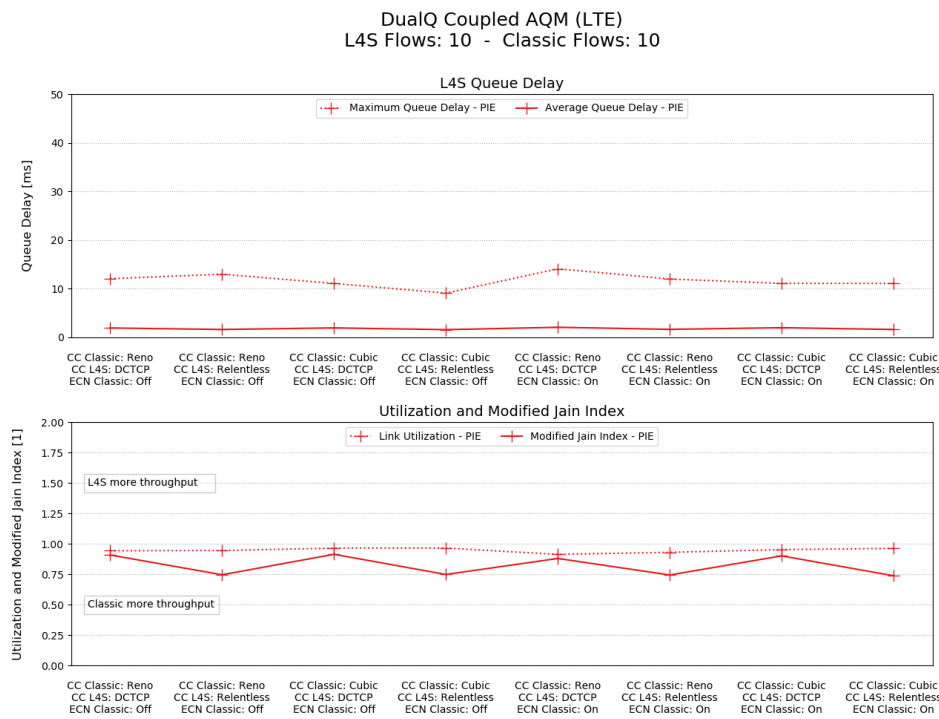


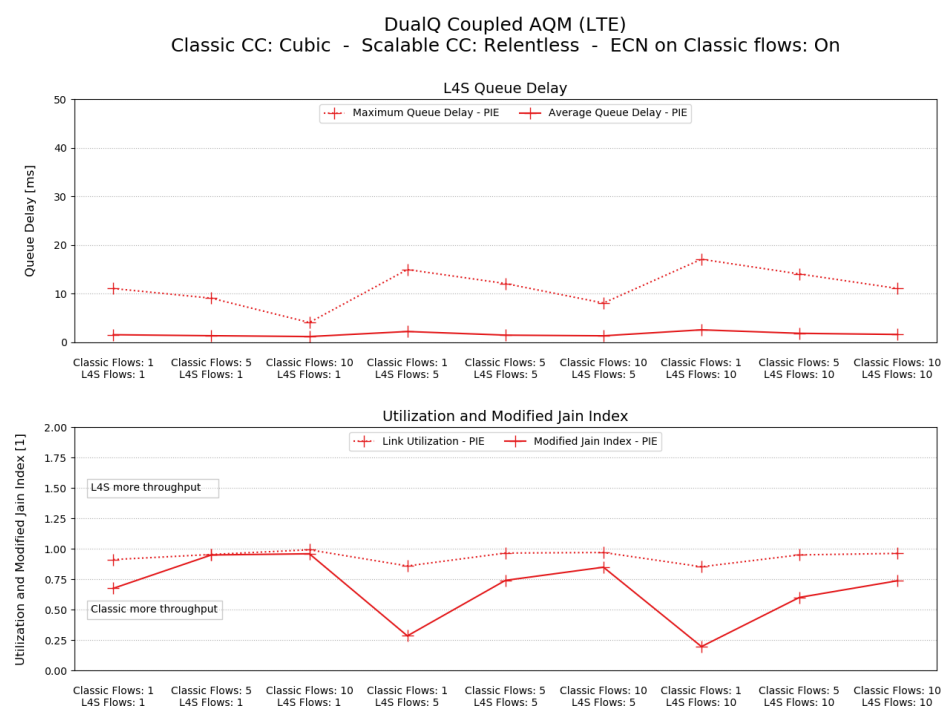
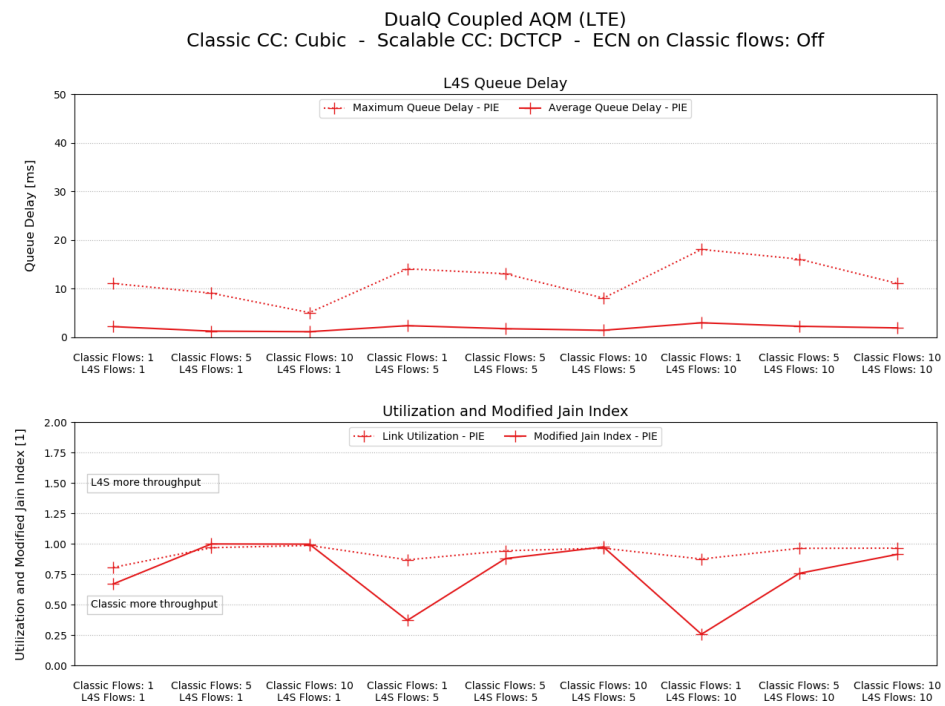


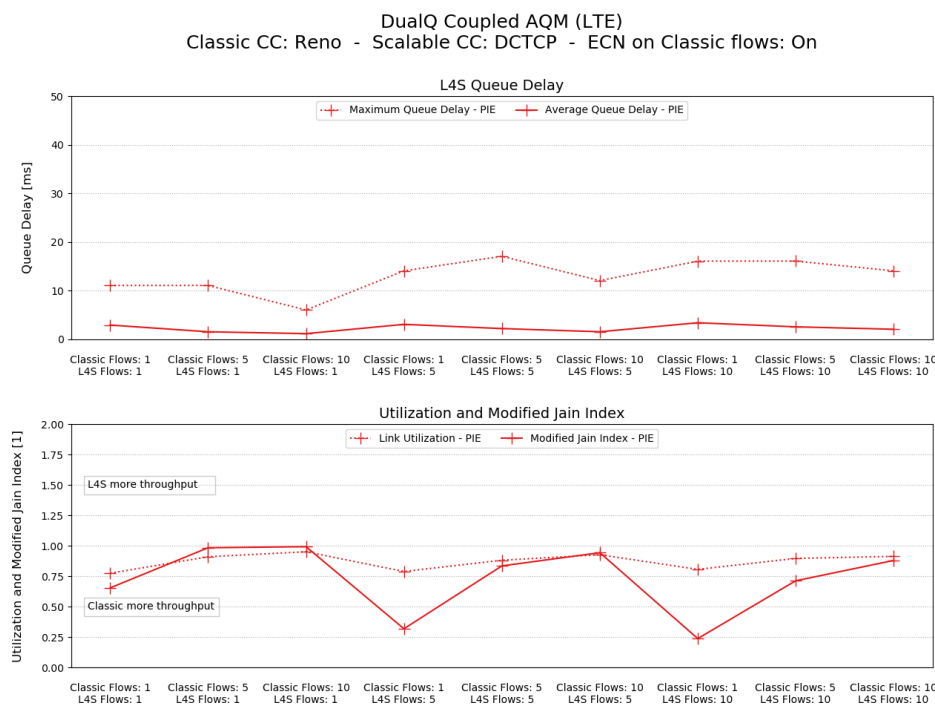
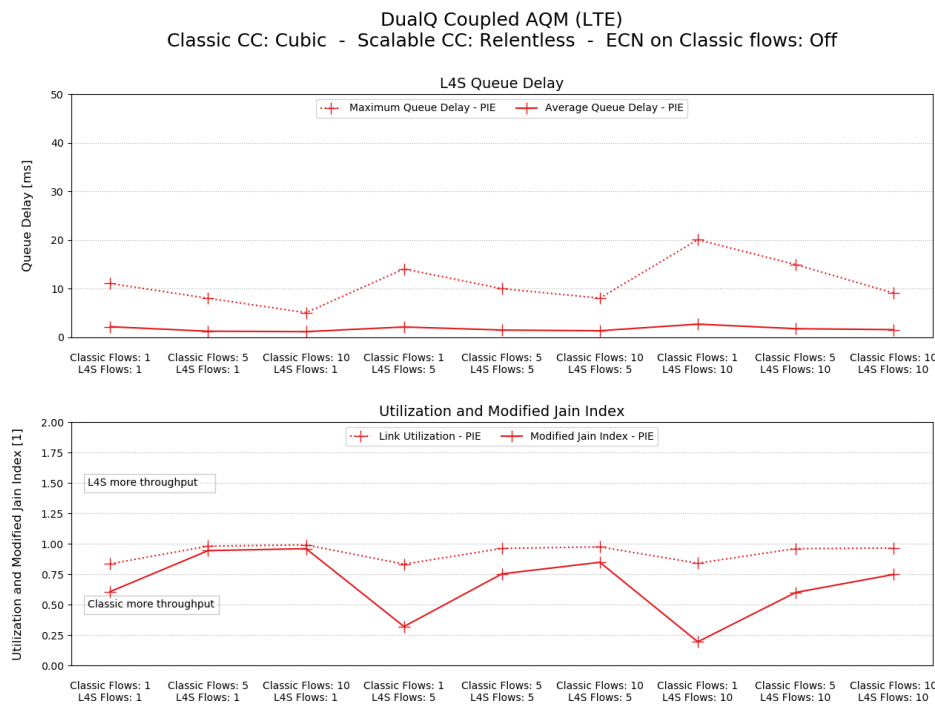


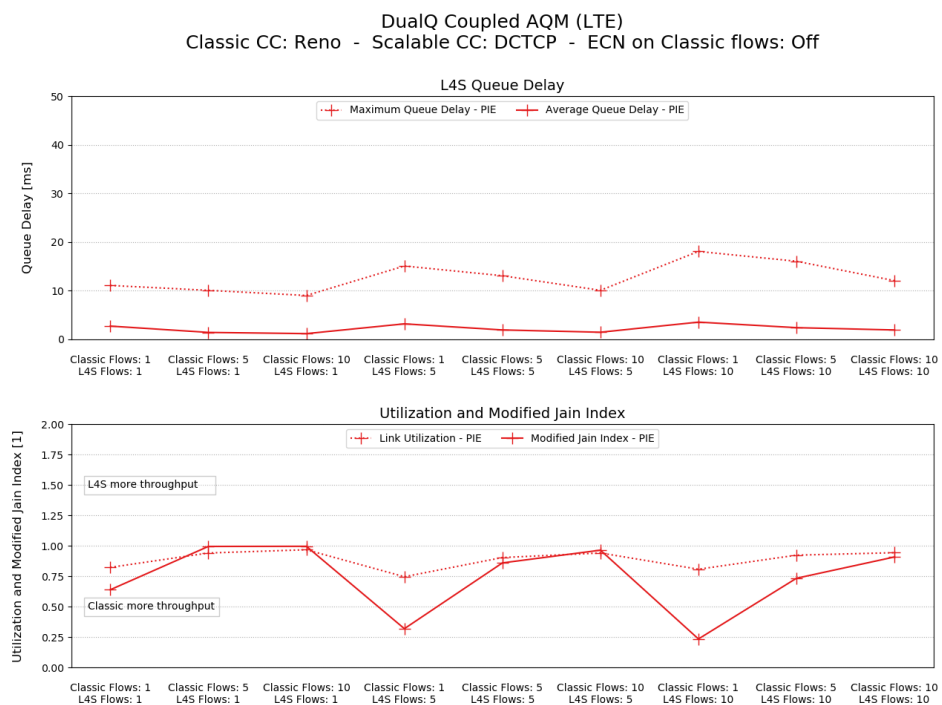
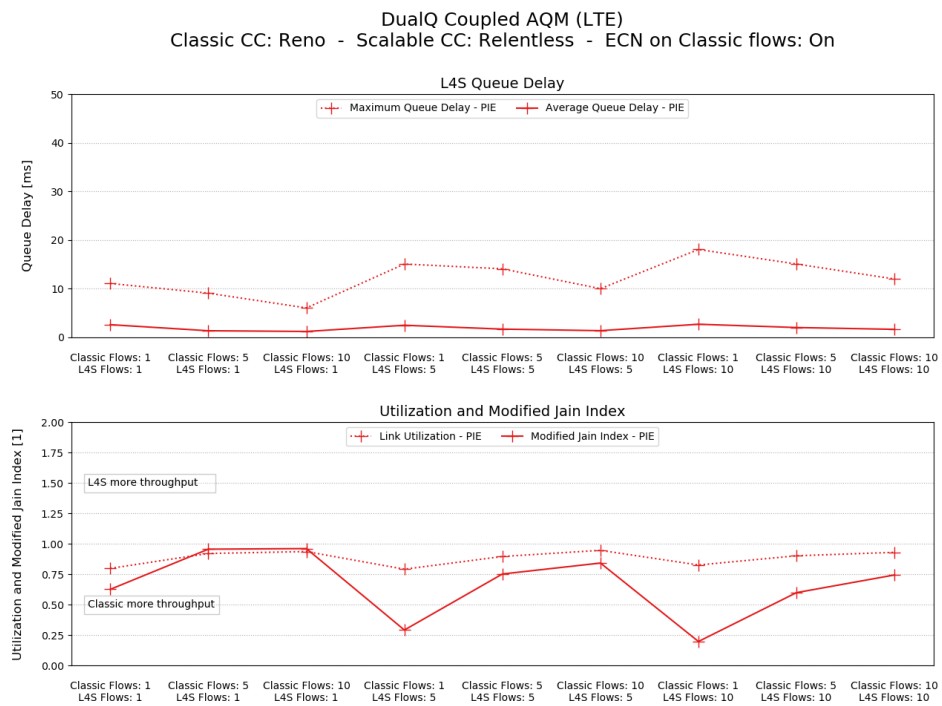


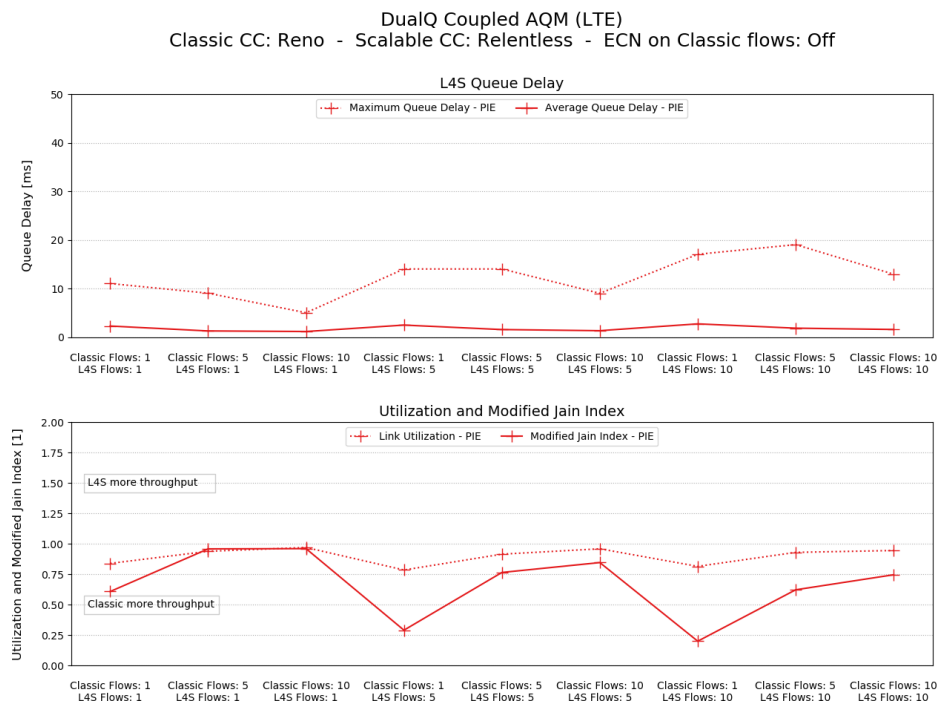












Appendix B

Data

This appendix contains the data from our simulations. Each line describes the set-up and metrics from one simulation.

aqm denotes the AQM scheme that was used.

- *sq – pie* stands for Single Queue AQM with PIE.
- *sq – red* stands for Single Queue AQM with RED.
- *dq – pie* stands for Dual Queue Uncoupled AQM with PIE.
- *dq – red* stands for Dual Queue Uncoupled AQM with RED.
- *l4s – cred* stands for DualQ Coupled AQM with PIE.
- *l4s – pi2* stands for DualQ Coupled AQM with RED.
- *l4s – pie* stands for DualQ Coupled AQM with PIE.

nLF and *nCF* denote, how many low-latency/L4S flows and how many classic flows were simulated.

ccC and *ccL* denote the congestion controls that were used for the classic and the low-latency/L4S flows.

utilization gives the achieved link utilization.

jainmod gives the value of the modified Jain index (See Section 4.1).

qDelayAvgC and *qDelayAvgL* give the average queue delays of the classic and the low-latency/L4S queue in milliseconds.

qDelayMaxC and *qDelayMaxL* give the maximum queue delays of the classic and the low-latency/L4S queue in milliseconds.

B.1 Data from Static Link Simulations

agm	nLF	nCF	ccc	ccL	ecn	utilization	jainmod	qDelayAvgL	qDelayMaxL	qDelayAvgC	qDelayMaxC
sq-pie	1	1	1	cubic	cubic	0	0.9327019833	0.9825588836	4.5812023216	26.1002000000	4.5812023216
sq-pie	1	1	1	cubic	cubic	1	0.958075500	1.0014803126	5.0823677495	18.8906000000	5.0823677495
sq-pie	1	1	1	reno	reno	0	0.8512934433	1.0069029858	4.8617030386	23.7090000000	4.8617030386
sq-pie	1	1	1	reno	cubic	1	0.8253590500	0.9884629599	4.6523527629	24.8986000000	4.6523527629
sq-pie	1	1	5	cubic	cubic	0	0.9844708533	1.0000324765	6.5527367117	26.1002000000	6.5527367117
sq-pie	1	1	5	cubic	cubic	1	0.9665670233	1.0000115010	7.0108909343	32.1082000000	7.0108909343
sq-pie	1	1	5	reno	reno	0	0.9263374533	1.0001454165	8.2447015062	38.1620000000	8.2447015062
sq-pie	1	1	5	reno	cubic	1	0.8991172100	0.9995622130	8.7673660838	40.5940000000	8.7673660838
sq-pie	1	10	10	cubic	cubic	0	0.9902060700	1.0000222322	6.2246818596	26.1122000000	6.2246818596
sq-pie	1	10	10	cubic	cubic	1	0.9734162200	0.9996908418	6.6831443076	33.3098000000	6.6831443076
sq-pie	1	10	10	reno	reno	0	0.9628822067	1.0000128928	7.3396243951	38.4392000000	7.3396243951
sq-pie	1	10	10	reno	cubic	1	0.9317606667	0.99955783	8.3436713974	44.4520000000	8.3436713974
sq-pie	5	1	1	cubic	cubic	0	0.9692106367	1.0019979837	7.0042691712	33.3098000000	7.0042691712
sq-pie	5	1	1	cubic	cubic	1	0.9721745567	1.0007470680	6.8665934242	32.1202000000	6.8665934242
sq-pie	5	1	1	reno	reno	0	0.9098515433	0.9998265646	8.2650321356	42.9226000000	8.2650321356
sq-pie	5	1	1	reno	cubic	1	0.9050451650	1.0000081825	6.6110787558	45.3258000000	6.6110787558
sq-pie	5	5	5	cubic	cubic	0	0.9831921333	1.0000039831	6.4558518211	26.4232000000	6.4558518211
sq-pie	5	5	5	cubic	cubic	1	0.9709729167	0.9979675733	6.9019883552	30.9066000000	6.9019883552
sq-pie	5	5	5	reno	reno	0	0.9518228000	1.0011210671	7.4581996435	35.7130000000	7.4581996435
sq-pie	5	5	5	reno	cubic	1	0.9259300000	0.9999628094	8.1908706928	48.0519000000	8.1908706928
sq-pie	5	10	10	cubic	cubic	0	0.9896551467	1.0000374185	6.2039653210	26.4208000000	6.2039653210
sq-pie	5	10	10	cubic	cubic	1	0.9745375333	1.0000440957	6.7746923901	29.7050000000	6.7746923901
sq-pie	5	10	10	reno	reno	0	0.9664446333	1.0000335584	7.4793728911	35.7130000000	7.4793728911
sq-pie	5	10	10	reno	cubic	1	0.9481624667	1.0000215024	8.0808807161	42.9106000000	8.0808807161
sq-pie	10	1	1	cubic	cubic	0	0.9737766400	0.9999999644	6.7677037380	30.9066000000	6.7677037380
sq-pie	10	1	1	cubic	cubic	1	0.9755203233	0.9997961069	6.5684635825	29.7050000000	6.5684635825
sq-pie	10	1	1	reno	reno	0	0.9371677886	1.0000424335	8.0305593857	46.5274000000	8.0305593857
sq-pie	10	1	1	reno	reno	1	0.9372880600	0.999912085	7.8618594628	41.7090000000	7.8618594628
sq-pie	10	5	5	cubic	cubic	0	0.9812666000	1.0000328278	6.4942827841	29.7050000000	6.4942827841
sq-pie	10	5	5	cubic	cubic	1	0.9774214833	0.9997506713	6.5655039875	29.7050000000	6.5655039875
sq-pie	10	5	5	reno	reno	0	0.9591045500	1.0000302035	7.6496288521	38.1282000000	7.6496288521
sq-pie	10	5	5	reno	cubic	1	0.9449583000	1.0000379386	8.0428404992	43.2016000000	8.0428404992
sq-pie	10	10	10	cubic	cubic	0	0.9865957800	0.0052648313	6.5725753501	25.1975000000	6.5725753501
sq-pie	10	10	10	cubic	cubic	1	0.9792080000	1.0000404645	6.9835383610	28.4914000000	6.9835383610
sq-pie	10	10	10	reno	reno	0	0.9664876500	1.003188819	7.9900252273	34.8825000000	7.9900252273
sq-pie	10	10	10	reno	cubic	1	0.9441772333	0.9999423433	8.5553806740	41.7090000000	8.5553806740
sq-red	1	1	5	cubic	cubic	0	0.9779624833	0.9995785367	10.7070301599	32.1105000000	10.7070301599
sq-red	1	1	5	cubic	cubic	1	0.9882553333	0.9932137594	10.7677500692	38.1162000000	10.7677500692
sq-red	1	1	5	reno	reno	0	0.9183503667	1.003755930	7.8391551995	30.9066000000	7.8391551995
sq-red	1	1	5	reno	cubic	1	0.9319485667	0.9908032985	8.1360278764	32.0962000000	8.1360278764
sq-red	1	5	5	cubic	cubic	0	0.9991638167	1.0000540671	21.1208330375	39.3178000000	21.1208330375
sq-red	1	5	5	cubic	cubic	1	0.9995785367	0.9994414784	21.1518360141	45.3258000000	21.1518360141
sq-red	1	5	5	reno	reno	0	0.9927123667	1.0000903117	20.405548887	44.1242000000	20.405548887
sq-red	1	5	5	reno	cubic	1	0.9764248800	1.0012344298	18.9383782509	50.1322000000	18.9383782509
sq-red	10	1	10	cubic	cubic	0	0.9988620967	1.0081461075	21.0541820225	39.3228000000	21.0541820225
sq-red	10	1	10	cubic	cubic	1	0.9834045333	0.9999536876	24.7351198006	53.7370000000	24.7351198006

1	10	reno	reno	0	0.9924841933	1.0543859685	19.8754749348	44.1362000000	19.8754749348	44.1362000000
1	10	reno	cubic	1	0.8996080433	0.9999988775	20.1996958033	62.1362000000	20.1996958033	62.1362000000
1	1	cubic	cubic	0	0.9988187333	0.9992454696	20.9999918062	41.7210000000	20.9999918062	41.7210000000
5	1	cubic	cubic	1	0.9996862833	1.0004055562	21.6074529426	41.7210000000	21.6074529426	41.7210000000
5	1	reno	reno	0	0.9750609900	0.9996543377	18.9414346195	47.7290000000	18.9414346195	47.7290000000
5	1	reno	reno	1	0.9692982367	1.0015807672	18.3302290033	48.9306000000	18.3302290033	48.9306000000
5	1	cubic	cubic	0	0.9991062333	1.149311803	23.773029182	44.1242000000	23.773029182	44.1242000000
5	1	cubic	cubic	1	0.9933633000	0.999771551	25.8307632669	50.1322000000	25.8307632669	50.1322000000
5	1	reno	reno	0	0.9875950500	1.1868869379	21.1490511920	46.5394000000	21.1490511920	46.5394000000
5	1	reno	reno	1	0.9097014833	0.9998531467	20.5687141630	57.3418000000	20.5687141630	57.3418000000
5	10	cubic	cubic	0	0.9993588000	1.3780859882	23.603454850	45.3258000000	23.603454850	45.3258000000
5	10	cubic	cubic	1	0.9734939833	0.999662702	24.0517739893	57.3418000000	24.0517739893	57.3418000000
5	10	reno	reno	0	0.9871272500	1.4223633706	21.2670814879	48.0399000000	21.2670814879	48.0399000000
5	10	reno	reno	1	0.8745822667	0.9999880362	20.5784491224	66.9426000000	20.5784491224	66.9426000000
10	1	cubic	cubic	0	0.9966897933	1.0042288369	26.982812208	48.9306000000	26.982812208	48.9306000000
10	1	cubic	cubic	1	0.9720443867	0.999945151	24.5203472121	52.5354000000	24.5203472121	52.5354000000
10	1	reno	reno	0	0.9396738367	1.0042915534	21.2185900709	52.5354000000	21.2185900709	52.5354000000
10	1	reno	reno	1	0.8993877200	1.00066675565	19.2235235206	60.0559000000	19.2235235206	60.0559000000
10	5	cubic	cubic	0	0.9984321067	1.1363707015	28.2801990111	47.7290000000	28.2801990111	47.7290000000
10	5	cubic	cubic	1	0.9720396500	0.9999973735	23.186573735	56.1402000000	23.186573735	56.1402000000
10	5	reno	reno	0	0.9421170767	1.1381322996	20.489150799	51.6447000000	20.489150799	51.6447000000
10	5	reno	reno	1	0.8745822333	0.9999434670	20.5784491224	66.9426000000	20.5784491224	66.9426000000
10	10	cubic	cubic	0	0.9981197800	1.3196160485	28.2115130437	48.0519000000	28.2115130437	48.0519000000
10	10	cubic	cubic	1	0.9598781333	0.9999344732	23.2472975995	61.2695000000	23.2472975995	61.2695000000
10	10	reno	reno	0	0.95533799500	1.256159402	21.6114168215	52.5354000000	21.6114168215	52.5354000000
10	10	reno	reno	1	0.8541381333	0.9999829359	23.5547733152	72.9746000000	23.5547733152	72.9746000000
1	1	cubic	cubic	0	0.9999942333	0.9937148971	5.7202012670	21.2938000000	368.5985881270	708.9310000000
1	1	cubic	cubic	1	0.9999913333	0.9825761647	5.0918261957	23.6970000000	257.9429770180	912.0020000000
1	1	cubic	dctcp	0	0.1000000000	1.0000000000	6.22262518544	11.2615130437	385.4052158690	626.0210000000
1	1	cubic	dctcp	1	0.9999210000	0.9999999926	6.2837088985	11.6810000000	251.3012560260	816.7520000000
1	1	cubic	relentless	0	0.9934089167	1.0000001043	6.7848383888	16.5554000000	380.0180933280	629.3030000000
1	1	cubic	relentless	1	1.0000000000	0.9999998396	6.6841880862	16.4874000000	250.5172218830	816.7520000000
1	1	reno	dctcp	0	0.1000000000	1.0000000000	6.2318624308	11.6810000000	370.06310170	513.0710000000
1	1	reno	dctcp	1	0.9999922000	0.9999999926	6.2250776361	11.6810000000	379.999284810	521.1592000000
1	1	reno	relentless	0	0.1000000000	0.9999999925	6.6627857116	15.6088000000	335.8530158590	515.4740000000
1	1	reno	relentless	1	0.9999920333	0.9999999928	6.7299893014	16.4874000000	380.2703930310	521.1590000000
1	1	reno	reno	0	0.9999943333	0.9937148971	5.7202012670	21.2938000000	368.5985881270	708.9310000000
1	1	reno	reno	1	0.9999913333	0.9825761647	5.0918261957	23.6970000000	257.9429770180	912.0020000000
1	1	cubic	dctcp	0	0.1000000000	1.0000000000	6.22262518544	11.2615130437	385.4052158690	626.0210000000
1	1	cubic	dctcp	1	0.9999921000	0.9999999926	6.2837088985	11.6810000000	251.3012560260	816.7520000000
1	1	cubic	relentless	0	0.9999913333	0.9937148971	5.7202012670	21.2938000000	368.5985881270	708.9310000000
1	1	cubic	relentless	1	1.0000000000	0.9999998396	6.6841880862	16.4874000000	250.5172218830	816.7520000000
1	1	reno	dctcp	0	0.1000000000	1.0000000000	6.2318624308	11.6810000000	370.06310170	513.0710000000
1	1	reno	dctcp	1	0.9999922000	0.9999999926	6.2250776361	11.6810000000	379.999284810	521.1592000000
1	1	reno	relentless	0	0.1000000000	0.9999999925	6.6627857116	15.6088000000	335.8530158590	515.4740000000
1	1	reno	relentless	1	0.9999920333	0.9999999928	6.7299893014	16.4874000000	380.2703930310	521.1590000000
1	1	reno	reno	0	0.9999943333	0.9937148971	5.7202012670	21.2938000000	368.5985881270	708.9310000000
1	1	reno	reno	1	0.9999913333	0.9825761647	5.0918261957	23.6970000000	257.9429770180	912.0020000000
1	1	cubic	dctcp	0	0.1000000000	1.0000000000	6.2250776361	11.6810000000	379.999284810	521.1592000000
1	1	cubic	dctcp	1	0.9999921000	0.9999999926	6.2837088985	11.6810000000	251.3012560260	816.7520000000
1	1	cubic	relentless	0	0.1000000000	0.9999998396	6.6627857116	15.6088000000	335.8530158590	515.4740000000
1	1	cubic	relentless	1	0.9999920333	0.9937148971	6.7299893014	16.4874000000	380.2703930310	521.1590000000
1	1	reno	dctcp	0	0.1000000000	1.0000000000	6.2318624308	11.6810000000	370.06310170	513.0710000000
1	1	reno	dctcp	1	0.9999922000	0.9999999926	6.2250776361	11.6810000000	379.999284810	521.1592000000
1	1	reno	relentless	0	0.1000000000	0.9999999925	6.6627857116	15.6088000000	335.8530158590	515.4740000000
1	1	reno	relentless	1	0.9999920333	0.9937148971	6.7299893014	16.4874000000	380.2703930310	521.1590000000
1	1	cubic	dctcp	0	0.1000000000	1.0000000000	6.2318624308	11.6810000000	370.06310170	513.0710000000
1	1	cubic	dctcp	1	0.9999921000	0.9999999926	6.2837088985	11.6810000000	251.3012560260	816.7520000000
1	1	cubic	relentless	0	0.1000000000	0.9999998396	6.6627857116	15.6088000000	335.8530158590	515.4740000000
1	1	cubic	relentless	1	0.9999920333	0.9937148971	6.7299893014	16.4874000000	380.2703930310	521.1590000000
1	1	reno	dctcp	0	0.1000000000	1.0000000000	6.2318624308	11.6810000000	370.06310170	513.0710000000
1	1	reno	dctcp	1	0.9999922000	0.9999999926	6.2250776361	11.6810000000	379.999284810	521.1592000000
1	1	reno	relentless	0	0.1000000000	0.9999999925	6.6627857116	15.6088000000	335.8530158590	515.4740000000
1	1	reno	relentless	1	0.9999920333	0.9937148971	6.7299893014	16.4874000000	380.2703930310	521.1590000000
1	1	cubic	dctcp	0	0.1000000000	1.0000000000	6.2318624308	11.6810000000	370.06310170	513.0710000000
1	1	cubic	dctcp	1	0.9999921000	0.9999999926	6.2837088985	11.6810000000	251.3012560260	816.7520000000
1	1	cubic	relentless	0	0.1000000000	0.9999998396	6.6627857116	15.6088000000	335.8530158590	515.4740000000
1	1	cubic	relentless	1	0.9999920333	0.9937148971	6.7299893014	16.4874000000	380.2703930310	521.1590000000
1	1	reno	dctcp	0	0.1000000000	1.0000000000	6.2318624308	11.6810000000	370.06310170	513.0710000000
1	1	reno	dctcp	1	0.9999922000	0.9999999926	6.2250776361	11.6810000000	379.999284810	521.1592000000
1	1	reno	relentless	0	0.1000000000	0.9999999925	6.6627857116	15.6088000000	335.8530158590	515.4740000000
1	1	reno	relentless	1	0.9999920333	0.9937148971	6.7299893014	16.4874000000	380.2703930310	521.1590000000
1	1	cubic	dctcp	0	0.1000000000	1.0000000000	6.2318624308	11.6810000000	370.06310170	513.0710000000
1	1	cubic	dctcp	1	0.9999921000	0.9999999926	6.2837088985	11.6810000000	251.3012560260	816.7520000000
1	1	cubic	relentless	0	0.1000000000	0.9999998396	6.6627857116	15.6088000000	335.8530158590	515.4740000000
1	1	cubic	relentless	1	0.9999920333	0.9937148971	6.7299893014	16.4874000000	380.2703930310	521.1590000000

dq-pie	0	cubic	dctcp	1.0000011267	28.5664192485	407.9049652060	720.6240000000
dq-pie	1	cubic	dctcp	0.9999716400	28.751298546	57.3298000000	1078.6900000000
dq-pie	1	cubic	relentless	0.9999527819	22.975313669	70.8920000000	720.6360000000
dq-pie	1	cubic	relentless	0.999990867	0.9999143394	23.1016992715	57.3418000000
dq-pie	1	reno	dctcp	0.9999916833	1.0000000020	28.8474809220	540.3850000000
dq-pie	1	reno	dctcp	1.0000000000	0.9999999990	57.3298000000	553.6020000000
dq-pie	1	reno	relentless	0.9999915267	0.9999376366	23.0320977566	538.2920000000
dq-pie	1	reno	relentless	0.9999916100	0.9999376362	22.8604436570	552.4010000000
dq-pie	1	reno	reno	0	1.0000000000	0.9970678668	23.2052719535
dq-pie	1	reno	cubic	0	1.0000000000	0.9970226268	22.8235169703
dq-pie	1	cubic	relentless	0	1.0000000000	0.9987533533	6.7245422573
dq-pie	1	cubic	cubic	1	0.9998914667	0.9889298339	6.6107332248
dq-pie	1	cubic	dctcp	0	0.9999908633	0.9999143474	5.169892589
dq-pie	1	cubic	dctcp	1	1.0000000000	0.9999149119	5.9099901534
dq-pie	1	cubic	relentless	0	0.99999189167	0.9995499983	6.1657037021
dq-pie	1	cubic	relentless	1	1.0000000000	0.9995617371	6.2399108998
dq-pie	1	reno	dctcp	0	0.9999915833	0.9999333283	5.8666347160
dq-pie	1	reno	dctcp	1	0.9999915333	0.999917692	5.873825322
dq-pie	1	reno	relentless	0	1.0000000000	0.9996824535	6.1714308795
dq-pie	1	reno	relentless	1	1.0000000000	0.9995370630	6.2314371329
dq-pie	1	reno	reno	0	1.0000000000	0.9381628051	7.7190128881
dq-pie	1	reno	cubic	0	1.0000000000	0.947427263	7.7725578984
dq-pie	1	cubic	cubic	5	0.9996313500	0.9977487320	7.4141487803
dq-pie	1	cubic	cubic	5	1.0000000000	0.9968437256	7.7182433187
dq-pie	1	cubic	dctcp	0	0.9997413667	0.9998833479	8.0350019786
dq-pie	1	cubic	dctcp	1	1.0000000000	0.998922743	7.8498522195
dq-pie	1	cubic	relentless	0	0.9996787333	0.9993537245	7.8950921951
dq-pie	1	cubic	relentless	1	0.9999941333	0.9992812855	7.7603668992
dq-pie	1	reno	dctcp	0	0.9999914667	0.9999041034	8.0122621876
dq-pie	1	reno	relentless	1	0.9999915167	0.9998400000	27.6474000000
dq-pie	1	reno	relentless	0	0.9999915333	0.9993069332	7.9107784196
dq-pie	1	reno	reno	1	0.9999918933	0.9992201112	7.9287352364
dq-pie	1	reno	reno	0	0.9999916000	0.9905155967	8.6068346299
dq-pie	1	reno	reno	1	1.0000000000	0.9891124007	8.924529635
dq-pie	10	cubic	cubic	10	0.9998226667	0.9970912007	9.3207413998
dq-pie	10	cubic	cubic	10	0.9999941833	0.9966122743	9.2101251519
dq-pie	10	cubic	dctcp	0	0.9994586667	0.9997246150	10.6633712183
dq-pie	10	cubic	dctcp	1	0.9999941333	0.9996469260	10.5153663091
dq-pie	10	cubic	relentless	0	0.9994687833	0.998576750	10.2855973527
dq-pie	10	cubic	relentless	1	1.0000000000	0.999031510	11.33954615745
dq-pie	10	reno	dctcp	0	1.0000000000	0.9996575643	10.5390716172
dq-pie	10	reno	reno	0	1.0000000000	0.9996653754	10.4834855941
dq-pie	10	reno	relentless	0	1.0000000000	0.9984758823	10.3877936982
dq-pie	10	reno	relentless	1	1.0000000000	0.999031510	11.33954615745
dq-pie	10	reno	reno	0	1.0000000000	0.9996575643	10.5390716172
dq-pie	10	cubic	cubic	10	0.999591030	0.9933968307	6.111783493
dq-pie	10	cubic	cubic	10	0.9999514467	0.9831739464	6.2329540635
dq-pie	10	cubic	dctcp	0	0.99999113933	0.9991687803	5.6619031940
dq-pie	10	cubic	dctcp	1	0.99999313767	0.9992474661	6.0062352608
dq-pie	10	cubic	relentless	0	0.99999265500	0.9944872872	6.1342913233
dq-pie	10	cubic	relentless	1	0.9999990400	0.99946783747	6.1245732889
dq-pie	10	cubic	relentless	1	0.9999990400	0.9999990400	26.1002000000
dq-pie	10	cubic	relentless	1	0.9999990400	0.9999990400	394.5124634570
dq-pie	10	cubic	relentless	1	0.9999990400	0.9999990400	1220.4900000000

10	dq-pie	0	reno	0	0.9999715867	0.9992444025	6.0220036642	20.0922000000	359.4297259360
10	dq-pie	1	reno	1	1.0000000000	0.9993377268	6.0529612983	22.8184000000	368.4480128090
10	dq-pie	1	reno	0	0.9999515167	0.9993831375	6.1456836869	22.8456000000	383.05499988620
10	dq-pie	1	reno	1	0.9999916000	0.9948814307	6.0815567361	23.69702975233	373.7091834160
10	dq-pie	1	reno	0	0.9999909333	0.9505080923	6.070202659	33.6207000000	268.5090693900
10	dq-pie	1	reno	1	0.9998113000	0.9363973109	6.9043506999	38.4271000000	263.0291631680
10	dq-pie	5	cubic	0	0.9992607500	0.995457202	7.0004142067	28.7930000000	421.739087170
10	dq-pie	5	cubic	1	1.0000000000	0.9950297092	6.9634175233	26.1002000000	453.3050814350
10	dq-pie	5	cubic	0	0.9999692000	0.9993246098	7.3608390676	28.8264000000	414.4329469520
10	dq-pie	5	cubic	1	1.0000000000	0.9994148374	7.2991281831	30.0159000000	427.2296945860
10	dq-pie	5	cubic	0	0.9999116400	0.9969644006	7.5388396848	28.5159100000	417.4482306310
10	dq-pie	5	cubic	1	1.0000000000	0.9970325566	7.481702599	40.6408838780	1236.1000000000
10	dq-pie	5	cubic	0	0.9999916000	0.9994765802	7.3825038262	24.8986000000	563.2150000000
10	dq-pie	5	cubic	1	0.9998113500	0.999514530	7.25733901386	26.1002000000	359.2971746350
10	dq-pie	5	cubic	0	1.0000000000	0.9967192908	7.4478733938	29.7050000000	371.5129160280
10	dq-pie	5	cubic	1	1.0000000000	0.9995909333	7.6031270360	33.7098100000	590.8400000000
10	dq-pie	5	cubic	0	0.9999114833	0.9969597853	8.1974864148	38.1042000000	385.9478639180
10	dq-pie	5	cubic	1	0.9999916000	0.9870167990	8.422925176	49.2415000000	351.06334049140
10	dq-pie	10	reno	0	0.9998113500	0.9855470189	8.5253045099	33.3955000000	424.3484071550
10	dq-pie	10	reno	1	0.9994514167	0.9961216051	8.5253045099	1304.9200000000	1.0016953360
10	dq-pie	10	reno	0	1.0000000000	0.9962334328	8.5300000000	40.5074000000	481.752556640
10	dq-pie	10	reno	1	0.9997439900	0.9996839042	9.9630594106	37.2472000000	418.6552556640
10	dq-pie	10	reno	0	0.9999915500	0.9994762898	9.7131541971	38.1162000000	470.6813658220
10	dq-pie	10	reno	1	0.9995738167	0.9979968305	9.7375465640	38.1042000000	427.9093266940
10	dq-pie	10	reno	0	1.0000000000	0.9974756189	9.55652268953	45.3258000000	464.403945470
10	dq-pie	10	reno	1	0.9990742980	0.9995254743	9.6506348453	40.5074000000	370.041269970
10	dq-pie	10	reno	0	1.0000000000	0.9995347360	9.8944112100	40.5074000000	354.3157910110
10	dq-pie	10	reno	1	0.9999915500	0.9996839042	9.9630594106	37.2472000000	410.6440000000
10	dq-pie	10	reno	0	0.9995738167	0.9979968305	9.7375465640	38.1042000000	427.9093266940
10	dq-pie	10	reno	1	0.9999915500	0.9994762898	9.55652268953	45.3258000000	464.403945470
10	dq-pie	10	reno	0	1.0000000000	0.9995254743	9.6506348453	40.5074000000	370.041269970
10	dq-pie	10	reno	1	0.9999915500	0.9996839042	9.8944112100	40.5074000000	354.3157910110
10	dq-pie	10	reno	0	0.9999915500	0.9994762898	9.7131541971	38.1162000000	470.6813658220
10	dq-pie	10	reno	1	0.9999915500	0.9996839042	9.8944112100	40.5074000000	354.3157910110
10	dq-pie	10	reno	0	0.9999915500	0.9994762898	9.7131541971	38.1162000000	470.6813658220
10	dq-pie	10	reno	1	0.9999915500	0.9996839042	9.8944112100	40.5074000000	354.3157910110
10	dq-pie	10	reno	0	0.9999915500	0.9994762898	9.7131541971	38.1162000000	470.6813658220
10	dq-pie	10	reno	1	0.9999915500	0.9996839042	9.8944112100	40.5074000000	354.3157910110
10	dq-pie	10	reno	0	0.9999915500	0.9994762898	9.7131541971	38.1162000000	470.6813658220
10	dq-pie	10	reno	1	0.9999915500	0.9996839042	9.8944112100	40.5074000000	354.3157910110
10	dq-pie	10	reno	0	0.9999915500	0.9994762898	9.7131541971	38.1162000000	470.6813658220
10	dq-pie	10	reno	1	0.9999915500	0.9996839042	9.8944112100	40.5074000000	354.3157910110
10	dq-pie	10	reno	0	0.9999915500	0.9994762898	9.7131541971	38.1162000000	470.6813658220
10	dq-pie	10	reno	1	0.9999915500	0.9996839042	9.8944112100	40.5074000000	354.3157910110
10	dq-pie	10	reno	0	0.9999915500	0.9994762898	9.7131541971	38.1162000000	470.6813658220
10	dq-pie	10	reno	1	0.9999915500	0.9996839042	9.8944112100	40.5074000000	354.3157910110
10	dq-pie	10	reno	0	0.9999915500	0.9994762898	9.7131541971	38.1162000000	470.6813658220
10	dq-pie	10	reno	1	0.9999915500	0.9996839042	9.8944112100	40.5074000000	354.3157910110
10	dq-pie	10	reno	0	0.9999915500	0.9994762898	9.7131541971	38.1162000000	470.6813658220
10	dq-pie	10	reno	1	0.9999915500	0.9996839042	9.8944112100	40.5074000000	354.3157910110
10	dq-pie	10	reno	0	0.9999915500	0.9994762898	9.7131541971	38.1162000000	470.6813658220
10	dq-pie	10	reno	1	0.9999915500	0.9996839042	9.8944112100	40.5074000000	354.3157910110
10	dq-pie	10	reno	0	0.9999915500	0.9994762898	9.7131541971	38.1162000000	470.6813658220
10	dq-pie	10	reno	1	0.9999915500	0.9996839042	9.8944112100	40.5074000000	354.3157910110
10	dq-pie	10	reno	0	0.9999915500	0.9994762898	9.7131541971	38.1162000000	470.6813658220
10	dq-pie	10	reno	1	0.9999915500	0.9996839042	9.8944112100	40.5074000000	354.3157910110
10	dq-pie	10	reno	0	0.9999915500	0.9994762898	9.7131541971	38.1162000000	470.6813658220
10	dq-pie	10	reno	1	0.9999915500	0.9996839042	9.8944112100	40.5074000000	354.3157910110
10	dq-pie	10	reno	0	0.9999915500	0.9994762898	9.7131541971	38.1162000000	470.6813658220
10	dq-pie	10	reno	1	0.9999915500	0.9996839042	9.8944112100	40.5074000000	354.3157910110
10	dq-pie	10	reno	0	0.9999915500	0.9994762898	9.7131541971	38.1162000000	470.6813658220
10	dq-pie	10	reno	1	0.9999915500	0.9996839042	9.8944112100	40.5074000000	354.3157910110
10	dq-pie	10	reno	0	0.9999915500	0.9994762898	9.7131541971	38.1162000000	470.6813658220
10	dq-pie	10	reno	1	0.9999915500	0.9996839042	9.8944112100	40.5074000000	354.3157910110
10	dq-pie	10	reno	0	0.9999915500	0.9994762898	9.7131541971	38.1162000000	470.6813658220
10	dq-pie	10	reno	1	0.9999915500	0.9996839042	9.8944112100	40.5074000000	354.3157910110
10	dq-pie	10	reno	0	0.9999915500	0.9994762898	9.7131541971	38.1162000000	470.6813658220
10	dq-pie	10	reno	1	0.9999915500	0.9996839042	9.8944112100	40.5074000000	354.3157910110
10	dq-pie	10	reno	0	0.9999915500	0.9994762898	9.7131541971	38.1162000000	470.6813658220
10	dq-pie	10	reno	1	0.9999915500	0.9996839042	9.8944112100	40.5074000000	354.3157910110
10	dq-pie	10	reno	0	0.9999915500	0.9994762898	9.7131541971	38.1162000000	470.6813658220
10	dq-pie	10	reno	1	0.9999915500	0.9996839042	9.8944112100	40.5074000000	354.3157910110
10	dq-pie	10	reno	0	0.9999915500	0.9994762898	9.7131541971	38.1162000000	470.6813658220
10	dq-pie	10	reno	1	0.9999915500	0.9996839042	9.8944112100	40.5074000000	354.3157910110
10	dq-pie	10	reno	0	0.9999915500	0.9994762898	9.7131541971	38.1162000000	470.6813658220
10	dq-pie	10	reno	1	0.9999915500	0.9996839042	9.8944112100	40.5074000000	354.3157910110
10	dq-pie	10	reno	0	0.9999915500	0.9994762898	9.7131541971	38.1162000000	470.6813658220
10	dq-pie	10	reno	1	0.9999915500	0.9996839042	9.8944112100	40.5074000000	354.3157910110
10	dq-pie	10	reno	0	0.9999915500	0.9994762898	9.7131541971	38.1162000000	470.6813658220
10	dq-pie	10	reno	1	0.9999915500	0.9996839042	9.8944112100	40.5074000000	354.3157910110
10	dq-pie	10	reno	0	0.9999915500	0.9994762898	9.7131541971	38.1162000000	470.6813658220
10	dq-pie	10	reno	1	0.9999915500	0.9996839042	9.8944112100	40.5074000000	354.3157910110
10	dq-pie	10	reno	0	0.9999915500	0.9994762898	9.7131541971	38.1162000000	470.6813658220
10	dq-pie	10	reno	1	0.9999915500	0.9996839042	9.8944112100	40.5074000000	354.3157910110
10	dq-pie	10	reno	0	0.9999915500	0.9994762898	9.7131541971	38.1162000000	470.6813658220
10	dq-pie	10	reno	1	0.9999915500	0.9996839042	9.		

dq-red	5	reno	reno	0	1.0000000000	0.9976440099	19.8511654138	57.3538000000	153.6632574880	
dq-red	5	reno	cubic	1	1.0000000000	0.9980793810	22.0462071794	57.3418000000	208.7430000000	
dq-red	10	cubic	cubic	0	1.0000000000	0.9997077199	23.6941874491	57.3418000000	378.6240000000	
dq-red	10	cubic	cubic	1	1.0000000000	0.9996906490	24.8965451374	57.3418000000	328.9150000000	
dq-red	10	cubic	dctcp	0	1.0000000000	0.9999998633	214.0780982400	215.9735907440	316.8870000000	
dq-red	10	cubic	dctcp	1	0.9999994367	0.9999997343	16.4797598680	44.1242000000	220.0104680780	
dq-red	10	cubic	relentless	0	1.0000000000	0.9993345131	12.0569452582	30.9186000000	211.5279591769	
dq-red	10	cubic	relentless	1	0.9999793367	0.9993979887	12.388272754	30.9186000000	201.6594624930	
dq-red	10	reno	dctcp	0	0.9999817800	0.999999916	16.5084666806	44.1242000000	182.0591402250	
dq-red	10	reno	dctcp	1	1.0000000000	0.9999997303	16.7206959766	44.1242000000	245.9930000000	
dq-red	10	reno	relentless	0	1.0000000000	0.99999994367	12.2965601127	30.9186000000	176.8407871020	
dq-red	10	reno	relentless	1	0.9999915667	0.9994577335	11.5587112334	30.9186000000	177.687686050	
dq-red	10	reno	reno	0	0.9999791900	0.9959593921	21.4286110719	57.3538000000	226.7700000000	
dq-red	10	reno	reno	1	0.9999997667	0.9959677533	21.5112218220	57.3538000000	239.9850000000	
dq-red	5	cubic	cubic	0	0.9999938500	0.9999997300	20.7949637737	44.1242000000	178.4142207610	
dq-red	5	cubic	cubic	1	0.9999987500	0.9999979318	21.7564553765	45.3378000000	188.5651619770	
dq-red	5	cubic	dctcp	0	1.0000000000	0.9987722152	5.2578111809	20.8120200000	80.0339941229	
dq-red	5	cubic	dctcp	1	1.0000000000	0.9984793596	5.268679254	18.1204000000	77.6679245420	
dq-red	5	cubic	relentless	0	0.9996563333	0.9075071168	3.7338553010	18.8786000000	178.972423580	
dq-red	5	cubic	relentless	1	0.9999906667	0.9126487712	3.7248651380	18.8786000000	427.2165224120	
dq-red	5	reno	dctcp	0	0.9999910000	0.9984136506	5.2864016302	18.8786000000	587.9633548280	
dq-red	5	reno	dctcp	1	0.9999918333	0.9987293145	5.3027291451	18.8786000000	603.8972448530	
dq-red	5	reno	relentless	0	1.0000000000	0.8923249509	3.6987167243	16.8104000000	321.1232028730	
dq-red	5	reno	relentless	1	1.0000000000	0.9099632486	3.6780881239	18.8786000000	715.8180000000	
dq-red	5	reno	reno	0	0.9999915000	0.9889635156	18.1674173238	52.5474000000	427.2165224120	
dq-red	5	reno	reno	1	0.9999915000	0.9889605923	5.1836505962	50.1322000000	482.5824494400	
dq-red	5	cubic	cubic	0	0.9999851000	0.9996881500	22.8857735681	53.7370000000	835.9780000000	
dq-red	5	cubic	cubic	1	0.9999970167	0.9997231117	23.4596398184	54.9386000000	552.3910000000	
dq-red	5	cubic	dctcp	0	0.9999921500	0.9993055913	7.1831096172	25.2216000000	340.8224529770	
dq-red	5	cubic	dctcp	1	0.9999900000	0.99893541863	2.2953412422	28.1674173238	355.3148031750	
dq-red	5	cubic	relentless	0	0.9999947833	0.9777158930	5.2965999201	30.0280000000	334.2978428370	
dq-red	5	cubic	relentless	1	1.0000000000	0.9802260412	5.22216288642	26.0882000000	461.4120000000	
dq-red	5	reno	dctcp	0	0.9999817000	0.9994179578	7.2640583284	26.1122000000	288.3745993400	
dq-red	5	reno	dctcp	1	0.9999970167	0.9999790167	2.3084231820	26.0882000000	427.7570000000	
dq-red	5	reno	relentless	0	1.0000000000	0.97922656336	7.2468247633	24.68247633	269.7939723210	
dq-red	5	reno	relentless	1	1.0000000000	0.9791224922	5.19171917532	24.0790000000	364.9510000000	
dq-red	5	reno	reno	0	0.9999900000	0.9787464978	5.1632876249	24.7770000000	348.4520000000	
dq-red	5	reno	reno	1	1.0000000000	0.9885309331	19.9432421411	61.3411000000	231.040115830	
dq-red	5	reno	reno	0	0.9999979150	0.9884803222	19.2402194453	59.7450000000	352.0560000000	
dq-red	5	reno	reno	1	1.0000000000	0.9999824956	23.3084231820	57.3337848500	319.062812160	
dq-red	5	reno	reno	0	1.0000000000	0.9986906955	22.2498106925	60.9466000000	330.2670371160	
dq-red	5	cubic	cubic	0	1.0000000000	0.9992646121	9.1465232750	35.7130000000	252.0560000000	
dq-red	5	cubic	dctcp	1	1.0000000000	0.9989461471	9.1674564429	39.3058000000	334.1552161880	
dq-red	5	cubic	relentless	0	1.0000000000	0.986120369	6.6500876953	32.1082000000	245.074936240	
dq-red	5	cubic	relentless	1	0.9999845667	0.9867722630	6.7022851650	31.2175000000	247.3738477230	
dq-red	5	reno	dctcp	0	1.0000000000	0.9993121915	9.218265441	33.3098000000	371.2700000000	
dq-red	5	reno	dctcp	1	0.9999999833	0.9992133554	9.1176227218	35.7130000000	423.0770000000	
dq-red	5	reno	relentless	0	1.0000000000	0.95828251654	6.3389353662	32.1082000000	242.987124280	
dq-red	5	reno	relentless	1	1.0000000000	0.9841277978	6.7550720181	33.6207000000	447.5610000000	
dq-red	5	reno	reno	0	1.0000000000	0.9994205523	21.9815946246	70.8823000000	494.7510000000	
dq-red	5	reno	reno	1	0.9999865500	0.9887172011	22.4337205379	75.3658000000	305.8370000000	
dq-red	5	cubic	cubic	0	0.9999866900	0.99809939192	25.672036956	49.2535000000	3429.0200000000	
dq-red	10	cubic	cubic	1	1.0000000000	0.9979123182	24.6817662105	51.3458000000	1481.7685414400	
dq-red	10	cubic	cubic	10	1	1.0000000000	0.9979123182	2233.4330000000	2233.4330000000	

10	dq-red	cubic	dctcp	0	0.9999892167	0.9895989126	6.6225685868	26.0690000000	1223.4024987600	2710.4760000000
10	dq-red	cubic	dctcp	1	1.0000000000	0.9888758647	6.5494309709	24.8986000000	1386.7293381700	3452.3200000000
10	dq-red	cubic	relentless	0	0.9995187333	0.7663005541	4.8246947300	29.6930000000	1539.8300000000	3452.3200000000
10	dq-red	cubic	relentless	1	1.0000000000	0.7532243256	4.8224984789	24.8860000000	521.6142359620	1279.3800000000
10	dq-red	cubic	reno	0	1.0000000000	0.9887889339	6.5273274254	24.8965000000	979.1145323780	1356.2700000000
10	dq-red	cubic	dctcp	1	1.0000000000	0.9892480619	6.4837823487	23.1697000000	806.7408740500	1165.2200000000
10	dq-red	cubic	reno	0	1.0000000000	0.7722082552	4.8729584847	22.5075000000	394.5024097660	911.6790000000
10	dq-red	cubic	relentless	1	1.0000000000	0.7694165035	4.8014377830	24.8986000000	399.6225595870	1046.2500000000
10	dq-red	cubic	reno	0	0.9999749833	0.9113953497	20.2404738467	58.5434000000	538.7190165770	1376.7000000000
10	dq-red	cubic	reno	1	0.9999790401	0.8831383423	19.9185112123	59.7450000000	519.4748495450	1502.8700000000
10	dq-red	cubic	cubic	0	1.0000000000	0.9978244052	24.1576876537	63.3498000000	581.3262967030	842.4410000000
10	dq-red	cubic	dctcp	0	0.9999784533	0.9978191826	23.3584085224	52.0549000000	563.7472945150	930.9040000000
10	dq-red	cubic	reno	0	0.9999377987	0.9938777987	6.6150320844	28.5034000000	504.2851942460	817.2670000000
10	dq-red	cubic	dctcp	1	0.9999915333	0.9947155175	6.5781089604	30.9066000000	477.1736193020	651.2550000000
10	dq-red	cubic	relentless	0	1.0000000000	0.9383488851	4.8122685235	23.6970000000	387.5883731700	636.5130000000
10	dq-red	cubic	relentless	1	0.9999842667	0.9406522358	4.8089993805	28.2106000000	404.3605934240	760.2770000000
10	dq-red	cubic	reno	0	1.0000000000	0.9943248866	6.5253372468	28.5034000000	374.4716752590	524.7640000000
10	dq-red	cubic	dctcp	1	0.9999914833	0.9942971263	6.7760325115	33.3098000000	397.6957535000	539.1830000000
10	dq-red	cubic	relentless	0	1.0000000000	0.9420851200	4.7118539952	24.0200000000	311.2907589470	481.5060000000
10	dq-red	cubic	reno	1	0.9999747104	0.940127917230	2.7624800000	314.2848938360	546.4050000000	830.5130000000
10	dq-red	cubic	reno	0	0.9999866333	0.9663600573	21.7727884322	6.6954600000	338.9260288810	618.4890000000
10	dq-red	cubic	reno	1	1.0000000000	0.9610271125	21.5524149558	67.2655000000	327.5506471780	561.8800000000
10	dq-red	cubic	dctcp	0	1.0000000000	0.9983914381	23.7418792660	63.3498000000	463.7381237310	708.6110000000
10	dq-red	cubic	reno	1	0.9999818383	0.9977474540	23.6002273669	6.5514000000	677.3670000000	677.3670000000
10	dq-red	cubic	dctcp	0	1.0000000000	0.9974322370	9.6932935979	37.2255000000	470.297645970	694.3580000000
10	dq-red	cubic	reno	1	1.0000000000	0.9973935667	9.7950144861	42.5143000000	473.551688630	749.9280000000
10	dq-red	cubic	relentless	0	0.9999852333	0.9731334931	6.9048475783	37.2070000000	400.2707044350	679.0330000000
10	dq-red	cubic	reno	1	1.0000000000	0.9682777044	6.9661207021	36.0239000000	381.8631245500	590.5440000000
10	dq-red	cubic	dctcp	0	0.9999663333	0.99707408908	9.7587408934	40.8423000000	328.4451360270	449.3860000000
10	dq-red	cubic	reno	1	0.9999166667	0.9974534542	9.9438769163	40.8423000000	334.4097364940	435.8450000000
10	dq-red	cubic	dctcp	1	0.9999866333	0.9690426240	6.9193895605	35.7130000000	291.0582535350	411.9730000000
10	dq-red	cubic	reno	0	0.9999915090	0.9698033341	6.9828033341	40.5074000000	296.2554403030	427.4340000000
10	dq-red	cubic	relentless	1	1.0000000000	0.9972586693	24.6819710855	76.5674000000	302.6631642490	439.4500000000
10	dq-red	cubic	reno	0	0.9984361833	0.9999046393	1.3263000236	4.4714500000	10.4940351277	50.4551000000
10	dq-red	cubic	dctcp	1	0.9864210167	1.000035893648	1.3134241901	4.4714500000	10.6798292598	50.1442000000
10	dq-red	cubic	reno	0	0.9838113000	0.87135065	1.257459226	4.4714500000	8.361449482	46.5274000000
10	dq-red	cubic	relentless	1	0.9842381167	0.8606751306	1.2974016411	4.4834600000	7.6035087400	37.2376000000
10	dq-red	cubic	reno	0	0.9601933333	1.0062420735	1.1712938580	4.4714500000	11.2922926803	68.1562000000
10	dq-red	cubic	dctcp	1	0.9449181833	1.0151549293	1.0695219326	4.4714500000	12.5798302893	57.3418000000
10	dq-red	cubic	reno	0	0.9417441650	0.9417443342	1.0692293917	4.4714500000	8.181449482	45.3258000000
10	dq-red	cubic	relentless	1	0.9228964000	0.9496366493	1.0349143891	4.4714500000	8.0224845552	46.8553000000
10	dq-red	cubic	reno	0	0.9913301833	1.2362901589	1.2895001948	4.4834600000	15.2277018903	58.5554000000
10	dq-red	cubic	dctcp	1	1.0000000000	0.999957324	1.4626988887	4.4714500000	33.2571488350	70.5714000000
10	dq-red	cubic	reno	0	0.9882661833	1.0002475978	1.2973661315	4.4714500000	14.1608228185	46.5274000000
10	dq-red	cubic	dctcp	1	0.9999515233	0.9353829409	1.4503928381	4.4714500000	30.0432578453	59.7450000000
10	dq-red	cubic	reno	0	0.96339461000	1.3518711459	1.0577723479	4.7846700000	16.3518401811	75.3778000000
10	dq-red	cubic	dctcp	1	0.9987173167	1.0000426911	1.4564121015	4.4714500000	31.7659557828	76.5794000000
10	dq-red	cubic	reno	0	0.9433361000	1.0299269356	1.0795110533	4.4726700000	13.184732762	59.7450000000
10	dq-red	cubic	dctcp	1	0.9989652767	0.9474830763	1.449519626	4.4714500000	30.1060358165	66.9540000000
10	dq-red	cubic	reno	0	0.9308121333	1.4517733354	1.2735401153	4.7726700000	16.4193381717	59.7450000000
10	dq-red	cubic	dctcp	1	1.0000000000	1.0000751944	1.3829247024	4.4714500000	51.2743668497	86.1892000000

14s-cred	10	cubic	relentless	0	0.9864642667	1.1013705938	1.3002934871	4.4714500000	13.511693295
14s-cred	10	cubic	relentless	1	0.999941600	0.9725114210	1.4442870340	4.4594300000	49.7103078810
14s-cred	10	reno	dctcp	0	0.9681918500	1.6118636269	1.0890614524	4.7726700000	15.5507800483
14s-cred	10	reno	dctcp	1	0.9999790600	1.0018207589	1.3697430972	4.4714500000	52.1054088975
14s-cred	10	reno	relentless	0	0.952465933	1.2044115880	1.0879712926	4.7726700000	13.551452754
14s-cred	10	reno	relentless	1	0.9997512100	0.9745905480	1.4705609070	4.7703500000	49.6247433622
14s-cred	5	cubic	dctcp	0	0.9966141833	1.0021898149	1.9983868937	11.6690000000	89.7850000000
14s-cred	5	cubic	dctcp	1	0.9954405633	1.0026302834	2.0249284723	10.4794000000	32.7463757086
14s-cred	5	cubic	relentless	0	0.9954405633	0.8284840151	1.8139919895	17.796230922	187.1140000000
14s-cred	5	cubic	relentless	1	0.9930698333	0.7762237536	1.7821160913	9.4166600000	84.0939000000
14s-cred	5	reno	dctcp	0	0.9932778867	1.0071836322	2.0110227157	11.6810000000	18.0294183055
14s-cred	5	reno	dctcp	1	0.9910596767	1.0001805482	1.980039149	11.6810000000	32.1848319715
14s-cred	5	reno	relentless	0	0.9863617500	0.8013222239	1.7544390103	10.4794000000	34.1163537579
14s-cred	5	reno	relentless	1	0.9760871567	0.8551807503	1.7110156868	9.5844300000	103.0030000000
14s-cred	5	cubic	dctcp	0	0.9940672200	1.2307945144	1.8179136631	9.2778400000	141.7770000000
14s-cred	5	cubic	dctcp	1	0.9999906667	1.0034908041	1.6957006917	7.1855600000	243.9710000000
14s-cred	5	cubic	relentless	0	0.9930973667	1.0024255346	1.6605637050	9.2658300000	96.9946000000
14s-cred	5	cubic	relentless	1	0.9993979383	0.859679535	1.1791471660	5.8666600000	82.3889000000
14s-cred	5	reno	dctcp	0	0.9900659167	1.2264631373	1.7703172342	9.9974900000	75.6887000000
14s-cred	5	reno	dctcp	1	0.9990453667	1.0047374465	1.6567830953	8.3841800000	103.0030000000
14s-cred	5	reno	relentless	0	0.9784330333	1.0099676779	1.5705381663	8.3871600000	49.4996706761
14s-cred	5	reno	relentless	1	0.9976960000	0.8699671425	1.6341958710	22.470305885	98.1842000000
14s-cred	5	cubic	dctcp	0	0.99246256867	1.5135592354	1.882361027	9.5887000000	35.0298446004
14s-cred	5	cubic	dctcp	1	1.0000000000	1.012753734	1.5318284809	6.8745000000	22.6162559077
14s-cred	5	cubic	relentless	0	0.9932778833	1.2082073609	1.6946503265	8.0642300000	33.9164841016
14s-cred	5	cubic	relentless	1	0.9999866683	0.912559834	1.5447329793	7.7750606667	77.7810000000
14s-cred	5	cubic	dctcp	0	0.9921161167	1.4729472010	1.807523570	9.2413000000	55.0301549705
14s-cred	5	cubic	dctcp	1	0.9999866600	1.0134050729	1.547476103	8.0762500000	36.030087444
14s-cred	5	cubic	relentless	0	0.9801702833	1.2400091852	1.6514129479	9.2778400000	66.4582612647
14s-cred	5	reno	dctcp	1	1.0000000000	1.0049755033	1.5209588197	55.0380000000	116.2320000000
14s-cred	5	reno	dctcp	0	0.9811762340	1.0115791544	1.3137784698	17.6899000000	77.7810000000
14s-cred	5	reno	dctcp	1	0.9843884467	1.0023412270	2.8933422557	18.9027000000	51.2788201897
14s-cred	5	reno	dctcp	0	0.9695410933	0.9006721916	2.2215357378	13.2056000000	325.3100000000
14s-cred	5	reno	dctcp	1	0.9725576633	0.8628009171	2.2493800000	26.2497295445	205.4610000000
14s-cred	5	reno	dctcp	0	0.9766231167	0.8412646053	2.2493800000	15.2975000000	27.9050317179
14s-cred	5	reno	dctcp	1	0.9811762340	1.0049755033	1.5209588197	48.3766933679	194.6340000000
14s-cred	5	reno	dctcp	0	0.9832069467	1.0000425484	2.8633825899	15.2975000000	55.0323690434
14s-cred	5	reno	dctcp	1	0.9668851567	0.8896215281	2.2373166739	15.4688000000	26.8320751213
14s-cred	5	reno	dctcp	0	0.9897254033	1.0110426545	2.095354375	11.8682000000	55.5921636791
14s-cred	5	reno	dctcp	1	0.9998898167	1.0120775959	2.0755549732	11.6931000000	70.0693708362
14s-cred	5	reno	relentless	0	0.9855001333	1.0018757954	1.9331925409	12.0040000000	44.2883735085
14s-cred	5	reno	relentless	1	0.9998788833	0.8940728346	2.0568822745	12.8826000000	32.2450266446
14s-cred	5	reno	relentless	0	0.9897254033	1.145978993	1.938798099	11.6810000000	44.8084814734
14s-cred	5	reno	relentless	1	0.9990979200	1.0110426545	2.095354375	16.8104000000	57.1314261619
14s-cred	5	reno	relentless	0	0.9752317833	1.0076226806	1.05723019	11.8682000000	308.4659000000
14s-cred	5	reno	relentless	1	0.9971754167	0.8894077338	1.9331925409	12.0040000000	199.1180000000
14s-cred	5	reno	dctcp	0	0.9895473067	1.3588822745	2.0568822745	12.8826000000	44.2883735085
14s-cred	5	reno	dctcp	1	1.0000000000	1.28381626	1.8593822878	10.4915000000	34.9730000000
14s-cred	5	reno	dctcp	0	0.9858530500	1.0545956956	1.9222579157	12.5028000000	155.8850000000
14s-cred	5	reno	dctcp	1	0.9999991500	0.9209891506	1.7377225266	8.0642300000	35.7057745287
14s-cred	5	reno	dctcp	0	0.9894374833	1.311912520	2.3480115587	15.1698000000	112.6442609156
14s-cred	5	reno	dctcp	1	1.0000000000	1.0222578416	1.80477734867	10.4794000000	270.0410000000
14s-cred	10	cubic	relentless	0	0.999941600	1.6118636269	1.0890614524	15.5507800483	170.9430000000
14s-cred	10	cubic	relentless	1	0.9999790600	1.2044115880	1.0879712926	13.551452754	58.9842000000
14s-cred	10	reno	dctcp	0	0.9997512100	0.9745905480	1.4705609070	4.7703500000	89.7850000000
14s-cred	10	reno	dctcp	1	0.9996141833	1.0021898149	1.9983868937	11.6690000000	230.3720000000
14s-cred	10	reno	dctcp	0	0.9954405633	1.0026302834	2.0249284723	10.4794000000	187.1140000000
14s-cred	10	reno	dctcp	1	0.9954405633	0.8284840151	1.8139919895	17.796230922	84.0939000000
14s-cred	10	reno	dctcp	0	0.9930698333	0.7762237536	1.7821160913	9.4166600000	94.5914000000
14s-cred	10	reno	dctcp	1	0.9932778867	1.0071836322	2.0110227157	11.6810000000	279.6500000000
14s-cred	10	reno	dctcp	0	0.9910596767	1.0001805482	1.980039149	11.6810000000	257.9970000000
14s-cred	10	reno	dctcp	1	0.9863617500	0.8013222239	1.7544390103	10.4794000000	103.0030000000
14s-cred	10	reno	dctcp	0	0.9760871567	0.8551807503	1.7110156868	9.5844300000	187.1140000000
14s-cred	10	reno	dctcp	1	0.9940672200	1.2307945144	1.8179136631	9.2778400000	141.7770000000
14s-cred	10	reno	dctcp	0	0.9999906667	1.0034908041	1.6957006917	7.1855600000	243.9710000000
14s-cred	10	reno	dctcp	1	0.9930973667	1.0024255346	1.6605637050	9.2658300000	96.9946000000
14s-cred	10	reno	dctcp	0	0.9993979383	0.859679535	1.1791471660	5.8666600000	75.6887000000
14s-cred	10	reno	dctcp	1	0.9900659167	1.2264631373	1.7703172342	9.9974900000	183.5220000000
14s-cred	10	reno	dctcp	0	0.9990453667	1.0047374465	1.6567830953	8.3841800000	103.0030000000
14s-cred	10	reno	dctcp	1	0.9784330333	1.0099676779	1.5705381663	8.3871600000	49.4996706761
14s-cred	10	reno	dctcp	0	0.9976960000	0.8699671425	1.6341958710	7.7845000000	98.1842000000
14s-cred	10	reno	dctcp	1	0.99246256867	1.5135592354	1.882361027	9.5887000000	22.6162559077
14s-cred	10	reno	dctcp	0	0.9932778833	1.2082073609	1.6946503265	8.0642300000	77.7810000000
14s-cred	10	reno	dctcp	1	0.9999866683	0.912559834	1.5447329793	7.7750606667	93.4018000000
14s-cred	10	reno	dctcp	0	0.9921161167	1.4729472010	1.807523570	9.2413000000	36.0315497059
14s-cred	10	reno	dctcp	1	0.9999866600	1.0134050729	1.547476103	8.0762500000	66.030087444
14s-cred	10	reno	dctcp	0	0.9801702833	1.2400091852	1.6514129479	9.2778400000	92.1882000000
14s-cred	10	reno	dctcp	1	0.9900000000	1.0049755033	1.5209588197	55.0380000000	95.7930000000
14s-cred	10	reno	dctcp	0	0.9811762340	1.0115791544	1.3137784698	17.6899000000	349.3300000000
14s-cred	10	reno	dctcp	1	0.9843884467	1.0023412270	2.8933422557	18.9027000000	51.2788201897
14s-cred	10	reno	dctcp	0	0.9695410933	0.9006721916	2.2215357378	13.2056000000	325.3100000000
14s-cred	10	reno	dctcp	1	0.9725576633	0.8628009171	2.2493800000	26.2497295445	205.4610000000
14s-cred	10	reno	dctcp	0	0.9766231167	0.8412646053	2.2493800000	18.0100000000	55.5921636791
14s-cred	10	reno	dctcp	1	0.9811762340	1.0049755033	1.5209588197	48.3766933679	194.6340000000
14s-cred	10	reno	dctcp	0	0.9832069467	1.0000425484	2.8633825899	15.2975000000	55.0323690434
14s-cred	10	reno	dctcp						

14s-cred	10	reno	relentless	0	0.9873375500	1.0586760177	1.9221521437	10.7904000000	36.1969462994
14s-cred	10	reno	relentless	1	0.9999941333	0.9100011490	1.7174517460	10.4674000000	64.0729713618
14s-pi2	1	cubic	dctcp	0	0.9762799667	1.017334918169	1.7338827400	10.4794000000	39.3228000000
14s-pi2	1	cubic	dctcp	1	0.9819473333	1.0051913176	1.6729653619	11.6810000000	15.7130402753
14s-pi2	1	cubic	relentless	0	0.9759195500	0.9077477888	1.7060882369	11.6690000000	15.3346630514
14s-pi2	1	cubic	relentless	1	0.9741370500	0.9124636037	1.7490959464	11.6810000000	15.1802693563
14s-pi2	1	reno	dctcp	0	0.9337833000	1.0023624829	2.0073296792	10.4915000000	40.5194000000
14s-pi2	1	reno	dctcp	1	0.9255612433	1.0039945315	1.9895073211	10.4915000000	40.5194000000
14s-pi2	1	reno	relentless	0	0.9236298500	0.9827072495	1.7566329609	11.6810000000	16.3741928904
14s-pi2	1	reno	relentless	1	0.9110932000	0.9678473533	1.8580352992	11.6810000000	16.6365120823
14s-pi2	1	cubic	dctcp	0	0.9843582500	0.9999999037	1.9876870527	16.4874000000	47.7290000000
14s-pi2	1	cubic	dctcp	1	0.9778496000	0.0001189578	2.656813773	10.4915000000	48.9306000000
14s-pi2	1	cubic	relentless	0	0.989732467	0.9567522691	1.8860615371	11.6931000000	15.6915983902
14s-pi2	1	cubic	relentless	1	0.9837098733	0.9496376563	1.9943819654	14.0963000000	15.379656047
14s-pi2	1	reno	dctcp	0	0.9208394267	0.9994300259	2.2220128128	25.2338000000	55.2712000000
14s-pi2	1	reno	dctcp	1	0.9231507067	0.98893192	3.268641735	20.3018000000	56.1402000000
14s-pi2	1	reno	relentless	0	0.9466004567	0.9578805618	2.9851011483	24.9106000000	54.9386000000
14s-pi2	1	reno	relentless	1	0.9478421067	0.953407593	2.7776241006	21.2938000000	52.5354000000
14s-pi2	1	cubic	dctcp	0	0.9873346900	0.9991229930	1.6624581047	16.4874000000	46.1492000000
14s-pi2	1	cubic	dctcp	1	0.9759923333	0.9895031795	2.149931567	20.1043000000	53.7370000000
14s-pi2	1	cubic	relentless	0	0.9906688900	0.9889733640	1.7618301945	16.4995000000	57.7302615272
14s-pi2	1	cubic	relentless	1	0.9833560567	0.9623387090	1.8909818490	20.1639000000	51.3338000000
14s-pi2	1	reno	dctcp	0	0.9836898967	0.9981106340	2.0190110900	23.7900000000	53.7340000000
14s-pi2	1	reno	dctcp	1	0.9501050800	0.9978239555	2.5326850971	20.8264000000	60.9556000000
14s-pi2	1	reno	relentless	0	0.9771563100	0.9631236342	2.3453270847	21.3059000000	53.84895323
14s-pi2	1	reno	relentless	1	0.9427152100	0.9627093364	2.791849485	28.5154000000	60.9466000000
14s-pi2	1	cubic	dctcp	0	0.9893573833	0.9528755747	2.4345973608	15.2858000000	44.1342000000
14s-pi2	1	cubic	dctcp	1	0.9853346667	0.9217955079	2.3225532079	14.4192000000	42.9346000000
14s-pi2	1	cubic	relentless	0	0.9797979783	0.6569111254	2.2576168123	15.6088000000	45.6487000000
14s-pi2	1	cubic	relentless	1	0.9842906000	0.6021231858	2.2116085057	15.2738000000	45.3248000000
14s-pi2	1	reno	dctcp	0	0.97184967167	0.9065845477	2.3307557066	14.4072000000	44.1242000000
14s-pi2	1	reno	dctcp	1	0.9734436833	0.9253333227	2.439585128	15.2858000000	44.1242000000
14s-pi2	1	reno	relentless	0	0.9666074167	0.6238956167	2.3248920000	16.4192000000	42.9346000000
14s-pi2	1	reno	relentless	1	0.9572498333	0.6146891674	2.3891085527	18.0000000000	46.7290000000
14s-pi2	1	cubic	dctcp	0	0.9927570333	0.9910069536	1.9717024833	17.6890000000	48.0519000000
14s-pi2	1	cubic	dctcp	1	0.9839100667	0.9784455479	2.1237910198	16.4874000000	47.7290000000
14s-pi2	5	cubic	relentless	0	0.9903438800	0.9253333227	2.439585128	15.2858000000	44.1242000000
14s-pi2	5	cubic	relentless	1	0.9881757500	0.8167420388	1.9167541209	15.6208000000	46.5274000000
14s-pi2	5	reno	dctcp	0	0.9656597000	0.9664436625	2.5592154290	20.0922000000	49.2525000000
14s-pi2	5	reno	dctcp	1	0.9500650000	0.9807554594	2.8207302033	23.6970000000	53.7370000000
14s-pi2	5	reno	relentless	0	0.9666068167	0.8061150274	2.290418184	22.4954000000	52.5354000000
14s-pi2	5	reno	relentless	1	0.9616805333	0.8003198524	2.2949932187	23.6970000000	52.5354000000
14s-pi2	5	cubic	dctcp	0	0.9889367167	0.9883221079	1.9487440075	19.0267000000	49.930415510
14s-pi2	5	cubic	dctcp	1	0.9770210000	0.9974841079	2.1821001291	20.1043000000	50.1442000000
14s-pi2	5	reno	relentless	0	0.9924467667	0.8834100692	1.7145201913	20.1043000000	50.1322000000
14s-pi2	5	reno	relentless	1	0.9929621000	0.885390058	1.7404753705	16.4656000000	46.5274000000
14s-pi2	5	reno	dctcp	0	0.9828487500	0.9873087090	2.1450741938	22.8281000000	54.9246000000
14s-pi2	5	reno	dctcp	1	0.9634695833	0.9822025756	2.5699124968	28.3840000000	59.7450000000
14s-pi2	5	reno	relentless	0	0.9759555000	0.8778531264	2.2798649574	24.9106000000	55.4641000000
14s-pi2	5	reno	relentless	1	0.9597454800	0.8766173134	2.3934842105	16.0732719306	53.5986000000
14s-pi2	10	cubic	dctcp	0	0.9861531667	0.8239073320	3.1304783307	21.2818000000	47.7292000000
14s-pi2	10	cubic	dctcp	1	0.9870543500	0.8187150889	3.1846576071	18.8906000000	47.7410000000

14s-pi2	-	10	-	0	0.9662867000	0.4095875227	21.2938000000	50.1322000000
14s-pi2	-	10	-	1	0.9605948333	0.4152686333	2.9641803651	16.2065455761
14s-pi2	-	10	-	1	0.9777093800	0.8061732939	3.2043928908	22.4950000000
14s-pi2	-	10	-	1	0.9759948333	0.8297350382	3.3028712260	20.1043000000
14s-pi2	-	10	-	1	0.9759948333	0.8297350382	3.3028712260	18.9872660270
reno	-	dctcp	-	0	0.9483837000	0.4186079282	3.1026032362	23.6970000000
reno	-	dctcp	-	0	0.9516471333	0.4190360339	3.1105820963	16.7090000000
reno	-	dctcp	-	0	0.9893774500	0.9813064175	2.77938497	15.9449101082
cubic	-	dctcp	-	0	0.9873546667	0.9766070859	2.2308245620	45.3378000000
cubic	-	dctcp	-	0	0.9903967000	0.7396200960	2.0812111122	20.1043000000
cubic	-	dctcp	-	0	0.9888688333	0.7357658858	2.0839103435	17.9867000000
cubic	-	dctcp	-	0	0.9769609500	0.9863344802	2.4994877528	22.5075000000
reno	-	dctcp	-	1	0.9661464667	0.9420210161	2.7616068937	23.6970000000
reno	-	dctcp	-	1	0.99036250	0.7316278816	2.3483883166	53.7490000000
reno	-	dctcp	-	1	0.970772353	0.7247003253	2.4931479356	26.0882400000
reno	-	dctcp	-	0	0.9925533333	0.9885057160	1.860220485	18.8906000000
reno	-	dctcp	-	0	0.981343167	0.9926595397	2.123811421	18.9060000000
reno	-	dctcp	-	0	0.9949108667	0.8398577882	1.822223547	16.8201000000
cubic	-	dctcp	-	0	0.99036250	0.83951548	1.9753621147	21.2938000000
cubic	-	dctcp	-	0	0.9807561167	0.9833598828	2.1247743981	23.7090000000
cubic	-	dctcp	-	1	0.9611348157	0.9605882686	2.8056286252	28.5154000000
reno	-	dctcp	-	0	0.975094333	0.8285956560	2.2244442773	15.8736843153
reno	-	dctcp	-	0	0.9710129500	0.829347638	2.5012460333	16.2278000510
reno	-	dctcp	-	0	0.9246988500	1.0367223246	1.2774631122	4.4714500000
reno	-	dctcp	-	1	0.9182826633	1.0329281050	1.3784284109	4.4714500000
cubic	-	dctcp	-	0	0.9753863667	0.9889358026	1.4795450278	4.4714500000
cubic	-	dctcp	-	1	0.9837099167	0.9799169447	1.7997051828	8.4714500000
reno	-	dctcp	-	0	0.9129832500	1.0811318469	1.2920543867	4.7662000000
reno	-	dctcp	-	1	0.8712918167	1.0387084049	1.1393235911	4.4714500000
reno	-	dctcp	-	0	0.9629222000	1.0666632095	1.4069320420	4.4714500000
reno	-	dctcp	-	1	0.9311599500	0.9999513734	1.33015981346	31.4792321452
cubic	-	dctcp	-	0	0.9854298167	1.0005343628	1.3083529277	8.8843950994
cubic	-	dctcp	-	1	0.9633227500	0.9996714291	1.2982055573	30.8811688512
reno	-	dctcp	-	0	0.9933282100	0.9630510943	1.4602647396	14.7462000000
reno	-	dctcp	-	1	0.9879355100	0.9966815032	1.4385801326	27.3302033601
reno	-	dctcp	-	0	0.9544208533	0.9968839471	1.2130342071	4.4714500000
reno	-	dctcp	-	1	0.9379089600	0.9331031674	1.1741170705	4.4714500000
cubic	-	dctcp	-	0	0.9563331313	0.9437240598	1.3286086868	4.7665000000
cubic	-	dctcp	-	1	0.9274349533	0.9519767523	1.2864310290	4.4714500000
reno	-	dctcp	-	0	0.995687200	0.9992266602	1.23493216675	4.4714500000
reno	-	dctcp	-	1	0.9925816100	0.986712500	1.2502621957	4.4594300000
cubic	-	dctcp	-	0	0.995109767	0.959718477	1.2243817265	4.7605000000
cubic	-	dctcp	-	1	0.9882772700	0.9663809476	1.3152493948	5.6393200000
reno	-	dctcp	-	0	0.9874147867	0.995326392	1.1786194091	4.4714500000
reno	-	dctcp	-	1	0.9741771233	0.9953658301	1.1554221282	4.4714500000
reno	-	dctcp	-	0	0.9878954233	0.961948552	1.2502621957	4.4594300000
reno	-	dctcp	-	1	0.96528806	1.3604798677	1.2243817265	17.979946119
cubic	-	dctcp	-	0	0.9051249833	0.953913342	1.2208151930	52.5354000000
cubic	-	dctcp	-	1	0.9069952667	0.968302635	1.6008768558	10.4794000000
reno	-	dctcp	-	0	0.9734062333	0.8562441576	1.8711428407	9.2653000000
reno	-	dctcp	-	1	0.9748380667	0.790670786	1.8538424537	33.9485278788
cubic	-	dctcp	-	0	0.8995654333	0.9613131060	1.4759309312	27.321839669
cubic	-	dctcp	-	1	0.8786451167	0.9735954011	1.5332478466	206.3400000000

14s-pie	reno	relentless	reno	0.9484829333	0.8818538841	1.761002499	10.467400000	33.0313622739
14s-pie	reno	relentless	dctcp	1	0.9609696667	0.8267359476	1.784201945	9.277840000
14s-pie	cubic	relentless	dctcp	0	0.9749653667	0.9729502674	1.4482116246	8.076250000
14s-pie	cubic	relentless	dctcp	1	0.9450183000	0.96656580083	1.4456459589	10.351200000
14s-pie	cubic	relentless	dctcp	0	0.8869605000	0.8140968532	1.5115236885	20.9837162603
14s-pie	cubic	relentless	dctcp	1	0.9742172667	0.8300731266	1.5210346245	8.076250000
14s-pie	reno	relentless	dctcp	0	0.9631677333	0.9740871389	1.326482527	6.874650000
14s-pie	reno	relentless	dctcp	1	0.9360645400	0.9486468734	1.3378363175	7.388720000
14s-pie	reno	relentless	dctcp	0	0.9660416667	0.7892349477	1.4181995346	8.076250000
14s-pie	reno	relentless	dctcp	1	0.9492216500	0.8093385265	1.4399141902	21.5625931984
14s-pie	cubic	relentless	dctcp	0	0.9956634500	0.9987047462	1.4005639718	6.6084793398
14s-pie	cubic	relentless	dctcp	1	0.9900828333	0.9894079520	1.3710784883	8.6648430062
14s-pie	cubic	relentless	dctcp	0	0.9973791333	0.8855797616	1.4151187266	12.862630000
14s-pie	cubic	relentless	dctcp	1	0.9916804500	0.89774926283	1.4221273615	8.862300000
14s-pie	reno	relentless	dctcp	0	0.9881388000	0.9818548847	1.2351697424	7.185560000
14s-pie	reno	relentless	dctcp	1	0.9758943333	0.9754533664	1.2299141341	8.113950000
14s-pie	reno	relentless	dctcp	0	0.9789741833	0.8693455011	1.303575959	7.095090000
14s-pie	reno	relentless	dctcp	1	0.9710605733	0.8701013976	1.3178588040	6.874650000
14s-pie	cubic	relentless	dctcp	0	0.9263555167	0.8126948580	1.9035172737	12.882600000
14s-pie	cubic	relentless	dctcp	1	0.9325016967	0.9269057228	2.0318125756	11.681000000
14s-pie	cubic	relentless	dctcp	0	0.9673806000	0.7070178855	2.0478221196	10.802400000
14s-pie	cubic	relentless	dctcp	1	0.9688615000	0.7070949392	2.1176334340	11.270600000
14s-pie	reno	relentless	dctcp	0	0.9174415500	0.9080507639	1.9669476174	12.004000000
14s-pie	reno	relentless	dctcp	1	0.8734029700	0.9104405315	1.8471615697	13.084200000
14s-pie	reno	relentless	dctcp	0	0.9479886667	0.6831652554	1.985213656	13.193600000
14s-pie	reno	relentless	dctcp	1	0.9473389000	0.7534119121	1.9315563610	14.084200000
14s-pie	cubic	relentless	dctcp	0	0.976682000	0.9456953064	1.5869804916	9.289860000
14s-pie	cubic	relentless	dctcp	1	0.9425149500	0.9303434834	1.5373177590	10.790400000
14s-pie	cubic	relentless	dctcp	0	0.9807944167	0.7622494984	1.6779199757	9.588760000
14s-pie	cubic	relentless	dctcp	1	0.975646833	0.7480184948	1.6143916778	10.802400000
14s-pie	reno	relentless	dctcp	0	0.9606953000	0.938520415	1.4947048749	9.600780000
14s-pie	reno	relentless	dctcp	1	0.9404424167	0.9032296497	1.4499298772	9.289860000
14s-pie	reno	relentless	dctcp	0	0.9625173333	0.74581845111	1.6059730375	11.669000000
14s-pie	reno	relentless	dctcp	1	0.9425150167	0.7581845111	1.5659718460	14.155900000
14s-pie	cubic	relentless	dctcp	0	0.996393500	0.9896594115	1.51346754	10.479400000
14s-pie	cubic	relentless	dctcp	1	0.9818874333	0.9830240696	1.4841452196	9.600780000
14s-pie	cubic	relentless	dctcp	0	0.9935584000	0.850100926	1.5255660839	9.277840000
14s-pie	cubic	relentless	dctcp	1	0.9877675250	0.8246054422	1.4818762514	12.877840000
14s-pie	cubic	relentless	dctcp	0	0.9897030167	0.9705983743	1.379477362	9.277840000
14s-pie	cubic	relentless	dctcp	1	0.9788633500	0.956001856	1.375849635	16.5260559706
14s-pie	cubic	relentless	dctcp	0	0.9853601833	0.8136295430	1.4362483137	8.076250000
14s-pie	cubic	relentless	dctcp	1	0.9723547167	0.8122009188	1.403964936	9.265830000

B.2 Data from LTE Link Simulations

agm	nLF	nGF	ccC	cCL	ecn	utilization	jainmod	qDelayAvgL	qDelayMaxL	qDelayAvgC	qDelayMaxC
sq-pie	1	1	cubic	cubic	0	0.7634327249	0.9889424546	7.7497061215	41.044000000	7.7497061215	41.044000000
sq-pie	1	1	cubic	cubic	1	0.6608886195	0.9960126385	8.5269043924	46.022000000	8.5269043924	46.022000000
sq-pie	1	1	reno	reno	0	0.823681846	1.014737375	7.689255542	23.034000000	7.689255542	23.034000000
sq-pie	1	1	reno	reno	1	0.7410520346	1.0039266032	7.9071725089	25.046000000	7.9071725089	25.046000000
sq-pie	1	1	cubic	cubic	0	0.8382875166	0.9999322528	6.1131741344	20.044000000	6.1131741344	20.044000000
sq-pie	1	1	cubic	cubic	1	0.8513577771	0.9986969805	6.1517541160	21.022000000	6.1517541160	21.022000000
sq-pie	1	1	reno	reno	0	0.8097303836	1.0031103600	7.1542179125	36.046000000	36.046000000	36.046000000
sq-pie	1	1	reno	reno	1	0.8437586423	0.9936560781	6.27512273945	25.046000000	6.27512273945	25.046000000
sq-pie	1	10	cubic	cubic	0	0.9819141738	1.0012682321	5.2639459393	18.058000000	5.2639459393	18.058000000
sq-pie	1	10	cubic	cubic	1	0.9554926849	1.0001021329	6.0186011826	25.022000000	6.0186011826	25.022000000
sq-pie	1	10	reno	reno	0	0.9380777771	1.0008030912	6.2986981576	28.046000000	6.2986981576	28.046000000
sq-pie	1	10	reno	reno	1	0.9195516923	0.9992218242	6.8877147201	25.046000000	6.8877147201	25.046000000
sq-pie	5	1	cubic	cubic	0	0.8049302852	1.0000945370	6.8162964639	30.046000000	6.8162964639	30.046000000
sq-pie	5	1	cubic	cubic	1	0.7815967960	1.0004151478	7.0957104028	35.046000000	7.0957104028	35.046000000
sq-pie	5	1	reno	reno	0	0.8282945940	1.0100894233	6.4518648075	27.034000000	6.4518648075	27.034000000
sq-pie	5	1	reno	reno	1	0.8312487013	0.0044648477	6.0660258192	22.046000000	6.0660258192	22.046000000
sq-pie	5	5	cubic	cubic	0	0.9782995151	0.9999055621	5.2540700653	22.034000000	5.2540700653	22.034000000
sq-pie	5	5	cubic	cubic	1	0.9577805666	0.9999881733	5.9559642682	21.046000000	5.9559642682	21.046000000
sq-pie	5	5	reno	reno	0	0.9245804145	1.0026169337	6.6595530142	30.046000000	6.6595530142	30.046000000
sq-pie	5	5	reno	reno	1	0.903840825	1.0000082370	6.5152559734	30.046000000	6.5152559734	30.046000000
sq-pie	5	10	cubic	cubic	0	0.9722199087	1.0005181342	5.6234098995	23.044000000	5.6234098995	23.044000000
sq-pie	5	10	cubic	cubic	1	0.9501961304	0.9999388808	5.66647583447	30.022000000	5.66647583447	30.022000000
sq-pie	5	10	reno	reno	0	0.9287036794	1.0001212486	5.3747243811	22.046000000	5.3747243811	22.046000000
sq-pie	5	10	reno	reno	1	0.8959893015	0.9999893015	6.6198546251	26.034000000	6.6198546251	26.034000000
sq-pie	5	10	cubic	cubic	0	0.9604430462	1.014057264	5.9467131447	23.046000000	5.9467131447	23.046000000
sq-pie	5	10	cubic	cubic	1	0.9811525195	1.0008508266	5.7589790234	21.046000000	5.7589790234	21.046000000
sq-pie	5	10	reno	reno	0	0.9063570983	1.0003898254	6.7654261964	31.046000000	6.7654261964	31.046000000
sq-pie	10	1	reno	reno	1	0.8888593725	1.0002325941	7.0842423770	40.046000000	7.0842423770	40.046000000
sq-pie	10	1	cubic	cubic	0	0.9511623739	1.0016700660	5.6041966241	24.034000000	5.6041966241	24.034000000
sq-pie	10	1	cubic	cubic	1	0.9177806998	1.0014057264	5.7510822412	25.046000000	5.7510822412	25.046000000
sq-pie	10	1	reno	reno	0	0.9108249382	1.0000896302	5.4224942681	23.040000000	5.4224942681	23.040000000
sq-pie	10	5	reno	reno	1	0.8928861000	0.9998524458	5.5626223306	25.046000000	5.5626223306	25.046000000
sq-pie	10	5	cubic	cubic	0	0.9604519551	1.0016917966	5.0869195249	21.022000000	5.0869195249	21.022000000
sq-pie	10	5	cubic	cubic	1	0.9263964537	1.00000793838	5.2951875208	22.046000000	5.2951875208	22.046000000
sq-pie	10	10	reno	reno	0	0.938638658	1.0005768931	5.7129334978	27.046000000	5.7129334978	27.046000000
sq-pie	10	10	reno	reno	1	0.9129797955	1.0001047917	5.4540158143	24.046000000	5.4540158143	24.046000000
sq-pie	1	1	cubic	cubic	0	0.4345797949	0.9954981511	5.9446599751	11.058000000	5.9446599751	11.058000000
sq-red	1	1	cubic	cubic	1	0.4216681784	0.9733971766	6.0660655581	11.046000000	6.0660655581	11.046000000
sq-red	1	1	reno	reno	0	0.3647736357	0.9870020405	5.1238635045	11.046000000	5.1238635045	11.046000000
sq-red	1	1	reno	reno	1	0.3891286062	0.9972695228	5.7129334978	11.046000000	5.7129334978	11.046000000
sq-red	5	1	cubic	cubic	0	0.6683662674	1.005391182	6.6505313214	13.058000000	6.6505313214	13.058000000
sq-red	5	1	cubic	cubic	1	0.9766016163	1.0001389956	6.3390079163	19.044000000	6.3390079163	19.044000000
sq-red	1	5	reno	reno	0	0.6992312322	1.1044981660	6.3645372700	14.034000000	6.3645372700	14.034000000
sq-red	1	5	reno	reno	1	0.8602460202	1.0017445338	6.5867690124	23.034000000	6.5867690124	23.034000000
sq-red	1	10	cubic	cubic	0	0.77663058376	1.3422714778	5.9159766625	14.058000000	5.9159766625	14.058000000
sq-red	1	10	cubic	cubic	1	0.9580116106	1.00114683096	8.3472622335	24.044000000	8.3472622335	24.044000000

1	10	reno	reno	0.6498112930	1.2123819524	6.4217952590	13.0580000000
1	10	reno	cubic	0.8505508462	1.0007623268	8.4907677263	28.0460000000
1	1	cubic	cubic	0.9722545541	1.996181511	6.2443593084	18.0340000000
5	1	cubic	cubic	0.9830675530	1.0010106822	6.4442684336	18.0580000000
5	1	cubic	cubic	0.870333904	0.9990155680	6.414295470	20.0580000000
5	1	reno	reno	0.8653356399	0.9994357688	6.5368259874	21.0580000000
5	1	reno	cubic	0.9834829340	1.1681398449	6.80404644218	18.0460000000
5	5	cubic	cubic	0.974253086	0.998477300	8.327927639	25.0440000000
5	5	reno	reno	0.8948194999	1.1717874079	6.6072281370	23.0340000000
5	5	reno	reno	0.8401934683	1.0002681848	8.0455937475	27.0580000000
5	10	cubic	cubic	0.9884903974	1.4218397344	6.9866063013	18.0580000000
5	10	cubic	cubic	0.9397188154	1.0004665971	9.0704551766	27.0460000000
5	10	reno	reno	0.9041831432	1.4385297229	6.6784009146	21.0220000000
5	10	reno	reno	0.8231974520	0.9998836554	9.2971432617	30.0220000000
10	1	cubic	cubic	0.9750654573	1.0021470327	8.5989347543	22.0460000000
10	1	cubic	cubic	0.9721676797	0.9984637917	8.334841297	23.0460000000
10	1	reno	reno	0.8838226659	1.0010734792	8.1194077106	24.0580000000
10	1	reno	cubic	0.828552405	1.0003415041	8.1488252303	27.0340000000
10	5	cubic	cubic	0.9819563225	1.1195153203	9.0810224835	22.0100000000
10	5	cubic	cubic	0.93952997165	1.0003299607	8.8127533012	26.0460000000
10	5	reno	reno	0.8822999125	1.1412364901	8.3762490775	23.0340000000
10	5	reno	cubic	0.8083448850	0.9999998639	9.1980802320	31.0580000000
10	10	cubic	cubic	0.9824695189	1.3197204300	9.0073817108	21.0460000000
10	10	cubic	cubic	0.8955390378	0.9999999829	9.2134221596	29.0460000000
10	10	reno	reno	0.8784473664	1.324965858	8.2982643603	25.0340000000
10	10	reno	cubic	0.9788480319	1.0000173515	9.7838594257	34.0440000000
1	1	cubic	cubic	0.9823302529	0.9911645555	4.9952272711	47.0460000000
1	1	cubic	cubic	0.9824436870	0.98835382847	4.9716581000	360.0233952560
1	1	dctcp	dctcp	0.9985216777	1.0000000148	5.3889756801	811.0460000000
1	1	cubic	dctcp	0.9985160202	0.9999986018	5.2912875640	197.680227190
1	1	cubic	relentless	0.9974716187	1.0000015666	5.6390500634	369.5145000000
1	1	cubic	relentless	0.9988780757	0.9999998388	5.4833471565	17.0460000000
1	1	reno	dctcp	0.9990122932	1.0000000000	5.6887472667	349.035775330
1	1	reno	dctcp	0.9990122837	1.0000000000	5.4458590000	393.0460000000
1	1	reno	relentless	0.9987922894	0.9999998972	5.8284749975	18.0460000000
1	1	reno	relentless	0.9988043830	0.99999999243	5.5857490666	341.731503110
1	1	reno	dctcp	0.9713105656	0.999104236	5.2183207598	429.0460000000
1	1	reno	dctcp	0.9844287602	0.9723165959	5.4507128198	27.0460000000
1	1	cubic	dctcp	0.9819538182	1.3556391663	5.0124378137	46.0460000000
1	5	cubic	cubic	0.9806943335	1.3663151656	5.008805265	44.0440000000
1	5	cubic	dctcp	0.9988888572	1.4444742077	5.4602974117	302.9573409470
1	5	cubic	dctcp	0.999123027	1.4444444444	5.523435550	303.643295890
1	5	cubic	relentless	0.999123027	1.44442808365	8.0460000000	328.0187075670
1	5	cubic	relentless	0.9987435349	1.44442808365	5.8387069551	16.0460000000
1	5	reno	dctcp	0.998892489	1.44441254479	5.749610201	324.159708030
1	5	reno	dctcp	0.9988566589	1.4439891413	4.7754463911	528.0460000000
1	5	reno	dctcp	0.997239836	1.4411214848	5.2029217092	11.0460000000
1	5	reno	relentless	0.9986479749	1.4440998324	5.6434916243	337.3068435040
1	5	reno	relentless	0.9985389998	1.4440932538	5.915767700	17.0460000000
1	5	reno	reno	0.9838896463	1.3019509192	5.0844832658	340.198846900
1	5	reno	reno	0.9846062179	1.3224088232	5.466729832	290.8944354120
10	1	cubic	cubic	0.9841784845	1.6215090010	5.4197528019	35.6131639310
10	1	cubic	cubic	0.981104202	1.60002437841	5.2403647615	119.4022000000

dq-pie	0	cubic	dctcp	0	0.9970632915	1.66678909226	4.9751905485	12.0460000000	412.1928898530
dq-pie	10	cubic	dctcp	1	0.9990122932	1.66494214927	5.8237710000	8.0460000000	1117.0340000000
dq-pie	10	cubic	relentless	0	0.998815744	1.66693531404	5.7051486500	16.0460000000	419.0510756450
dq-pie	10	cubic	relentless	1	0.99883874311	1.66690192926	5.7473292384	18.0460000000	1089.0340000000
dq-pie	10	reno	dctcp	0	0.9990122932	1.66494214927	5.68120918378	8.0460000000	379.6044807430
dq-pie	10	reno	dctcp	1	0.9978486119	1.66811997690	5.1809304578	12.0460000000	538.0460000000
dq-pie	10	reno	relentless	0	0.9986193002	1.66692085144	5.8099481500	16.0460000000	545.0220000000
dq-pie	10	reno	relentless	1	0.9988418140	1.66691754786	5.6322461872	16.0460000000	540.0460000000
dq-pie	10	reno	reno	0	0.983340359	1.5533340355	5.0291181919	15.0220000000	552.0460000000
dq-pie	10	reno	reno	1	0.9807337897	1.5755539347	5.3394634659	28.0460000000	585.0460000000
dq-pie	5	cubic	relentless	0	0.9911926317	0.53520242425	6.0038052829	23.0460000000	595.0460000000
dq-pie	5	cubic	cubic	1	0.9927733314	0.5348300422	5.8685597817	28.0440000000	621.0560000000
dq-pie	5	cubic	dctcp	0	0.995625956	0.5052470458	5.0607269244	16.0460000000	545.0220000000
dq-pie	5	cubic	dctcp	1	0.9966012835	0.5514466552	5.0291181919	15.0220000000	606.0340000000
dq-pie	5	cubic	relentless	0	0.993862236	0.5433802727	5.1282491632	19.0460000000	732.0460000000
dq-pie	5	cubic	relentless	1	0.9953293687	0.5487579861	5.0890080601	21.0440000000	603.1263614560
dq-pie	5	reno	dctcp	0	0.9964133980	0.5515218246	5.1030353549	16.0460000000	735.3073553550
dq-pie	5	reno	dctcp	1	0.996862158	0.5519740331	5.0384344291	16.0460000000	429.0460000000
dq-pie	5	reno	relentless	0	0.9952690911	0.5484744445	5.0921501928	20.0440000000	385.0460000000
dq-pie	5	reno	relentless	1	0.9954125119	0.5480040377	5.0741477853	17.0460000000	429.0460000000
dq-pie	5	reno	reno	0	0.9875373765	0.4975245571	6.4390594718	39.0220000000	388.0460000000
dq-pie	5	reno	reno	1	0.986901504	0.49966697670	6.381387918	40.0460000000	442.0460000000
dq-pie	5	cubic	cubic	0	0.9923414432	0.99389421015	6.3458897093	25.0340000000	400.0460000000
dq-pie	5	cubic	cubic	1	0.9917821259	0.998059770	6.1039165766	29.0440000000	60.0460000000
dq-pie	5	cubic	dctcp	0	0.9964222571	0.9999587624	5.0699957500	19.0220000000	648.0460000000
dq-pie	5	cubic	dctcp	1	0.9961298631	0.9999556862	5.0100920202	325.2581958510	926.0340000000
dq-pie	5	cubic	relentless	0	0.9950728656	0.99988930268	5.1591876017	21.0460000000	404.3086443190
dq-pie	5	cubic	relentless	1	0.9951473569	0.9998968674	5.0966119328	19.0460000000	657.0460000000
dq-pie	5	reno	dctcp	0	0.9967019205	0.9999653672	5.0627607219	14.0460000000	944.0340000000
dq-pie	5	reno	dctcp	1	0.9966180738	0.9999673027	5.018445202	318.6056477270	529.0460000000
dq-pie	5	reno	relentless	0	0.9952122076	0.99988742627	5.0676541535	19.0220000000	935.0460000000
dq-pie	5	reno	relentless	1	0.9950313366	0.999886666455	5.1410954444	19.0460000000	530.0460000000
dq-pie	5	reno	reno	0	0.9868194809	0.9935013662	6.2068872608	34.0440000000	532.0460000000
dq-pie	5	reno	reno	1	0.9861751569	0.9914437360	6.03044074530	40.0440000000	542.0460000000
dq-pie	10	cubic	cubic	0	0.9902518294	1.0894378758	5.8971861841	30.0440000000	535.0460000000
dq-pie	10	cubic	cubic	1	0.9919397604	1.0928089421	5.8460681317	28.0460000000	530.0460000000
dq-pie	10	cubic	dctcp	0	0.996230956	1.1080092937	5.0776178167	15.0460000000	728.0340000000
dq-pie	10	cubic	dctcp	1	0.9964542974	1.10756323286	5.0185955255	14.0460000000	359.9838585710
dq-pie	10	cubic	relentless	0	0.995701603047	5.0831598369	5.151445152	20.0580000000	391.1377602320
dq-pie	10	cubic	relentless	1	0.9957065697	1.1050355478	5.1308935363	18.0460000000	508.0786554340
dq-pie	10	reno	dctcp	0	0.9963668093	1.1069420773	5.0189510219	15.0440000000	774.0460000000
dq-pie	10	reno	dctcp	1	0.9964055239	1.1073969987	5.1069639153	17.0440000000	1163.0460000000
dq-pie	10	reno	relentless	0	0.9951518350	1.11054515024	5.1158069352	20.0340000000	397.8802698170
dq-pie	10	reno	relentless	1	0.9950749857	1.1049651293	5.151445152	20.0580000000	1084.0580000000
dq-pie	10	reno	reno	0	0.9870315554	1.0619888588	6.3257750682	40.0460000000	711.0460000000
dq-pie	10	reno	reno	1	0.9878190721	1.0683020997	6.6212213755	30.0440000000	1152.0460000000
dq-pie	1	cubic	cubic	0	0.9892765545	0.3094716930	5.261646172	365.1905229010	544.0460000000
dq-pie	10	cubic	cubic	1	0.9912866990	0.3102755411	5.2762676609	25.0340000000	558.0460000000
dq-pie	10	cubic	dctcp	0	0.9933362331	0.3234418557	5.00336845055	18.0220000000	544.0460000000
dq-pie	10	cubic	dctcp	1	0.9940677030	0.3222374663	5.043495900	17.0460000000	556.0460000000
dq-pie	5	cubic	relentless	0	0.9897250533	0.3119634453	5.2277955636	34.0340000000	569.0220000000
dq-pie	10	cubic	relentless	1	0.9913461590	0.31333342334	5.1123041990	25.0340000000	674.0460000000
dq-pie	10	cubic	relentless	1	0.9913461590	0.31333342334	5.1123041990	25.0340000000	654.0460000000
dq-pie	10	cubic	relentless	1	0.9913461590	0.31333342334	5.1123041990	25.0340000000	747.0460000000
dq-pie	10	cubic	relentless	1	0.9913461590	0.31333342334	5.1123041990	25.0340000000	216.6893717230

10	dq-pie	0	reno	dctcp	0.9941954174	0.3232572765	5.0667359236	20.046000000	336.650454440
	dq-pie	1	reno	dctcp	0.9938280567	0.3219405364	5.0334464436	19.046000000	387.046000000
	dq-pie	0	reno	relentless	0.9912243202	0.3143963384	5.1132018885	21.044000000	427.046000000
	dq-pie	1	reno	relentless	0.9915314984	0.3161628080	5.1513647071	21.046000000	388.046000000
	dq-pie	0	reno	reno	0.9861413482	0.285826597	5.5995525743	32.044000000	322.154744180
	dq-pie	1	reno	reno	0.9867181593	0.2898770788	5.5578274751	34.022000000	398.046000000
	dq-pie	0	cubic	cubic	0.8616391487	0.613776255	5.2042653484	26.046000000	667.046000000
	dq-pie	1	cubic	cubic	0.9906024434	0.9907413320	5.0961558532	20.046000000	969.034000000
	dq-pie	0	reno	dctcp	0.9935965976	0.8791431413	5.019898062	18.044000000	428.894053690
	dq-pie	1	reno	dctcp	0.9933647078	0.8789963345	5.0471855161	18.046000000	402.451385820
	dq-pie	0	cubic	dctcp	0.9913299487	0.8629926049	5.1660219545	24.046000000	322.0624584980
	dq-pie	1	reno	relentless	0.9912397034	0.8702331714	5.1031150815	23.046000000	652.046000000
	dq-pie	0	cubic	relentless	0.9914771535	0.8780390434	5.0414578875	20.046000000	917.046000000
	dq-pie	1	reno	dctcp	0.9939092793	0.8794489356	5.0583772138	16.046000000	530.046000000
	dq-pie	0	reno	dctcp	0.9941723712	0.8794489356	5.0583772138	16.046000000	540.046000000
	dq-pie	1	reno	relentless	0.9913299487	0.8629926049	5.1660219545	24.046000000	534.046000000
	dq-pie	0	reno	reno	0.9912397034	0.8702331714	5.1031150815	23.046000000	528.046000000
	dq-pie	1	reno	reno	0.986885111	0.8367826542	5.5850963981	30.034000000	554.046000000
	dq-pie	0	reno	reno	0.9865070165	0.8363223417	5.5007631475	32.056000000	542.046000000
	dq-pie	1	cubic	cubic	0.9902363662	0.9980707492	5.25950624319	32.044000000	723.058000000
	dq-pie	0	reno	cubic	0.9901621126	0.9976649893	5.2818162937	41.7526009510	1094.034000000
	dq-pie	1	reno	cubic	0.9938848926	0.9997251064	5.0722805193	17.046000000	407.4940515220
	dq-pie	0	reno	dctcp	0.9937557045	0.9999727025	5.0582886634	17.034000000	716.046000000
	dq-pie	1	cubic	relentless	0.9908477657	0.99990981724	5.1354336363	21.034000000	1094.034000000
	dq-pie	0	reno	reno	0.99116850257	0.9990483341	5.1965505061	23.046000000	712.034000000
	dq-pie	1	cubic	relentless	0.9902363662	0.9980707492	5.25950624319	32.044000000	1073.058000000
	dq-pie	0	reno	dctcp	0.9945716106	0.9998078698	5.0539505761	18.034000000	353.8619832950
	dq-pie	1	reno	dctcp	0.9941138334	0.9997586313	5.0179517449	17.046000000	543.058000000
	dq-pie	0	reno	relentless	0.9919626260	0.99991832587	5.1710232550	21.044000000	558.046000000
	dq-pie	1	reno	relentless	0.9914848926	0.9988964463	5.0932148296	20.010000000	543.058000000
	dq-pie	0	reno	reno	0.9870612379	0.9932936212	5.6698582532	20.020779310	561.046000000
	dq-pie	1	reno	reno	0.9863427172	0.9928652274	5.4977489312	30.046000000	602.010000000
	dq-pie	0	cubic	cubic	0.9891451322	0.9976131629	4.0345649044	13.046000000	434.058000000
	dq-pie	1	cubic	cubic	0.9844624834	0.9959509247	3.1035084000	13.046000000	357.3190413060
	dq-pie	0	reno	dctcp	0.9990123122	1.0000000000	5.0932148296	20.010000000	361.1688716800
	dq-pie	1	reno	dctcp	0.9990123122	1.0000000000	5.0932148296	20.010000000	555.046000000
	dq-pie	0	reno	reno	0.9998387970	0.9999999997	14.8769853662	23.046000000	561.046000000
	dq-pie	1	reno	reno	0.9998350180	0.9999999997	12.7611905190	21.046000000	359.4726948040
	dq-pie	0	cubic	cubic	0.99990123027	1.0000000000	12.3635868167	21.046000000	602.010000000
	dq-pie	1	cubic	cubic	0.9981578437	0.9700136150	3.0450761991	19.046000000	227.9207221900
	dq-pie	0	reno	dctcp	0.9990122932	1.0000000000	14.4387047500	21.044000000	317.046000000
	dq-pie	1	reno	dctcp	0.9990122932	1.0000000000	14.4387047500	21.044000000	431.8164207710
	dq-pie	0	reno	reno	0.99990123027	1.0000000000	14.8466726500	22.046000000	438.046000000
	dq-pie	1	reno	reno	0.99990123027	1.0000000000	14.8466726500	22.046000000	555.046000000
	dq-pie	0	reno	reno	0.9999999997	14.8769853662	23.046000000	227.5330699330	561.046000000
	dq-pie	1	reno	reno	0.9999999997	12.7611905190	21.046000000	256.701262710	366.046000000
	dq-pie	0	cubic	cubic	0.9999999997	12.3635868167	21.046000000	257.7941098670	325.046000000
	dq-pie	1	cubic	cubic	0.9984624834	0.9959509247	3.1035084000	13.046000000	434.058000000
	dq-pie	0	reno	dctcp	0.9990123122	1.0000000000	14.4387047500	21.044000000	555.046000000
	dq-pie	1	reno	dctcp	0.9990123122	1.0000000000	14.4387047500	21.044000000	555.046000000
	dq-pie	0	reno	reno	0.9999999997	14.8769853662	23.046000000	227.5330699330	561.046000000
	dq-pie	1	reno	reno	0.9999999997	12.7611905190	21.046000000	256.701262710	366.046000000
	dq-pie	0	cubic	cubic	0.9999999997	12.3635868167	21.046000000	257.7941098670	325.046000000
	dq-pie	1	cubic	cubic	0.9984624834	0.9959509247	3.1035084000	13.046000000	434.058000000
	dq-pie	0	reno	dctcp	0.9990123122	1.0000000000	14.4387047500	21.044000000	555.046000000
	dq-pie	1	reno	dctcp	0.9990123122	1.0000000000	14.4387047500	21.044000000	555.046000000
	dq-pie	0	reno	reno	0.9999999997	14.8769853662	23.046000000	227.5330699330	561.046000000
	dq-pie	1	reno	reno	0.9999999997	12.7611905190	21.046000000	256.701262710	366.046000000
	dq-pie	0	cubic	cubic	0.9999999997	12.3635868167	21.046000000	257.7941098670	325.046000000
	dq-pie	1	cubic	cubic	0.9984624834	0.9959509247	3.1035084000	13.046000000	434.058000000
	dq-pie	0	reno	dctcp	0.9990123122	1.0000000000	14.4387047500	21.044000000	555.046000000
	dq-pie	1	reno	dctcp	0.9990123122	1.0000000000	14.4387047500	21.044000000	555.046000000
	dq-pie	0	reno	reno	0.9999999997	14.8769853662	23.046000000	227.5330699330	561.046000000
	dq-pie	1	reno	reno	0.9999999997	12.7611905190	21.046000000	256.701262710	366.046000000
	dq-pie	0	cubic	cubic	0.9999999997	12.3635868167	21.046000000	257.7941098670	325.046000000
	dq-pie	1	cubic	cubic	0.9984624834	0.9959509247	3.1035084000	13.046000000	434.058000000
	dq-pie	0	reno	dctcp	0.9990123122	1.0000000000	14.4387047500	21.044000000	555.046000000
	dq-pie	1	reno	dctcp	0.9990123122	1.0000000000	14.4387047500	21.044000000	555.046000000
	dq-pie	0	reno	reno	0.9999999997	14.8769853662	23.046000000	227.5330699330	561.046000000
	dq-pie	1	reno	reno	0.9999999997	12.7611905190	21.046000000	256.701262710	366.046000000
	dq-pie	0	cubic	cubic	0.9999999997	12.3635868167	21.046000000	257.7941098670	325.046000000
	dq-pie	1	cubic	cubic	0.9984624834	0.9959509247	3.1035084000	13.046000000	434.058000000
	dq-pie	0	reno	dctcp	0.9990123122	1.0000000000	14.4387047500	21.044000000	555.046000000
	dq-pie	1	reno	dctcp	0.9990123122	1.0000000000	14.4387047500	21.044000000	555.046000000
	dq-pie	0	reno	reno	0.9999999997	14.8769853662	23.046000000	227.5330699330	561.046000000
	dq-pie	1	reno	reno	0.9999999997	12.7611905190	21.046000000	256.701262710	366.046000000
	dq-pie	0	cubic	cubic	0.9999999997	12.3635868167	21.046000000	257.7941098670	325.046000000
	dq-pie	1	cubic	cubic	0.9984624834	0.9959509247	3.1035084000	13.046000000	434.058000000
	dq-pie	0	reno	dctcp	0.9990123122	1.0000000000	14.4387047500	21.044000000	555.046000000
	dq-pie	1	reno	dctcp	0.9990123122	1.0000000000	14.4387047500	21.044000000	555.046000000
	dq-pie	0	reno	reno	0.9999999997	14.8769853662	23.046000000	227.5330699330	561.046000000
	dq-pie	1	reno	reno	0.9999999997	12.7611905190	21.046000000	256.701262710	366.046000000
	dq-pie	0	cubic	cubic	0.9999999997	12.3635868167	21.046000000	257.7941098670	325.046000000
	dq-pie	1	cubic	cubic	0.9984624834	0.9959509247	3.1035084000	13.046000000	434.058000000
	dq-pie	0	reno	dctcp	0.9990123122	1.0000000000	14.4387047500	21.044000000	555.046000000
	dq-pie	1	reno	dctcp	0.9990123122	1.0000000000	14.4387047500	21.044000000	555.046000000
	dq-pie	0	reno	reno	0.9999999997	14.8769853662	23.046000000	227.5330699330	561.046000000
	dq-pie	1	reno	reno	0.9999999997	12.7611905190	21.046000000	256.701262710	366.046000000
	dq-pie	0	cubic	cubic	0.9999999997	12.36			

5	-	reno	-	0.9769135197	1.1510757926	1.6536501207	9.0460000000	211.020422080	
5	-	reno	reno	0.9754749477	1.1698168805	1.5904622454	7.0460000000	214.4263762330	
10	-	cubic	cubic	0.9911152101	0.9989961877	1.240239497	5.0460000000	194.0376217380	
10	-	cubic	cubic	0.9918192337	0.9975437177	1.2651158404	6.0440000000	265.0580000000	
10	-	cubic	dctcp	0.9676072637	1.5679450558	1.3563705623	6.0460000000	506.0460000000	
10	-	cubic	dctcp	0.9683397034	1.534198131	1.3569847937	6.0460000000	494.0340000000	
10	-	cubic	relentless	0.9698334740	1.4515360547	1.2648070298	6.0460000000	418.0460000000	
10	-	cubic	relentless	0.9715264889	1.4027296168	1.2643633132	6.0440000000	401.0340000000	
10	-	reno	dctcp	0	0.9681541548	1.5491950459	1.3095160501	6.0440000000	340.0460000000
10	-	reno	dctcp	0	0.9689423179	1.5319703888	1.3623457200	6.0440000000	337.0460000000
10	-	reno	relentless	0	0.9705136737	1.4377112435	1.2660535994	6.0100000000	315.0460000000
10	-	reno	relentless	1	0.9721308023	1.3865678883	1.2609754577	6.0460000000	315.0220000000
10	-	reno	reno	0	0.9918193345	0.9882155521	1.3036578989	5.0220000000	221.0220000000
10	-	reno	reno	1	0.9922150295	0.9833768780	1.3099221404	5.0240000000	208.0460000000
1	-	cubic	cubic	0	0.9981382392	0.5524007395	14.9276551834	35.0460000000	319.0580000000
1	-	cubic	cubic	1	0.9977025100	0.5504656057	14.4097183682	36.0460000000	348.0460000000
1	-	cubic	dctcp	0	0.9990122932	0.5555555262	27.9464123333	41.0460000000	320.0580000000
1	-	cubic	dctcp	1	0.9991122932	0.5555555623	27.910065933	41.0460000000	321.0460000000
1	-	cubic	relentless	0	0.9929422324	0.5219658105	16.7925658158	43.0440000000	323.0580000000
1	-	cubic	relentless	1	0.991583096	0.5185559624	15.77364779320	42.0460000000	252.758240130
1	-	reno	dctcp	0	0.9990122932	0.5555555485	27.7687836333	42.0340000000	288.0460000000
1	-	reno	dctcp	1	0.9991123027	0.555555556	27.9530189833	42.0340000000	289.0460000000
1	-	reno	relentless	0	0.991357758	0.5194746578	16.275250330	42.0460000000	293.0460000000
1	-	reno	relentless	1	0.9913268587	0.5138499422	15.5456096510	41.0460000000	227.4473227110
1	-	reno	reno	0	0.9905326583	0.4940758316	12.1701202490	43.0440000000	295.0460000000
1	-	reno	reno	1	0.9912178076	0.5031940509	12.2057630479	42.0340000000	181.4257171500
1	-	cubic	cubic	0	0.9939459498	0.99991220188	7.9468304497	12.0460000000	181.4244948000
1	-	cubic	cubic	1	0.9911553908	0.9974221191	7.6787256231	17.8932044540	293.0460000000
1	-	cubic	dctcp	0	0.9989940388	0.9999999993	15.8240805627	31.0340000000	292.0460000000
5	-	cubic	dctcp	1	0.9990122932	0.5031940509	15.809734167	31.0340000000	295.0460000000
5	-	cubic	relentless	0	0.9872629017	0.9993102077	8.42996035688	30.0460000000	171.4733482630
5	-	cubic	relentless	1	0.9857183495	0.9879494739	8.2435415977	31.0340000000	297.0460000000
5	-	reno	dctcp	0	0.9990122932	1.0000000000	15.8679499833	30.0460000000	321.926577330
5	-	reno	dctcp	1	0.9990123027	1.0000000000	27.0220000000	318.4593129850	465.0460000000
5	-	reno	relentless	1	0.9863371839	0.9889717488	8.2280211282	30.0100000000	332.4385426640
5	-	reno	relentless	1	0.9873695189	0.99111727332	8.6692448332	30.0460000000	492.0340000000
5	-	reno	reno	0	0.9845504469	0.9760713483	6.6129477666	31.0340000000	481.0340000000
5	-	reno	reno	1	0.9852697661	0.9792116363	6.9339959545	30.0460000000	458.0460000000
5	-	reno	reno	1	0.9802922094	0.9707333885	4.62021378276	29.0460000000	348.0460000000
5	-	cubic	cubic	1	0.9888334874	0.723799199	4.7330552911	30.0340000000	359.0580000000
5	-	cubic	dctcp	0	0.9980962350	1.1097473836	9.241405581	30.0460000000	360.0220000000
5	-	cubic	dctcp	1	0.9980933039	1.1097636321	9.2847768821	30.0460000000	371.0460000000
5	-	cubic	relentless	0	0.9830964442	1.0434976091	5.507173789	24.0220000000	348.0220000000
5	-	cubic	relentless	1	0.9833481080	1.0421378276	5.5961640289	24.0220000000	349.0100000000
5	-	reno	dctcp	0	0.9980483267	1.1050808036	9.213797801	25.0340000000	349.0100000000
5	-	reno	dctcp	1	0.9981727990	1.1038619091	9.2458945998	24.0460000000	350.0460000000
5	-	reno	relentless	0	0.983529036	1.0441620188	5.5050920659	24.0460000000	351.0460000000
5	-	reno	relentless	1	0.9834681974	1.0427504208	5.5952088005	24.0460000000	352.0460000000
5	-	reno	reno	0	0.9822824336	1.024857503	4.1267901817	21.0580000000	353.0460000000
5	-	reno	reno	1	0.98227541833	1.0222447543	4.5104066457	21.0460000000	354.0460000000
5	-	cubic	cubic	0	0.9944001806	0.3119462519	17.6965791441	45.0460000000	326.0460000000
5	-	cubic	cubic	1	0.9957934033	0.31174294968	18.8021078877	46.0340000000	391.0460000000

10	dq-red	0	0.99990122932	0.3305785073	29.6036022833	52.0340000000	220.6084715500	349.0460000000
10	dq-red	1	0.99991122932	0.3305785073	29.6851666167	53.0460000000	257.3728690670	321.0460000000
10	dq-red	1	0.9873395608	0.2847072015	16.539637187	52.9980000000	245.6951349490	416.0340000000
10	dq-red	1	0.9881359764	0.2865900201	16.5404846876	54.0460000000	234.2032259790	338.0460000000
10	dq-red	1	0.99990122932	0.3305785175	29.4416891833	52.0340000000	182.4321095330	288.0460000000
10	dq-red	1	0.99991122932	0.3305785073	29.7838370500	54.0580000000	181.8216517330	289.0460000000
10	dq-red	1	0.99873395608	0.2848048339	16.5681217316	52.0440000000	167.6777791900	295.0460000000
10	dq-red	1	0.9876482221	0.2840021157	16.581768873	53.0460000000	167.222917600	296.0460000000
10	dq-red	1	0.9881918521	0.2686327409	14.982264952	54.0460000000	158.3026889430	308.0460000000
10	dq-red	1	0.988491538	0.2681062297	15.5027630899	56.0340000000	161.610644680	296.0460000000
10	dq-red	1	0.99991122932	0.3305785073	11.5014284781	36.0460000000	309.2702137850	468.0460000000
10	dq-red	1	0.99873395608	0.2848048339	11.5533272808	41.0460000000	411.0220000000	411.0220000000
10	dq-red	1	0.9876482221	0.2840021157	20.3550380692	43.0580000000	333.8300947120	528.0460000000
10	dq-red	1	0.9881918521	0.2686327409	20.3639715981	42.0460000000	331.8789084200	493.0340000000
10	dq-red	1	0.988491538	0.2681062297	12.0341807778	46.0340000000	290.2972513140	477.0340000000
10	dq-red	1	0.99991122932	0.3305785073	11.8096474015	11.9080521	299.0381525140	494.0100000000
10	dq-red	1	0.99873395608	0.2848048339	12.03550380692	44.0220000000	347.0460000000	347.0460000000
10	dq-red	1	0.9876482221	0.2840021157	20.2845582620	44.0340000000	278.4616991670	343.0460000000
10	dq-red	1	0.9881918521	0.2686327409	20.4047723224	42.0340000000	283.1137200430	372.0340000000
10	dq-red	1	0.988491538	0.2681062297	12.0250311767	45.0340000000	255.5775786560	380.0460000000
10	dq-red	1	0.99991122932	0.3305785073	12.0336953460	45.0460000000	240.7257525600	356.0460000000
10	dq-red	1	0.99873395608	0.2848048339	10.864237410	43.0460000000	374.0460000000	374.0460000000
10	dq-red	1	0.9876482221	0.2840021157	10.8319190968	44.0460000000	247.0595850000	529.0100000000
10	dq-red	1	0.9881918521	0.2686327409	8.6635395985	34.0460000000	368.5067930460	504.0220000000
10	dq-red	1	0.988491538	0.2681062297	8.7447502857	31.0340000000	322.5455289820	529.0460000000
10	dq-red	1	0.99991122932	0.3305785073	15.3879696787	41.0340000000	409.0340000000	577.0580000000
10	dq-red	1	0.9985666011	0.7714956615	10.864237410	43.0460000000	240.7257525600	356.0460000000
10	dq-red	1	0.98534313387	0.7706746558	10.8319190968	44.0460000000	247.0595850000	374.0460000000
10	dq-red	1	0.98999971953	0.9933927907	8.6635395985	34.0460000000	368.5067930460	529.0100000000
10	dq-red	1	0.9900285796	0.9940731357	8.7447502857	31.0340000000	322.5455289820	529.0460000000
10	dq-red	1	0.99811266381	0.81154544640	12.0250311767	45.0340000000	255.5775786560	380.0460000000
10	dq-red	1	0.9984528561	0.8029046610	12.0341807778	46.0340000000	290.2972513140	477.0340000000
10	dq-red	1	0.99991122932	0.3305785073	10.8096474015	43.0460000000	240.7257525600	356.0460000000
10	dq-red	1	0.99873395608	0.2848048339	10.864237410	43.0460000000	240.7257525600	356.0460000000
10	dq-red	1	0.9876482221	0.2840021157	8.6635395985	34.0460000000	368.5067930460	529.0100000000
10	dq-red	1	0.9881918521	0.2686327409	8.7447502857	31.0340000000	322.5455289820	529.0460000000
10	dq-red	1	0.988491538	0.2681062297	15.4313135330	38.0460000000	410.572377730	577.0580000000
10	dq-red	1	0.99991122932	0.3305785073	9.7895852889	39.0460000000	361.6212319310	505.0580000000
10	dq-red	1	0.99873395608	0.2848048339	9.6778347045	38.0340000000	481.0460000000	529.0100000000
10	dq-red	1	0.9876482221	0.2840021157	15.3804545972	38.0460000000	387.0340000000	405.0220000000
10	dq-red	1	0.9881918521	0.2686327409	15.2972266126	39.0220000000	327.7983386400	396.0460000000
10	dq-red	1	0.988491538	0.2681062297	9.6001942843	37.0460000000	12.0620894939	62.0460000000
10	dq-red	1	0.99991122932	0.3305785073	9.7317871633	38.0340000000	284.3300128240	401.0100000000
10	dq-red	1	0.9985666011	0.7714956615	9.7317871633	38.0340000000	361.6212319310	505.0580000000
10	dq-red	1	0.98534313387	0.7706746558	9.7317871633	38.0340000000	481.0460000000	529.0100000000
10	dq-red	1	0.98999971953	0.9933927907	9.6778347045	38.0340000000	387.0340000000	405.0220000000
10	dq-red	1	0.9900285796	0.9940731357	15.3804545972	38.0340000000	327.7983386400	396.0460000000
10	dq-red	1	0.99811266381	0.81154544640	15.2972266126	39.0220000000	322.5455289820	529.0460000000
10	dq-red	1	0.9984528561	0.8029046610	9.6001942843	37.0460000000	281.5513132380	388.0460000000
10	dq-red	1	0.99991122932	0.3305785073	9.7317871633	38.0340000000	284.3300128240	401.0100000000
10	dq-red	1	0.99873395608	0.2848048339	9.6778347045	38.0340000000	361.6212319310	505.0580000000
10	dq-red	1	0.9876482221	0.2840021157	15.3804545972	38.0340000000	387.0340000000	405.0220000000
10	dq-red	1	0.9881918521	0.2686327409	15.2972266126	39.0220000000	327.7983386400	396.0460000000
10	dq-red	1	0.988491538	0.2681062297	9.6001942843	37.0460000000	281.5513132380	388.0460000000
10	dq-red	1	0.99991122932	0.3305785073	9.7317871633	38.0340000000	284.3300128240	401.0100000000
10	dq-red	1	0.99873395608	0.2848048339	9.6778347045	38.0340000000	361.6212319310	505.0580000000
10	dq-red	1	0.9876482221	0.2840021157	15.3804545972	38.0340000000	387.0340000000	405.0220000000
10	dq-red	1	0.9881918521	0.2686327409	15.2972266126	39.0220000000	327.7983386400	396.0460000000
10	dq-red	1	0.988491538	0.2681062297	9.6001942843	37.0460000000	281.5513132380	388.0460000000
10	dq-red	1	0.99991122932	0.3305785073	9.7317871633	38.0340000000	284.3300128240	401.0100000000
10	dq-red	1	0.99873395608	0.2848048339	9.6778347045	38.0340000000	361.6212319310	505.0580000000
10	dq-red	1	0.9876482221	0.2840021157	15.3804545972	38.0340000000	387.0340000000	405.0220000000
10	dq-red	1	0.9881918521	0.2686327409	15.2972266126	39.0220000000	327.7983386400	396.0460000000
10	dq-red	1	0.988491538	0.2681062297	9.6001942843	37.0460000000	281.5513132380	388.0460000000
10	dq-red	1	0.99991122932	0.3305785073	9.7317871633	38.0340000000	284.3300128240	401.0100000000
10	dq-red	1	0.99873395608	0.2848048339	9.6778347045	38.0340000000	361.6212319310	505.0580000000
10	dq-red	1	0.9876482221	0.2840021157	15.3804545972	38.0340000000	387.0340000000	405.0220000000
10	dq-red	1	0.9881918521	0.2686327409	15.2972266126	39.0220000000	327.7983386400	396.0460000000
10	dq-red	1	0.988491538	0.2681062297	9.6001942843	37.0460000000	281.5513132380	388.0460000000
10	dq-red	1	0.99991122932	0.3305785073	9.7317871633	38.0340000000	284.3300128240	401.0100000000
10	dq-red	1	0.99873395608	0.2848048339	9.6778347045	38.0340000000	361.6212319310	505.0580000000
10	dq-red	1	0.9876482221	0.2840021157	15.3804545972	38.0340000000	387.0340000000	405.0220000000
10	dq-red	1	0.9881918521	0.2686327409	15.2972266126	39.0220000000	327.7983386400	396.0460000000
10	dq-red	1	0.988491538	0.2681062297	9.6001942843	37.0460000000	281.5513132380	388.0460000000
10	dq-red	1	0.99991122932	0.3305785073	9.7317871633	38.0340000000	284.3300128240	401.0100000000
10	dq-red	1	0.99873395608	0.2848048339	9.6778347045	38.0340000000	361.6212319310	505.0580000000
10	dq-red	1	0.9876482221	0.2840021157	15.3804545972	38.0340000000	387.0340000000	405.0220000000
10	dq-red	1	0.9881918521	0.2686327409	15.2972266126	39.0220000000	327.7983386400	396.0460000000
10	dq-red	1	0.988491538	0.2681062297	9.6001942843	37.0460000000	281.5513132380	388.0460000000
10	dq-red	1	0.99991122932	0.3305785073	9.7317871633	38.0340000000	284.3300128240	401.0100000000
10	dq-red	1	0.99873395608	0.2848048339	9.6778347045	38.0340000000	361.6212319310	505.0580000000
10	dq-red	1	0.9876482221	0.2840021157	15.3804545972	38.0340000000		

14s-pie	10 cubic	relentless	0 0.9915500894 0.9603139373 1.1406492587 5.0460000000 15.6192571888
14s-pie	10 cubic	relentless	1 0.9921589846 0.9591847502 1.1516972766 4.0460000000 15.5363335638
14s-pie	10 reno	dctcp	0 0.9677009527 0.9950992293 1.1380705223 8.0840000000 16.896062405
14s-pie	10 reno	dctcp	1 0.9511838298 0.9931344664 1.1337641736 6.0080000000 16.9134480175
14s-pie	10 reno	relentless	0 0.9693539781 0.9603043553 1.1609400135 5.0220000000 16.4454036959
14s-pie	10 reno	relentless	1 0.9364003841 0.9606591956 1.1695489697 6.0100000000 17.8104339898
14s-pie	1 cubic	dctcp	0 0.8684255467 0.9704662245 2.3551058741 1.4.0580000000 11.5005771017
14s-pie	1 cubic	dctcp	1 0.8274893041 0.2924644078 2.9554394678 14.0460000000 10.1335429563
14s-pie	1 cubic	relentless	0 0.8326541624 0.3192211507 2.0970859221 2.0790000000 12.5016461446
14s-pie	1 cubic	relentless	1 0.8589868416 0.2838521093 2.1913092226 14.9370000000 12.0523329931
14s-pie	5 reno	dctcp	0 0.7457026051 0.31841274160 3.1504933551 1.5.0460000000 10.19371969271
14s-pie	5 reno	dctcp	1 0.7899027477 0.3176085732 3.0488155673 14.0460000000 10.6906070797
14s-pie	5 reno	relentless	0 0.7847186062 0.7846471665 2.0860719462 1.4.0220000000 9.6781565836
14s-pie	5 reno	relentless	1 0.7912155638 0.2910284156 2.4517295986 1.5.0440000000 10.4157676881
14s-pie	5 cubic	dctcp	0 0.9430394086 0.8785513378 1.745715353 1.3.0460000000 17.69946744221
14s-pie	5 cubic	dctcp	1 0.9239107910 0.53037005 1.8915958424 17.0340000000 17.64226559473
14s-pie	5 cubic	relentless	0 0.9621202320 0.7526181250 1.4667880397 9.9720000000 19.1156495926
14s-pie	5 cubic	relentless	1 0.9649607055 0.9043894222 1.4476154653 12.0580000000 18.5657381502
14s-pie	5 cubic	dctcp	0 0.9035134436 0.8594276121 1.8964135188 1.3.0460000000 19.892403720
14s-pie	5 reno	dctcp	1 0.8813861285 0.8318191605 2.1792538281 17.1460000000 19.5028006869
14s-pie	5 reno	relentless	0 0.9148807473 0.7643759262 1.5628597065 14.0220000000 19.7039675011
14s-pie	5 reno	dctcp	1 0.8958078532 0.7517457729 1.6547737028 14.0220000000 16.0460000000
14s-pie	10 cubic	dctcp	0 0.9638951332 0.9742451013 1.4153409111 8.0340000000 17.0808866407
14s-pie	10 cubic	dctcp	1 0.9458730272 0.9582732730 1.4631694530 11.0460000000 17.4936083838
14s-pie	10 cubic	relentless	0 0.9748767446 0.8481337255 1.3222463515 8.0340000000 16.4530314159
14s-pie	10 cubic	relentless	1 0.969826982 0.8481337255 1.3222463515 8.0340000000 16.4530314159
14s-pie	10 reno	dctcp	0 0.9410105153 0.9642410256 1.4250104863 10.0460000000 16.69103873
14s-pie	10 reno	dctcp	1 0.9266642575 0.9455323302 1.5238799736 12.0440000000 17.0460000000
14s-pie	10 reno	relentless	0 0.9591086613 0.8457329555 1.3341143680 9.0220000000 17.8359193981
14s-pie	10 reno	relentless	1 0.9463813558 0.8457329555 1.3341143680 9.0220000000 16.9409064273
14s-pie	10 cubic	dctcp	0 0.8749111323 0.2562273883 2.9550928735 1.8.0340000000 17.37188704
14s-pie	10 cubic	dctcp	1 0.8351293877 0.2225666005 3.3221943360 1.9.0340000000 12.7655649558
14s-pie	10 cubic	relentless	0 0.8403837231 0.1940405887 2.6797681313 20.0440000000 10.3178470393
14s-pie	10 cubic	relentless	1 0.8524181118 0.19584046899 2.5881366858 17.0560000000 11.4172052310
14s-pie	10 cubic	dctcp	0 0.8075129292 0.2338166815 3.2360211531 18.0460000000 16.8962095458
14s-pie	10 reno	dctcp	1 0.8061276193 0.2369144831 3.3761084716 16.0460000000 12.0460000000
14s-pie	10 reno	relentless	0 0.8146354345 0.1989984009 2.7371427822 17.0460000000 10.717223983
14s-pie	10 reno	dctcp	1 0.8259064176 0.1964974555 2.6576568428 18.0340000000 16.6785962826
14s-pie	10 reno	dctcp	1 0.9629907492 0.7575831310 2.2365140935 16.0580000000 15.5308000000
14s-pie	10 reno	relentless	0 0.9442206918 0.7406554448 2.3604171912 15.0560000000 17.9663873143
14s-pie	10 reno	relentless	1 0.9607493535 0.5998427648 1.7467817508 14.0440000000 17.952742099
14s-pie	10 cubic	dctcp	1 0.9500385435 0.6003714015 1.8173390731 14.0220000000 19.7176311955
14s-pie	10 cubic	dctcp	1 0.9231818977 0.7331035768 2.3656949806 11.0560000000 18.5926836778
14s-pie	10 cubic	relentless	0 0.9650857577 0.7478760878 1.5336585173 9.0580000000 17.0176513133
14s-pie	10 cubic	relentless	1 0.9622967389 0.7373298222 1.5849300515 11.0460000000 17.1941853774
14s-pie	10 reno	dctcp	0 0.9434933923 0.9024444252 1.8915403778 12.0320000000 18.023304132
14s-pie	10 reno	dctcp	1 0.9132164005 0.878962515328 2.0351247095 14.0560000000 18.897972454

14s-pie	10	10	reno	relentless	0	0.9449737973	0.745444304	1.5810303367	12.9490000000	17.92215454433	58.0460000000
14s-pie	10	10	reno	relentless	1	0.9299741110	0.7437206168	1.6112951049	11.9610000000	17.5716614105	67.0460000000

Appendix C

Original Problem

Evaluation of AQM schemes to support Low Latency in the Internet

Master thesis

Background

Many modern applications require low latency transmission in the Internet which is not explicitly supported today. Most networks are optimized for high throughput and low loss. This increases latency due to high queuing delays. Only very few applications actually need both high throughput and low latency, therefore the network could offer a new parallel Internet service that provides lower latency compared to the best effort service that is usually offered today. This can be achieved by separating flows into different queues at the bottleneck link that operate either independently or could be coupled as proposed by the DualQ Coupled AQM for Low Latency, Low Loss and Scalable Throughput (L4S) [1].

Thesis Goals

The goal of this project is to evaluate different solutions for the realization of such an low latency service, including DualQ for L4S.

This leads to the following tasks:

1. Implementation and configuration of different AQM setups in the ns-3 network simulator [2].
2. Design of an experimental setup focusing on traffic conditions and cases that may have scalability or fairness issues.
3. Evaluation and representation of simulation results.

Contact: Mirja Kühlewind, mirja.kuehlewind@tik.ee.ethz.ch, ETZ H93
Brian Trammell, trammell@tik.ee.ethz.ch, ETZ H93

Professor: Prof. Laurent Vanbever

References:

1. K. De Schepper, B. Briscoe, O. Bondarenko, I. Tsang: DualQ Coupled AQM for Low Latency, Low Loss and Scalable Throughput. Internet-Draft, IETF (Oct 2016): <https://datatracker.ietf.org/doc/draft-briscoe-tsvwg-aqm-dualq-coupled/>
2. ns-3: <https://www.nsnam.org/>

Bibliography

- [1] Network simulator 3. <https://www.nsnam.org/>. Last Accessed: August 2017.
- [2] Network simulator 3 - direct code execution. <https://www.nsnam.org/overview/projects/direct-code-execution/>. Last Accessed: August 2017.
- [3] Network simulator 3 - lte module. <https://www.nsnam.org/docs/models/html/lte.html>. Last Accessed: August 2017.
- [4] Linux kernel (4.7.0-rc5) [operating system], 2016. Retrieved from <https://github.com/libos-nuse/net-next-nuse> on 10. August 2017.
- [5] M. Alizadeh, A. Greenberg, D. A. Maltz, J. Padhye, P. Patel, B. Prabhakar, S. Sengupta, and M. Sridharan. Data center tcp (dctcp). In *Proceedings of the ACM SIGCOMM 2010 Conference, SIGCOMM '10*, pages 63–74, New York, NY, USA, 2010. ACM.
- [6] F. Baker and G. Fairhurst. IETF Recommendations Regarding Active Queue Management. RFC 7567, July 2015.
- [7] S. Bensley, D. Thaler, P. Balasubramanian, L. Eggert, and G. Judd. Datacenter TCP (DCTCP): TCP Congestion Control for Datacenters. Internet-Draft draft-ietf-tcpm-dctcp-10, Internet Engineering Task Force, Aug. 2017. Work in Progress.
- [8] E. Blanton, D. V. Paxson, and M. Allman. TCP Congestion Control. RFC 5681, Sept. 2009.
- [9] O. Bondarenko, K. Schepper, I. Tsang, B. Briscoe, A. Petlund, and C. Griwodz. Ultra-low delay for all: Live experience, live analysis, 05 2016.
- [10] B. Briscoe. Insights from curvy red (random early detection). Technical report, 05/2015 2015.
- [11] B. J. Briscoe, K. D. Schepper, and M. Bagnulo. Low Latency, Low Loss, Scalable Throughput (L4S) Internet Service: Architecture. Internet-Draft draft-ietf-tsvwg-l4s-arch-00, Internet Engineering Task Force, May 2017. Work in Progress.
- [12] D. D. Clark, G. Minshall, L. Zhang, S. Shenker, D. C. Partridge, L. Peterson, D. K. K. Ramakrishnan, J. T. Wroclawski, J. Crowcroft, R. T. Braden, D. S. E. Deering, S. Floyd, D. B. S. Davie, V. Jacobson, and D. D. Estrin. Recommendations on Queue Management and Congestion Avoidance in the Internet. RFC 2309, Apr. 1998.
- [13] K. De Schepper, O. Bondarenko, I.-J. Tsang, and B. Briscoe. Pi2 : A linearized aqm for both classic and scalable tcp. pages 105–119, New York, NY, USA, 12/2016 2016. ACM.
- [14] R. Diana and E. Lochin. TCP relentless congestion control model. *CoRR*, abs/1102.3270, 2011.
- [15] S. Floyd, D. K. K. Ramakrishnan, and D. L. Black. The Addition of Explicit Congestion Notification (ECN) to IP. RFC 3168, Sept. 2001.
- [16] A. Gurkov, T. Henderson, S. Floyd, and Y. Nishida. The NewReno Modification to TCPs Fast Recovery Algorithm. RFC 6582, Apr. 2012.
- [17] S. Ha, I. Rhee, and L. Xu. Cubic: A new tcp-friendly high-speed tcp variant. *SIGOPS Oper. Syst. Rev.*, 42(5):64–74, July 2008.

- [18] R. Jain, D.-M. Chiu, and W. R. Hawe. *A quantitative measure of fairness and discrimination for resource allocation in shared computer system*, volume 38. Eastern Research Laboratory, Digital Equipment Corporation Hudson, MA, 1984.
- [19] D. Lin and R. Morris. Dynamics of random early detection. In *Proceedings of the ACM SIGCOMM '97 Conference on Applications, Technologies, Architectures, and Protocols for Computer Communication*, SIGCOMM '97, pages 127–137, New York, NY, USA, 1997. ACM.
- [20] M. Mathis. Relentless congestion control. In *Proc. PFLDNeT*, 2009.
- [21] M. Mathis. Relentless Congestion Control. Internet-Draft draft-mathis-icrcg-relentless-tcp-00, Internet Engineering Task Force, Mar. 2009. Work in Progress.
- [22] R. Pan, P. Natarajan, F. Baker, and G. White. Proportional Integral Controller Enhanced (PIE): A Lightweight Control Scheme to Address the Bufferbloat Problem. RFC 8033, Feb. 2017.
- [23] R. Pan, P. Natarajan, C. Piglione, M. S. Prabhu, V. Subramanian, F. Baker, and B. VerSteeg. Pie: A lightweight control scheme to address the bufferbloat problem. In *High Performance Switching and Routing (HPSR), 2013 IEEE 14th International Conference on*, pages 148–155. IEEE, 2013.
- [24] I. Rhee, L. Xu, S. Ha, A. Zimmermann, L. Eggert, and R. Scheffenegger. CUBIC for Fast Long-Distance Networks. Internet-Draft draft-ietf-tcpm-cubic-05, Internet Engineering Task Force, July 2017. Work in Progress.
- [25] K. D. Schepper and B. J. Briscoe. Identifying Modified Explicit Congestion Notification (ECN) Semantics for Ultra-Low Queuing Delay. Internet-Draft draft-ietf-tsvwg-ecn-l4s-id-00, Internet Engineering Task Force, May 2017. Work in Progress.
- [26] K. D. Schepper, B. J. Briscoe, O. Bondarenko, and I. J. Tsang. DualQ Coupled AQM for Low Latency, Low Loss and Scalable Throughput. Internet-Draft draft-ietf-tsvwg-aqm-dualq-coupled-01, Internet Engineering Task Force, July 2017. Work in Progress.